Control of constrained multi-agent systems with cooperative and antagonistic interactions

Pelin Sekercioglu

▶ **To cite this version:**

Pelin Sekercioglu. Control of constrained multi-agent systems with cooperative and antagonistic interactions. Engineering Sciences [physics]. Université Paris-Saclay, 2024. English. NNT : 2024UPAST130 . tel-04837019

HAL Id: tel-04837019

https://theses.hal.science/tel-04837019v1

Submitted on 13 Dec 2024

HAL is a multi-disciplinary open access archive for the deposit and dissemination of scientific research documents, whether they are published or not. The documents may come from teaching and research institutions in France or abroad, or from public or private research centers.

L'archive ouverte pluridisciplinaire **HAL**, est destinée au dépôt et à la diffusion de documents scientifiques de niveau recherche, publiés ou non, émanant des établissements d'enseignement et de recherche français ou étrangers, des laboratoires publics ou privés.

université PARIS-SACLAY

Control of constrained multi-agent systems with cooperative and antagonistic interactions

Commande de systèmes multi-agents sous contraintes par des interactions coopératives et antagonistes

Thèse de doctorat de l'université Paris-Saclay

École doctorale n° 580, Sciences et Technologies de l'Information et de la Communication (STIC)
Spécialité de doctorat: Automatique
Graduate School : Sciences de l'Ingénierie et des Systèmes
Référent : Faculté des sciences d'Orsay

Thèse préparée dans le Département **Traitement de l'Information et Systèmes** (Université Paris-Saclay, ONERA),
sous la direction d'**Antonio LORIA**, Directeur de recherche, CNRS, L2S,
le co-encadrement de **Julien MARZAT**, Directeur de recherche, ONERA, DTIS,
et le co-encadrement de **Ioannis SARRAS**, Ingénieur de recherche, ONERA, DTIS

Thèse soutenue à Paris-Saclay, le 5 Novembre 2024, par

Pelin SEKERCIOGLU

Composition du jury

Membres du jury avec voix délibérative

Cristina STOICA Professeur, CentraleSupélec/L2S, Université Paris-Saclay	Présidente
Claudio ALTAFINI Professeur, Linkoping University	Rapporteur & Examinateur
Ming CAO Professeur, University of Groningen	Rapporteur & Examinateur
Maria Elena VALCHER Professeur, University of Padova	Examinatrice

THESE DE DOCTORAT

NNT : 2024UPAST130

université PARIS-SACLAY

ÉCOLE DOCTORALE
Sciences et technologies de l'information et de la communication (STIC)

Titre: Commande de systèmes multi-agents sous contraintes par des interactions coopératives et antagonistes

Mots clés: Véhicules autonomes, automatique, robotique, coordination

Résumé: Dans cette thèse, nous abordons des problèmes de commande de systèmes multi-agents sous contraintes, avec des interactions coopératives et compétitives, en présence de leaders multiples. Certaines de nos contributions traitent des problèmes de consensus biparti pour des systèmes linéaires de premier et de second ordre sur des réseaux contenant plusieurs leaders ou sous contraintes inter-agents, ainsi que pour des systèmes non linéaires, par exemple des robots manipulateurs sous contraintes et avec des perturbations. Nous utilisons la théorie des graphes signés pour traiter la présence d'interactions compétitives.

Concernant les réseaux signés contenant plusieurs leaders ou soumis à des contraintes, nous étudions le problème de suivi de confinement biparti pour des systèmes de premier et de second ordres. L'originalité de ce travail repose sur le développement d'une nouvelle analyse de stabilité pour les systèmes multi-agents contenant des interactions coopératives et compétitives, plusieurs leaders et avec des perturbations. L'analyse de stabilité repose sur la théorie de Lyapunov, et nous établissons des propriétés de stabilité et de robustesse, au sens de la stabilité exponentielle et de la stabilité entrée-sortie, via la construction de fonctions de Lyapunov strictes. Nous considérons ensuite des réseaux signés soumis à des contraintes d'évitement des collisions et de maintien d'une distance maximale ou de la connectivité. Tout d'abord, nous concevons un nouveau contrôleur basé sur le gradient d'une fonction de Lyapunov barrière garantissant le respect des contraintes imposées pour les systèmes du premier et du second ordre afin de résoudre le problème de la formation bipartie. Ensuite, nous considérons des robots manipulateurs modélisés par des systèmes d'Euler-Lagrange et nous traitons le problème de la formation bipartie des effecteurs terminaux sous des contraintes inter-agents et des perturbations. Nous utilisons une approche basée sur le modèle interne pour compenser les perturbations. Nous considérons ensuite un réseau de satellites soumis à des contraintes d'évitement des collisions et de maintien de la connectivité. Dans les deux cas, nous établissons la stabilité asymptotique du système en boucle fermée.

université PARIS-SACLAY

ÉCOLE DOCTORALE
Sciences et technologies de l'information et de la communication (STIC)

Title: Control of constrained multi-agent systems with cooperative and antagonistic interactions

Keywords: Autonomous vehicles, automatic control, robotics, coordination

Abstract: In this thesis, we address several problems of control of multi-agent systems with competitive interactions, under inter-agent constraints, and for the presence of multiple leaders. Some of our contributions address problems of bipartite consensus for linear systems, *e.g.,* first- and second-order systems over networks containing multiple leaders or under inter-agent constraints, and for non-linear systems, *e.g.,* robot manipulators under constraints and with disturbance. We use the signed graph theory to address the presence of competitive interactions.

Concerning the signed networks containing multiple leaders or under constraints, we study the bipartite containment tracking problem for first- and second-order systems, and the originality of this work relies on developing a new stability analysis for multi-agent systems containing cooperative and competitive interactions, multiple leaders and with disturbances.

The stability analysis relies on Lyapunov theory, and we establish strong stability and robustness properties, in the sense of exponential stability and input-to-state stability, via the construction of strict Lyapunov functions. Then, we consider signed networks under collision avoidance and connectivity maintenance constraints. First, we design a new controller based on the gradient of a barrier-Lyapunov function encoding the imposed constraints for first- and second-order systems to address the bipartite formation problem. Then, we consider robot manipulators modeled by Euler-Lagrange systems and address the bipartite formation problem of end-effectors under inter-agent constraints and disturbances. We use an internal-model-based approach to compensate for the disturbance. Then, we consider a network of satellites under collision-avoidance and connectivity-maintenance constraints. In both cases, we establish asymptotic stability of the bipartite formation manifold.

ACKNOWLEDGEMENTS

I would like to express my gratitude to all the people who helped me during my PhD journey.

First, I would like to thank my jury for accepting to be on my defense committee. Thank you, Prof. Claudio Altafini, Prof. Ming Cao, Prof. Cristina Stoica, and Prof. Maria Elena Valcher, for your constructive reviews and insightful suggestions, which greatly helped me improve both my presentation and manuscript. I deeply appreciate the time and effort you dedicated to being part of my jury and for your interesting questions. It was a great honor and privilege to have you all on my committee, especially as I began my PhD journey by reading your work and concluded it with a meaningful discussion with you about my own research.

I owe immense gratitude to my supervisor team for believing in me from the very beginning and for always being there when I needed guidance. Thank you, Julien, for your support and valuable feedback, especially in the robotics aspects of my thesis. I would like to extend special thanks to Antonio for his high standards and for consistently pushing me to perform at my best. Thank you for always making time for me, whether I needed to finalize a paper or prepare for an important presentation. I will, of course, miss your humorous emails that brightened my days. I also want to express a special thanks to Ioannis for constantly motivating me to work harder, inspiring me with new ideas, and reminding me that my work was good enough, even when I doubted myself. Thank you for ensuring that I maximized my PhD experience by exploring opportunities, such as conferences around the world and mobility.

A special thanks to Elena Panteley for our collaboration during my PhD and for being an invited jury member on my defense committee. Thank you for your keen interest in my results, for your valuable assistance in improving my work, and for always spotting my mathematical errors. Most of all, thank you for your invaluable advice as a woman in the control community, which I will carry forward in my career.

On the other hand, I would like to express my gratitude to all PhD students, postdocs, and researchers from L2S. Beyond the academic environment, I sincerely appreciate the warm and welcoming atmosphere you created during my time in the laboratory. A special thank you for the encouragement and support you provided throughout my journey, which made my time at L2S not only productive but also incredibly enjoyable.

I would also like to thank Prof. Bayu Jayawardhana for hosting me at the University of Groningen in the Netherlands for two and a half months and for the collaboration that

followed. It was an incredible experience that allowed me to engage with numerous international researchers from the control community. A big thank you to Linda, Vaibhav, Luis, Mireny, Arijit, Santiago, Kathinka, Matthijs, Bahadir, Yiling, Sepide, Ridho, Azin, Bangguo, Brenda, Emmanuel, Zaki, Yulyan, Jin, Lihua, Saeed, and all the other wonderful people I met there for your warm welcome and support.

J'aimerais remercier chaleureusement tous les doctorants de l'ONERA. Sans vous tous, ces trois années n'auraient pas été aussi agréables. Tout d'abord, un immense merci aux doctorants de ma promotion. Peps, merci pour les cafés que tu nous as préparés, ton humour que j'apprécie beaucoup, et nos discussions sur les livres. Joules, merci pour les jus de fruits, les madeleines, les compotes, ainsi que pour tes précieux conseils en escalade. Renato, merci d'avoir toujours été mon fidèle compagnon dans toutes les démarches administratives et celles de la CSE. Shon, merci d'avoir partagé avec moi ta dernière année de thèse dans le même bureau, ありがとうございます。Antoine, je suis ravie de notre belle rencontre à Singapour, et fais un bisou à Elina de ma part. Romaigne, tu nous as quittés un peu tôt, mais je sais que Paris et nous te manquons beaucoup, adieu. Thomas, merci pour ton sourire constant et tes blagues qui rendent chaque journée plus agréable. Ensuite, j'aimerais remercier Lulu, Lucas 2, Amina et Juan: merci de rendre le 3ème étage si génial, je vous adore <3. Enfin, j'aimerais remercier tous les doctorants, docteurs, et ingénieurs: Esteban, Mathieu, Clara, Hanae, Clément, Matthieu, Eliot, Thibaud, Bastien, Enzo, Wilfried, Anne-So, et Thomas (Chevet). Merci pour les pauses café, thé, les jeux de société, les soirées, et les karaokés. Merci aussi à tous les autres doctorants, stagiaires, ingénieurs et chercheurs avec qui j'ai pu intéragir pendant ma présence à l'ONERA.

Enfin et surtout, j'aimerais remercier tous mes amis et ma famille qui m'ont soutenu pendant mes trois ans de thèse. Merci d'être toujours là pour moi quand j'en avais besoin et de m'avoir aidé avec toutes les préparations. Je tiens à remercier tout particulièrement Ananda pour son soutien inconditionnel tout au long de mes études supérieures, pour m'avoir encouragé à entreprendre une thèse, pour m'avoir accompagné à des conférences à l'autre bout du monde, et maintenant pour placer ma carrière en priorité en acceptant de me suivre dans une nouvelle aventure en Suède.

Ve en önemlisi, aileme çok teşekkür etmek istiyorum. Anne, baba ve Doruk, her zaman bana güvendiğiniz ve destek olduğunuz için çok teşekkürler, iyi ki varsınız. Özellikle de bana her zaman inanan, bu olanakları sağlayan ve beni destekleyen babama yürekten teşekkür ediyorum.

PREAMBLE

Coordination control of multi-agent systems consists in making several systems coordinate their motion according to their mission objective and the constraints imposed between agents or in the environment. It is used in many engineering applications. For instance, it is used in Robotics to deploy several autonomous vehicles in an unknown and uncertain environment, when the objective is to guide the vehicles to a safe zone while avoiding collisions between agents and obstacles. This problem may also be related to problems addressed in opinion dynamics, in which the agents' behavior is studied in a social network, e.g., in a scenario involving consumers that are influenced by their neighbors and external influential entities, such as two competing marketers. In these scenarios, unlike the consensus problems widely studied in the literature, the system may have multiple leaders that are either cooperative or competitive, and there are distrust/dislike interactions between some agents.

Motivated by the above, the aim of this thesis is to design distributed control laws for multi-agent robotic systems required to execute coordination tasks under the assumption that these systems communicate over a network that comprises both collaborative and antagonistic agents. More precisely, the objective is to control a swarm of autonomous vehicles to gather and advance in formation or to be contained in a safe zone in realistic, constrained environments. To that end, in the analysis of the control problems and the design of the control laws, the following challenges are addressed:

- *Control in presence of* ***cooperative*** *and* ***competitive*** *interactions among agents.*
- *Control in presence of* ***multiple leaders*** *in the network.*
- *Control under* ***inter-agent constraints****.*
- ***Disturbance rejection****.*

ORGANIZATION OF THE THESIS

The dissertation is organized into five chapters addressing the problems posed above. The first chapter is a brief summary of the state of the art prior to this thesis. The content of the remaining chapters is explained below.

- Chapter 2: In this chapter we recall elements of graph theory used to model the dynamics of multi-agent systems. Then, by revisiting the classical consensus algorithm for

cooperative networks, we introduce the basic control law to address networks having competitive interactions to achieve *bipartite consensus*. We also introduce important properties of signed networks through simple examples. At the end of the chapter, we introduce an alternative representation of the networks, called the *edge-based formulation*.

- Chapter 3: In this chapter we address the bipartite containment tracking-control problem over structurally balanced and unbalanced signed networks with multiple cooperative and competitive leaders for first-order and second-order systems. We present a Lyapunov approach to analyze the exponential stability of the bipartite containment tracking set by expressing the system in terms of two interconnected dynamical systems evolving in orthogonal spaces: dynamics of the leaders and synchronization errors relative to the group of leaders. Thus, the bipartite containment problem is transformed into one of stability of a set of appropriately defined errors. Then, we establish a bound for the convergence set of the followers, as well as the limiting set points for all the agents. Moreover, we provide strict Lyapunov functions. Disposing of strict Lyapunov functions allows us to establish the system's robustness with a bounded disturbance.
  These results were originally presented in [1, 4].

- Chapter 4: In this chapter we present a BLF-based distributed control law to solve the bipartite formation-consensus control problem for simple and double integrators over structurally balanced, connected undirected, and structurally balanced, strongly connected directed signed networks. The proposed control laws ensure that connectivity is maintained for all cooperative agents and that both cooperative and competitive agents do not collide. We analyze the asymptotic stability of the system using Lyapunov's direct method.
  These results were originally presented in [2, 5].

- Chapter 5: In this chapter we address the problem of constrained bipartite formation of cooperative-competitive Euler-Lagrange systems. We first study robot manipulators and then flying spacecraft, both modeled by Euler-Lagrange equations, and we consider structurally balanced and undirected signed graphs. First, we present a bipartite formation control law based on the gradient of a barrier-Lyapunov function that guarantees that robot manipulators' end-effectors do not collide and stay within the maximum distance imposed by the task requirements. Then, in order to deal with perturbed robot manipulators, we robustify our controller with an internal model-based approach to reject disturbances. We establish asymptotic stability of the bipartite formation manifold in the absence and the presence of disturbance. Next, we consider networked satellites interconnected over a signed graph and under collision avoidance and connectivity maintenance constraints. We establish asymptotic stability of the bipartite formation manifold.
  These results were originally presented in [3, 6].

Publications

The following is a list of the publications written during the past three years that are either accepted for publication or published.

Journal articles

[1] P. Sekercioglu, E. Panteley, I. Sarras, A. Loría and J. Marzat "Distributed Bipartite Containment Tracking over Signed Networks with Multiple Leaders," *IEEE Transactions on Control of Network Systems*(2024) (Early Access).

[2] P. Sekercioglu, I. Sarras, A. Loría, E. Panteley and J. Marzat, "Leader-follower and Leaderless Bipartite Formation-consensus over Undirected Coopetition Networks and under Proximity and Collision-avoidance Constraints," *International Journal of Control*(2024), pp. 1–15.

[3] P. Sekercioglu, B. Jayawardhana, I. Sarras, A. Loría and J. Marzat "Robust Formation Control of Robot Manipulators with Inter-agent Constraints over Undirected Signed Networks," *IEEE Transactions on Control of Network Systems*(2024) (Early Access).

Conference proceedings

[4] P. Sekercioglu, E. Panteley, I. Sarras, A. Loría and J. Marzat, "Exponential Bipartite Containment Tracking over Multi-leader Coopetition Networks," in *Proc. American Control Conference,* 2023. pp. 509–514.

[5] P. Sekercioglu, I. Sarras, A. Loría, E. Panteley and J. Marzat, "Bipartite Formation over Undirected Signed Networks with Collision Avoidance," in *Proc. IEEE Conference on Decision and Control,* 2023, pp. 1438–1443.

[6] P. Sekercioglu, B. Jayawardhana, I. Sarras, A. Loría, J. Marzat "Formation Control of Cooperative-Competitive Robot Manipulators with Inter-agent Constraints," *IFAC-PapersOnLine*, 2024, vol. 58, no. 21, pp. 49–54.

RÉSUMÉ ÉTENDU EN FRANÇAIS

La commande de systèmes multi-agents permet de coordonner le mouvement de plusieurs systèmes en fonction de l'objectif de la mission qui leur est donné et des contraintes imposées entre les agents et/ou par l'environnement. La coordination de systèmes multi-agents est utilisée dans de nombreuses applications techniques, telles que la robotique, pour déployer plusieurs véhicules autonomes dans un environnement inconnu et incertain, où l'objectif est de guider les véhicules vers une zone sûre tout en évitant les collisions entre les agents et avec les obstacles. Ce problème peut également être lié aux problèmes abordés dans la dynamique des opinions, où le comportement de chaque agent est étudié dans un réseau social. Par exemple, dans le cas où des consommateurs sont influencés par leurs voisins ou par des entités influentes et extérieures, comme deux spécialistes du marketing concurrents. Dans ces scénarios, contrairement aux problèmes de consensus étudiés dans la littérature, le système peut avoir plusieurs leaders qui sont soit coopératifs, soit compétitifs, et des interactions de méfiance ou d'aversion entre certains agents.

Motivé par ces scénarios précédents, le but de cette thèse est de concevoir des lois de commande distribuées pour les systèmes robotiques multi-agents qui éxecutent des tâches de coordination en prennant en compte les interactions coopératives et compétitives entre les agents. Plus particulièrement, l'objectif est de contrôler un essaim de véhicules autonomes pour qu'ils se rassemblent et avancent en formation ou pour qu'ils soient contenus dans une zone sécurisée dans des environnements réalistes et contraints. À cette fin, dans l'analyse des problèmes de commande et la conception des lois de commande, les aspects suivants sont abordés :

- *Interactions **coopératives** et **compétitives** entre les agents:* La nature des interactions de deux agents détermine si ces systèmes interconnectés ont les mêmes objectifs ou non. Les interactions coopératives sont utilisées pour les agents censés collaborer à l'exécution de la tâche. Les interactions compétitives sont utilisées pour représenter la présence de groupes d'agents ennemis, de zones dangereuses et d'obstacles dans le système.
- *Présence de **multiple leaders** dans le réseau:* Les leaders sont utilisés afin de définir les zones dangereuses à éviter et les zones de sécurité vers lesquelles les agents doivent converger. Les leaders qui sont coopératifs avec les agents définissent la zone de sécurtié vers laquelle les suiveurs doivent converger, tandis que les leaders compétitifs représentent les obstacles et les zones dangereuses à éviter.

- ***Contraintes inter-agents:*** Dans cette thèse, nous utilisons les distances relatives pour garantir la sécurité et le succès de la mission du système multi-agents. Cela signifie que, pour que la mission réussisse, les agents doivent toujours rester à portée de leurs capteurs afin que l'échange d'informations se poursuive et que la connectivité soit maintenue. De plus, pour assurer la sécurité du système, les agents doivent également éviter les collisions avec les obstacles, les agents ennemis présents dans l'environnement, ainsi qu'avec les autres agents de leur équipe.

- ***Perturbations:*** Dans les environnements réalistes des systèmes robotiques, il existe, par exemple, des perturbations aérodynamiques, qui sont généralement inconnues et variables, et qui peuvent avoir un impact important sur les performances des véhicules.

Cette thèse se concentre sur les aspects présentés ci-dessus et nous les adressons en reformulant les problèmes de commande comme des problèmes de stabilisation. A cette fin, nous utilisons la théorie de Lyapunov et étendons certains travaux récents sur celle-ci pour les systèmes multi-agents.

L'ORGANISATION DE CETTE THÈSE

Ce mémoire est organisé en cinq chapitres traitant les problèmes posés ci-dessus. Le premier chapitre est un bref résumé de l'état de l'art avant cette thèse. Le contenu des autres chapitres est expliqué ci-dessous.

- Chapitre 2 : Dans ce chapitre, nous rappelons les éléments de la théorie des graphes utilisés pour modéliser la dynamique des systèmes multi-agents. Ensuite, en reconsidérant l'algorithme de consensus classique pour les réseaux coopératifs, nous introduisons la loi de commande basique pour traiter les réseaux ayant des interactions coopératives et compétitives afin que les agents atteignent *consensus biparti*. Nous introduisons également des propriétés importantes des réseaux signés à travers des exemples simples. À la fin du chapitre, nous rappelons une autre façon de représenter les réseaux, appelée *formulation basée sur les arêtes*.

- Chapitre 3 : Dans ce chapitre, nous abordons le problème de suivi de confinement biparti sur des réseaux signés structurellement équilibrés et déséquilibrés (structurally balanced et unbalanced, en anglais) qui contiennent multiples leaders coopératifs et compétitifs pour des systèmes du premier ordre et du second ordre. Nous présentons une approche de Lyapunov pour analyser la stabilité exponentielle de l'ensemble de suivi du confinement biparti en exprimant le système en termes de deux systèmes dynamiques interconnectés évoluant dans des espaces orthogonaux : la dynamique des leaders et les erreurs de synchronisation relatives aux groupes de leaders. Ainsi, le problème du confinement biparti est transformé en un problème de stabilité d'un ensemble d'erreurs. Ensuite, nous présentons une borne de convergence pour l'ensemble des suiveurs ainsi que les valeurs limites finales pour tous les agents. En outre, nous généralisons la caractérisation de l'équation de Lyapunov de la propriété de Hurwitz d'une matrice aux matrices ayant plusieurs valeurs propres nulles, ce qui nous permet de construire des fonctions de Lyapunov strictes. Disposer de fonctions de Lyapunov strictes nous permet d'établir la robustesse du système avec une perturbation bornée en termes de stabilité entrée-état.
  Ces résultats ont été initialement présentés dans les publications [1, 4].

- Chapitre 4 : Dans ce chapitre, nous présentons des lois de commande distribuées basées sur les fonctions barrières de Lyapunov pour résoudre le problème de la formation bipartie pour les simples et doubles intégrateurs sur des réseaux signés structurellement équilibrés, connectés et non dirigés, ainsi que pour les réseaux structurellement équilibrés et fortement connectés. Les lois de commande proposées garantissent l'évitement des collisions entre chaque couple d'agents interconnectés ainsi que le maintien de la connectivité pour les agents coopératifs. Nous analysons la stabilité asymptotique du système à l'aide de la méthode directe de Lyapunov.
  Ces résultats ont été initialement présentés dans les publications [2, 5].
- Chapitre 5 : Dans ce chapitre, nous abordons le problème de la formation bipartie des systèmes Euler-Lagrange coopératifs-compétitifs sous contraintes. Nous étudions d'abord les robot manipulateurs et ensuite les vaisseaux spatiaux volants, modélisés par des équations d'Euler-Lagrange, et nous considérons des graphes signés structurellement équilibrés et non dirigés. Tout d'abord, nous présentons une loi de commande de la formation bipartie basée sur le gradient d'une fonction de Lyapunov barrière qui garantit que les effecteurs terminaux n'entrent pas en collision et restent dans leurs régions de portée. Ensuite, afin de considérer les robot manipulateurs perturbés, nous robustifions notre contrôleur avec une approche basée sur un modèle interne pour rejeter les perturbations. Nous établissons la stabilité asymptotique de l'ensemble de formation bipartie à la fois en l'absence et en présence de perturbations. Puis, nous considérons un groupe de satellites interconnectés sur un graphe signé et soumis à des contraintes d'évitement de collision et de connectivité. Nous établissons la stabilité asymptotique de l'ensemble de formation bipartie.
  Ces résultats ont été initialement présentés dans les publications [3, 6].

Contents

List of Figures

Notations

$\mathbb{R}$	Set of real numbers
$\mathbb{R}_{\geq 0}$	Set of nonnegative real numbers
$\mathbb{R}^n$	Vector space of real vectors of dimension n
$\mathbb{R}^{n\times m}$	Set of real matrices of size $n \times m$
$\lvert \cdot \rvert$	Euclidean norm for vectors, absolute value for scalars, and induced norm for matrices
$\mathrm{diag}(v)$	Diagonal matrix whose non-zero elements correspond to the elements of the vector v
$\mathrm{blkdiag}(A_i)$	Block diagonal matrix formed by the matrices A_i
$\mathbf{1}_n$	Vector of all ones of size $n \times 1$
I_n	Identity matrix of size $n \times n$
$\lambda_i(A)$	ith eigenvalue of matrix A
$A^\top$	Transpose of matrix A
A^{-1}	Inverse of matrix A
$\mathcal{G}$	Graph
$\mathcal{V}$	Vertex set
$\mathcal{E}$	Edge set
$L(\mathcal{G})$	Laplacian matrix of an unsigned graph $\mathcal{G}$; also denoted as L
$L_s(\mathcal{G})$	Laplacian matrix of a signed graph $\mathcal{G}$; also denoted as L_s
$L_e(\mathcal{G})$	Edge Laplacian matrix of an unsigned graph $\mathcal{G}$; also denoted as L_e
$L_{e_s}(\mathcal{G})$	Edge Laplacian matrix of a signed graph $\mathcal{G}$; also denoted as L_{e_s}
E	Incidence matrix of an unsigned graph
E_s	Incidence matrix of a signed graph
$E_\odot$	In-incidence matrix of an unsigned graph
$E_{s\odot}$	In-incidence matrix of a signed graph

CHAPTER 1

CONTEXT

1.1 MOTIVATION

The objective of this thesis is to design distributed controllers for multi-agent robotic systems required to execute complex tasks. This thesis addresses the general problem of guiding a swarm of autonomous vehicles required to gather and advance in formation or to be contained in a safe zone in realistic, constrained environments—see Figure 1.1 for an illustration. Such problems are also relevant in applications, such as collaborative human-robot interactions, where teams of robot manipulators or mobile robots equipped with manipulators are controlled to perform tasks in constrained workspaces with safety guarantees—see Figure 1.2.

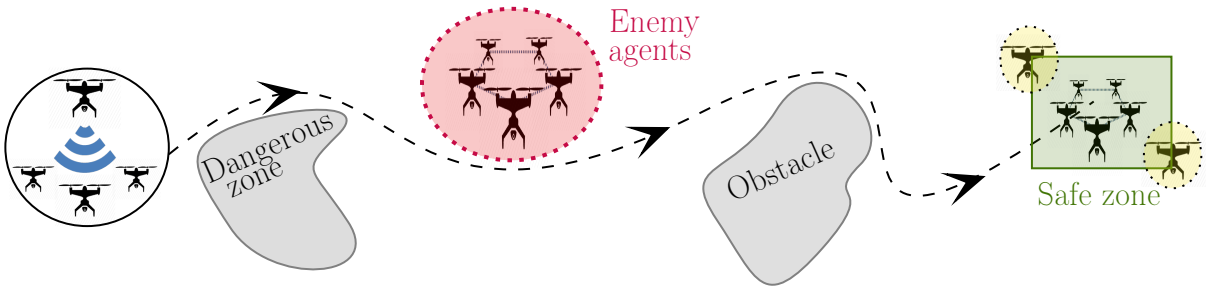

Figure 1.1: Guiding a group of drones in formation to a safe zone while avoiding collisions with obstacles, dangerous zones, and other agents.

More precisely, we consider problems of containment and formation for multi-agent systems in the presence of:

- ***Cooperative*** *and* ***competitive*** *interactions among the agents:* The nature of the interconnections between two agents defines whether these interconnected systems have the same objectives or not. Cooperative interactions are used for

agents expected to collaborate in executing the task. Then, competitive interactions represent the presence of enemy agent groups, dangerous zones, and obstacles in the system.

- ***Multiple leaders*** *in the network:* Multiple leaders can be used to define dangerous zones to avoid and identify the safe zone to which agents should converge. Leaders that are cooperative towards which followers must converge are illustrated in Figure 1.1 determining a safe zone, whereas competitive leaders with agents represent the obstacles and dangerous zones to avoid.

- ***Inter-agent constraints****:* In this thesis, we use relative distances to guarantee the safety and mission success of the multi-agent system, which means that for the mission to succeed, the agents should always stay in their sensors' range so that the information exchange continues and the connectivity is maintained. Moreover, for the systems' safety, agents should also avoid collisions with the obstacles or enemy agents present in the environment as well as with other agents of their team.

- ***Disturbances****:* In realistic settings of robotics systems, there are, *e.g.,* aerodynamic disturbances, which are generally unknown and varying, significantly impacting the performance of the vehicles.

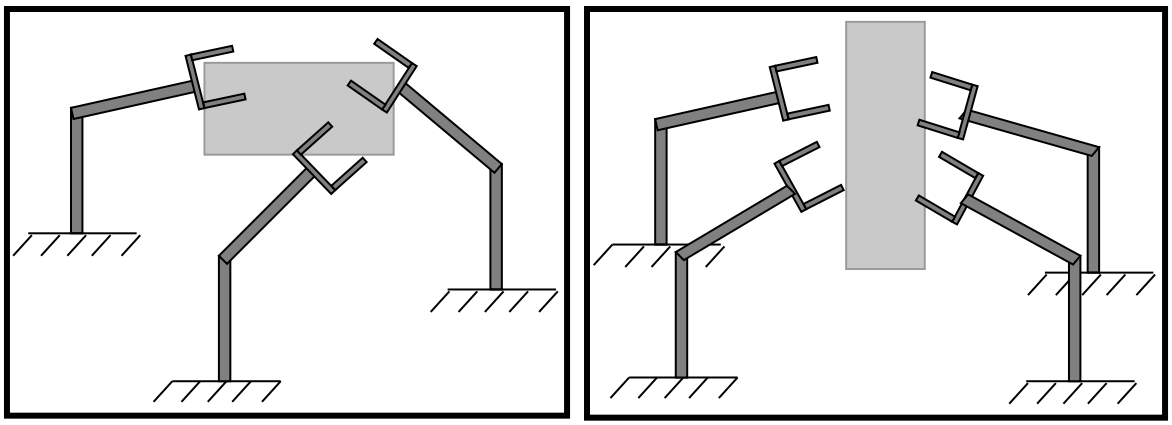

Figure 1.2: A team of robot manipulators performing tasks in a constrained workspace with guaranteed safety: (a) collaboration of manipulators to move a product, (b) two groups of manipulators working on opposite sides of a product.

To address the aspects above, we recast the pertinent control problems as stabilization ones. In turn, to that end, we use Lyapunov theory and extend some recent work on Lyapunov theory for multi-agent systems. Such methods are briefly put in perspective below.

1.2 PRESENCE OF COOPERATIVE AND COMPETITIVE INTERACTIONS

The literature on consensus and synchronization of multi-agent systems is abundant. Still, it is largely focused on networks containing only cooperative interactions [100],

such as consensus for first-order [62], second-order [74] and linear high-order dynamics [100]. In these cases, all the agents may reach a global agreement regarding a certain quantity of interest through collaboration [75]. However, this excludes several scenarios where some agents cooperate, while others compete as, *e.g.*, in the context of herding control [15, 26, 80], in social networks [2, 72], or in aerospace applications [48, 113]. The cooperative *vs* competitive nature of the links, which is at the center of attention here, may be analyzed using the formalism of *signed networks* [2], also known as *coopetition networks* [30], in which the edges may have positive or negative weights. Some of such networks are called *structurally balanced*[1]. For the latter, agreement on a common value is generally not attainable. However, an achievable goal is *bipartite consensus* [95], [2], in which all the agents converge to the same state in modulus but opposite in signs. There are multiple studies on the bipartite consensus-control problem for single-integrators [2, 52], double-integrators [104], and linear high-order dynamics [95].

In this thesis, we focus on consensus-like problems, but in which the interconnections between agents are represented both by positive and negative weights on the edges. We use the tools introduced in [2, 52], but as we will see, in contrast to [95, 2], even bipartite consensus may be out of reach, notably due to the presence of multiple leaders. In this case, we give conditions to achieve bipartite *containment*.

1.3 PRESENCE OF MULTIPLE LEADERS IN THE NETWORK

In the coordination of multi-agent networks containing a single leader (defined as either a single root agent or a strongly connected subgraph containing multiple nodes but without any incoming edges), all the followers adopt the leader's trajectory or converge to the leader's state [58]. However, this so-called leader-follower consensus does not occur if the network contains more than one leader. In this case, multiple consensus equilibria may appear [55], and it is more appropriate to speak of *containment* control [7]—see Figure 1.3 below. This problem consists of ensuring all followers converge to a containment set determined by the leaders' initial conditions and is solvable if, for each follower, there exists at least one leader from which emanates a directed path to that follower. There are multiple studies on distributed containment control, e.g., for social networks [36] or for networks of single-integrators [8, 35], double-integrators [9, 44], and general linear autonomous systems [41]. However, most of the current research on the consensus or containment problems for multi-agent systems is on cooperative networks, *i.e.*, the coordination of nodes is achieved only by cooperative interactions.

To analyze directed signed networks containing multiple leaders, in [49], the notion of containment control is extended to *bipartite containment tracking-control*. The latter consists in having all the followers' states converge to containment sets determined by the leaders' states and their symmetric states, and more than two consensus equilibria appear because of the presence of multiple leaders. Succeeding [49], bipartite containment has also been studied in [110, 53] and [98]. On the other hand, in [50, 30], the interval bipartite problem is studied for directed signed networks, where multiple

[1] A signed network is structurally balanced if all the nodes may be split into two disjoint subsets, where agents cooperative with each other are in the same subset and agents competitive with each other are in different ones— see Definition 1 in Section 2.3.

equilibria appear, which is similar to the bipartite containment problem. The difference is that in [50, 30], multiple equilibria appear because of only one leader and the structural unbalance property.

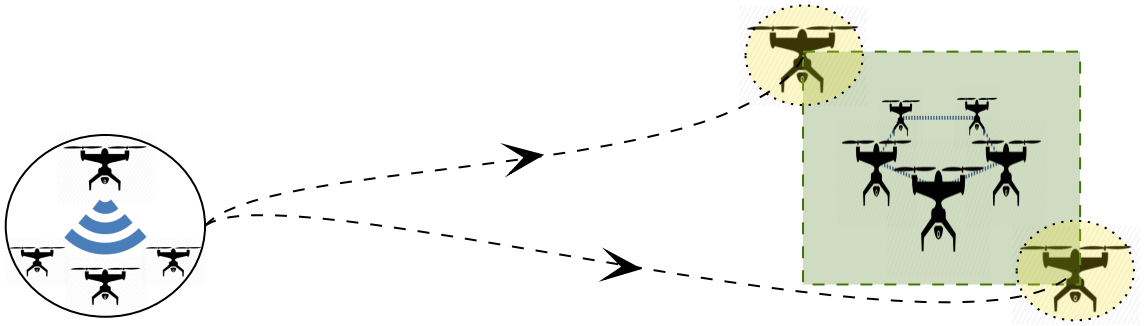

Figure 1.3: Containment of a group of robots inside a safe zone defined by the leaders' states.

In the context of this thesis, we are interested in signed networks containing multiple leaders. In this setting, a competitive leader may define, *e.g.*, a group of enemy agents or an obstacle to avoid, whereas a cooperative leader defines the safe final destination to attain; that is, a leader is not bound to being a single agent. In the case of a directed signed graph containing a root agent, defining a *leader*, all agents achieve leader-follower bipartite consensus. This means that all the agents that cooperate with the leader node converge to the leader's state, and the competitive agents converge to the leader's symmetric state. In that regard, bipartite containment [49] over multileader signed networks is similar to the leader-follower bipartite consensus problem. But, in the context of the containment problem, the equilibrium points are defined by the leaders' states and their symmetric states, called containment sets.

In the case where multiple (cooperative and/or antagonistic) leaders appear, a significant difficulty that appears in the analysis is that of the properties of the Laplacian matrix and the construction of the eigenvectors associated with its zero eigenvalues [51]. This is because the Laplacian matrix has multiple zero eigenvalues (as many as the number of the leader groups in the network) and multiple right and left eigenvectors associated with each zero eigenvalues. Moreover, since the graph is signed, the elements of the eigenvectors are also signed, depending on the interaction topology. The eigenvectors are useful for calculating where the agents' states converge. For instance, in [49] and [98], limit points for the followers' states are given explicitly.

In this thesis, in contrast to [110, 53, 98], where bipartite containment is studied only over structurally balanced networks, we address the problem regardless of whether the graph is structurally balanced or unbalanced. Furthermore, in [110], only cooperative leaders are considered, and in [98], interconnections between the followers are assumed to be only undirected. We consider both cooperative and competitive leaders, with followers interconnected over a directed signed graph. As in [49] and [98], we calculate the explicit limit values of the followers, but regardless of the structural balance property, and for second-order systems.

For the purpose of analysis, we recast the problem into one of stability of the set of containment errors, and our analysis relies on Lyapunov theory. More precisely, it is based on the framework introduced in [67], and we extend the results from [68] to

the case of containment. The contributions and innovations of our work on bipartite containment with respect to the literature are:

(i) the construction of the right and left eigenvectors for both structurally balanced and unbalanced signed networks containing multiple cooperative and competitive leaders;

(ii) the extension of the definition of the average system (defining the explicit limit values of the followers) and the synchronization errors for general multi-leader signed networks;

(iii) the extension of the well-known Lyapunov equation to the case of matrices having multiple zero eigenvalues (corresponding to the Laplacian matrix of a multi-leader signed network);

(iv) the construction of strict Lyapunov functions for multi-leader signed networks (exponential stability and input-to-state stability).

1.4 COLLISION AVOIDANCE AND CONNECTIVITY MAINTENANCE FOR SIGNED NETWORKS

In many instances where multi-agent vehicles are used, besides attaining the goal destination, the safe zone, or following a reference trajectory, autonomous vehicles must also satisfy other objectives, such as guaranteeing collision avoidance between two agents or maintaining information exchange between the ones cooperating with each other. Those objectives are encoded as inter-agent constraints, and various approaches based on artificial potential functions are exploited in the literature to enforce them—see *e.g.*, [22, 12, 97, 85, 77, 105] and [66]. The latter uses Lyapunov-like barrier functions to encode collision avoidance and connectivity maintenance control goals and assures the convergence to desired destinations for a network of multiple nonholonomic vehicles. Alternative methods that address the constrained consensus-control problem include those that use repulsive vector fields [4], employ a nonlinear learning error function [106], or apply various optimization-based approaches such as Voronoi diagrams [14, 32, 13, 93] and control barrier functions [3, 87]. However, only a few works in the literature focus on constrained control problems for networks containing both cooperative and competitive interactions.

In [15] the multi-swarm herding problem is solved under connectivity constraints using a mixed integer quadratically constrained program; in [26] a control strategy is proposed for the non-cooperative herding problem described by first-order dynamics and control barrier functions are used to prevent some agents from escaping from a protected zone. Yet, in [15] and [26] the system is modeled by a network in which all the agents cooperate and the control laws are optimization-based. Moreover, in [26] only a two-agent scenario is considered. In [24] the bipartite flocking-control problem is studied, and artificial potential functions are used to guarantee collision avoidance and connectivity maintenance. The statements rely on LaSalle's invariance principle [39]. Collisions are avoided in [24], but a minimal safety distance between agents is not guaranteed. Thus, only a few works in the literature focus on inter-agent constrained control problems for coopetition networks.

One of the goals of this thesis is to address constrained control problems in the presence of cooperative and competitive interactions. For this purpose, we encode the constraints using barrier-Lyapunov functions (BLF). Then, the distributed control laws are designed in terms of the gradient of the BLFs and consequently grow unboundedly as the agents' state approaches the boundaries of the set where the constraints hold. The contributions of this thesis on control of constrained multi-agent systems rely on providing, for the first time in the literature, barrier-Lyapunov-function-gradient-based controllers guaranteeing collision avoidance and connectivity maintenance for agents interconnected over both cooperative and competitive edges for first- and second-order systems over undirected and strongly connected directed signed graphs.

Compared to [100, 75, 22, 12, 66, 105, 4, 106, 77], which focus on traditional cooperative networks, our results apply to a more general and complex scenario where agents have both cooperative and competitive interactions. Compared to [2, 30, 104, 95], in which bipartite consensus-control problem of signed networks is studied, we address the problem under collision avoidance and connectivity maintenance constraints. The innovations of our work with respect to related literature reside in the construction of barrier-Lyapunov functions encoding collision avoidance and connectivity maintenance constraints for agents interconnected over both cooperative and competitive edges and the design of a bipartite consensus control law satisfying the control objective while ensuring inter-agent constraints are respected.

1.5 CONTROL OF COOPERATIVE AND COMPETITIVE EULER-LAGRANGE SYSTEMS

The challenge of considering constraints and collision avoidance is most naturally associated with applications involving mobile robots. However, the aspects previously described are also pertinent in the context of control of cooperative and competitive manipulators. In all of the previous references, generic first, second, or higher-order linear models are used. These are less suitable for robot manipulators, which are most commonly modeled by the Euler-Lagrange equations. In that regard, the literature on control of multi-agent Euler-Lagrange systems is also rich, but most often, only cooperative networks are considered. For instance, in [112, 90], the tracking-consensus problem for mobile robots with nonholonomic constraints is addressed, in [16] the formation control of flying spacecraft, in [17] the synchronization of multi-Lagrangian systems, and in [78, 59, 73, 61] the synchronization of multiple robot manipulators. In all of these references, the synchronization problem is studied in joint coordinates. Formation of manipulators in end-effector coordinates is considered in [79, 103, 102]. Nonetheless, in all of the previously cited references, only networks of cooperative agents are considered. For signed networks, the bipartite consensus of networked robot manipulators is addressed, *e.g.*, in [45, 29, 111, 20, 115], while the leader-follower bipartite consensus is studied in [31, 46, 42, 40] (in the latter parametric uncertainty is also considered). In end-effectors coordinates, the bipartite formation-control problem is considered in [65].

In the last part of the thesis, we consider the distributed bipartite formation-control problem of robot manipulators' end-effectors under relative distance constraints and

in the presence of disturbances. We consider a networked system of cooperative-competitive robot manipulators modeled by the Euler-Lagrange equations and interconnected over a structurally balanced undirected signed graph. The desired formation goal is imposed on the manipulators' end effectors. Such scenarios are motivated, for example, by applications in industrial robotics' where robots share the same workspace but are assigned symmetric tasks by the team. Ideally, the robot manipulators should occupy the minimum space while evolving with guaranteed safety and increased reactivity. Compared to the literature, we contribute with a robust bipartite formation control law that ensures that the manipulator's end effectors achieve the desired formation while avoiding inter-agent collisions and staying within the maximum distance imposed by the task requirements.

Next, we consider the bipartite formation-control problem of networked satellites under collision avoidance and connectivity maintenance constraints. In the related literature, the formation-control problem of cooperative flying spacecraft has been addressed—see *e.g.,* [64, 16, 70, 1, 47]. In this memoir, we address a group of cooperative-competitive satellites modeled by the Euler-Lagrange equations, following the developments in [1], over a structurally balanced undirected signed graph. Such a scenario is motivated by a group of spacecraft working in cooperation with the objective of observing objects in space while avoiding competitive space vehicles and debris to achieve their mission. Compared to the literature, we contribute with a bipartite formation control law that ensures the satellites achieve the desired formation while avoiding inter-agent collisions and staying in their sensors' range. To the best of our knowledge, similar results are not available in the literature for robot manipulators or for satellites interconnected over networks containing competitive interactions.

1.6 DISTURBANCE REJECTION

Besides the presence of cooperative/competitive interactions, the existence of multiple leaders, and the constraints imposed on the agents, another important aspect that must be considered in the control of multi-agent robot systems is the effect of external disturbances. Considering that a disturbance may be modeled by a multi-periodic signal [102], an effective method to compensate for its effect is the internal-model-based approach, see, *e.g.*, [99, 61, 102, 33, 34] for works on consensus among cooperative robots, and [20, 31, 115] and [65] for works on coopetitive networks of robot manipulators. Yet, none of the references cited above considers the presence of constraints. One additional contribution of this thesis is the design of controllers for constrained manipulators' end-effectors in the presence of matching disturbances. For that purpose, we rely on an internal-model-based approach [33]. In the case of this thesis, while addressing constrained control problems, we reject the disturbances using an internal model-based compensator.

CHAPTER 2

CONSENSUS PROTOCOLS FOR ANTAGONISTIC MULTI-AGENT SYSTEMS

In this chapter we recall elements of graph theory that we use to model the dynamics of multi-agent systems. Then, by revisiting the classical consensus algorithm for cooperative networks, we recall the basic control law to address networks with competitive interactions for achieving *bipartite consensus*. We also recall important properties of signed networks through simple examples. At the end of the chapter, we recall an alternative representation of the networks, called the *edge-based formulation*.

2.1 GRAPH THEORY FOR COOPERATIVE SYSTEMS

Under distributed control, multi-agent systems communicate via neighbor-to-neighbor interactions and only have access to their own measurements. Therefore, a natural way to model their interaction topology is using elements of graph theory [54], [75]. To that end, we recall some basic notations and definitions of graph theory.

A *graph* describes the information exchange, defined as the interaction topology between a set of agents. A graph is denoted by $\mathcal{G} = (\mathcal{V}, \mathcal{E})$, where $\mathcal{V} := \{\nu_1, \nu_2, \ldots, \nu_N\}$ is the set of N nodes corresponding to the agents in the system and $\mathcal{E} := \{\varepsilon_1, \varepsilon_2, \ldots, \varepsilon_M\} \subseteq \mathcal{V} \times \mathcal{V}$ is a set containing M edges, corresponding to the information exchange (interconnections) between agents. If there exists an edge between a pair of agents, they are said to be *adjacent*. If the information flow between a pair of agents is bidirectional, the graph is said to be *undirected*. The edge $\varepsilon_k = \{v_i, v_j\} \in \mathcal{E}$ of an undirected graph denotes that the agents ν_i and ν_j can obtain information from each other. Thus, in an undirected graph, we have the property that $\varepsilon_k = \{v_i, v_j\} = \{v_j, v_i\}$. Otherwise, if the information flow is only in one direction, the graph is said to be *directed*, and is commonly referred to as a *digraph*. The edge $\varepsilon_k = \{v_j, v_i\} \in \mathcal{E}$ of a digraph denotes that the agent v_j, which is the terminal node (tail of the edge), can obtain information from the agent v_i, which is the initial node (head of the edge)—see Figure 2.1. It is also assumed that the graph is defined in such a way that there are

no self-loops, i.e., edges of the form $\varepsilon_k = \{v_i, v_i\}$ are not included in $\mathcal{E}$. For instance, for the undirected graph at the left of Figure 2.1 we have the following edge set: $\mathcal{E} = \{\{\nu_1, \nu_2\}, \{\nu_1, \nu_3\}, \{\nu_1, \nu_4\}, \{\nu_2, \nu_5\}, \{\nu_2, \nu_6\}, \{\nu_3, \nu_4\}, \{\nu_5, \nu_6\}\}$, and for the directed graph at the right of Figure 2.1 we have $\mathcal{E} = \{\{\nu_2, \nu_1\}, \{\nu_3, \nu_1\}, \{\nu_1, \nu_4\}, \{\nu_5, \nu_2\}, \{\nu_2, \nu_6\}, \{\nu_4, \nu_3\}, \{\nu_6, \nu_5\}\}$.

On the other hand, a *weighted graph* is denoted by $\mathcal{G} = (\mathcal{V}, \mathcal{E}, \mathcal{W})$, where $\mathcal{W} : \mathcal{E} \to \mathbb{R}$ associates a value to each edge ε_k. For weighted graphs, we define a matrix called the *adjacency* matrix that contains the weights of interconnections. The adjacency matrix is defined as $\mathcal{A}(\mathcal{G}) = [a_{ij}] \in \mathbb{R}^{N \times N}$. For an undirected graph, we have $a_{ij} = a_{ji}, \forall i \neq j$ and $a_{ij} > 0$ if $\{\nu_j, \nu_i\}, \{\nu_i, \nu_j\} \in \mathcal{E}$ and $a_{ij} = 0$ if $\{\nu_j, \nu_i\}, \{\nu_i, \nu_j\} \notin \mathcal{E}$, and $a_{ii} = 0$. For a digraph, we have $\mathcal{A}(\mathcal{G}) = [a_{ij}] \in \mathbb{R}^{N \times N}$, where $a_{ij} > 0$ if $\{\nu_j, \nu_i\} \in \mathcal{E}$ and $a_{ij} = 0$ if $\{\nu_j, \nu_i\} \notin \mathcal{E}$, and $a_{ii} = 0$.

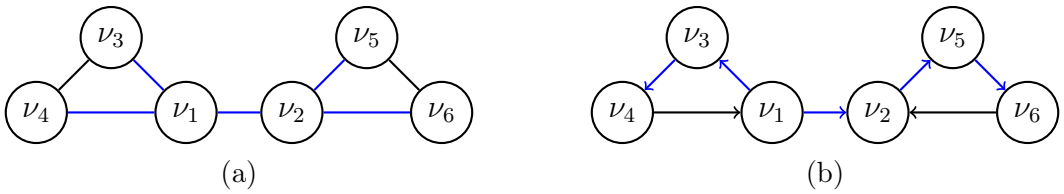

Figure 2.1: Example of two graphs: (a) an undirected graph; (b) a directed graph.

A (directed) *path* is a sequence of distinct adjacent vertices in a graph. When the vertices of the path are distinct except for its end vertices, the (directed) path is called a *(directed) cycle*. An undirected graph is said to be *connected* if there exists a path between every pair of nodes. For instance, the undirected graph on the left of Figure 2.1 is connected. A connected graph without any cycles is called a *tree*, meaning that any two vertices are connected by exactly one path. A digraph is said to be *strongly connected* if there exists a *directed path* between every pair of nodes. The directed graph in Figure 2.1b is not strongly connected, as, for instance, there is no directed path from node ν_2 to nodes ν_3 or ν_4. A (directed) *spanning tree* is a (directed) tree subgraph containing all the nodes of the graph. A (directed) spanning tree of the (directed) graph in Figure 2.1b is shown with the edges colored in blue. In a directed spanning tree, every agent has a *parent* node, except for the *root node*. A root node is a node without incoming edges and has a directed path to every other node. Notice that a directed spanning tree has no cycles, as every edge is oriented from the root node to the other nodes. For undirected graphs, containing a spanning tree equals a graph being connected, but for directed graphs, containing a directed spanning tree does not mean that the digraph is strongly connected.

2.2 THE CONSENSUS-CONTROL PROBLEM

The consensus control problem, loosely speaking, consists in making a team of agents work in a coordinated fashion and agree on a common value [75]. It may be studied using different tools, including graph theory and stability theories, both of which are

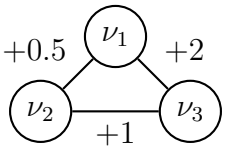

Figure 2.2: Example of three vehicles interconnected over an undirected graph.

extensively used in this memoir. For illustration, let us consider a robotic system containing three autonomous vehicles, as illustrated in Figure 2.2. They are interconnected over an unsigned, undirected, and connected graph with the objective of meeting at a rendezvous point before beginning their task. Since they all cooperate, they are interconnected over an unsigned graph, and their interactions are represented by the positive weights associated with each edge. Each vehicle only communicates with its neighbors, and if we assume that each node's dynamics corresponds to a simple integrator in closed loop with a diffusive control law, the multi-agent system dynamics are described by

$$\dot{x}_1 = -0.5(x_1 - x_2) - 2(x_1 - x_3) \tag{2.1a}$$
$$\dot{x}_2 = -0.5(x_2 - x_1) - 1(x_2 - x_3) \tag{2.1b}$$
$$\dot{x}_3 = -2(x_3 - x_1) - 1(x_3 - x_2), \tag{2.1c}$$

where $x_i \in \mathbb{R}$ is the state of each agent, *e.g.,* the position of each vehicle, and the factors 0.5, 1 and 2 correspond to the values of the adjancency weights a_{12}, a_{23} and a_{13} of the interconnections.

Remark 1 *In this chapter, and throughout the whole dissertation, for notational simplicity and without loss of generality, we assume that $x_i \in \mathbb{R}$, but all contents of this thesis apply to systems of higher dimension $x_i \in \mathbb{R}^n$, $n > 1$, using a Kronecker product* [27]. •

Then, to study the behavior of the solutions of (2.1), we start by rewriting these equations in the compact form

$$\dot{x} = -\begin{bmatrix} (2+0.5) & -0.5 & -2 \\ -0.5 & (0.5+1) & -1 \\ -2 & -1 & (2+1) \end{bmatrix} x, \tag{2.2}$$

where $x = [x_1\ x_2\ x_3]^\top$ is the vector containing the states x_i of all agents and the matrix in (2.2) is called the Laplacian matrix, which in the N-agents' case reads $L := [\ell_{ij}] \in \mathbb{R}^{N\times N}$. It describes the topology corresponding to the graph in Figure 2.2 and, in general, is defined as

$$\ell_{ij} = \begin{cases} \sum\limits_{k\in\mathcal{I}_\mathcal{N}} a_{ik} & i = j \\ -a_{ij} & i \neq j. \end{cases} \qquad i, j \leq N \tag{2.3}$$

Since the agents are interconnected over a connected undirected graph, the Laplacian matrix L is symmetric and positive semidefinite. Moreover, the sum of each row of

L is equal to zero, so L has a unique zero eigenvalue, and all nonzero eigenvalues are positive, such that,

$$\lambda_1(\mathcal{G}) = 0 < \lambda_2(\mathcal{G}) = 2.2 \leq \lambda_3(\mathcal{G}) = 4.8.$$

Moreover, $\mathbf{1}_3 := [1\ 1\ 1]^\top$ the eigenvector associated with $\lambda_1(\mathcal{G})$. Also, since $L = L^\top$, we have that $L\mathbf{1}_3 = 0$ and $\mathbf{1}_3^\top L = 0$.

Thus, the system in (2.1) is linear time-invariant, since it has the form $\dot{x} = -Lx$. The Laplacian matrix in (2.2) plays an important role in the analysis of the consensus problem via tools involving linear systems theory, which we use and extend to address the problems of bipartite consensus and containment of interest in this memoir. For clarity and to put our contributions in perspective, we describe below two approaches to analyze the behavior of the solutions of the otherwise well-known equation $\dot{x} = -Lx$ [75, 54, 7].

2.2.1 Limit values for the network solutions over an undirected graph

The solution of the system (2.1) is given by

$$x(t) = e^{-Lt}x_0, \tag{2.4}$$

where $x_0 = x(0)$ is the vector containing the initial conditions of all agents and $L \in \mathbb{R}^{3\times 3}$, which is symmetric and positive semidefinite, is defined in (2.3). Let

$$U = [v_{D_1} \quad v_{D_2} \quad v_{D_3}]$$

be a matrix containing normalized and orthogonal eigenvectors of the Laplacian matrix associated with its eigenvalues. Using the Jordan decomposition of L such that, $L = U\Lambda(\mathcal{G})U^\top$ and the spectral factorization of the Laplacian matrix [75], we have

$$e^{-Lt} = e^{-U\Lambda(\mathcal{G})U^\top t} = Ue^{-\Lambda(\mathcal{G})t}U^\top,$$

where $\Lambda(\mathcal{G}) = \text{diag}([\lambda_1(\mathcal{G}),\ \lambda_2(\mathcal{G}),\ \lambda_3(\mathcal{G})])$. Then, (2.4) can be decomposed as

$$\begin{aligned} x(t) &= Ue^{-\Lambda(\mathcal{G})t}U^\top x_0 \\ &= e^{-\lambda_1(\mathcal{G})t}v_{D_1}v_{D_1}^\top x_0 + e^{-\lambda_2(\mathcal{G})t}v_{D_2}v_{D_2}^\top x_0 + e^{-\lambda_3(\mathcal{G})t}v_{D_3}v_{D_3}^\top x_0. \end{aligned}$$

Since $\lambda_1(\mathcal{G}) = 0$, we have that $e^{-\lambda_1(\mathcal{G})t} = 1$, and for all $1 < i \leq 3$, we have $e^{-\lambda_i(\mathcal{G})t} \to 0$ as $t \to \infty$. Then,

$$\lim_{t\to\infty} x(t) = v_{D_1}v_{D_1}^\top x_0 = \frac{1}{3}\mathbf{1}_3\mathbf{1}_3^\top x_0. \tag{2.5}$$

Thus, the trajectories of the system in (2.4) converge to the agreement set

$$\{x \in \mathbb{R} : x_1 = x_2 = x_3\}.$$

In addition, from the expression in (2.5), we notice that the convergence point is the average of the initial conditions of all agents. Then, all agents achieve *average*

consensus. Indeed, note that here each x_i converges to $\frac{1}{3}\mathbf{1}_3^\top x_0$, which corresponds to an average. This is a particular case of consensus, but in the more general coordination setting, the average is defined as $\frac{1}{3}\mathbf{1}_3^\top x$ and not with the initial conditions x_0, as the system may be moving [67].

The above development allowed us to establish the convergence of the network containing three autonomous vehicles. The same conclusion is obtained after analyzing the stability of the system using Lyapunov stability tools [38].

2.2.2 Lyapunov stability of the consensus set over an undirected graph

Here, we analyze the stability of the origin in the space of the synchronization errors. We saw above that three agents interconnected over a connected and undirected graph achieve average consensus. Then, it makes sense to define the synchronization errors with respect to the average value of the system. To that end, we use the approach introduced in [67] and express the system in terms of two interconnected dynamical systems: the dynamics of the weighted average system x_m, which is actually the consensus equilibrium, and of the synchronization errors e_i relative to x_m. The consensus equilibrium is calculated by the left eigenvector associated with the zero eigenvalue and the states of the agents, such that,

$$x_m := \frac{1}{3}\mathbf{1}_3^\top x. \tag{2.6}$$

Here, x_m is scalar since all the agents converge to the same state, which is the rendezvous point. Then, we define the synchronization errors as the difference between the agents' states and the average system, that is,

$$e := x - \mathbf{1}_3 x_m. \tag{2.7}$$

Remark 2 *In (2.6), $\frac{1}{3}\mathbf{1}_3$ corresponds to the left eigenvector associated with the zero eigenvalue. In (2.7), $\mathbf{1}_3$ corresponds to the right eigenvector associated with the zero eigenvalue. In this example, left and right eigenvectors differ only by a scalar factor because the graph under consideration is undirected. However, this is generally not the case, as will be demonstrated in Chapter 3 for directed graphs.* •

Then, differentiating the errors, and from (2.2), we obtain

$$\begin{aligned}\dot{e} &= \dot{x} - \mathbf{1}_3\dot{x}_m \\ &= -[1 - \frac{1}{3}\mathbf{1}_3\mathbf{1}_3^\top]Lx.\end{aligned}$$

Since $\mathbf{1}_3^\top L = 0$ and $L\mathbf{1}_3 = 0$, note that $\dot{x}_m = 0$ and the error dynamics can be expressed as

$$\dot{e} = -Le. \tag{2.8}$$

Consider the following Lyapunov function candidate[1]

$$V(e) = \frac{1}{2} e^\top e. \tag{2.9}$$

Its derivative along the trajectories of (2.8) reads

$$\begin{aligned} \dot{V}(e) &= \frac{1}{2}\left[(-Le)^\top e + e^\top(-Le)\right] \\ &= -e^\top Le, \end{aligned} \tag{2.10}$$

which is negative semi-definite. Next, we use Barbashin-Krasovskii's theorem [5, 38]. On the set $\{e \in \mathbb{R} : \dot{V} = 0\}$, we have

$$Le = Lx - L\mathbf{1}_3\mathbf{1}_3^\top x = Lx = 0,$$

as $L\mathbf{1}_3 = 0$. The only solution of (2.10) that remains in the set $\{e \in \mathbb{R} : \dot{V} = 0\}$, is

$$x_i = x_j = x_m \quad \Leftrightarrow \quad e = 0.$$

Thus, global asymptotic stability of $\{e = 0\}$ follows, which means that the agents achieve consensus. Moreover,

$$\lim_{t\to\infty} x(t) = \frac{1}{3}\mathbf{1}_3\mathbf{1}_3^\top x(0).$$

Let us now consider the consensus control problem for networks containing N dynamical systems modeled by

$$\dot{x}_i = u_i, \quad x_i, u_i \in \mathbb{R}, \quad i \in \mathcal{I}_\mathcal{N} \tag{2.11}$$

where $\mathcal{I}_\mathcal{N} := \{1, 2, \ldots, N\}$. Each right-hand-side in (2.1) may be assimilated to a control input of the generic form

$$u_i = -\sum_{j=1}^{N} a_{ij}(x_i - x_j), \tag{2.12}$$

where $a_{ij} \in \mathbb{R}_{\geq 0}$ is the interconnection weight between the nodes ν_i and ν_j. More precisely, $a_{ij} > 0$ if there is a (directed) interconnection between the ith and the jth nodes, and $a_{ij} = 0$ if there is not. The control law in (2.12) is a well-known consensus algorithm that ensures that,

$$\lim_{t\to\infty}[x_j(t) - x_i(t)] = 0 \quad \forall\, i, j \leq N, \tag{2.13}$$

which is the property that we established to hold for the system (2.1). In general, (2.13) holds if and only if the underlying (directed) graph contains a (directed) spanning tree

[1] See Appendix A.2 for the definition of a Lyapunov function.

[7]. Indeed akin to (2.2), the system (2.11) interconnected via the distributed consensus algorithm in (2.13) may be analyzed by expressing it in the multi-agent form

$$\dot{x} = -Lx, \tag{2.14}$$

where

$$L = \begin{bmatrix} \sum_{k=2}^{N} a_{1k} & -a_{12} & \dots & -a_{1N} \\ -a_{21} & \sum_{k=1,\ k\neq 2}^{N} a_{2k} & \dots & -a_{23} \\ \dots & \dots & \ddots & \dots \\ -a_{N1} & -a_{N2} & \dots & \sum_{k=1}^{N-1} a_{Nk} \end{bmatrix}, \tag{2.15}$$

is the resulting Laplacian matrix corresponding to the considered graph. Now, the Laplacian matrix may also be defined as

$$L := \mathcal{D} - \mathcal{A}, \tag{2.16}$$

where $\mathcal{D}$ is a diagonal matrix, called the *degree matrix* and $\mathcal{A}$ is the *adjacency matrix*.

For an undirected graph, $\mathcal{D}$ contains the vertex degrees $d(\nu_i)$, such that

$$\mathcal{D} := \text{diag}([d(\nu_1)\ d(\nu_2) \cdots\ d(\nu_N)]).$$

For instance, the degrees of the vertices of the graph in Figure 2.2 are $d(\nu_1) = 2.5$, $d(\nu_2) = 1.5$, $d(\nu_3) = 3$, which also corresponds to the diagonal of the matrix in (2.2). Then, the resulting Laplacian matrix is symmetric and positive semi-definite, and all nonzero eigenvalues of L are positive, such that

$$0 = \lambda_1(\mathcal{G}) < \lambda_2(\mathcal{G}) \leq \cdots \leq \lambda_N(\mathcal{G}),$$

with $\mathbf{1}_N$ the eigenvector associated with the zero eigenvalue. Moreover, since $L = L^\top$, we have that $L\mathbf{1}_N = 0$ and $\mathbf{1}_N^\top L = 0$.

We now move forward with the case of directed graphs.

2.2.3 Limit values for the network solutions over a directed graph

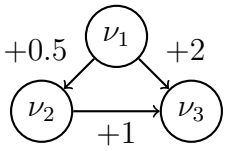

Figure 2.3: Example of three vehicles interconnected over a directed graph.

For a directed graph, $\mathcal{D}$ contains the in-degree of each vertex on the diagonal, such that

$$\mathcal{D} := \text{diag}([d_{in}(\nu_1)\ d_{in}(\nu_2)\ \cdots\ d_{in}(\nu_N)]),$$

where the in-degree is the sum of the weights of the incoming edges to the node. On the other hand, the out-degree is the sum of the weights of the outcoming edges. If the in-degree and out-degree are equal for every vertex, the directed graph is called *balanced*. Thus, every undirected graph is naturally balanced. For instance, the in- and out-degrees of the vertices of the graph in Figure 2.3 are $d_{in}(\nu_1) = 0$, $d_{in}(\nu_2) = 0.5$, $d_{in}(\nu_3) = 3$ and $d_{out}(\nu_1) = 2.5$, $d_{out}(\nu_2) = 1$, $d_{out}(\nu_3) = 0$. Then, the resulting Laplacian matrix is generally not symmetric and all its nonzero eigenvalues have positive real parts, such that,

$$0 = \lambda_1(\mathcal{G}) < \mathrm{Re}(\lambda_2(\mathcal{G})) \leq \cdots \leq \mathrm{Re}(\lambda_N(\mathcal{G})),$$

with $\mathbf{1}_N$ the right eigenvector associated with the zero eigenvalue. Moreover, if the digraph is balanced, in addition to having $L\mathbf{1}_N = 0$, we also have $\mathbf{1}_N^\top L = 0$.

Following the steps of the latter example, we now consider the system (2.11) interconnected with the control law (2.12) under a directed graph containing a spanning tree.

The solution of (2.11) is given by $x(t) = e^{-Lt}x_0$, where $x_0 = x(0)$ and $L \neq L^\top$. Let $L = UJ(\Lambda)U^{-1}$ be the Jordan decomposition of the Laplacian of the digraph, where $U = [v_{D_1}\ v_{D_2}\ \ldots\ v_{D_N}]$ with $v_{D_1} = \mathbf{1}_N$, contains the right eigenvectors and $U^{-1} = [w_{D_1}\ w_{D_2}\ \ldots\ w_{D_N}]$ contains the left eigenvectors associated with the eigenvalues. Moreover, $\lambda_i(\mathcal{G})$, $2 \leq i \leq N$ have positive real parts and $J(\lambda_1(\mathcal{G})) = J(0) = 0$ [54]. Then,

$$U^{-1}LU = J(\Lambda(\mathcal{G})) = \begin{bmatrix} 0 & 0 & \ldots & 0 \\ 0 & J(\lambda_2(\mathcal{G})) & \ldots & 0 \\ \vdots & \vdots & \vdots & \vdots \\ 0 & 0 & 0 & J(\lambda_N(\mathcal{G})) \end{bmatrix}.$$

We also have $LU = UJ(\Lambda(\mathcal{G}))$ and $U^{-1}L = J(\Lambda(\mathcal{G}))U^{-1}$, which implies that $\mathbf{1}_N$ and w_{D_1} are the right and left eigenvectors associated with the 0 eigenvalue such that $L\mathbf{1}_N = 0_N$ and $w_{D_1}^\top L = 0$. In addition, since $UU^{-1} = I_N$, we also have $\mathbf{1}_N^\top w_{D_1} = 1$. Thus,

$$\lim_{t\to\infty} e^{-Lt} = U \begin{bmatrix} e^0 & 0 & \ldots & 0 \\ 0 & e^{J(-\lambda_2(\mathcal{G}))t} & \ldots & 0 \\ \vdots & \vdots & \vdots & \vdots \\ 0 & 0 & 0 & e^{J(-\lambda_N(\mathcal{G}))t} \end{bmatrix} U^{-1}.$$

Since $\mathrm{Re}(\lambda_i) > 0$ for all $i > 1$, we have $\lim_{t\to\infty} e^{-J(\lambda_i(\mathcal{G}))t} = 0$. Consequently,

$$\lim_{t\to\infty} x(t) = \mathbf{1}_N w_{D_1}^\top x_0, \tag{2.17}$$

Hence, all the agents converge to the agreement set

$$\{x \in \mathbb{R} : x_i = x_j,\ \forall i, j \leq N\}.$$

Furthermore, if the digraph is balanced, all agents achieve average consensus, *i.e.,* $\lim_{t\to\infty} x(t) = \frac{1}{N}\mathbf{1}_N\mathbf{1}_N^\top x_0$.

Next, we show how to analyze the stability of the agreement set using Lyapunov-stability tools.

2.2.4 Lyapunov stability of the consensus set over a directed graph

Once again, we analyze the stability of the origin in space of the synchronization errors by using the approach introduced in [67] and express the system in terms of two interconnected dynamical systems. To that end, we define the weighted average system as

$$x_m := w_D^\top x, \tag{2.18}$$

and the synchronization errors as

$$e := x - \mathbf{1}_N x_m. \tag{2.19}$$

Then, differentiating the expression above and using $\dot{x}_m = w_D^\top L x = 0$ and $L\mathbf{1}_N = 0$, we obtain

$$\dot{e} = -Le. \tag{2.20}$$

Next, consider the following Lyapunov function candidate in (2.9) whose derivative along the trajectories of (2.20) reads

$$\dot{V}(e) = -e^\top (L^\top + L)e.$$

Since the graph is directed, the Laplacian matrix is not symmetric, and $L^\top + L$ is not positive semi-definite. Therefore, we cannot conclude that $\dot{V}$ is negative semi-definite. However, there are some works in the literature on Lyapunov-function design for balanced or strongly connected digraphs based on M-matrices concepts [69]. For instance, if the considered digraph is *balanced*, then $L^\top + L \geq 0$ and the derivative of the Lyapunov function is negative semi-definite [109]. Then, invoking LaSalle's invariance principle [39], we can conclude that the system converges to the invariant set $\{e \in \mathbb{R} : \dot{V} = 0\}$, that is, $\{e = 0\}$. On the other hand, if the digraph is *strongly connected*, then the left eigenvector associated with the zero eigenvalue of L has all positive elements, and using this property, a quadratic Lyapunov function of the form $V(e) := e^\top P e$, where P is diagonal and contains the elements of w_{D_1}, may be constructed [109]. However, if the digraph is not strongly connected, the left eigenvector may contain zero elements, so this construction cannot be used. That is, in general, the analysis of consensus over general digraphs is more complicated than for undirected graphs. In [68] a Lyapunov approach for the study of consensus problems for the systems over general digraphs containing a directed spanning tree is presented. The following statement, repeated here for convenience, provides a Lyapunov characterization of the necessary and sufficient condition to achieve consensus over digraphs.

Proposition 1 ([68]) *Let $\mathcal{G}$ be a directed graph of order N and let $L \in \mathbb{R}^{N\times N}$ be its associated, non-symmetric, Laplacian matrix. The following statements are equivalent:*

1. *the graph $\mathcal{G}$ contains a directed spanning tree;*

2. *for any matrix* $Q \in \mathbb{R}^{N\times N}$, $Q = Q^\top > 0$, *and any real* $\alpha > 0$, *there exists matrix* $P(\alpha) \in \mathbb{R}^{N\times N}$, $P = P^\top > 0$ *such that*

$$PL + L^\top P = Q - \alpha[P\mathbf{1}_N w_D^\top + w_D \mathbf{1}_N^\top P], \tag{2.21}$$

where $w_D \in \mathbb{R}^N$ *is the left eigenvector of* L *corresponding to the zero eigenvalue.*

In particular, Proposition 1 gives the guidelines to construct a strict Lyapunov function for the consensus problem in the space of the synchronization errors defined in (2.19) [68]. Consider the system (2.20) and the Lyapunov function candidate

$$V(e) = e^\top P e, \tag{2.22}$$

where $P = P^\top > 0$ is to be defined. Its derivative gives

$$\dot{V}(e) = -e^\top (PL + L^\top P)e.$$

Let $Q = Q^\top > 0$ and $\alpha > 0$ be arbitrarily fixed. Under the assumption that the digraph contains a directed spanning tree, from Proposition 1, there exists $P = P^\top > 0$ such that (2.21) holds. Then, using such P in (2.22) we obtain

$$\dot{V}(e) = -e^\top Q e + \alpha e^\top [P\mathbf{1}_N w_D^\top + w_D \mathbf{1}_N^\top P]e.$$

However, from (2.18) and (2.19), and from the fact that $w_D^\top \mathbf{1}_N = 1$ we have

$$P\mathbf{1}_N w_D^\top e = P\mathbf{1}_N w_D^\top [I - \mathbf{1}_N w_D^\top]x = 0,$$

so

$$\dot{V}(e) = -e^\top Q e,$$

which is negative definite for all e satisfying (2.19). Thus, the consensus manifold $\{e = 0\}$ is globally exponentially stable.

Remark 3 *Disposing of strict Lyapunov functions is important as it provides a basis to establish input-to-state stability (ISS). In Chapter 3, we construct strict Lyapunov functions to analyze the stability of the synchronization errors, and then we conduct a robustness analysis of the error set in the sense of ISS.* •

The previous developments allowed us to establish *convergence* and asymptotic or exponential *stability* to the consensus set over networks of agents that evolve with cooperative interactions having the same objectives. They set the basis to consider the more general case of networks containing both cooperative and *competitive* interactions between agents, modeled by *signed graphs*, which is discussed next.

2.3 THE BIPARTITE CONSENSUS-CONTROL PROBLEM

In a network with signed interconnections, the agents generally do not have a unique consensus equilibrium, but at least two equilibria [2], [30], [95]. However, it is not impossible for them to converge to a consensus equilibrium. This depends on the *structural balance* property of the graph [2]—see below.

Definition 1 (Structural balance) *Let $\mathcal{V}$ denote a set of cardinality N, of vertices (nodes) ν_l, let $\mathcal{E} \subseteq \mathcal{V}^2$ denote the set of cardinality M, of edges (interconnections) $\varepsilon_k := \{v_i, v_j\}$, and let $\mathcal{G}(\mathcal{V}, \mathcal{E})$ denote the corresponding graph. Then, a signed graph is structurally balanced if it may be split into two disjoint sets of vertices $\mathcal{V}_1$ and $\mathcal{V}_2$, where $\mathcal{V}_1 \cup \mathcal{V}_2 = \mathcal{V}, \mathcal{V}_1 \cap \mathcal{V}_2 = \emptyset$ such that for every $v_i, v_j \in \mathcal{V}_p, p \in \{1, 2\}$, if $a_{ij} \geq 0$, while for every $v_i \in \mathcal{V}_p, v_j \in \mathcal{V}_q$, with $p, q \in \{1, 2\}, p \neq q$, if $a_{ij} \leq 0$. It is structurally unbalanced, otherwise.*

Figure 2.4: Example of two signed networks: (a) a structurally balanced signed network (b) a structurally unbalanced network.

An example of two signed networks is given in Figure 2.4, where the cooperative interactions are represented by solid black lines and the competitive interactions by red dashed lines. The nodes of the signed graph in Figure 2.4a can be separated into two disjoint subsets such as $\mathcal{V}_1 = \{\nu_1\}$ and $\mathcal{V}_2 = \{\nu_2,\ \nu_3\}$, so the graph is structurally balanced. However, the nodes of the signed graph in Figure 2.4b cannot be separated into two disjoint subsets, so the graph is structurally unbalanced.

We first address undirected and directed graphs that are structurally balanced.

2.3.1 Structurally-balanced undirected signed networks

Figure 2.5: Example of two undirected graphs with three agents: (a) an undirected unsigned graph; (b) an undirected signed graph.

For the purpose of illustration, consider a robotic system containing three autonomous vehicles interconnected over an undirected and connected graph but with

cooperative and competitive interactions. Suppose that if two vehicles are cooperative, they aim to meet at a rendezvous point, whereas if they are competitive, they have the objective of going in opposite directions. To illustrate these interactions, we consider a signed graph with both positive and negative signs on its adjacency weights. More precisely, if the interactions are *cooperative* for *some* i, $j \leq N$ then, $a_{ij} > 0$ whereas if they are *competitive* for *some* i, $j \leq N$, then $a_{ij} < 0$—see Figure 2.5. Thus, $\{\nu_i, \nu_j\} \in \mathcal{E}$ if and only if $a_{ij} \neq 0$; otherwise, $\{\nu_i, \nu_j\} \notin \mathcal{E}$ and $a_{ij} = 0$. Each vehicle only communicates with its neighbors, and each agent's dynamics correspond to a simple integrator interconnected with a diffusive control law. Then, the system dynamics are described by

$$\dot{x}_1 = -0.5(x_1 + x_2) - 2(x_1 + x_3) \tag{2.23a}$$
$$\dot{x}_2 = -0.5(x_2 + x_1) - 1(x_2 - x_3) \tag{2.23b}$$
$$\dot{x}_3 = -2(x_3 + x_1) - 1(x_3 - x_2), \tag{2.23c}$$

where $x_i \in \mathbb{R}$ is the position of vehicle i and the factors -0.5, 1 and -2 correspond to the values of the adjacency weights a_{12}, a_{23} and a_{13}. Notice that in equations (2.23a) and (2.23b), for agents that are interconnected with a competitive edge, *i.e.*, agents ν_1 and ν_2 or agents ν_1 and ν_3, we have the sum of the agents' states whereas in equations (2.23b) and (2.23c), for agents that are cooperative with each other *i.e.*, agents ν_2 and ν_3, we have the difference of the agents' states, as for the case of unsigned graphs. Then, by rearranging (2.23), we obtain

$$\dot{x} = -\begin{bmatrix} (2+0.5) & 0.5 & 2 \\ 0.5 & (0.5+1) & -1 \\ 2 & -1 & (2+1) \end{bmatrix} x, \tag{2.24}$$

where the matrix on the right-hand side corresponds to the signed Laplacian matrix associated with the signed graph describing the cooperative and competitive interactions, which in the N-agents' case reads $L_s := [\ell_{s_{ij}}] \in \mathbb{R}^{N \times N}$. Its elements are defined as

$$\ell_{s_{ij}} = \begin{cases} \sum\limits_{k \in \mathcal{I}_N} |a_{ik}| & i = j \\ -a_{ij} & i \neq j. \end{cases} \tag{2.25}$$

Moreover, the signed graph in Figure 2.5 is *digon sign-symmetric*. A signed graph is said to be digon sign-symmetric if $a_{ij}a_{ji} \geq 0$. It means that the interaction between two interconnected agents always has the same sign in both directions.

Assumption 1 (Standing assumption) *Throughout this manuscript, signed graphs are assumed to be digon sign-symmetric.*

Furthermore, the signed graph in Figure 2.5 is said to be structurally balanced [2]—see Definition 1. More precisely, we recall the following characterization of structurally balanced and undirected signed graphs [2, 30, 108].

Lemma 1 *(Structural balance for undirected signed graphs) A connected and undirected signed graph $\mathcal{G} = (\mathcal{V}, \mathcal{E})$ is said to be structurally balanced if and only if one of the following equivalent conditions holds:*

(i) *All the cycles of the graph are positive.*

(ii) *There exists a matrix* $D \in \mathfrak{D}$ *such that all off-diagonal elements of* DL_sD *are negative and is equivalent to the Laplacian matrix of an unsigned graph through a gauge transformation, where* $\mathfrak{D} = \{D = diag(\sigma),\ \sigma = [\sigma_1, \sigma_2, \ldots, \sigma_N], \sigma_i \in \{-1, 1\},\ i \leq N\}$.

(iii) $\lambda_1(L_s) = 0$ *is a simple eigenvalue of* L_s *and the rest of the eigenvalues are positive.*

The condition (i) of Lemma 1 means that the signed graph is structurally balanced if the multiplication of the signs of the interconnections on a cycle is positive [10]. The signed graph in Figure 2.4b is structurally balanced because the cycle is positive, such that, for one cooperative and two competitive edges, we have $1 \times (-1) \times (-1) = 1$. On the other hand, the graph in Figure 2.4a is structurally unbalanced because the cycle is negative, such that, for two cooperative and one competitive edges, we have $1 \times 1 \times (-1) = -1$.

The condition (ii) of Lemma 1 implies that if the considered graph is structurally balanced, then the resulting Laplacian matrix of the signed graph L_s is equivalent to the Laplacian matrix L of an unsigned graph through a *gauge transformation*. The gauge transformation consists in a change of coordinates performed by a diagonal invertible matrix $D \in \mathfrak{D}$, such that $L = DL_sD$. Consider the signed graph in Figure 2.5. The corresponding Laplacian matrix is given in (2.24). On the other hand, as there are three agents in the considered graph, the set $\mathfrak{D}$ contains $2^N = 8$ possible matrices, as shown below.

$$D_1 = \begin{bmatrix} 1 & 0 & 0 \\ 0 & 1 & 0 \\ 0 & 0 & 1 \end{bmatrix},\ D_2 = \begin{bmatrix} -1 & 0 & 0 \\ 0 & -1 & 0 \\ 0 & 0 & -1 \end{bmatrix},\ D_3 = \begin{bmatrix} 1 & 0 & 0 \\ 0 & 1 & 0 \\ 0 & 0 & -1 \end{bmatrix},\ D_4 = \begin{bmatrix} -1 & 0 & 0 \\ 0 & -1 & 0 \\ 0 & 0 & 1 \end{bmatrix},$$
$$D_5 = \begin{bmatrix} 1 & 0 & 0 \\ 0 & -1 & 0 \\ 0 & 0 & 1 \end{bmatrix},\ D_6 = \begin{bmatrix} -1 & 0 & 0 \\ 0 & 1 & 0 \\ 0 & 0 & -1 \end{bmatrix},\ D_7 = \begin{bmatrix} 1 & 0 & 0 \\ 0 & -1 & 0 \\ 0 & 0 & -1 \end{bmatrix},\ D_8 = \begin{bmatrix} -1 & 0 & 0 \\ 0 & 1 & 0 \\ 0 & 0 & 1 \end{bmatrix}.$$

Remark 4 *The entries of the matrix* D *are either* $+1$ *or* -1. *The signs indicate that agents correspond to two distinct disjoint subsets, as explained in the structural balanced property in Definition 1. For instance, from matrices* D_7 *and* D_8, *it is clear that agents* ν_2 *and* ν_3 *belong to the same subset* $\mathcal{V}_p$, $p \in \{1, 2\}$, *as the last two diagonal entries have the same signs. In contrast, agent* ν_1 *belongs to the other subset* $\mathcal{V}_q$, $p \in \{1, 2\}$, *where* $p \neq q$, *since the first diagonal entry has the opposite sign.* •

Then, there exist $2^{N-1} = 4$ possibilities of gauge equivalent Laplacian matrices

$\mathcal{L}(L) = \{DL_sD, D \in \mathfrak{D}\}$, as $DL_sD = (-D)L_s(-D)$, such that,

$$L_1 = D_1L_sD_1 = D_2L_sD_2 = \begin{bmatrix} 2.5 & 0.5 & 2 \\ 0.5 & 1.5 & -1 \\ 2 & -1 & 3 \end{bmatrix},$$

$$L_2 = D_3L_sD_3 = D_4L_sD_4 = \begin{bmatrix} 2.5 & 0.5 & -2 \\ 0.5 & 1.5 & 1 \\ -2 & 1 & 3 \end{bmatrix},$$

$$L_3 = D_5L_sD_5 = D_6L_sD_6 = \begin{bmatrix} 2.5 & -0.5 & 2 \\ -0.5 & 1.5 & 1 \\ 2 & 1 & 3 \end{bmatrix},$$

$$L_4 = D_7L_sD_7 = D_8L_sD_8 = \begin{bmatrix} 2.5 & -0.5 & -2 \\ -0.5 & 1.5 & -1 \\ -2 & -1 & 3 \end{bmatrix}.$$

All the matrices above are symmetric and positive semi-definite, and their eigenvalues are $\lambda(L_i) = 0,\ 4,\ 4$. However, the only matrix corresponding to the Laplacian matrix of an unsigned graph is L_4, as it is the only matrix for which all off-diagonal entries are nonpositive.

Condition (iii) of Lemma 1 holds if and only if the signed graph is structurally balanced. This comes from the fact that L and L_s are both square $N \times N$ matrices and $L_s \to DLD$ is a similarity transformation as $D = D^\top = D^{-1}$ so L and L_s have the same eigenvalues and the same geometric multiplicities of eigenvalues [2].

Now, we analyze the solutions of the system of three autonomous vehicles interconnected over a signed graph.

2.3.1.1 Limit values for the network solutions

Let us first transform the system in (2.24) into a system of agents interconnected over an unsigned graph, *e.g.,* the one on Figure 2.5a, using the gauge transformation defined in Lemma 1 [2], [108]. To that end, we define

$$z := Dx, \tag{2.26}$$

where $z = [z_1\ z_2,\ z_3]^\top$ are the states of agents of the unsigned graph with $z_i = \sigma_i x_i$, and $\sigma_i \in \{1, -1\}$. Its derivative along the trajectories reads

$$\dot{z} = D\dot{x}.$$

Replacing (2.24) in the latter and using (2.26), we obtain

$$\dot{z} = -DL_sx = -DL_sDz,$$

which is equivalent to

$$\dot{z} = -Lz, \tag{2.27}$$

since $L = DL_sD$, where L is the Laplacian associated with the transformed unsigned graph. Then, the solution of (2.27) is

$$z(t) = e^{-\lambda_1(\mathcal{G})t}\frac{1}{3}\mathbf{1}_3\mathbf{1}_3^\top z_0 + e^{-\lambda_2(\mathcal{G})t}v_{D_2}v_{D_2}^\top z_0 + e^{-\lambda_N(\mathcal{G})t}v_{D_3}v_{D_3}^\top z_0.$$

Coming back to the original coordinates corresponding to the signed graph by $x = Dz$, since $D = D^{-1}$, we obtain

$$x(t) = e^{-\lambda_1(\mathcal{G})t}D\frac{1}{3}\mathbf{1}_3\mathbf{1}_3^\top Dx_0 + e^{-\lambda_2(\mathcal{G})t}Dv_{D_2}v_{D_2}^\top Dx_0 + e^{-\lambda_N(\mathcal{G})t}Dv_{D_3}v_{D_3}^\top Dx_0.$$

Since the considered undirected signed graph is structurally balanced, from Lemma 1 we have $\lambda_1(G) = 0$ and for $1 < i \leq 3$, $\lambda_i(\mathcal{G}) > 0$. Then,

$$\lim_{t\to\infty} x(t) = \frac{1}{3}D\mathbf{1_3}\mathbf{1_3}^\top Dx_0.$$

On the other hand, let

$$U_s = [v_{r_1}\ v_{r_2}\ v_{r_3}]$$

be a matrix containing normalized and orthogonal eigenvectors of the signed Laplacian matrix associated with its eigenvalues. Then, we have $v_{r_1} = D\mathbf{1}_N$ and $v_{l_1} = \frac{1}{3}D\mathbf{1_N}$, which means that the right and left eigenvectors associated with the zero eigenvalue of the signed Laplacian matrix have positive and negative entries. Thus, the trajectories of the system converge to the set $\{x \in \mathbb{R} : \sigma_i x_i = \sigma_j x_j,\ \forall i, j \leq 3\}$, where $\sigma_i = \pm 1$. More precisely, they converge to the disagreement set

$$\{x \in \mathbb{R} : x_1 = -x_2 = -x_3\}. \tag{2.28}$$

With the above disagreement set (2.28) for the networked system, we established the convergence of the network. Now, to analyze the stability of the system, we use Lyapunov stability theory, similar to Subsection 2.2.2.

2.3.1.2 Lyapunov stability of the bipartite consensus set

As in the ordinary consensus problem discussed in Section 2.2, we follow the approach of [67]. It relies on representing the network dynamics as two interconnected dynamical systems. One corresponds to average dynamics, and the other to the dynamics of synchronization errors relative to the trajectories of that average system. More precisely, we define the state of the average system as

$$x_m := v_{l_1}^\top x, \tag{2.29}$$

where v_{l_1} is the left eigenvector associated with the zero eigenvalue. For instance, for the example in Figure 2.5b, $v_{l_1} = \frac{1}{3}[1\ -1\ -1]^\top$. Then, we define the synchronization errors as

$$e := x - v_{r_1}x_m, \tag{2.30}$$

where v_{r_1} is the right eigenvector associated with the zero eigenvalue. For instance, for the example in Figure 2.5b, $v_{r_1} = [1 \ -1 \ -1]^\top$. Then, the error dynamics can again be expressed as

$$\dot{e} = -L_s e, \tag{2.31}$$

which is equivalent to $\dot{x} = -L_s x$, because

$$L_s e = L_s x - L_s v_{r_1} v_{l_1}^\top x = L_s x$$

since $L_s v_{r_1} = \mathbf{0}_N$. Then, we reconsider the Lyapunov function candidate in (2.9). Its derivative along the trajectories reads

$$\dot{V}(e) = -e^\top L_s e, \tag{2.32}$$

which is negative semi-definite. Next, we use Barbashin-Krasovskii's theorem [5, 38]. The only solution of (2.32) that remains in the set $\{e \in \mathbb{R} : \dot{V} = 0\}$, is

$$x = v_{r_1} x_m \qquad \Leftrightarrow \qquad e = 0.$$

Thus, global asymptotic stability of $\{e = 0\}$ follows.

Remark 5 *Here, the right eigenvector v_{r_1} is not a vector of all ones. It also contains negative valued elements, so the agents converge to two symmetric equilibrium points x_m and $-x_m$.* •

The previous arguments apply to generic signed networks containing more than $N = 3$ agents. Let us now consider the bipartite consensus-control problem for signed networks containing N dynamical systems modeled by (2.11). Then, the distributed consensus control law in (2.12) becomes, for signed networks,

$$u_i = -\sum_{j=1}^{N} |a_{ij}|(x_i - \text{sgn}(a_{ij})x_j), \tag{2.33}$$

where we clearly see that the sign of the edge interconnecting two agents ν_i and ν_j appears.

Remark 6 *Notice that for the case of a graph with all cooperative interactions, the control law in (2.33) is equivalent to the consensus control law in (2.12) since $a_{ij} > 0$ for all $i, j \leq N$.* •

The control law in (2.33) is a well-known bipartite consensus algorithm that solves the bipartite consensus problem [2], [30], that is,

$$\lim_{t\to\infty}[x_j(t) - \text{sgn}(a_{ij})x_i(t)] = 0 \quad \forall\, i, j \leq N, \tag{2.34}$$

if and only if the underlying (directed) graph contains a (directed) spanning tree and is structurally balanced [2]—see Definition 1.

Indeed akin to (2.23), the system (2.11) interconnected with the bipartite consensus algorithm (2.33) may be expressed in the multi-agent form

$$\dot{x} = -L_s x, \tag{2.35}$$

where

$$L_s = \begin{bmatrix} \sum_{k=2}^{N} |a_{1k}| & -a_{12} & \dots & -a_{1N} \\ -a_{21} & \sum_{k=1,\ k\neq 2}^{N} |a_{2k}| & \dots & -a_{23} \\ \dots & \dots & \ddots & \dots \\ -a_{N1} & -a_{N2} & \dots & \sum_{k=1}^{N-1} |a_{Nk}| \end{bmatrix}, \tag{2.36}$$

is the resulting signed Laplacian matrix, which can also be defined as

$$L_s := |\mathcal{D}| - \mathcal{A}, \tag{2.37}$$

where $\mathcal{D}$ is the degree matrix and $\mathcal{A}$ is the adjacency matrix corresponding to the signed graph.

2.3.2 Structurally-balanced and directed signed networks

The properties of the signed Laplacian matrix depend on the structural balance property of the signed graph. Now, for generic directed signed graphs, we have the following characterization of the structural balance property [2, 30, 108].

Lemma 2 *(Structural balance for directed signed graphs) For a digon sign-symmetric structurally balanced directed signed graph $\mathcal{G} = (\mathcal{V}, \mathcal{E})$ containing a spanning tree, the following statements are equivalent:*

(i) *All directed cycles of the graph are positive.*

(ii) *There exists a matrix $D \in \mathfrak{D}$ such that DL_sD has all nonpositive off-diagonal entries and is equivalent to the Laplacian matrix of an unsigned directed graph through a gauge transformation, where $\mathfrak{D} = \{D = diag(\sigma),\ \sigma = [\sigma_1, \sigma_2, \dots, \sigma_N],$ $\sigma_i \in \{-1, 1\},\ i \leq N\}$.*

Lemma 3 ([30]). *If a signed network $\mathcal{G} = (\mathcal{V}, \mathcal{E})$ has a spanning tree and is structurally balanced, then all eigenvalues of its signed Laplacian matrix have nonnegative real parts, and 0 is a simple eigenvalue.*

Corollary 1 ([2]). *A (directed) spanning tree is always structurally balanced since no (directed) cycles are present in the graph.*

Following the steps of the analysis for unsigned digraphs, we address a system of autonomous vehicles interconnected over a structurally balanced signed digraph containing a directed spanning tree.

2.3.2.1 Limit values for the network solutions

From (2.17) and using the gauge transformation, we obtain

$$\lim_{t\to\infty} x(t) = D\mathbf{1}_N w_{D_1}^\top Dx_0,$$

where $D\mathbf{1}_N$ is the right eigenvector v_{r_1} and $w_{D_1}^\top D$ is the left eigenvector v_{l_1} associated with the zero eigenvalue of L_s. This comes from the fact that $\mathbf{1}_N$ and w_{D_1} are the right and left eigenvectors associated with the zero eigenvalue of the Laplacian matrix of the unsigned graph, as in (2.17), before applying the gauge transformation. Hence, the trajectories of the system converge to the disagreement set

$$\{x \in \mathbb{R} : \sigma_i x_i = \sigma_j x_j,\ \forall i, j \leq N\},$$

where $\sigma_i \in \{1, -1\}$. Furthermore, if the signed digraph is balanced, we have

$$\lim_{t\to\infty} x(t) = \frac{1}{N} D\mathbf{1}_N \mathbf{1}_N^\top Dx_0.$$

Remark 7 *For the analysis of signed networks, we used the gauge transformation to show the similarities between the consensus and bipartite consensus problems. However, the gauge transformation cannot be used in every situation. For instance, it is ineffective on structurally unbalanced signed networks (containing multiple leaders)—see Chapter 3, as well as for bipartite consensus problems with inter-agent constraints—see Chapters 4 and 5.* •

Now, we analyze the Lyapunov stability of the disagreement set.

2.3.2.2 Lyapunov stability of the bipartite consensus set

The weighted average system and the synchronization errors are defined as in (2.29) and (2.30), where $v_{r_1}, v_{l_1} \in \mathbb{R}^N$ are the right and left eigenvectors associated with the zero eigenvalue of the signed Laplacian matrix. Then, considering the Lyapunov function candidate in (2.22), and using Proposition 1, it may be concluded that the derivative of V is negative definite and the bipartite consensus manifold $\{e = 0\}$ is globally exponentially stable.

Next, we look at the case of structurally unbalanced networks.

2.3.3 Structurally-unbalanced and undirected signed networks

Agents in a structurally unbalanced and undirected graph cannot achieve bipartite consensus because the graph cannot be partitioned into two disjoint subsets. Instead, the agents' states converge to the origin. We follow the same steps of analysis of solutions and Lyapunov stability as before. In the case the undirected signed graph is not structurally balanced, we have the following.

Lemma 4 *(Structural unbalance for undirected signed graphs [2]). A connected undirected signed graph $\mathcal{G} = (\mathcal{V}, \mathcal{E})$ is structurally unbalanced if and only if one of the following equivalent conditions holds:*

(i) *One or more cycles of* $\mathcal{G}$ *are negative.*

(ii) *There does not exist a matrix* $D \in \mathfrak{D}$ *such that* DL_sD *has all nonpositive off-diagonal entries.*

(iii) $\lambda_1(L_s) > 0$.

If a graph is structurally unbalanced, the resulting Laplacian matrix is positive definite, and the eigenvalues are all positive. Consequently, we have that $e^{-\lambda_i(\mathcal{G})t} \to 0$ as $t \to \infty$ for all $1 \leq i \leq N$. Then,

$$\lim_{t\to\infty} x(t) = 0.$$

Moreover, for the stability of the agreement set, consider the Lyapunov function candidate

$$V(x) = \frac{1}{2}x^\top x.$$

Its derivative along the trajectories reads

$$\dot{V}(x) = -2x^\top L_s x \leq -2\lambda_1(L_s)|x|^2 < 0,$$

which is strictly negative since $L_s > 0$. Then, the origin of the system is globally exponentially stable, and agents achieve consensus at the origin $\{x = 0\}$.

2.3.4 Structurally-unbalanced and directed signed networks

For strongly connected signed digraphs that are structurally unbalanced, we have the following.

Lemma 5 *(Structural unbalance for directed signed graphs [2]). A strongly connected, digon sign-symmetric signed digraph* $\mathcal{G} = (\mathcal{V}, \mathcal{E})$ *is structurally unbalanced if and only if one of the following equivalent conditions holds:*

(i) $\mathcal{G}$ *has at least one negative directed cycle.*

(ii) *There does not exist a matrix* $D \in \mathfrak{D}$ *such that* DL_sD *has all nonpositive off-diagonal entries.*

(iii) $\lambda_1(L_s) > 0$, *i.e.,* $-L_s$ *is Hurwitz.*

After Lemma 5, it follows that the state trajectories of all agents interacting over a strongly connected and structurally unbalanced digraph converge to zero, as for structurally unbalanced and undirected signed graphs. Since the eigenvalues of the signed Laplacian matrix associated with the digraph are all positive, we have $\lim_{t\to\infty} x(t) = 0_N$. Moreover, considering the Lyapunov function candidate $V(x) = \frac{1}{2}x^\top x$, we have that $\dot{V}(x) = -x^\top(L_s^\top + L_s)x \leq -\underline{\lambda}|x|^2 < 0$, which is strictly negative since $L_s^\top + L_s > 0$ and $\underline{\lambda} > 0$ is the smallest eigenvalue of $L_s^\top + L_s$. Then, the origin of the system is globally exponentially stable, and all the agents' states converge to the origin, that is, $\{x = 0\}$.

On the other hand, several possible scenarios exist for the convergence of agents interconnected over directed signed networks that are structurally unbalanced, whereas Lemma 5 only applies to strongly connected digraphs. However, if the structurally unbalanced digraph contains one root agent (also called as *leader*), the states of all agents do not converge to zero, but at least two equilibrium points appear [30]. We illustrate this by the following example.

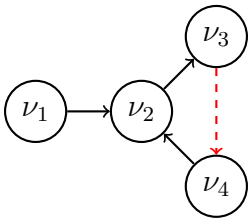

Figure 2.6: Example of a structurally unbalanced signed digraph with a root node.

Example 1 In Figure 2.6, ν_1 is the root agent as it is a node without any incoming edges, meaning its state is not influenced by other agents. The agents ν_2, ν_3, and ν_4 are interconnected over a strongly connected digraph that is also structurally unbalanced. As a result, all their states will converge to zero. However, as agent ν_2 is also getting information from the root node ν_1, its state will converge to a value between the state of the root node ν_1 and 0. This is because the system has three distinct equilibrium points but not two symmetric equilibria. Consequently, the agents do not achieve *bipartite consensus*, but instead reach *multi-consensus*. This will be studied and explained in more detail in Chapter 3. □

2.4 EDGE-BASED FORMULATION

In Sections 2.2 and 2.3, we studied the solutions of the trajectories of the system in node coordinates, meaning the states were represented using the nodes of the graph. We represented the networked system in terms of two interconnected dynamical systems: weighted average and synchronization error dynamics. The synchronization errors e were defined as the difference between the states of the agents x and the weighted average x_m, so the errors were dependent on the graph topology, as the left eigenvector associated with the zero eigenvalue was used to define x_m.

Another way to address the consensus or the bipartite consensus problems, which we use in this memoir, relies on the so-called edge-based formulation. In this case, we also look at the synchronization errors, and the network model is expressed in terms of its interconnections; that is, the states represent relative differences between pairs of nodes. This is a natural way, for instance, to address constrained control problems, where constraints are defined between a pair of interconnected agents. Below, we recall first some elements of the edge-based formulation, originally proposed in [54] for unsigned networks; then we recall some material for signed networks [23]. The edge-based formulation is used in Chapters 4 and 5.

2.4.1 The edge-based formulation for unsigned networks

The construction of edge-based models of graphs $\mathcal{G}(\mathcal{V}, \mathcal{E})$ starts with the definition of the incidence matrix $E \in \mathbb{R}^{N\times M}$, where N is the cardinality of $\mathcal{V}$ and M is the cardinality of $\mathcal{E}$. According to [54], for an unsigned and arbitrarily oriented graph $\mathcal{G}$ containing N nodes and M edges, the incidence matrix is defined as

$$[E]_{ik} := \begin{cases} +1, & \text{if } v_i \text{ is the initial node of the edge } \varepsilon_k; \\ -1, & \text{if } v_i \text{ is the terminal node of the edge } \varepsilon_k; \\ 0, & \text{otherwise.} \end{cases} \tag{2.38}$$

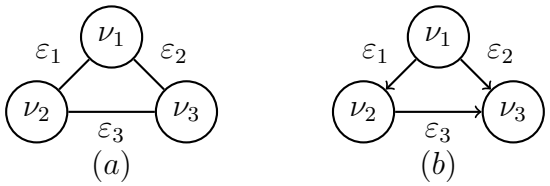

Figure 2.7: Example of two undirected graphs with three agents: (a) an undirected unsigned graph, where all interconnections are cooperative; (b) an undirected and structurally balanced signed graph, where some interconnections are competitive.

Example 2 Consider the unsigned graph containing three nodes on the left of Figure 2.7. We define the orientations of the edges as follows,

$$\varepsilon_1 := x_1 - x_2, \quad \varepsilon_2 := x_1 - x_3, \quad \varepsilon_3 := x_2 - x_3.$$

Then, from the definition in (2.38), the incidence matrix reads

$$E = \begin{bmatrix} 1 & 1 & 0 \\ -1 & 0 & 1 \\ 0 & -1 & -1 \end{bmatrix}.$$

□

Moreover, using the definition of incidence matrix we can define the *edge* Laplacian matrix $L_e \in \mathbb{R}^{M\times M}$ as

$$L_e := E^\top E. \tag{2.39}$$

It is also useful to remark that the *node* Laplacian matrix $L \in \mathbb{R}^{N\times N}$ defined in (2.3), may also be rewritten in terms of the incidence matrix, as

$$L := EE^\top. \tag{2.40}$$

With these definitions, for an undirected connected signed graph, we have the following linear algebraic properties [107]:

(i) the non-zero eigenvalues of L and L_e coincide.

(ii) $\operatorname{rank}(L) = \operatorname{rank}(L_e) = N - 1$.

Now, for digraphs, we recall the definitions of two incidence matrices: the first defines the incoming edges to a node, and the second defines the outgoing edges from a node. The so-called in-incidence matrix of an unsigned graph is defined as

$$[E_{\odot}]_{ik} := \begin{cases} -1, & \text{if } v_i \text{ is the terminal node of the edge } \varepsilon_k; \\ 0, & \text{otherwise,} \end{cases} \tag{2.41}$$

whereas the out-incidence matrix is defined as

$$[E_{\otimes}]_{ik} := \begin{cases} +1, & \text{if } v_i \text{ is the initial node of the edge } \varepsilon_k; \\ 0, & \text{otherwise.} \end{cases} \tag{2.42}$$

Then, the node and edge Laplacian matrices of a digraph can be defined as

$$L = E_{\odot} E^{\top}, \quad L_e = E^{\top} E_{\odot}, \tag{2.43}$$

where E is defined in (2.38).

In both node-based and edge-based representations, spanning trees and cycles play a crucial role in the network. They determine whether the graph is connected, and the null space of the edge Laplacian characterizes the graph's cycles [107]. Then, to simplify the representation of the network, by following the labeling algorithm proposed in [56], we may partition the incidence matrix as

$$E = [E_t \quad E_c \,],$$

where $E_t \in \mathbb{R}^{N \times N-1}$ corresponds to the incidence matrix of a spanning tree contained in the graph and $E_c \in \mathbb{R}^{N \times M-N+1}$ corresponds to the rest of the edges (cycles). Then, we have the following.

Theorem 1 ([54]) *Consider an undirected graph $\mathcal{G}$ with cycles, and a tree subgraph $\mathcal{G}_t$, with corresponding edge Laplacians $L_e(\mathcal{G}) = [E_t \; E_c]^{\top}[E_t \; E_c]$ and $L_e(\mathcal{G}_t) = E_t \top E_t$, respectively. Then, there exists a matrix $R = [I_{N_1} \quad T]$, where $T = (E_t^{\top} E_t)^{-1} E_t^{\top} E_c$ such that*

$$L_e(\mathcal{G}) = R^{\top} L_e(\mathcal{G}_t) R.$$

The reduced-order edge-based formulation is useful because it allows us to express the system in terms of the spanning tree and analyze only a part of the graph. This will be used later in Chapter 4.

2.4.2 The edge-based formulation for signed networks

We recall the edge-based formulation for signed networks. Using the edge-based formulation, we analyze directly the edge states, corresponding to the relative states of agents. This representation can be very useful and more direct than the node-based formulation in tackling some linear interconnections between agents and taking into account some inter-agent constraints. Moreover, using the reduced-order edge-based formulation has the advantage that it is only needed to analyze the behavior of the

agents corresponding to the spanning tree graph. This is because all the agents' behavior can be expressed in terms of those corresponding to the spanning tree agents. This will be used later in Chapters 4 and 5.

In the following definitions [23], we introduce the elements of the incidence matrices of a structurally balanced signed graph.

Definition 2 *Consider a structurally balanced undirected signed network $\mathcal{G}$, organized into two disjoint sets of vertices $\mathcal{V}_1$ and $\mathcal{V}_2$, that contains M signed edges and N nodes. Let $l,\ p,\ q \in \{1,2\}$. Then, the incidence matrix $E_s \in \mathbb{R}^{N\times M}$ of $\mathcal{G}$ is defined as*

$$[E_s]_{ik} := \begin{cases} +1 & \text{if } v_i \text{ is the initial node of the edge } \varepsilon_k; \\ -1 & \text{if } v_i, v_j \text{ are cooperative such that } v_i, v_j \in \mathcal{V}_l, \\ & \text{and } v_i \text{ is the terminal node of the edge } \varepsilon_k; \\ +1 & \text{if } v_i, v_j \text{ are competitive such that } v_i \in \mathcal{V}_p, v_j \in \mathcal{V}_q, \\ & \text{and } v_i \text{ is the terminal node of the edge } \varepsilon_k; \\ 0 & \text{otherwise,} \end{cases}$$

where $\varepsilon_k = \{v_i, v_j\},\ k \leq M,\ i,j \leq N$ are arbitrarily oriented edges.

To see that the signed incidence matrix is equivalent to the incidence matrix of an unsigned graph, we use the gauge transformation described in Section 2.3.1. For the incidence matrix of a structurally balanced signed graph, we may apply the *edge gauge transformation* on E_s, performed by the matrix $D = \text{diag}(\sigma)$ and $D_e = \text{diag}(\sigma_e)$, where $\sigma_e = [\sigma_{e_1},\ \ldots,\ \sigma_{e_n}]$, $i \in \mathcal{I}_M$ with $\sigma_{e_i} = 1$ if $v_i \in \mathcal{V}_1$ and $\sigma_{e_i} = -1$ if $v_i \in \mathcal{V}_2$ with v_i being the initial node of the edge, to obtain the incidence matrix $E = DE_sD_e$ of the unsigned graph [23, Lemma 4].

Then, the Laplacian matrix L_s and the edge Laplacian matrix $L_{e_s} \in \mathbb{R}^{M\times M}$ of a structurally-balanced undirected graph $\mathcal{G}$ satisfy

$$L_s = E_sE_s^\top, \quad L_{e_s} = E_s^\top E_s. \tag{2.44}$$

The following defines the in-incidence and out-incidence matrices of a signed network.

Definition 3 *Consider a structurally balanced directed signed network $\mathcal{G}$, organized into two disjoint sets of vertices $\mathcal{V}_1$ and $\mathcal{V}_2$, that contains M signed edges and N nodes. Let $l,\ p,\ q \in \{1,2\}$. Then, the in-incidence matrix $E_s \in \mathbb{R}^{N\times M}$ of $\mathcal{G}$ is defined as*

$$[E_{s\odot}]_{ik} := \begin{cases} -1 & \text{if } v_i, v_j \in \mathcal{V}_l \text{ and } v_i \text{ is the terminal node of the edge } \varepsilon_k; \\ +1 & \text{if } v_i \in \mathcal{V}_p, v_j \in \mathcal{V}_q \text{ and } v_i \text{ is the terminal node of the edge } \varepsilon_k; \\ 0 & \text{otherwise.} \end{cases} \tag{2.45}$$

Definition 4 *The out-incidence matrix $E_{s\otimes} \in \mathbb{R}^{N\times M}$ of a structurally balanced directed signed graph is given as*

$$[E_{s\otimes}]_{ik} := \begin{cases} +1 & \text{if } v_i \text{ is the initial node of the edge } \varepsilon_k; \\ 0 & \text{otherwise.} \end{cases} \tag{2.46}$$

Then, for directed networks, the incidence matrix may be expressed as the sum of two incidence matrices: $E_s = E_{s\odot} + E_{s\otimes}$.

The Laplacian matrix of the unsigned directed network was defined as $L = E_{\odot}E^{\top}$ in (2.43). Using the edge gauge transformation, we obtain the following.

$$L = DE_{s\odot}D_e(DE_sD_e)^{\top} = DE_{s\odot}D_eD_e^{\top}E_s^{\top}D^{\top} = DE_{s\odot}E_s^{\top}D \tag{2.47}$$

as $D_eD_e^{\top} = I_{M\times M}$. The edge Laplacian matrix of the unsigned directed network was defined as $L_e = E^{\top}E_{\odot}$ in (2.43). Applying edge gauge transformation, we obtain

$$L_e = E^{\top}E_{\odot} = (DE_sD_e)^{\top}DE_{s\odot}D_e = D_eE_s^{\top}D^{\top}DE_{s\odot}D_e = D_eE_s^{\top}E_{s\odot}D_e \tag{2.48}$$

as $D^{\top}D = I_{N\times N}$.

The Laplacian matrix L_s and the edge Laplacian matrix L_{e_s} of a signed digraph are defined as

$$L_s = E_{s\odot}E_s^{\top} \tag{2.49}$$

$$L_{e_s} = E_s^{\top}E_{s\odot}. \tag{2.50}$$

With these definitions, for a directed signed graph containing a spanning tree, we have the following linear algebraic properties:

(i) the non-zero eigenvalues of L_s and L_{e_s} coincide.

(ii) $\text{rank}(L_s) = \text{rank}(L_{e_s}) = N - 1$.

2.4.3 Edge convergence problems

Let us now address the bipartite consensus problem for a signed network in edge coordinates. Consider N scalar dynamical systems modeled by (2.11) and (2.33) and interconnected over a directed spanning tree. The states of the edges are given by

$$e_x = E_s^{\top}x. \tag{2.51}$$

Then, by differentiating the edge states, we obtain

$$\dot{e}_x = E_s^{\top}(-L_sx), \tag{2.52}$$

and from the definition of the Laplacian matrices in (2.50), we obtain

$$\dot{e}_x = -L_{e_s}e_x. \tag{2.53}$$

Since the considered graph is a spanning tree, it consists of $N-1$ edges, so $L_{e_s} \in \mathbb{R}^{(N-1)\times(N-1)}$ and the rank of the edge-Laplacian matrix L_{e_s} is $N-1$. Moreover, it only has eigenvalues with positive real parts, so $-L_{e_s}$ is Hurwitz. Then, given any symmetric positive definite matrix $Q \in \mathbb{R}^{N-1\times N-1}$, there exists a symmetric positive definite matrix $P \in \mathbb{R}^{N-1\times N-1}$ such that

$$PL_{e_s} + L_{e_s}^{\top}P = Q. \tag{2.54}$$

Consider the following Lyapunov function candidate.

$$V(e_x) = \frac{1}{2} e_x^\top P e_x,$$

where $P = P^\top > 0$. Its derivative along the trajectories yields

$$\dot{V}(e_x) = -e_x^\top Q e_x < 0,$$

which is strictly negative. Thus, since $V(e_x)$ is a strict Lyapunov function for (2.53), the origin $\{e_x = 0\}$ is exponentially stable.

Remark 8 *In the case of structurally balanced signed graphs containing more than $N-1$ edges, the edge-Laplacian matrix contains $M-N+1$ zero eigenvalues. $-L_{e_s}$ is not Hurwitz, and the Lyapunov equation (2.54) cannot be used to show the stability of the origin. The same technical problem appears when a network contains multiple leaders; the Laplacian matrix L_s associated with the graph also has more than one zero eigenvalue, so Proposition 1 cannot be used to construct a strict Lyapunov function. The stability analysis for Laplacian matrices containing more than one zero eigenvalue will be addressed in Chapter 3.* •

2.5 CONCLUSIONS

In this chapter, we presented elements of graph theory and an introduction to the fundamental coordination algorithms for networks with both cooperative and competitive interactions. The agreement and disagreement of agents depend on the network topology and on the signs of the interactions between them. In addition, for a class of signed networks that are structurally balanced, the graph can be transformed into an unsigned graph, enabling the tools adopted for traditional cooperative networks to be used. In particular, we saw that as signed networks represent a larger class of networks, the obtained results remain valid for networks with only cooperative interactions.

In the next chapters, we present our main contributions, which build upon these previous results.In particular, we present stronger stability results using strict Lyapunov functions and establishing robustness in terms of input-to-state stability for sets pertinent in the context of signed networked multi-agent systems. Furthermore, we also work on more general signed networks containing multiple roots or interconnected over a graph with nonlinear interconnections.

CHAPTER 3

BIPARTITE CONTAINMENT TRACKING OVER MULTI-LEADER SIGNED NETWORKS

In this chapter, we address the bipartite containment tracking-control problem over structurally balanced and unbalanced signed networks. We consider cooperative or competitive leaders for first-order and second-order systems. A leader is defined either as a single root agent or a strongly connected subgraph containing multiple nodes but without any incoming edges, as in [49]. In this setting, competitive leaders model enemy agents or obstacles to avoid, whereas cooperative leaders define the safe final destination. In contrast to [49], however, our results apply both to first- and second-order systems. Second-order systems better describe mechanical systems and a variety of feedback linearizable autonomous vehicles [94]. In contrast to [110, 53, 98], our main statements hold for the general case of signed networks that are either structurally balanced or unbalanced, and beyond bipartite containment tracking, we provide explicit estimates of the limit points of the followers.

Furthermore, we provide sufficient conditions for exponential stability of the containment set. In contrast to all references mentioned previously, our proofs are constructive; we provide strict Lyapunov functions regardless of whether the network is structurally balanced or unbalanced. Exponential stability is important because it is a stronger result than convergence to the limit points (or to the interior of a convex hull). In particular, it is equivalent to the existence of strict Lyapunov functions which in turn are significant because they are a basis for establishing input-to-state stability. Thus, our main results additionally guarantee the robustness of the containment set with respect to additive perturbations.

From a technical viewpoint, the contributions of this chapter are based on the framework introduced in [67]. But, we extend the method of the latter to general signed graphs containing multiple leaders and consider the multi-leader signed network in terms of two interconnected dynamical systems evolving in orthogonal spaces: dynamics of the leaders and synchronization errors relative to the leader groups. Thus, the bipartite containment problem is recast into one of stability of a set of appropriately

defined errors. Then, we generalize a statement in [68] on the Lyapunov characterization of exponential stability of sets to linear systems with one pole at zero and others having negative real parts. The technical results we provide here apply to systems with several poles at the origin. Then, in addition to exponential stability of the containment set, we provide the explicit limit values of the followers by a matrix determined by all eigenvectors associated with the zero eigenvalues in a similar way as explained in Sections 2.2 and 2.3. We demonstrate a possible form of these eigenvectors both for structurally balanced and unbalanced networks, and the elements of the eigenvectors are defined in more detail in Lemmata 7 and 8. In particular, as we consider *signed* networks, which are a more general representation than the traditional cooperative networks, our bipartite containment tracking results are valid in the context of containment *tracking*.

3.1 MOTIVATION AND PROBLEM FORMULATION

As we mentioned earlier, the bipartite containment tracking problem may appear in the context of herding control [80, 15, 26], in social network theory when deceiving influencers inject disinformation [2] or in aerospace applications involving the attitude control of multiple rigid bodies [48], to mention a few.

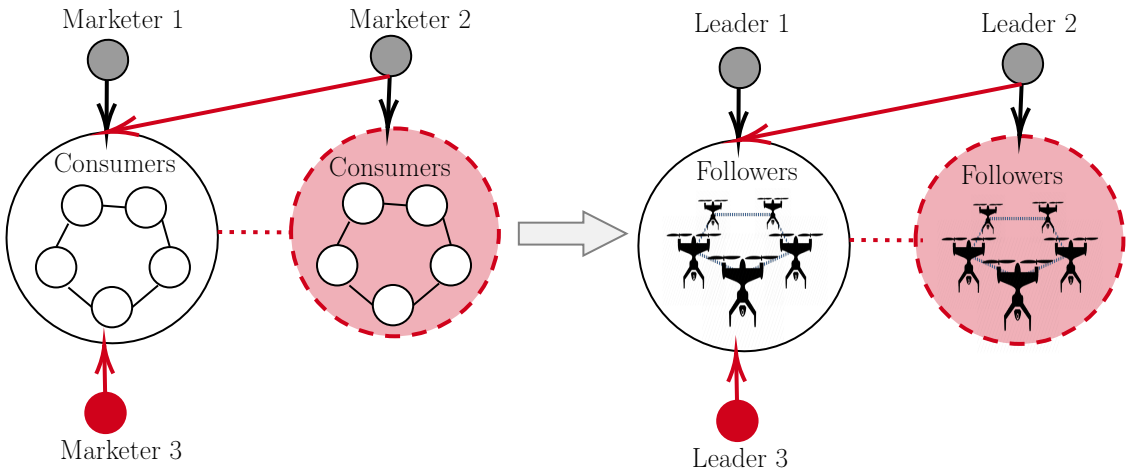

Figure 3.1: Presence of multiple cooperative and competitive leaders in two different scenarios: social networks and robotic applications.

To provide more concrete application scenarios, consider the following examples. In herding control, the objective is to herd a flock of birds (followers) away from the air space around an airport, where the air space can be seen as an obstacle to avoid and can be represented by a competitive agent, and toward a safe zone using unmanned aerial vehicles acting as cooperative leaders. In aerospace applications, the objective is to control multiple satellites, represented as cooperative agents, following one or more leaders. These leaders must navigate while avoiding debris or groups of enemy agents, which are modeled as non-cooperative agents. In the context of opinion dynamics within social networks, the behavior of consumers (followers) is influenced by both their neighbors and external influential entities, *e.g.*, marketers (represented by

the leaders). These marketers, often in competition, may be modeled as cooperative or competitive leaders belonging to two distinct disjoint subsets. The consumers' behavior is shaped by their level of trust, preference, and susceptibility to the influence of these marketers. If a consumer distrusts or dislikes one marketer, they may act oppositely, moving closer to the opposing marketer's position. Conversely, if a consumer trusts and favors both marketers, they are likely to position themselves between the two, leaning closer to the one who exerts a stronger influence.

For the sake of clarity and simplicity, let us first consider a group of N dynamical systems, containing the leaders and the followers, modeled by simple integrators, *i.e.,*

$$\dot{x}_i = u_i, \quad i \in \mathcal{I}_{\mathcal{N}} \tag{3.1}$$

where $x_i \in \mathbb{R}$ is the state[1] and $u_i \in \mathbb{R}$ is the input, and $\mathcal{I}_{\mathcal{N}} := \{1, 2, \ldots, N\}$. Agents interconnected over a directed signed graph containing a leader or a directed spanning tree achieve *bipartite consensus*, under the distributed control law

$$u_i = -\sum_{j=1}^{N} |a_{ij}|(x_i - \operatorname{sgn}(a_{ij})x_j), \tag{3.2}$$

if and only if the underlying graph is structurally balanced [2]. As we also explained in Chapter 2, the Laplacian matrix of a structurally balanced graph has a single zero eigenvalue [2], and the right eigenvector associated with the unique zero eigenvalue has all entries equal to either $+1$ or -1. Thereby, agents converge to the same state in modulus but with different signs.

In some cases, moreover, there may be several competitive agents, described as *competitive leaders*, that inject disinformation into the network. In this case, the agents can no longer achieve bipartite consensus, but instead they can achieve *bipartite containment* [49], where followers converge to the bipartite containment set defined by all cooperative leaders' trajectories and competitive leaders' symmetric trajectories. More precisely, for a multi-leader directed signed network, the achievable objective is *bipartite containment tracking*, that is,

$$\lim_{t\to\infty}[|x_j(t)| - \max_{i\in\mathcal{L}}|x_i(t)|] \leq 0, \quad \forall j \in \mathcal{F}, \tag{3.3}$$

where $\mathcal{L}$ and $\mathcal{F}$ are sets containing leader and follower nodes, respectively—see Assumption 2 below. For a more restrictive case of structurally balanced multi-leader signed networks, the bipartite containment set in (3.3) is refined to

$$\lim_{t\to\infty}[x_j(t) - \max_{i\in\mathcal{L}}\{\sigma_i x_i(t)\}][x_j(t) - \min_{i\in\mathcal{L}}\{\sigma_i x_i(t)\}] \leq 0, \tag{3.4}$$

where $j \in \mathcal{F}$, $\sigma_i = 1$ if $(i,j) \in \mathcal{V}_p, p \in \{1,2\}$ or $\sigma_i = -1$ if $i \in \mathcal{V}_p$, $j \in \mathcal{V}_q$ with $p, q \in \{1,2\}, p \neq q$. In contrast to the convex hull resulting from (3.3), that is

$$x_j(t) \in \left[-\max_{i\in\mathcal{L}}|x_i(t)|, \quad \max_{i\in\mathcal{L}}|x_i(t)|\right], \ \forall j \in \mathcal{F}, \quad \text{as } t \to \infty$$

[1]The following exposition applies to systems such that $x_i \in \mathbb{R}^n$ with appropriate modifications in the notation.

from (3.4), follower nodes in a structurally balanced signed network converge to a disconnected set composed of two disjoint convex subsets, that is

$$x_j(t) \in \left[\min_{i\in\mathcal{L}}\{\sigma_i x_i(t)\}, \quad \max_{i\in\mathcal{L}}\{\sigma_i x_i(t)\}\right], \ \forall j \in \mathcal{F}, \qquad \text{as } t \to \infty$$

—see Section 3.5

In what follows, we analyze the behavior of the networked systems modeled by simple integrators as in (3.1) in closed-loop with the distributed control law (3.2), and double integrators interconnected with the control law that will be presented later in Subsection 3.4. Moreover, we also assume that multiple cooperative and competitive leaders interfere in the network. Beyond the inequality in (3.3), commonly found in the literature—cf. [49], we give the explicit limit values of the followers' states depending only on the initial conditions of the leaders. To that end, we pose the following.

Assumption 2 *[Networks with multiple leaders]*

1. *The network contains N_L leaders, which can be organized into K groups of p_i leader(s), with $i \in \{1, 2, \ldots, K\}$, interconnected over a strongly connected subgraph, where $1 \leq K \leq N_L < N$, and $\sum_{i=1}^{K} p_i = N_L$ —cf.* [49, Definition 1].

2. *Given each follower ν_j, i.e., with $j \in \mathcal{F}$ with $\mathcal{F} := \{N_L + 1, N_L + 2, \ldots, N\}$, there exists at least one leader ν_i i.e., with $i \in \mathcal{L} := \{1, 2, \ldots, N_L\}$, such that there exists at least one path from ν_i to ν_j —cf.* [49, Condition 1].

In the case of a network containing only one leader, Assumption 2 boils down to the necessary condition for consensus that requires the existence of a directed spanning tree. As the networks considered here contain, *a priori*, more than one leader, the resulting Laplacian matrix has as many zero eigenvalues as the number of groups of leaders [11], and right and left eigenvectors associated with each zero eigenvalues. This results in multiple convergence points for the agents' trajectories.

In Chapter 2, we showed that under the distributed control law (2.12), the consensus problem (2.13) is solved if and only if the underlying graph contains a directed spanning tree. Moreover, we defined the consensus equilibrium with the left eigenvector associated with the zero eigenvalue as $x_m = v_l^\top x(0)$. We showed that since the network contains a directed spanning tree, the Laplacian matrix has a unique zero eigenvalue, and an associated right eigenvector of all ones, and all agents converge to the same equilibrium point. Furthermore, as we saw in Chapter 2, a strict Lyapunov function can be constructed to establish exponential stability of the origin in the space of the synchronization errors

$$e := x - v_r x_m,$$

where v_r is the right eigenvector associated with the zero eigenvalue [68]. Here, because of the presence of multiple leaders, the asymptotic values of the states of the agents are determined by all eigenvectors associated with the zero eigenvalues. One of this

chapter's contributions is to show that under the control law (3.2) and the Assumption 2, the limit values of the agents are given by

$$x_m := \mathbb{V}x, \tag{3.5}$$

where $\mathbb{V}$ is a matrix determined by all the eigenvectors associated with the N_L zero eigenvalues of the Laplacian matrix and $x = [x_1 \; x_2 \; \dots \; x_N]^\top$. More precisely,

$$\mathbb{V} := \sum_{i=1}^{K} \begin{bmatrix} v_{r_{i,1}} \\ v_{r_{i,2}} \\ \vdots \\ v_{r_{i,N}} \end{bmatrix} \begin{bmatrix} v_{l_{i,1}} & v_{l_{i,2}} & \dots & v_{l_{i,N}} \end{bmatrix}, \tag{3.6}$$

where v_{r_i} and v_{l_i} denote respectively the right and left eigenvectors of the Laplacian matrix L_s corresponding to the ith 0 eigenvalue and, for each $j \leq N$, $v_{r_{i,j}}$ and $v_{l_{i,j}}$ denote the jth element of the ith right and left eigenvectors, respectively. In particular, as we demonstrate further below, a possible form of the right and left eigenvectors associated with the zero eigenvalues is

$$v_{r_1} = \begin{bmatrix} 1_{p_1} \\ 0_{p_2} \\ \vdots \\ 0_{p_K} \\ \xi_1 \end{bmatrix}, \quad v_{r_2} = \begin{bmatrix} 0_{p_1} \\ 1_{p_2} \\ \vdots \\ 0_{p_K} \\ \xi_2 \end{bmatrix}, \quad \dots, \quad v_{r_K} = \begin{bmatrix} 0_{p_1} \\ 0_{p_2} \\ \vdots \\ 1_{p_K} \\ \xi_K \end{bmatrix}, \tag{3.7a}$$

$$v_{l_1} = \begin{bmatrix} \rho_{p_1} \\ 0_{p_2} \\ \vdots \\ 0_{p_K} \\ 0_{N-N_L} \end{bmatrix}, \; v_{l_2} = \begin{bmatrix} 0_{p_1} \\ \rho_{p_2} \\ \vdots \\ 0_{p_k} \\ 0_{N-N_L} \end{bmatrix}, \; \dots, \; v_{l_K} = \begin{bmatrix} 0_{p_1} \\ 0_{p_2} \\ \vdots \\ \rho_{p_K} \\ 0_{N-N_L} \end{bmatrix}, \tag{3.7b}$$

where $\xi_i \in \mathbb{R}^{N-N_L}$, $\mathbf{1}_{p_i} \in \mathbb{R}^{p_i}$ is a vector of ones, $0_{p_i} \in \mathbb{R}^{p_i}$ and $0_{N-N_L} \in \mathbb{R}^{N-N_L}$ are vectors of zeros, and $\rho_{p_i} \in \mathbb{R}^{p_i}$.

The structure of the right eigenvectors in (3.7a) provides information on the number of leaders in each leader group as well as the interactions between leaders and followers. For instance, if $p_1 = 1$, then $1_{p_1} = 1$, and all other elements of v_{r_1} up to ξ_1 are equal to zero. This indicates that the first leader group contains only one leader. Similarly, if $p_2 = 3$, then $1_{p_2} = [1 \; 1 \; 1]^\top$, and all other elements of v_{r_2} up to ξ_2 are equal to 0. In this case, the second leader group consists of three leaders, and so on. The elements of ξ_i, where $i \leq K$, can be positive, negative, or equal to zero depending on the follower's interactions with the leader groups. This will be defined more in detail in Lemmata 7 and 8 further below. The structure of the left eigenvectors in (3.7b) provides information about the interactions between the leaders, while the elements corresponding to the followers are zero. If $p_i = 1$, where $i \leq K$, then $\rho_{p_i} = 1$, meaning the corresponding left eigenvector v_{l_i} has a single non-zero element equal to 1. For $p_i > 1$, v_{l_i} has p_i elements within $(-1, 1)$, satisfying $\sum_{l=1}^{p_i} |\rho_l| = 1$ [83]. The definition of

the eigenvectors given in (3.7) covers that of [11, Corollary 4.2] and [55, Proposition 3], which are restricted to unsigned networks. With this under consideration, we establish bipartite containment of the system (3.1) and, more significantly, that $x \to x_m$—as defined in (3.5)—exponentially.

3.2 ANALYSIS APPROACH

The main results presented in this Chapter are based on original statements for signed networks with an associated Laplacian having multiple zero eigenvalues. First, following the framework laid in [67] and extending it to multi-leader signed networks, we show how to construct the matrix $\mathbb{V}$ in (3.5)-(3.6), to define the average states of the agents and the synchronization errors. Then, we extend the method of [68] to construct strict Lyapunov functions for linear systems with one zero eigenvalue to the case of multiple null eigenvalues. To that end, we first recall certain notations and definitions.

Definition 5 ([83]). *For any vertex i, we define the reachable set R_i as the set containing vertex i and all vertices j such that there exists a directed path from vertex i to vertex j. A reachable set is a maximal reachable set if $R = R_i$ for some i and there is no j such that $R_i \subset R_j$. The reachable set of vertices R is called a reach if it is a maximal reachable set, that consists of a leader group and its followers. For each reach $\mathcal{R}_i$ of a graph, we define the exclusive part of $\mathcal{R}_i$ as the set $\mathcal{H}_i = \mathcal{R}_i \backslash \bigcup_{j \neq i} \mathcal{R}_j$, i.e., the set of followers influenced only by the leader group i, and the common part of $\mathcal{R}_i$ as the set $\mathcal{C}_i = \mathcal{R}_i \backslash \mathcal{H}_i$, i.e., the set of followers influenced by leaders other than the ith leader group.*

The following statements, which lead to the construction of the matrix $\mathbb{V}$ in (3.6), are original contributions of this chapter, and they were presented in [83]. They extend Corollary 4.2 of [11] and Proposition 3 of [55] to the case of general signed networks.

Lemma 6 ([83]). *Let $\mathcal{G}$ denote a directed signed graph and let L_s denote the associated Laplacian matrix. Suppose $\mathcal{G}$ has N vertices and K reaches. Then, the algebraic and geometric multiplicity of the eigenvalue 0 is equal to K.*

Proof: Let $L := \mathcal{D} - |A|$ denote the Laplacian matrix of the unsigned graph $\mathcal{G}_+$, where $\mathcal{G}_+$ is obtained from $\mathcal{G}$ by applying a gauge transformation, $\mathcal{D}$ is the in-degree matrix and A is the adjacency matrix of $\mathcal{G}$. $\mathcal{G}_+$ and $\mathcal{G}$ have identical reaches. Then, the fact that the algebraic and geometric multiplicity of 0 equals K follows from [11, Theorem 3.2]. ■

Lemma 7 ([83]). *Let $\mathcal{G}$ denote a structurally unbalanced directed signed graph. Then, the eigenspace generated by the eigenvectors associated with the null eigenvalues has a basis defined by the vectors $\gamma_i \in \mathbb{R}^N$, with $i \leq K$, whose elements satisfy the following:*

(i) $\gamma_{i,j} = 0$ *for* $j \notin \mathcal{R}_i$,

(ii) $|\gamma_{i,j}| = 1$ *for* $j \in \mathcal{H}_i$,

(iii) $|\gamma_{i,j}| \leq 1$ *for* $j \in \mathcal{C}_i$,

(iv) $\sum_i |\gamma_{i,j}| \leq 1, \ \forall j \in \mathcal{I}_{\mathcal{N}}$,

where $j \in \mathcal{I}_{\mathcal{N}}$, *and* $\gamma_{i,j}$ *denotes the* j*th element of* γ_i.

Proof: For structurally unbalanced graphs satisfying Assumption 2, Items (i) and (ii), follow from Definition 5. Item (iii) follows from [51], while Item (iv) results from computing the null space of L, which is generated by $\gamma_i \in \mathbb{R}^N$ such that $L_s\gamma_i = 0$ for each $i \leq K$. This gives $L_s \sum_{i=1}^{K} \gamma_i = 0$. Then, under Assumption 2, the Laplacian matrix satisfies

$$L_s = \begin{bmatrix} L_l & 0 \\ -A_{lf} & L_f + \Delta_{|A_{lf}|} \end{bmatrix},$$

where $L_l \in \mathbb{R}^{N_L \times N_L}$ represents the interactions between the leaders, *i.e.,* the leader-leader part of the Laplacian matrix, $A_{lf} \in \mathbb{R}^{(N-N_L)\times N_L}$ represents the part of the adjacency matrix corresponding to the interactions between the leaders and the followers, while $L_f + \Delta_{|A_{lf}|} \in \mathbb{R}^{(N-N_L)\times(N-N_L)}$ denotes the sum of two matrices: L_f, which corresponds to the interactions between the followers, *i.e.,* the follower-follower part of the Laplacian matrix, and $\Delta_{|A_{lf}|}$, which is the in-degree matrix corresponding to the interactions between the leaders and the followers. Then, we have

$$-A_{lf} \sum_{i=1}^{K} \gamma_{i_{N_L}} + (L_f + \Delta_{|A_{lf}|}) \sum_{i=1}^{K} \gamma_{i_{N-N_L}} = 0,$$

where $\gamma_i = [\gamma_{i_{N_L}} \ \gamma_{i_{N-N_L}}]^\top$, $\gamma_{i_{N_L}} \in \mathbb{R}^{N_L}$ is the vector containing the first N_L elements of γ_i and $\gamma_{i_{N-N_L}} \in \mathbb{R}^{N-N_L}$ is the vector containing the last $N - N_L$ elements of γ_i. This yields

$$(L_f + \Delta_{|A_{lf}|}) \sum_{i=1}^{K} \gamma_{i_{N-N_L}} = A_{lf} \sum_{i=1}^{K} \gamma_{i_{N_L}},$$

where $\sum_{i=1}^{K} \gamma_{i_{N_L}} = \mathbf{1}_{N_L}$ from (3.7). Therefore, the sum of the remaining rows of γ_is gives the following,

$$\sum_{i=1}^{K} \gamma_{i_{N-N_L}} = (L_f + \Delta_{|A_{lf}|})^{-1} A_{lf} \mathbf{1}_{N_L}$$

and it follows that $\sum_{i=1}^{K} |\gamma_{i_{N-N_L}}| \leq \mathbf{1}_{N-N_L}$ from Lemma 6 of [49]. Thus, we conclude that $\gamma_{i,j} = 0$ for $j \notin \mathcal{R}_i$, $|\gamma_{i,j}| = 1$ for $j \in \mathcal{H}_i$, $|\gamma_{i,j}| \leq 1$ for $j \in \mathcal{C}_i$, and $\sum_j |\gamma_i| \leq \mathbf{1}_N$. ■

In the more restrictive case that $\mathcal{G}$ is structurally balanced, we have the following.

Lemma 8 ([83]). *Let* $\mathcal{G}$ *denote a structurally balanced directed signed graph. Then, the eigenspace generated by the eigenvectors associated with the null eigenvalues has a basis defined by the vectors* $\gamma_i \in \mathbb{R}^N$, *with* $i \leq K$, *whose elements satisfy the following:*

(i) $\gamma_{i,j} = 0$ *for* $j \notin \mathcal{R}_i$

(ii) $\gamma_{i,j} = \begin{cases} 1, & \text{if } (\nu_j, \nu_i) \in \mathcal{V}_l \\ -1, & \text{if } \nu_j \in \mathcal{V}_p, \ \nu_i \in \mathcal{V}_q, \end{cases}$ *for* $j \in \mathcal{H}_i$

(iii) $\gamma_{i,j} \in \begin{cases} (0,1), & \text{if } (\nu_j, \nu_i) \in \mathcal{V}_l \\ (-1,0), & \text{if } \nu_j \in \mathcal{V}_p,\ \nu_i \in \mathcal{V}_q \end{cases}$ *for* $j \in \mathcal{C}_i$

(iv) $\sum_i |\gamma_{i,j}| = 1,\ \forall j \in \mathcal{I}_{\mathcal{N}}$,

where $l \in \{1,2\}$, $p, q \in \{1,2\}$, $p \neq q$, $\mathcal{V}_1$ *and* $\mathcal{V}_2$ *are the two disjoint sets of vertices,* $i \in \mathcal{I}_{\mathcal{K}}$, $j \in \mathcal{I}_{\mathcal{N}}$, *and* $\gamma_{i,j}$ *denotes the* j*th element of* γ_i.

Proof: Since the graph is structurally balanced, we apply the *gauge transformation*, which consists in a change of coordinates performed by the matrix $D = \text{diag}(\sigma)$, where $\sigma = [\sigma_1, \ldots, \sigma_N], \sigma_j \in \{1, -1\}, j \in \mathcal{I}_{\mathcal{N}}$ [2]—see Chapter 2. Let $L = DL_sD$ denote the unsigned Laplacian matrix of the transformed network. Then, we may express the Laplacian L in Jordan canonical form, as $L_s = DLD = DP_D\Lambda P_D^{-1}D$, where $P_D = [v_{D_1}, \ldots, v_{D_K}, P_{D_1}] \in \mathbb{C}^{N\times N}$, $P_D^{-1} = \left[w_{D_1}^\top, \ldots, w_{D_K}^\top, P_{D_1}^\dagger\right]^\top \in \mathbb{C}^{N\times N}$, and $\Lambda \in \mathbb{C}^{N\times N}$, with v_{D_i} and $w_{D_i}, i \leq N_L$ are the right and left eigenvectors associated to K zero eigenvalues of L. From the Jordan decomposition, we can see that the basis of the null space of L_s is given by $L_sD\gamma_{D_i} = L_sDv_{D_i} = 0, i \leq K$ and has a basis defined by the columns of $\gamma = D\gamma_D$, where $\gamma_D = [\gamma_{D_1} \ \cdots \ \gamma_{D_K}]$ and the columns $\{\gamma_{D_i}\}$ constitute the basis of the associated eigenspace of L. Then, using [11, Corollary 4.2], we obtain the following for a structurally balanced signed network: $\gamma_{i,j} = \sigma_j\gamma_{D_{i,j}} = 0$ for $j \notin \mathcal{R}_i$, $\gamma_{i,j} = \sigma_j\gamma_{D_{i,j}} = \sigma_j$ for $i \in \mathcal{H}_i$, $\gamma_{i,j} = \sigma_j\gamma_{D_{i,j}} \in \sigma_j(0,1)$ for $j \in \mathcal{C}_i$ and $\sum_j \gamma_i = \sum_j D\gamma_{D_i} = D\mathbf{1}_N$, which gives $\sum_j |\gamma_i| = \mathbf{1}_N$. Items (i) to (iv) follow. ■

In general, for signed networks, after Lemma 7 and setting $v_{r_{i,j}} = \gamma_{i,j}$, we obtain the form given in (3.7a) for the K right eigenvectors associated to the K zero eigenvalues, such that for each $j \leq N_L$, $v_{r_{i,j}}$ is either equal to 1 or to 0, because the jth leader can only be in the exclusive part of its corresponding reach. The remaining rows $\xi_{i,j}$ of v_{r_i} belong, either to $\{-1, 1\}$ or to $(-1, 1)$, depending on the network's topology and signs of the interconnections. Moreover, under Assumption 2 and the given form in (3.7a) for right eigenvectors, as the Laplacian matrix has all entries equal to 0 for its first N_L rows, we obtain (3.7b) for K left eigenvectors associated to zero eigenvalues. Notice that, because of the form of the left eigenvectors, each column of the matrix $\mathbb{V}$ has the same properties as the basis defined in Lemma 7. Therefore, we may split $\mathbb{V}$ in four blocks, as follows:

$$\mathbb{V} = \sum_{i=1}^{K} v_{r_i} v_{l_i}^\top = \left[\begin{array}{c|c} V_l & 0_{N_L\times(N-N_L)} \\ \hline V_f & 0_{(N-N_L)\times(N-N_L)} \end{array}\right], \tag{3.8}$$

where $V_l \in \mathbb{R}^{N_L\times N_L}$ is a matrix that represents the interactions among the leaders and $V_f \in \mathbb{R}^{(N-N_L)\times N_L}$ represents those between leaders and followers.

If the leaders in the considered directed network are only single nodes, we have that $N_L = K$, and we have the following form for the N_L left eigenvectors associated with the zero eigenvalues:

$$v_{l_{i,j}} = \begin{cases} 1 & i = j \\ 0 & i \neq j \end{cases} \quad \forall i \leq N_L, \quad \forall j \leq N. \tag{3.9}$$

More precisely,

$$V_l = \begin{bmatrix} v_{r_{1,1}} v_{l_{1,1}} & & \\ & \ddots & \\ & & v_{r_{N_L,N_L}} v_{l_{N_L,N_L}} \end{bmatrix} = I_{N_L \times N_L}, \tag{3.10a}$$

$$V_f = \begin{bmatrix} v_{r_{1,N_L+1}} & \cdots & v_{r_{N_L,N_L+1}} \\ \vdots & \vdots & \vdots \\ v_{r_{1,N}} & \cdots & v_{r_{N_L,N}} \end{bmatrix}, \tag{3.10b}$$

so $\mathbb{V}$ has the following particular form

$$\mathbb{V} = \left[\begin{array}{c|c} I_{N_L \times N_L} & 0_{N_L \times (N-N_L)} \\ \hline V_f & 0_{(N-N_L)\times(N-N_L)} \end{array}\right]. \tag{3.11}$$

It is also important to remark that the elements of V_f have the properties stated in Lemma 7. This is significant because, owing to the fact that $x \to x_m$ where x_m is defined by (3.27), it is clear that V_f is the matrix that defines the limit point for the followers. Such limit points are determined purely by the leaders' initial conditions, as reflected by the columns of zeros in $\mathbb{V}$—see (3.8).

Now, similarly to the case of networks with one leader, where the error is defined as $e := x - v_r x_m$, with $x_m := v_l^\top x$, for multi-leader coopetition networks, we define the consensus errors as

$$e := [I - \mathbb{V}]x. \tag{3.12}$$

Then, to establish that $x_i \to x_m$ for all $i \leq N$ and, consequently, that the bipartite containment objective defined by (3.3) is achieved, we prove the stronger property of global exponential stability of the set $\{e = 0\}$. For that, we show how to construct strict—in the space of e— Lyapunov functions, based on the following proposition. Proposition 2 is another original contribution of this chapter and was originally presented in [83] and [18]. It extends Proposition 1 of [68] to the case of signed networks with multiple leaders.

Proposition 2 ([83]). *Let $\mathcal{G}$ be a directed signed network with multiple leaders. Then the following are equivalent:*

(i) *The graph has N_L leaders organized in K groups and, given each follower ν_j, with $j \in \mathcal{F}$, there exists at least one leader ν_i, with $i \in \mathcal{L}$, such that there exists at least one path from ν_i to ν_j.*

(ii) *For any $Q \in \mathbb{R}^{N\times N}, Q = Q^\top > 0$ and for any $\{\alpha_1, \alpha_2, \ldots, \alpha_K\}$ with $\alpha_i > 0$, there exists a matrix $P(\alpha_i) \in \mathbb{R}^{N\times N}$, $P = P^\top > 0$ such that*

$$PL_s + L_s^\top P = Q - \sum_{i=1}^{K} \alpha_i (P v_{ri} v_{li}^\top + v_{li} v_{ri}^\top P), \tag{3.13}$$

where $v_{ri}, v_{li} \in \mathbb{R}$ are the right and left eigenvectors of L_s associated with the ith eigenvalue equal to 0.

Proof of Proposition 2: (i) $\Rightarrow$ (ii): By assumption, the graph $\mathcal{G}$ has K leader groups and is connected. Then, from Lemma 6, it follows that L_s has K zero eigenvalues, and the rest of its eigenvalues have positive real parts:

$$0 = \lambda_1 = \cdots = \lambda_K < \mathrm{Re}(\lambda_{K+1}) \leq \cdots \leq \mathrm{Re}(\lambda_N).$$

Following the lines of proof as for Lemma 2 in [68], we can write the Jordan decomposition of L as

$$L_s = U\Lambda U^{-1} = \sum_{i=1}^{K} \lambda_i(L_s) v_{ri} v_{li}^\top + U_1 \Lambda_1 U_1^\dagger$$

with $\Lambda_1 \in \mathbb{C}^{N-K\times N-K}$, $U = [v_{r_1}, \ldots, v_{r_K}, U_1] \in \mathbb{C}^{N\times N}$ and $U^{-1} = \left[v_{l_1}^\top, \ldots, v_{l_K}^\top, U_1^\dagger\right]^\top \in \mathbb{C}^{N\times N}$. For any $\{\alpha_1, \alpha_2, \ldots, \alpha_K\}$ with $\alpha_i > 0$ define $R = L_s + \sum_{i=1}^{K} \alpha_i v_{ri} v_{li}^\top$. From this decomposition and the properties of Λ_1, $\mathrm{Re}\{\lambda_j(R)\} > 0$ for all $j \leq N$. $-R$ is Hurwitz, therefore for any $Q = Q^\top > 0$ and $\alpha_i > 0, i \leq N_L$, there exists $P = P^\top > 0$ such that

$$-PR - R^\top P = -Q,$$

$$-P(L_s + \sum_{i=1}^{K} \alpha_i v_{ri} v_{li}^\top) - (L_s + \sum_{i=1}^{K} \alpha_i v_{ri} v_{li}^\top)^\top P = -Q,$$

$$-PL_s - P\sum_{i=1}^{m} \alpha_i v_{ri} v_{li}^\top - L_s^\top P - \sum_{i=1}^{m} \alpha_i v_{li} v_{ri}^\top P = -Q$$

$$PL_s + L_s^\top P = Q - \sum_{i=1}^{K} \alpha_i (P v_{ri} v_{li}^\top + v_{li} v_{ri}^\top P).$$

(ii) $\Rightarrow$ (i): Let statement (ii) hold and assume that the Laplacian matrix has $K+1$ zero eigenvalues and the rest of its eigenvalues have positive real parts. In view of Lemma 6, the assumption that the system has K groups of leaders does not hold. Now, the Jordan decomposition of L_s has the form

$$L_s = U\Lambda U^{-1} = \sum_{i=1}^{K+1} \lambda_i(L_s) v_{ri} v_{li}^\top + U_1 \Lambda_1 U_1^\dagger$$

with $U = \left[v_{r_1}, \ldots, v_{r_{K+1}}, U_1\right]$ and $U^{-1} = \left[v_{l_1}^\top, \ldots, v_{l_{K+1}}^\top, U_1^\dagger\right]^\top$. Next let us consider $R(\alpha_i) = L_s + \sum_{i=1}^{K} \alpha_i v_{ri} v_{li}^\top$ which admits the Jordan decomposition $R := U\Lambda_R U^{-1}$, where

$$\Lambda_R := \begin{bmatrix} \alpha_1 & & & & \\ & \ddots & & & \\ & & \alpha_K & & \\ & & & 0 & \\ & & & & \Lambda_1 \end{bmatrix}.$$

Clearly, R is not positive definite because one of its eigenvalues is equal to zero. Then, there exists a matrix $Q = Q^\top$ for which there does not exist a matrix $P = P^\top$ such that $-PR - R^\top P = -Q$, which contradicts statement (ii). ■

Remark 9 *Proposition 2 provides a Lyapunov characterization of the second part of the Assumption 2.* •

3.3 FIRST-ORDER SYSTEMS

Exploiting the tools of the previous section, we now study exponential bipartite containment-tracking for first-order systems. In particular, we establish robustness in the sense of input-to-state stability with respect to external bounded perturbations.

3.3.1 Exponential stability

Consider the system (3.1), interconnected with the bipartite containment control law (3.2). Then, consider the errors defined in (3.12). Differentiating those, we get

$$\dot{e} = [I - \mathbb{V}]\dot{x} \tag{3.14}$$

and using (3.1), (3.2) and the fact that $L_s\mathbb{V} = 0$, we obtain

$$\begin{aligned}\dot{e} &= -[I - \mathbb{V}]L_s x \\ &= -[I - \mathbb{V}]L_s[I - \mathbb{V}]x\end{aligned}$$

and since $\mathbb{V}L_s = 0$, the closed-loop error dynamics read

$$\dot{e} = -L_s e. \tag{3.15}$$

This is a familiar equation, but in the present context, stability of the origin for (3.15) implies bipartite containment and not consensus. Accordingly, the bipartite containment problem is now recast as a problem of stability analysis of the dynamical system (3.15). Thus, relying on Proposition 2, the next statement provides sufficient conditions to achieve global exponential stability of the set $\{e = 0\}$, which is equivalent to the bipartite containment tracking objective (3.3).

Proposition 3 ([18]). *Consider the system (3.1) with the bipartite containment control law (3.2). Under the Assumption 2, for any $Q = Q^\top > 0$ there exists $P = P^\top > 0$ such that*

$$V(e) = e^\top P e, \quad \dot{V}(e) = -e^\top Q e. \tag{3.16}$$

Hence, the containment set $\{e = 0\}$ is exponentially stable for all initial states $x(0) \in \mathbb{R}^n$.

Proof: Let $Q = Q^\top > 0$, let $\alpha > 0$ be arbitrarily fixed, and let Proposition 2 generate $P = P^\top > 0$, such that (3.13) holds. Then, consider the Lyapunov function candidate $V(e) := e^\top P e$. The total time derivative of V along the trajectories yields

$$\dot{V}(e) = -e^\top Q e + e^\top \sum_{i=1}^{K} \alpha_i (P v_{ri} v_{li}^\top + v_{li} v_{ri}^\top P) e.$$

On the other hand, replacing (3.12) we obtain

$$\begin{aligned}\sum_{i=1}^{K} \alpha_i P v_{ri} v_{li}^\top e &= \sum_{i=1}^{K} \alpha_i P v_{ri} v_{li}^\top [I - \sum_{i=1}^{K} v_{ri} v_{li}^\top] x \\ &= \sum_{i=1}^{K} \alpha_i (P v_{ri} v_{li}^\top - P v_{ri} v_{li}^\top) x = 0,\end{aligned}$$

for which we used the identity $v_{li}^\top v_{ri} = 1, i \leq K$. Similarly, we obtain

$$e^\top \sum_{i=1}^{K} \alpha_i v_{li} v_{ri}^\top P = 0.$$

It follows that,

$$\dot{V}(e) = -e^\top Q e \leq -q_m |e|^2, \tag{3.17}$$

where $q_m > 0$ is the smallest eigenvalue of Q, so the statement of the proposition follows. ■

The following statement provides explicit expressions for the limit values of the followers' states.

Proposition 4 ([18]). *Consider system (3.1) with the bipartite containment control law (3.2). Under Assumption 2, the bipartite containment objective is achieved; that is, inequality (3.3) holds. Furthermore, if the leaders are static (i.e., $\dot{x}_l = 0$) , the final states of the followers satisfy*

$$\lim_{t\to\infty} x_f(t) = V_f x_l, \tag{3.18}$$

where x_l and x_f are the leaders' and the followers' states respectively and V_f is given in (3.10b).

Proof: Differentiating the weighted average of the system (3.5), we obtain the dynamical equation below

$$\dot{x}_m = \mathbb{V}\dot{x} = -\mathbb{V}L_s x = 0, \tag{3.19}$$

with $v_{l_i}^\top L_s = 0$ for each $i \leq K$. Its solution gives $x_m(t) = x_m(0)$. From Proposition 3, we have $\lim_{t\to\infty} e(t) = 0$, which gives $\lim_{t\to\infty} x(t) = x_m(t) = x_m(0)$. Then, using (3.11), we obtain the relation in (3.18). Under the Assumption 2 and from Item 4 of Lemmata 7 and 8, we have

$$\begin{aligned}\lim_{t\to\infty} |x_{f_j}(t)| = \left| \sum_{i=1}^{N_L} v_{N_L+j,i} x_{l_i} \right| &\leq \sum_{i=1}^{N_L} |v_{N_L+j,i}| \max_{1\leq i\leq N_L} |x_{l_i}| \\ &\leq \max_{1\leq i\leq N_L} |x_{l_i}|,\end{aligned}$$

where $v_{i,j}$ are the elements of the matrix $\mathbb{V}$ in (3.8) and $1 \leq j \leq N - N_L$. Then, the bipartite containment objective in (3.3) is achieved. ■

It is worth noting that for unsigned networks, the achievable objective is *containment* [7], that is,

$$\lim_{t\to\infty} [x_j(t) - \max_{i\in\mathcal{L}} x_i(t)][x_j(t) - \min_{i\in\mathcal{L}} x_i(t)] \leq 0. \tag{3.20}$$

Then, for such networks, we recover the following statement from Proposition 4.

Corollary 2 . *Consider the system (3.1) with the bipartite containment control law (3.2) and let the associated digraph be unsigned. Under the Assumption 2, the containment objective is achieved; that is, the inequality (3.20) holds.*

The advantage of disposing of a strict Lyapunov function is that the robustness of the bipartite containment set with respect to matching perturbations is also guaranteed. We discuss this in the following subsection.

3.3.2 Robustness analysis

Consider the perturbed first-order systems

$$\dot{x}_i = u_i + d_i(t), \tag{3.21}$$

where the disturbances $d_i : \mathbb{R}_{\geq 0} \to \mathbb{R}^n$ are assumed to be locally integrable functions. Under the control law (3.2), the system (3.21) becomes

$$\dot{x} = -L_s x + d(t). \tag{3.22}$$

Differentiating the errors in (3.14) on both sides, and using (3.22) we obtain

$$\dot{e} = -L_s e + [I - \mathbb{V}]d(t). \tag{3.23}$$

Then, we have the following.

Proposition 5 ([18]). *Under Assumption 2, the closed-loop system (3.23) is ISS.*

Proof: Consider the Lyapunov function candidate in (3.16). Its derivative gives

$$\dot{V}(e) = \frac{\partial V}{\partial e}[-L_s e] + \frac{\partial V}{\partial e}[I - \mathbb{V}]d.$$

From (3.17), we have

$$\begin{aligned}\dot{V}(e) &\leq -e^\top Q e + \frac{\partial V}{\partial e}[I - \mathbb{V}]d \\ &\leq -q_m|e|^2 + 2\overline{\lambda}_P|e||[I - \mathbb{V}]||d|.\end{aligned}$$

We know that $0 \leq |[I - \mathbb{V}]| \leq |I| + |\mathbb{V}| \leq 2$, because all eigenvalues of I are equal to 1 and all eigenvalues of $|\mathbb{V}|$ are either 1 or 0. Let $\delta > 0$ be such that $c := q_m - \frac{2\overline{\lambda}_P}{\delta} > 0$. Then,

$$\dot{V}(e) \leq -c|e|^2 + 2\delta|d|^2.$$

So V is an ISS Lyapunov function [88]. The statement follows. ■

3.4 SECOND-ORDER SYSTEMS

We now proceed with the extension of our analysis to more realistic agent dynamics. In particular, we consider a group of N second-order dynamical systems modeled by

$$\dot{x}_{1_i} = x_{2_i}, \quad x_{1_i},\ x_{2_i} \in \mathbb{R} \tag{3.24a}$$

$$\dot{x}_{2_i} = u_i, \quad u_i \in \mathbb{R},\ i \in \mathcal{I}_{\mathcal{N}}. \tag{3.24b}$$

The system (3.24) is a simple representation of an autonomous vehicle, in which x_{1_i} represents position and x_{2_i} denotes velocity—cf. [71]. More generally, such a model

may represent feedback-linearizable nonlinear systems that include a large class of systems.

To put our contributions in perspective, let us first recall that the consensus problem for (3.24), that is, to ensure that (2.13) holds, where $x_i = \begin{bmatrix} x_{1_i} & x_{2_i} \end{bmatrix}^\top$, via distributed control, is completely solved under various conditions on the interconnections and the resulting network's topology. For instance, for static directed networks, it is well-known that under the consensus-control law—*cf.* [7, Section 8],

$$u_i = -k_1 \sum_{j=1}^{N} a_{ij}(x_{1_i} - x_{1_j}) - k_2 \sum_{j=1}^{N} a_{ij}(x_{2_i} - x_{2_j}) - k_3 x_{2_i}, \tag{3.25}$$

with k_1, $k_2 > 0$ and $k_3 \geq 0$, the expressions in (2.13) hold if and only if the underlying graph contains a directed spanning tree [75]. The first two terms in (3.25) ensure position and velocity consensus respectively, *i.e.*, that (2.13) holds, but the latter does not necessarily imply that the systems *stabilize* at a common set-point, for which it is required, in addition, that $x_{2i} \to 0$. Indeed, we show in Section 3.4.1 that $x_{2i} \to 0$ is possible only if $k_3 > 0$. If $k_3 = 0$ the closed-loop solutions may grow unboundedly, but this is not necessarily nocuous; *e.g.*, the goal may be for a group of vehicles to continue advancing in formation at equal velocity without ever stopping, *i.e.,* achieve flocking [89, 24]. Thus, the gain k_3 may be freely chosen to be positive or null, depending on whether it is required that $x_{2i} \to 0$ or not, respectively—see Proposition 7 on p. 75.

For networks in which some of the nodes are *competitive*, the distributed consensus control law (3.25) may be replaced with

$$u_i = -k_1 \sum_{j=1}^{N} |a_{ij}|(x_{1_i} - \operatorname{sgn}(a_{ij}) x_{1_j}) - k_2 \sum_{j=1}^{N} |a_{ij}|(x_{2_i} - \operatorname{sgn}(a_{ij}) x_{2_j}) - k_3 x_{2_i}, \tag{3.26}$$

where $k_1, k_2 > 0$, and $k_3 \geq 0$. The first two terms result from a natural modification of (3.25), to take into account the signs of the interconnections—cf. [104]. Under the distributed control law (3.26), agents on a directed connected signed network containing a directed spanning tree achieve *bipartite consensus* if and only if the underlying graph is structurally balanced [2].

In this memoir, we consider bipartite containment protocols for second-order systems, with and without absolute velocity damping, *i.e.,* $k_3 > 0$ and $k_3 = 0$. We show that under the control law (3.26) and the Assumption 2, the agents' states converge to

$$x_m := (\mathbb{V} \otimes I_2)x, \tag{3.27}$$

where $\mathbb{V}$ is defined in (3.6) and the synchronization errors are given as

$$e := ([I - \mathbb{V}] \otimes I_2)x, \tag{3.28}$$

where $e = \begin{bmatrix} e_1 & e_2 \end{bmatrix}^\top$. Then, to establish beyond the convergence statements that $x_1 \to x_{1_m}$ and $x_2 \to x_{2_m}$ and, consequently, the bipartite containment objectives defined by (3.3), we prove the stronger property of global exponential stability of the set $\{x \in \mathbb{R}^{2N} : (e_1, e_2) = (0, 0)\}$. For that, we construct strict—in the space of (e_1, e_2)—Lyapunov functions, based on Proposition 2. Furthermore, we establish robustness of the bipartite containment tracking in the sense of input-to-state stability with respect to external bounded perturbations.

3.4.1 Exponential stability

Consider the system (3.24), interconnected with the bipartite containment control law (3.26) and the errors defined in (3.28). Differentiating the errors along closed-loop trajectories, we obtain

$$\dot{e} = ([I - \mathbb{V}] \otimes I_2)\dot{x}$$

and using (3.24) and (3.26), we obtain the closed-loop dynamical equations

$$\dot{e}_1 = e_2 \tag{3.29a}$$
$$\dot{e}_2 = -k_1 L_s e_1 - k_2 L_s e_2 - k_3 e_2. \tag{3.29b}$$

Guaranteeing the bipartite containment problem is now recast as a problem of stability analysis of the dynamical system (3.29). Thus, relying on Proposition 2, our next statement provides sufficient conditions on the controller gains to achieve global exponential stability of the set $\{(e_1, e_2) = (0, 0)\}$, which covers the bipartite containment tracking objective (3.3).

Proposition 6 ([83]). *Consider the system (3.29) and let P be generated by (3.13) with $Q = I_N$. Then, under the Assumption 2, the set $\{(e_1, e_2) = (0, 0)\}$ is exponentially stable if*

$$k_1 > 0, \tag{3.30a}$$
$$k_2 > 2\sqrt{k_1 \overline{\lambda}_P}, \tag{3.30b}$$
$$\frac{k_2}{k_3} \geq \overline{\lambda}_P, \quad k_3 \geq 0, \tag{3.30c}$$

where $\overline{\lambda}_P \geq |P|$ is the largest eigenvalue of P.

Proof of Proposition 6: Let $Q = Q^\top > 0$ and $\alpha > 0$ be arbitrarily fixed. Since by the Assumption 2 and Proposition 2, $\exists P = P^\top > 0$ such that (3.13) holds. Then, consider the following Lyapunov function candidate

$$V(e) = \frac{1}{2}|e_1|^2 + \epsilon e_1^\top P e_2 + \mu e_2^\top P e_2, \tag{3.31}$$

which is positive definite (for all e as in (3.28)), under the condition $\epsilon \leq \sqrt{\frac{2\mu}{|P|}}$, $\mu > 0$. This can be shown by rewriting the Lyapunov function in vector form

$$V(e) = \frac{1}{2}\begin{bmatrix} e_1 \\ e_2 \end{bmatrix}^\top \begin{bmatrix} I & \epsilon P \\ \epsilon P & 2\mu P \end{bmatrix} \begin{bmatrix} e_1 \\ e_2 \end{bmatrix}. \tag{3.32}$$

For the matrix in (3.32) to be positive definite, the Schur complement condition requires $2\mu P - \epsilon^2 P^2 > 0$, which simplifies to $2\mu - \epsilon^2 |P| \geq 0$. This is satisfied when $\epsilon \leq \sqrt{\frac{2\mu}{|P|}}$ and $\mu > 0$.

The total time derivative of V along the trajectories yields

$$\begin{aligned}\dot{V}(e) = &- k_1\epsilon e_1^\top P L_s e_1 - e_2^\top [k_2\mu(PL_s + L_s^\top P) + 2k_3\mu P - \epsilon P]e_2 \\ &+ e_1^\top (I - k_2\epsilon P L_s - 2k_1\mu L^\top P - k_3\epsilon P)e_2.\end{aligned}$$

Let $\mu > 0$ be such that $2k_1\mu = k_2\epsilon = 1$. Using (3.13) with $Q = I_N$ and the identity

$$P\sum_{i=1}^{K} v_{r_i} v_{l_i}^\top e_1 = P\sum_{i=1}^{K} v_{r_i} v_{l_i}^\top e_2 = 0$$

we obtain the following:

$$\begin{aligned}-k_1\epsilon e_1^\top P L_s e_1 &= - k_1\epsilon e_1^\top (PL_s + L_s^\top P)e_1 \\ &= -\frac{1}{2}k_1\epsilon |e_1|^2, \\ -e_2^\top \mu k_2 (PL_s + L_s^\top P)e_2 &= - \mu k_2 e_2^\top e_2, \\ e_1^\top [I - (L_s^\top P + PL_s)]e_2 &= - e_1^\top [I - I]e_2 \\ &= 0.\end{aligned}$$

Hence, in compact form, we have

$$\dot{V}(e) = -\frac{1}{2}\begin{bmatrix} e_1 \\ e_2 \end{bmatrix}^\top \begin{bmatrix} k_1\epsilon I & k_3\epsilon P \\ k_3\epsilon P & 2\mu k_2 I + 4k_3\mu P - 2\epsilon P \end{bmatrix} \begin{bmatrix} e_1 \\ e_2 \end{bmatrix} \tag{3.33}$$

or, equivalently,

$$\dot{V}(e) = -\frac{1}{2}e^\top \begin{bmatrix} \frac{1}{2}k_1\epsilon I & k_3\epsilon P \\ k_3\epsilon P & 4k_3\mu P \end{bmatrix} e - \frac{1}{4}k_1\epsilon |e_1|^2 - e_2^\top [k_2\mu I - \epsilon P]e_2. \tag{3.34}$$

That is, $\dot{V}$ is negative definite if the matrix in (3.34) is positive semi-definite and $[k_2\mu I - \epsilon P]$ is positive definite. The latter holds, in view of the fact that $2k_1\mu = k_2\epsilon = 1$, if and only if

$$k_2 I - 2\frac{k_1}{k_2}\overline{\lambda}_P I > 0.$$

In turn, the previous inequality holds if $k_2 > \sqrt{2k_1\overline{\lambda}_P}$, that is, under condition (3.30b). Then, computing the Schur complement [28], the condition for the matrix in (3.34) to be positive semi-definite, is $4k_3\mu P - (k_3\epsilon P)^\top \frac{2}{k_1\epsilon} k_3\epsilon P \geq 0$. If $k_3 = 0$ the latter holds trivially. Otherwise, considering $k_3 > 0$, and using $2\frac{k_1}{k_2} = \frac{\epsilon}{\mu}$, we see that the latter inequality is equivalent to

$$\begin{aligned}2\frac{\mu}{\mu}I - \frac{k_3}{k_1}\frac{\epsilon}{\mu}P &= 2\frac{\mu}{\mu}I - \frac{k_3}{k_1}\frac{2k_1}{k_2}P \\ &= 1 - \frac{k_3}{k_2}\overline{\lambda}_P \geq 0,\end{aligned}$$

which is satisfied under (3.30c). We conclude that

$$\dot{V}(e) \leq -\frac{1}{4}\Big[\, \epsilon k_1 |e_1|^2 + [k_2\mu - \epsilon\bar{\lambda}_P]|e_2|^2 \,\Big], \tag{3.35}$$

so the statement of the proposition follows. ■

Remark 10 *For conciseness, we consider in one statement the two interesting and distinct cases evoked previously, that $k_3 = 0$ or $k_3 > 0$. Note that if k_3 is chosen to be null (3.30c) trivially holds, but if it is positive (3.30c) defines a condition on k_2 and k_3, relative to $\bar{\lambda}_P$, which depends on the Laplacian L_s—see (3.13).* •

From the proof of Proposition 6 it is clear that the value of $k_3 \geq 0$ is inconsequential to the exponential stability of the containment set. Nevertheless, as mentioned above, it plays a role in the solutions' behavior. This is stated next.

Proposition 7 ([83]). *Consider the system (3.24) and the bipartite containment control law (3.26). Under the Assumption 2, the bipartite containment objective is achieved, that is, the inequalities (3.3) hold. Furthermore, if $k_3 > 0$, the final states of the followers satisfy*

$$\lim_{t\to\infty} x_{1_f}(t) = V_f x_{1_l}(0) + \frac{1}{k_3} V_f x_{2_l}(0), \tag{3.36a}$$

$$\lim_{t\to\infty} x_{2_f}(t) = 0. \tag{3.36b}$$

On the other hand, if $k_3 = 0$,

$$\lim_{t\to\infty} x_{1_f}(t) = V_f x_{1_l}(0) + t V_f x_{2_l}, \tag{3.37a}$$

$$\lim_{t\to\infty} x_{2_f}(t) = V_f x_{2_l}, \tag{3.37b}$$

where x_l and x_f are leaders' and followers' states respectively and $V_f \in \mathbb{R}^{(N-N_L)\times N_L}$ is given in (3.8).

Proof: Differentiating the weighted average of the system (3.27), we obtain the dynamical equations below

$$\dot{x}_{1_m} = \mathbb{V}\dot{x}_1 = \mathbb{V}x_2 = x_{2_m}, \tag{3.38a}$$

$$\begin{aligned} \dot{x}_{2_m} &= \mathbb{V}\dot{x}_2 \\ &= \mathbb{V}(-k_1 L_s x_1 - k_2 L_s x_2 - k_3 x_2) \\ &= -k_3 x_{2_m}, \end{aligned} \tag{3.38b}$$

with $v_{li}^\top L_s = 0$ for $i \leq K$. Their solutions yield

$$x_{2_m}(t) = x_{2_m}(0) e^{-k_3 t}, \tag{3.39a}$$

$$x_{1_m}(t) = x_{1_m}(0) + x_{2_m}(0) \int_0^t e^{-k_3 s} ds. \tag{3.39b}$$

Now, from Proposition 6, we have $\lim_{t\to\infty} e(t) = 0$, which results in

$$\lim_{t\to\infty} x(t) = x_m(t).$$

On the other hand, from (3.39), we obtain

$$\lim_{t\to\infty} x_2(t) = 0$$

and

$$\lim_{t\to\infty} x_1(t) = x_{1_m}(0) + \frac{1}{k_3} x_{2_m}(0).$$

Then, using (3.8), we obtain the relations in (3.36). Under the Assumption 2 and from Item (iv) of Lemmata 7 and 8,

$$\begin{aligned}
\lim_{t\to\infty} |x_{1_{fj}}(t)| &= \sum_{i=1}^{N_L} |v_{N_L+j,i} x_{1_{li}}(0) + \frac{1}{k_3} v_{N_L+j,i} x_{2_{li}}(0)| \\
&\leq \sum_{i=1}^{N_L} |v_{N_L+j,i}||x_{1_{li}}(0) + \frac{1}{k_3} x_{2_{li}}(0)| \\
&\leq \sum_{i=1}^{N_L} |v_{N_L+j,i} x_{1_{li}}(0)| + |\frac{1}{k_3} v_{N_L+j,i} x_{2_{li}}(0)| \\
&\leq \sum_{i=1}^{N_L} |v_{N_L+j,i}||x_{1_{li}}(t)| \leq \max_{1\leq i\leq N_L} |x_{1_{li}}(t)|,
\end{aligned}$$

where $1 \leq j \leq N - N_L$ and $v_{i,j}$ are the elements of the matrix $\mathbb{V}$ in (3.8). In the case when $k_3 = 0$, (3.38) becomes

$$\begin{aligned}
\dot{x}_{1_m} &= x_{2_m}, \\
\dot{x}_{2_m} &= 0,
\end{aligned}$$

so

$$x_{2_m}(t) = x_{2_m}(0), \tag{3.40a}$$

$$x_{1_m}(t) = x_{1_m}(0) + t x_{2_m}(0). \tag{3.40b}$$

From (3.40), we obtain $\lim_{t\to\infty} x_2(t) = x_{2_m}(0)$ and $\lim_{t\to\infty} x_1(t) = x_{1_m}(0) + x_{2_m}(0)t$. Then using (3.8), we obtain the relations in (3.37). Under the Assumption 2 and from Items (iv) of Lemmata 7 and 8, we have

$$\begin{aligned}
\lim_{t\to\infty} |x_{2_{fj}}(t)| &= \sum_{i=1}^{N_L} |v_{N_L+j,i} x_{2_{li}}| \leq \sum_{i=1}^{N_L} |v_{N_L+j,i}| \max_{1\leq i\leq N_L} |x_{2_{li}}| \\
&\leq \max_{1\leq i\leq N_L} |x_{2_{li}}|, \\
\lim_{t\to\infty} |x_{1_{fj}}(t)| &= \sum_{i=1}^{N_L} |v_{N_L+j,i} x_{1_{li}}(0) + t v_{N_L+j,i} x_{2_{li}}| \\
&\leq \max_{1\leq i\leq N_L} |x_{1_{li}}(0)| + t \max_{1\leq i\leq N_L} |x_{2_{li}}| \\
&\leq \max_{1\leq i\leq N_L} |x_{1_{li}}(t)|,
\end{aligned}$$

so (3.3) follows. ■

On the other hand, we recover the following statement from Proposition 7.

Corollary 3 ([83]). *Consider the system (3.24) with the containment control law (3.26) and let the associated digraph be unsigned. Under the Assumption 2, the containment objective is achieved, that is the inequality (3.20) holds.*

Next, we use the strict Lyapunov functions constructed above to conduct a robustness analysis of the control law (3.26), in the sense of input-to-state stability of the bipartite containment tracking.

3.4.2 Robustness analysis

Consider the perturbed second-order systems

$$\dot{x}_{1_i} = x_{2_i} \tag{3.41a}$$
$$\dot{x}_{2_i} = u_i + d_i(t), \tag{3.41b}$$

where the disturbances $d_i : \mathbb{R}_{\geq 0} \to \mathbb{R}^N$ are assumed to be essentially bounded locally integrable functions, $d_i(t) \leq \bar{d} := \text{ess sup}_{t\geq 0}|d(t)|$. Under the action of the control law (3.26), the system (3.41) becomes

$$\dot{x}_1 = x_2 \tag{3.42a}$$
$$\dot{x}_2 = -k_1 L_s x_1 - k_2 L_s x_2 - k_3 x_2 + d(t), \tag{3.42b}$$

where $d := [d_i] \in \mathbb{R}^N$. Differentiating the errors in (3.28) on both sides and using (3.42) we obtain

$$\dot{e}_1 = e_2 \tag{3.43a}$$
$$\dot{e}_2 = -k_1 L_s e_1 - k_2 L_s e_2 - k_3 e_2 + [I - \mathbb{V}]d(t). \tag{3.43b}$$

Then, we have the following.

Proposition 8 *([83]). The closed-loop system (3.43), under the Assumption 2, is input-to-state stable with respect to essentially bounded, locally integrable external disturbances if the conditions in (3.30) hold.*

Proof: Consider the Lyapunov function (3.31) which is positive definite, under the condition $\epsilon \leq \sqrt{\frac{2\mu}{|P|}}$, $\mu > 0$. The total time derivative of V along the trajectories of (3.43) yields

$$\dot{V}(e) = \frac{\partial V}{\partial e_1} e_2 + \frac{\partial V}{\partial e_2}\left[-k_1 L_s e_1 - k_2 L_s e_2 - k_3 e_2\right] + \frac{\partial V}{\partial e_2}[I - \mathbb{V}]d. \tag{3.44}$$

Then, from (3.35), we obtain

$$\begin{aligned}\dot{V}(e) &\leq -\frac{1}{4}[\epsilon k_1 |e_1|^2 + (k_2\mu - \epsilon\overline{\lambda}_P)|e_2|^2] + \frac{\partial V}{\partial e_2}|[I - \mathbb{V}]||d| \\ &\leq -\frac{1}{4}\epsilon k_1 |e_1|^2 - \frac{1}{4}(k_2\mu - \epsilon\overline{\lambda}_P)|e_2|^2 \\ &\quad + \epsilon\overline{\lambda}_P e_1^\top |[I - \mathbb{V}]|d + 2\mu\overline{\lambda}_P e_2^\top |[I - \mathbb{V}]||d|.\end{aligned} \tag{3.45}$$

Now, we know that $0 \leq |[I - \mathbb{V}]| \leq |I| + |\mathbb{V}| \leq 2$, because all eigenvalues of I are equal to 1 and all eigenvalues of $|\mathbb{V}|$ are either 1 or 0. Let $\delta > 0$ be such that

$$c_1 := \frac{1}{4}(\epsilon k_1 - \frac{4}{\delta}\epsilon\overline{\lambda}_P) > 0$$

and

$$c_2 := \frac{1}{4}(k_2\mu - \epsilon\overline{\lambda}_P - \frac{8}{\delta}\mu\overline{\lambda}_P) > 0.$$

Then, since $|I - \mathbb{V}| \leq 2$, it follows from (3.45) that

$$\dot{V}(e) \leq -c_1|e_1|^2 - c_2|e_2|^2 + c_3|d|^2,$$

with $c_3 = \overline{\lambda}_P\delta(\epsilon + 2\mu) > 0$. Thus, V is an ISS Lyapunov function for the system (3.43), and the latter is input-to-state stable with respect to matched disturbances. ■

In the case of cooperative systems, Proposition 8 boils down to the following corollary.

Corollary 4 ([83]). *The system (3.43), under the Assumption 2 and over an unsigned network, is input-to-state stable with respect to an essentially bounded, locally integrable external disturbance if the conditions in (3.30) hold.*

3.5 NUMERICAL EXAMPLES

To illustrate our theoretical findings, we present a numerical example of a system of multi-wheeled mobile robots modeled as unicycles over both structurally balanced and unbalanced networks. As mentioned in Remark 1, we apply our results presented for one-dimension systems to systems of higher dimensions.

3.5.1 First-order systems

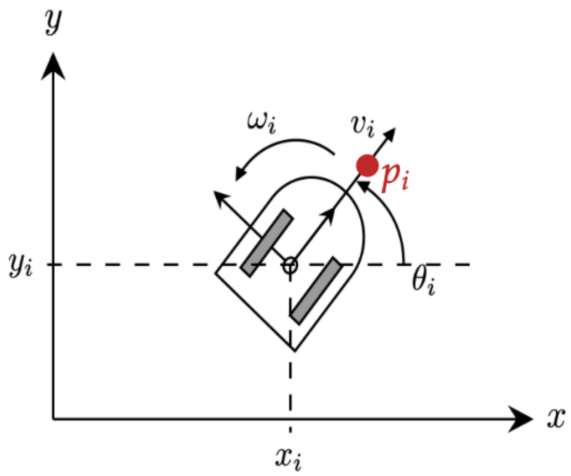

Figure 3.2: Schematic representation of a unicycle

Consider a unicycle vehicle as the one illustrated in Figure 3.2. Let

$$r_i = [r_{x_i}\ r_{y_i}]^\top \in \mathbb{R}^2$$

be the inertial position, θ_i the orientation, s_i the linear speed, and ω_i the angular speed of the ith robot. The objective of the team of unicycles is to make the follower unicycles converge to a safe zone defined by the cooperative leader unicycles and away from the competitive leader unicycles—see the bipartite containment set defined in (3.3). Then, the dynamics of such a wheeled mobile robot can be modeled as [94]

$$\begin{bmatrix} \dot{r}_{x_i} \\ \dot{r}_{y_i} \\ \dot{\theta}_i \end{bmatrix} = \begin{bmatrix} s_i \cos\theta_i \\ s_i \sin\theta_i \\ \omega_i \end{bmatrix}. \tag{3.46}$$

To apply the consensus control law (3.2)—designed for (3.1)—to this system we apply a preliminary feedback linearizing control. To that end, we rewrite the system's dynamics in terms of the position of a point located at a distance δ_i from the axis connecting the wheels. This allows us to control the system's position using the coordinates of this reference point. We choose the reference point p_i

$$p_i = r_i + \delta_i \begin{pmatrix} \cos\theta_i \\ \sin\theta_i \end{pmatrix}$$

located at a distance $\delta_i = 0.1$m ffrom the axis connecting the wheels, along a direction perpendicular to the wheels' axis. Now, to achieve bipartite containment on the reference points p_i, we look at its dynamics. Differentiating p_i with respect to time, we obtain

$$\begin{bmatrix} \dot{p}_{x_i} \\ \dot{p}_{y_i} \end{bmatrix} = \begin{bmatrix} s_i \cos\theta_i - \delta_i \omega_i \sin\theta_i \\ s_i \sin\theta_i + \delta_i \omega_i \cos\theta_i \end{bmatrix}. \tag{3.47}$$

Since we can control the velocity, let

$$\begin{bmatrix} s_i \\ \omega_i \end{bmatrix} = \begin{bmatrix} \cos(\theta_i) & \sin(\theta_i) \\ -\frac{1}{\delta_i}\sin(\theta_i) & \frac{1}{\delta_i}\cos(\theta_i) \end{bmatrix} \begin{bmatrix} u_{x_i} \\ u_{y_i} \end{bmatrix}, \tag{3.48}$$

so (3.47) becomes

$$\begin{bmatrix} \dot{p}_{x_i} \\ \dot{p}_{y_i} \end{bmatrix} = \begin{bmatrix} u_{x_i} \\ u_{y_i} \end{bmatrix},$$

which is a simplified kinematic equation in the form of first-order dynamics. For the simulations examples, we implemented (3.46) with u_i as in (3.2), where $x_i = [p_{x_i}\ p_{y_i}]^\top$.

3.5.1.1 Structurally balanced networks

We consider a coopetition network containing $N = 7$ agents with three leaders $\nu_i, i \leq 3$ and four followers $\nu_j, 4 \leq j \leq 7$, communicating over a structurally balanced directed graph as the one depicted in Figure 3.3. The competitive leader ν_3 represents an obstacle in the system. For clarity, we stress that, in this example, we consider a leader node to be one that has no incoming edges, and we assume them to be static.

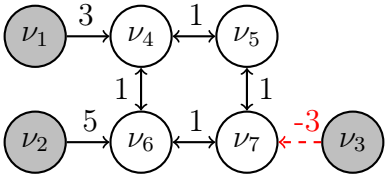

Figure 3.3: A network of seven mobile robots with 2 cooperative and 1 competitive leaders.

According to (2.25), the Laplacian matrix corresponding to the graph is

$$L_s = \begin{bmatrix} 0 & 0 & 0 & 0 & 0 & 0 & 0 \\ 0 & 0 & 0 & 0 & 0 & 0 & 0 \\ 0 & 0 & 0 & 0 & 0 & 0 & 0 \\ -3 & 0 & 0 & 5 & -1 & -1 & 0 \\ 0 & 0 & 0 & -1 & 2 & 0 & -1 \\ 0 & -5 & 0 & -1 & 0 & 7 & -1 \\ 0 & 0 & 3 & 0 & -1 & -1 & 5 \end{bmatrix}$$

and its eigenvalues are $\lambda_L = 0,\ 0,\ 0,\ 1.38,\ 4.80,\ 7.81$, and 5. The network may be bipartitioned into two subgroups as

$$\mathcal{V}_1 = \{\nu_1, \nu_2, \nu_4, \nu_5, \nu_6, \nu_7\}, \quad \mathcal{V}_2 = \{\nu_3\}$$

so it is structurally balanced. Then, the right and left eigenvectors associated with each zero eigenvalue are given by

$$\begin{aligned} v_{r_1} &= \begin{bmatrix} 1 & 0 & 0 & 0.7038 & 0.4038 & 0.1154 & 0.1038 \end{bmatrix}^\top, & v_{l_1} &= \begin{bmatrix} 1 & 0 & 0 & 0 & 0 & 0 & 0 \end{bmatrix}^\top \\ v_{r_2} &= \begin{bmatrix} 0 & 1 & 0 & 0.1923 & 0.1923 & 0.7692 & 0.1923 \end{bmatrix}^\top, & v_{l_2} &= \begin{bmatrix} 0 & 1 & 0 & 0 & 0 & 0 & 0 \end{bmatrix}^\top \\ v_{r_3} &= \begin{bmatrix} 0 & 0 & 1 & -0.1038 & -0.4038 & -0.1154 & -0.7038 \end{bmatrix}^\top, & v_{l_3} &= \begin{bmatrix} 0 & 0 & 1 & 0 & 0 & 0 & 0 \end{bmatrix}^\top. \end{aligned}$$

The matrices V_l and V_f in (3.8) are then calculated to be

$$V_l = \begin{bmatrix} 1 & 0 & 0 \\ 0 & 1 & 0 \\ 0 & 0 & 1 \end{bmatrix}, \ V_f = \begin{bmatrix} 0.7038 & 0.1923 & -0.1038 \\ 0.4038 & 0.1923 & -0.4038 \\ 0.1154 & 0.7692 & -0.1154 \\ 0.1038 & 0.1923 & -0.7038 \end{bmatrix}.$$

Notice that since in the graph considered above, the leaders have no neighbors, V_l has the form as in (3.11). We also remark that V_f has the properties stated in Items (i)–(iv) of Lemma 8. Since each follower is influenced by the three leaders, 0 is not an element of V_f (Item (i)). Moreover, none of the followers corresponds to the exclusive part of a reach, so V_f does not have an element equal to ± 1 (Item (ii)). From the structural-balance property, all elements corresponding to leaders ν_1 and ν_2 (the first two columns) are positive and less than one, whereas the elements corresponding to leader ν_3 (on the last column) are negative and greater than -1 (Item (iii)). We also remark that the sum of the absolute values of the terms on each row is equal to 1 (Item (iv)).

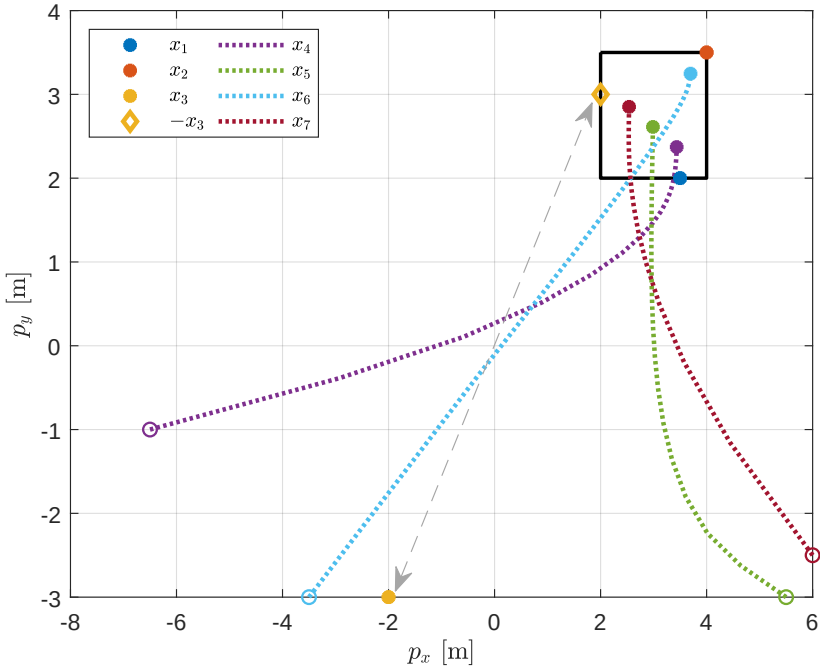

Figure 3.4: Bipartite containment tracking of system (3.50) with control input (3.48), $[u_{x_i}\ u_{y_i}] =: u_i$ and u_i as in (3.2). The filled dots are the final states of the mobile robots, and the dotted lines represent the trajectory of the four followers. The yellow diamond represents the symmetric state of the antagonistic leader x_3.

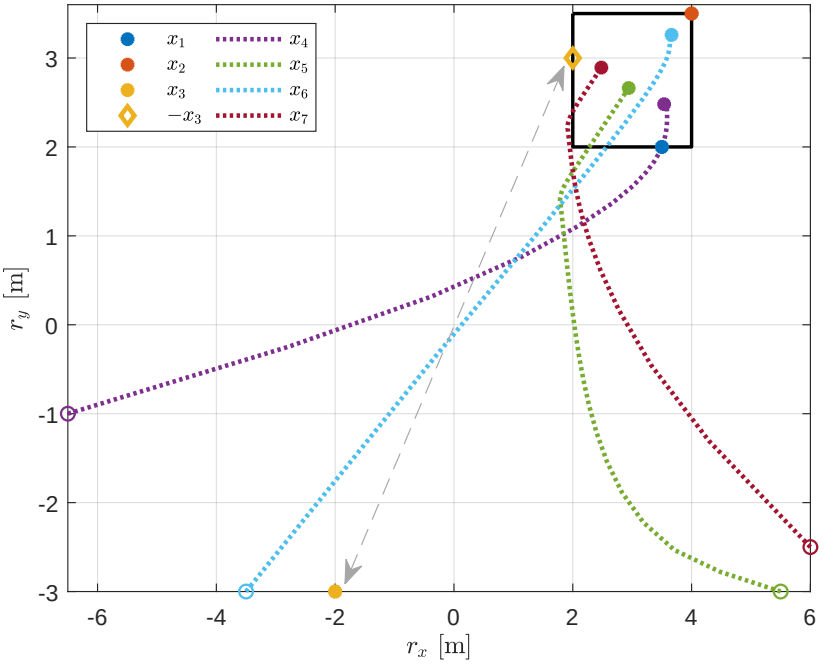

Figure 3.5: Bipartite containment tracking of system (3.50) under the same conditions as in Figure 3.4 and under the effect of the perturbation in (3.49).

Let P be generated by (3.13) with $Q = I_N$ and $\alpha = 20$, then we obtain $\overline{\lambda}_P = 0.6247$. Consider the system (3.50) and the bipartite containment law (3.2). The respective

initial states of the robots are

$$r_x(0) = \begin{bmatrix} 3.5 & 4 & -2 & -6.5 & 5.5 & -3.5 & 6 \end{bmatrix}^\top,$$

$$r_y(0) = \begin{bmatrix} 2 & 3.5 & -3 & -1 & -3 & -3 & -2.5 \end{bmatrix}^\top,$$

and $\theta_i(0) = \frac{\pi}{2}$ for all $i \in \mathcal{I}_{\mathcal{N}}$. Figure 3.4 depicts the simulation results. The followers converge to the convex hull spanned by cooperative leaders' states and competitive leader's ν_3 symmetric state. Using (3.18) and the coordinate transformation, we obtain the following limit values for the followers' states:

$$\lim_{t\to\infty} r_{x_f}(t) = \begin{bmatrix} 3.44 & 2.99 & 3.69 & 2.54 \end{bmatrix}^\top, \quad \lim_{t\to\infty} r_{y_f}(t) = \begin{bmatrix} 2.37 & 2.61 & 3.25 & 2.85 \end{bmatrix}^\top.$$

We now perform simulations for the system (3.50) with the bipartite containment law (3.2), with $d_i(t) = \sigma_i(t) \begin{bmatrix} 1 & 1 \end{bmatrix}^\top$ where $\sigma_i(t)$ is given as below

$$\sigma_i(t) = \begin{cases} \tanh(t-10) - 1 + \frac{1}{(t+10)} & i \in \{5, 6\} \\ -\tanh(t-10) + 1 - \frac{1}{(t+10)} & i = 4 \\ 0 & i \in \{1, 2, 3, 7\}. \end{cases} \tag{3.49}$$

Figure 3.5 depicts the simulation results. During the first $10s$, the perturbation $d(t)$ prevents the achievement of bipartite containment tracking, and the followers reach a stable state with a steady-state error. However, as the perturbation vanishes, after $10s$, the trajectories of the followers move towards the convex hull, spanned by the cooperative leaders' states and the antagonistic leader's symmetric state. We obtain the same limit values for the followers as before.

3.5.1.2 Structurally unbalanced networks

We consider now a coopetition network containing three leaders $\nu_i, i \leq 3$ and four followers $\nu_j, 4 \leq j \leq 7$, communicating over a structurally unbalanced directed graph as the one depicted in Figure 3.6. The competitive leader ν_3 represents a static obstacle in the system. For clarity, we stress that, in this example, we consider a leader node to be one that has no incoming edges, and we assume them to be static.

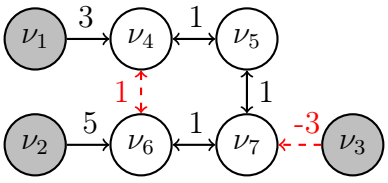

Figure 3.6: A network of seven mobile robots with 3 leaders over a structurally unbalanced signed graph.

According to (2.25), the Laplacian matrix corresponding to the graph is

$$L_s = \begin{bmatrix} 0 & 0 & 0 & 0 & 0 & 0 & 0 \\ 0 & 0 & 0 & 0 & 0 & 0 & 0 \\ 0 & 0 & 0 & 0 & 0 & 0 & 0 \\ -3 & 0 & 0 & 5 & -1 & 1 & 0 \\ 0 & 0 & 0 & -1 & 2 & 0 & -1 \\ 0 & -5 & 0 & 1 & 0 & 7 & -1 \\ 0 & 0 & 3 & 0 & -1 & -1 & 5 \end{bmatrix}$$

and its eigenvalues are $\lambda_L = 0,\ 0,\ 0,\ 1.44,\ 4.27,\ 5.56$, and 7.73. The network may not be bipartitioned into two subgroups so is structurally unbalanced. Then, the right and left eigenvectors associated with each zero eigenvalue are given by

$$\begin{aligned} v_{r_1} &= \begin{bmatrix} 1 & 0 & 0 & 0.6932 & 0.3750 & -0.0909 & 0.0568 \end{bmatrix}^\top, & v_{l_1} &= \begin{bmatrix} 1 & 0 & 0 & 0 & 0 & 0 & 0 \end{bmatrix}^\top \\ v_{r_2} &= \begin{bmatrix} 0 & 1 & 0 & -0.1515 & 0 & 0.7576 & 0.1515 \end{bmatrix}^\top, & v_{l_2} &= \begin{bmatrix} 0 & 1 & 0 & 0 & 0 & 0 & 0 \end{bmatrix}^\top \\ v_{r_3} &= \begin{bmatrix} 0 & 0 & 1 & -0.0568 & -0.3750 & -0.0909 & -0.6932 \end{bmatrix}^\top, & v_{l_3} &= \begin{bmatrix} 0 & 0 & 1 & 0 & 0 & 0 & 0 \end{bmatrix}^\top. \end{aligned}$$

The matrices V_l and V_f in (3.8) are calculated as below.

$$V_l = \begin{bmatrix} 1 & 0 & 0 \\ 0 & 1 & 0 \\ 0 & 0 & 1 \end{bmatrix}, \ V_f = \begin{bmatrix} 0.6932 & -0.1515 & -0.0568 \\ 0.3750 & 0 & -0.3750 \\ -0.0909 & 0.7576 & -0.0909 \\ 0.0568 & 0.1515 & -0.6932 \end{bmatrix}.$$

Notice that, as in the considered graph, leaders have no neighbors, V_l has the form as in (3.11). We also notice that V_f has the properties stated in Items (i)–(iv) of Lemma 7, since the network under consideration is structurally unbalanced. Since each follower is influenced by the three leaders, there are no agents corresponding to the exclusive part of a reach, and as a result, V_f does not have an element equal to ± 1. Moreover, the sum of the absolute values of the terms on each row is less than 1.

Let P be generated by (3.13) with $Q = I_N$ and $\alpha = 20$, then we obtain $\overline{\lambda}_P = 0.5161$. Consider the system (3.50) and the bipartite containment law (3.2). The respective initial states of the robots are

$$r_x(0) = \begin{bmatrix} 1.5 & -0.5 & -0.5 & -6.5 & 5.5 & -3.5 & 6 \end{bmatrix}^\top,$$

$$r_y(0) = \begin{bmatrix} 1 & 1.5 & -1 & -1 & -3 & -3 & -2.5 \end{bmatrix}^\top,$$

and $\theta_i(0) = \frac{\pi}{2}$ for all $i \in \mathcal{I}_\mathcal{N}$. Figure 3.7 depicts the simulation results. The followers converge to the convex hull spanned by the leaders' states and their symmetric states. Using (3.18) and the coordinate transformation, we obtain the following limit values for the followers' states:

$$\lim_{t\to\infty} r_{x_f}(t) = \begin{bmatrix} 1.20 & 0.81 & -0.39 & 0.42 \end{bmatrix}^\top, \quad \lim_{t\to\infty} r_{y_f}(t) = \begin{bmatrix} 0.49 & 0.67 & 1.14 & 0.85 \end{bmatrix}^\top.$$

We now perform simulations for the system (3.50) with the bipartite containment law (3.2), with $d_i(t) = \sigma_i(t) \begin{bmatrix} 1 & 1 \end{bmatrix}^\top$, where $\sigma_i(t)$ is in (3.49). Figure 3.8 depicts the

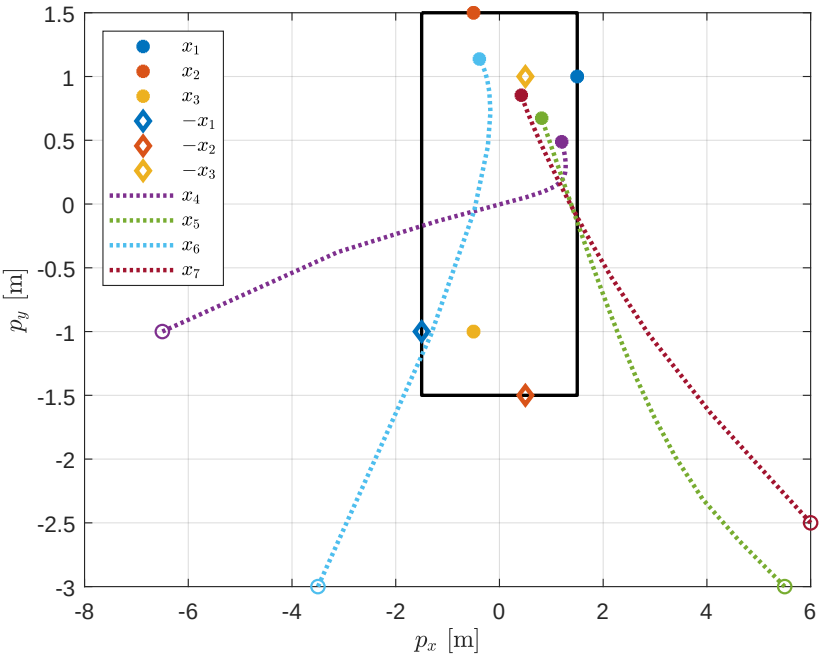

Figure 3.7: Bipartite containment tracking of system (3.50) with control input (3.48), $[u_{x_i}\ u_{y_i}] =: u_i$ and u_i as in (3.2). The filled dots are the final states of the mobile robots, and the dotted lines represent the trajectory of the four followers. The diamonds represent the symmetric states of the leaders.

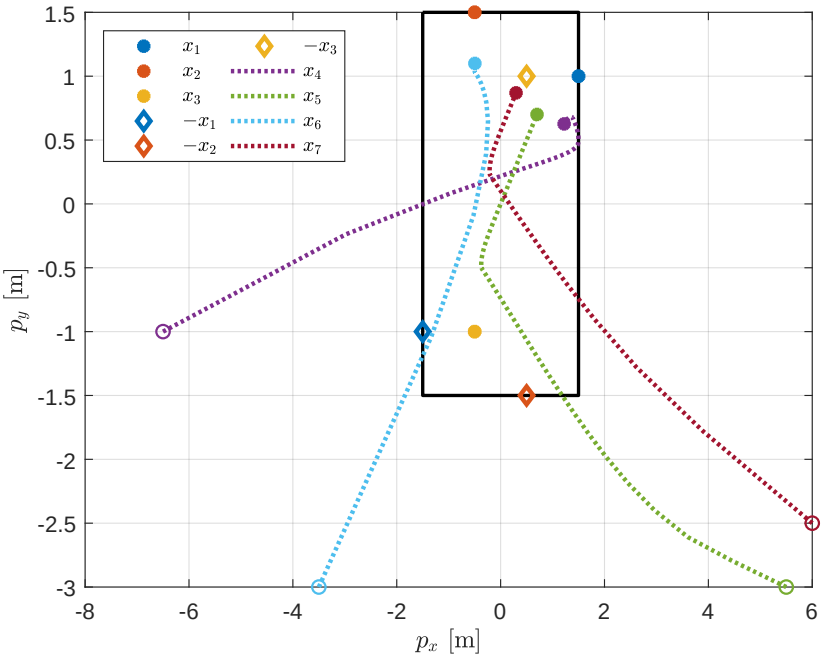

Figure 3.8: Bipartite containment tracking of system (3.50) under the same conditions as in Figure 3.7 and under the effect of the perturbation in (3.49).

simulation results. The trajectories of the followers move towards the convex hull, spanned by leaders' states and their symmetric states. We obtain the same limit

values as before for the followers.

3.5.2 Second-order systems

Let us consider next a group of force-controlled unicycles, hence modeled by the second-order equations

$$\begin{bmatrix} \dot{r}_{x_i} \\ \dot{r}_{y_i} \\ \dot{\theta}_i \end{bmatrix} = \begin{bmatrix} s_i \cos\theta_i \\ s_i \sin\theta_i \\ \omega_i \end{bmatrix}, \quad \begin{bmatrix} \dot{s}_i \\ \dot{\omega}_i \end{bmatrix} = \begin{bmatrix} \frac{1}{m_i} & 0 \\ 0 & \frac{1}{J_i} \end{bmatrix} \eta_i, \tag{3.50}$$

where m_i the mass, J_i the moment of inertia, F_i the applied force and τ_i the applied torque, and $\eta_i := \begin{bmatrix} F_i & \tau_i \end{bmatrix}^\top$. To apply the consensus control law (3.26)—designed for (3.24)—to the system (3.50), we apply a preliminary feedback linearizing control. To that end, we rewrite the system's dynamics in terms of the position of a reference point located at a distance δ_i from the axis connecting the wheels, as before. We define

$$\zeta := \begin{bmatrix} r_{x_i} + \delta_i \cos\theta_i \\ r_{y_i} + \delta_i \sin\theta_i \\ s_i \cos\theta_i - \delta_i \omega_i \sin\theta_i \\ s_i \sin\theta_i + \delta_i \omega_i \cos\theta_i \\ \theta_i \end{bmatrix}. \tag{3.51}$$

In transformed coordinates, with $p_i = [\zeta_{1_i}^\top \ \zeta_{2_i}^\top]^\top$, we have

$$\begin{bmatrix} \dot{\zeta}_{1_i} \\ \dot{\zeta}_{2_i} \end{bmatrix} = \begin{bmatrix} \zeta_{3_i} \\ \zeta_{4_i} \end{bmatrix}, \tag{3.52a}$$

$$\begin{bmatrix} \dot{\zeta}_{3_i} \\ \dot{\zeta}_{4_i} \end{bmatrix} = \begin{bmatrix} -s_i\omega_i \sin\theta_i - \delta_i\omega_i^2 \cos\theta_i \\ s_i\omega_i \cos\theta_i - \delta_i\omega_i^2 \sin\theta_i \end{bmatrix} + \begin{bmatrix} \frac{1}{m_i}\cos\theta_i & -\frac{\delta_i}{J_i}\sin\theta_i \\ \frac{1}{m_i}\sin\theta_i & \frac{\delta_i}{J_i}\cos(\theta_i) \end{bmatrix} \eta_i, \tag{3.52b}$$

$$\dot{\zeta}_{5_i} = -\frac{1}{2\delta_i}\zeta_{3_i} \sin\zeta_{5_i} + \frac{1}{2\delta_i}\zeta_{4_I} \cos\zeta_{5_i}. \tag{3.52c}$$

The feedback linearizing control η_i is given by

$$\eta_i = \begin{bmatrix} \frac{1}{m_i}\cos\theta_i & -\frac{\delta_i}{J_i}\sin\theta_i \\ \frac{1}{m_i}\sin\theta_i & \frac{\delta_i}{J_i}\cos(\theta_i) \end{bmatrix}^{-1} \times \left[u_i - \begin{bmatrix} -s_i\omega_i \sin\theta_i - \delta_i\omega_i^2 \cos\theta_i \\ s_i\omega_i \cos\theta_i - \delta_i\omega_i^2 \sin\theta_i \end{bmatrix} \right], \tag{3.53}$$

which gives $[\dot{\zeta}_{1_i} \ \dot{\zeta}_{2_i}]^\top = [\zeta_{3_i} \ \zeta_{4_i}]^\top$ and $[\dot{\zeta}_{3_i} \ \dot{\zeta}_{4_i}]^\top = u_i$. Thus, we implemented (3.53) with u_i as in (3.26), $x_{1_i} = [\zeta_{1_i} \ \zeta_{2_i}]^\top$, $x_{2_i} = [\zeta_{3_i} \ \zeta_{4_i}]^\top$, $m_i = 8\text{kg}$ and $J_i = 0.12\text{kg/m}^2$ for each $i \in \mathcal{I}_\mathcal{N}$.

Remark 11 *Nonholonomic systems, such as unicycles, are constrained in their movement, typically unable to move in certain directions, like sideways. Feedback linearization is used above to transform the nonlinear dynamics of the unicycles into linear ones, simplifying control design by placing the control point at an offset from the robot's center, allowing it to control the system while ignoring its exact orientation. This can make*

the robots behave like a holonomic system, simplifying trajectory tracking but introducing errors due to the robot's nonholonomic nature, such as tracking errors, especially during sharp turns. Moreover, in feedback linearization, the parameters of the robot are assumed to be perfectly known, so modeling errors or uncertainties in parameters and unmodeled dynamics, such as friction, may lead to control errors. On the other hand, the choice of considering nonholonomic systems in the first place is because they are more practical for many real-world applications. •

We provide some numerical examples of a system of nonholonomic unicycle mobile robots over both structurally balanced and unbalanced networks.

3.5.2.1 Structurally balanced networks

Consider a network of $N = 9$ agents with five leaders $\nu_i, i \leq 5$, organized in three leader groups $\{\nu_1, \nu_2, \nu_3\}$, $\{\nu_4\}, \{\nu_5\}$, and four followers $\nu_j, 6 \leq j \leq 9$, communicating over a directed graph as the one depicted in Figure 3.9, below.

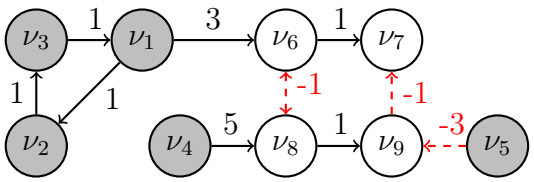

Figure 3.9: Network 1: A network of nine mobile robots

The Laplacian matrix corresponding to the graph is

$$L = \begin{bmatrix} 1 & 0 & -1 & 0 & 0 & 0 & 0 & 0 & 0 \\ -1 & 1 & 0 & 0 & 0 & 0 & 0 & 0 & 0 \\ 0 & -1 & 1 & 0 & 0 & 0 & 0 & 0 & 0 \\ 0 & 0 & 0 & 0 & 0 & 0 & 0 & 0 & 0 \\ 0 & 0 & 0 & 0 & 0 & 0 & 0 & 0 & 0 \\ -3 & 0 & 0 & 0 & 0 & 4 & 0 & 1 & 0 \\ 0 & 0 & 0 & 0 & 0 & -1 & 2 & 0 & 1 \\ 0 & 0 & 0 & -5 & 0 & 1 & 0 & 6 & 0 \\ 0 & 0 & 0 & 0 & 3 & 0 & -1 & 0 & 4 \end{bmatrix}$$

and its eigenvalues are $\lambda_L = 0, 0, 0, 1.5 \pm 0.86i, 2, 3.59, 4$, and 6.41. The network may be bipartitioned into two subgroups,

$$\mathcal{V}_1 = \{\nu_1, \nu_2, \nu_3, \nu_5, \nu_6, \nu_7\}, \quad \mathcal{V}_2 = \{\nu_4, \nu_8, \nu_9\},$$

so is structurally balanced, and

$$V_l = \begin{bmatrix} 0.33 & 0.33 & 0.33 & 0 & 0 \\ 0.33 & 0.33 & 0.33 & 0 & 0 \\ 0.33 & 0.33 & 0.33 & 0 & 0 \\ 0 & 0 & 0 & 1 & 0 \\ 0 & 0 & 0 & 0 & 1 \end{bmatrix}, \; V_f = \begin{bmatrix} 0.26 & 0.26 & 0.26 & -0.22 & 0 \\ 0.14 & 0.14 & 0.14 & -0.22 & 0.37 \\ -0.04 & -0.04 & -0.04 & 0.87 & 0 \\ -0.01 & -0.01 & -0.01 & 0.22 & -0.75 \end{bmatrix}. \tag{3.54}$$

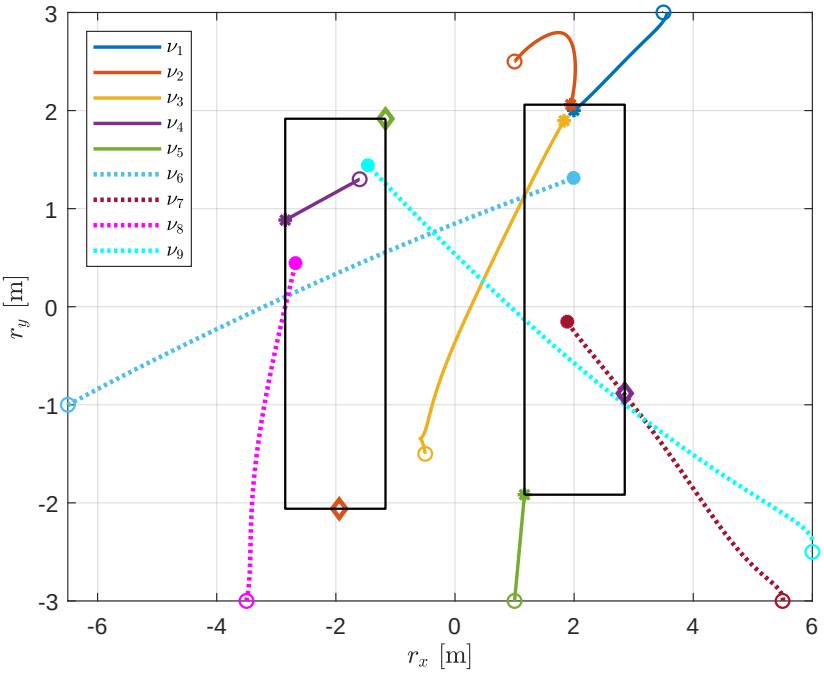

Figure 3.10: Bipartite containment tracking of (3.50) with the control (3.26) on the plane. The filled dots are the final states of the agents. The diamonds represent the mirrored final states of the leaders. The rectangles represent the containment set.

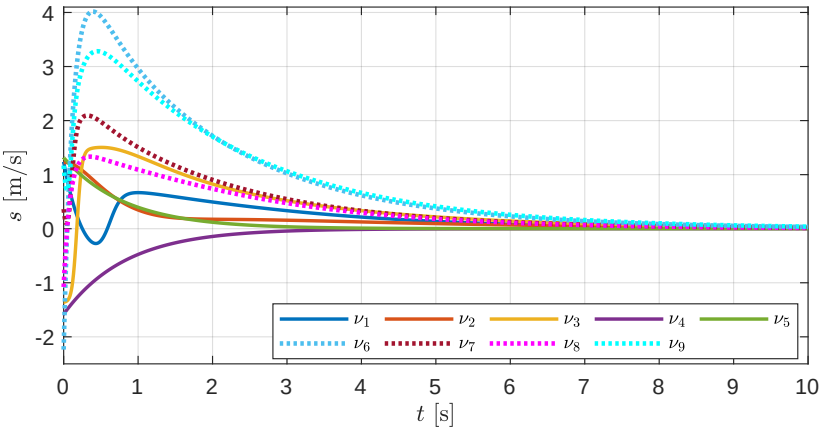

Figure 3.11: Bipartite containment tracking of (3.50) with (3.26) on velocity.

We notice that V_l and V_f have the properties stated in Items (i)-(iv) of Lemma 8, as the network is structurally balanced. For V_l, we have two elements equal to one, corresponding to isolated leaders ν_4 and ν_5, as they are in the exclusive part of the reaches. Leaders ν_1, ν_2, and ν_3 are in the exclusive part of a reach, so the corresponding elements of the right eigenvector are equal to one. Thus, as they are interconnected within a strongly connected graph, the absolute value of the elements of the left eigenvector is less than one. V_f does not have an element equal to ± 1 since all the followers are influenced by more than one leader. Followers ν_6 and ν_8 are not influenced by the leader ν_5, so the corresponding elements on the fifth column are equal to zero. We also remark that the sum of the absolute values of the terms on each row

is equal to 1.

Now, to compute P in (3.13) we proceed as follows. We set $Q = I_N$ and $\alpha_i = 20$. Then, in Matlab, we use `lyap(-R,Q)` with $Q = I_N$ to obtain the solution of $-PR - R^\top P = -Q$ with $R := L + \sum_{i=1}^{K} \alpha_i v_{r_i} v_{l_i}^\top$. We obtain $\overline{\lambda}_P = 0.5193$. Consider the system (3.50) and the bipartite containment law (3.53) with $k_1 = 0.8, k_2 = 1.5$, and $k_3 = 1.2$, which satisfy the conditions in (3.30). The respective agents' initial states are

$$
\begin{aligned}
r_x(0) &= [3.5 \;\; 1 \;\; -0.5 \;\; -1.6 \;\; 1 \;\; -6.5 \;\; 5.5 \;\; -3.5 \;\; 6]^\top, \\
r_y(0) &= [3 \;\; 2.5 \;\; -1.5 \;\; 1.3 \;\; -3 \;\; -1 \;\; -3 \;\; -3 \;\; -2.5]^\top, \\
\theta(0) &= [0.25 \;\; 0.61 \;\; -1.27 \;\; 0.32 \;\; 1.42 \;\; 0.46 \;\; 0.98 \;\; 1.19 \;\; 1.03]^\top, \\
s(0) &= [1.2 \;\; 1.2 \;\; -1.4 \;\; -1.6 \;\; 1.3 \;\; -2.2 \;\; 0.4 \;\; -1.1 \;\; 1.2]^\top.
\end{aligned}
$$

The simulation results are shown in Figures 3.10 and 3.11. The followers converge to the bipartite containment set spanned by cooperative leaders' final states and competitive leaders' mirrored final states and all agents' velocities converge to zero. Using the relations in (3.36) and the coordinate transformation, we obtain the following limit values for followers' states,

$$
\lim_{t\to\infty} r_x(t) = [1.99 \;\; 1.89 \;\; -2.68 \;\; -1.46]^\top, \quad \lim_{t\to\infty} r_y(t) = [1.31 \;\; -0.15 \;\; 0.44 \;\; 1.44]^\top,
$$

and

$$
\lim_{t\to\infty} s(t) = [0 \;\; 0 \;\; 0 \;\; 0]^\top.
$$

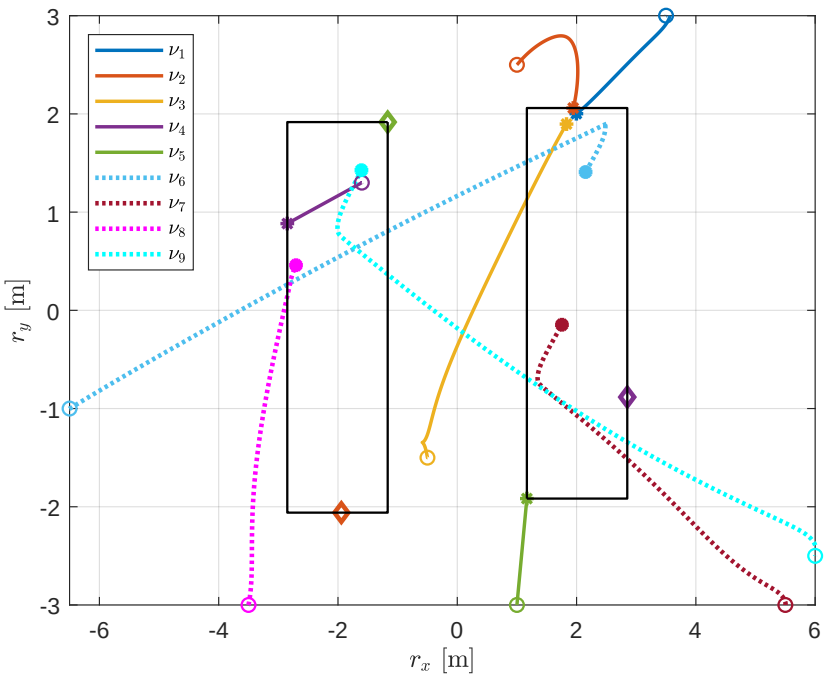

Figure 3.12: Bipartite containment tracking of (3.41) on the plane.

In a second run of simulations, we tested the bipartite-containment control law (3.53) on the system (3.50), using the same initial conditions and controller gains

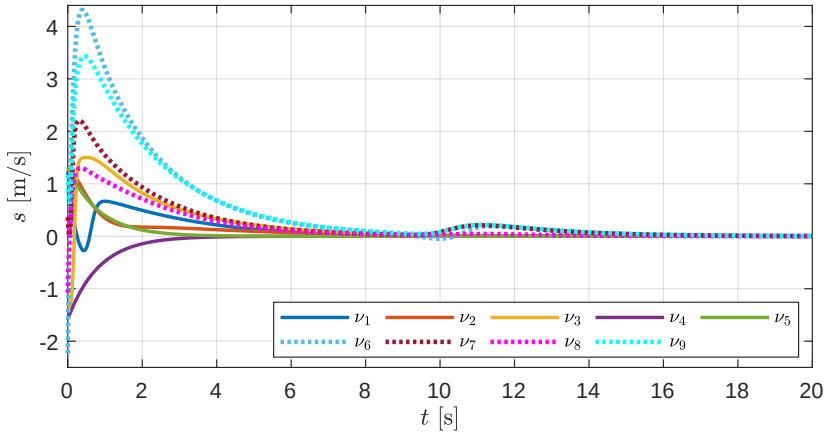

Figure 3.13: Bipartite containment tracking of (3.41) on velocity.

as above. Therefore, in the simulations we consider that the system is subject to a disturbance $d_i = \sigma_i(t) \begin{bmatrix} 1 & 1 \end{bmatrix}^\top$, where $\sigma_i(t)$ is given by

$$\sigma_i(t) = \begin{cases} \tanh(t-10) - 1 + \frac{1}{(t+10)} & i \in \{7, 9\} \\ -\tanh(t-10) + 1 - \frac{1}{(t+10)} & i = 6 \\ 0 & i \in \{1, 2, 3, 4, 5, 8\}. \end{cases}$$

The simulation results can be appreciated in Figures 3.12 and 3.13. During the first 10s, the perturbation $d(t)$ prevents the achievement of bipartite containment tracking, the trajectories of the followers 6, 7, and 9 shift because of the presence of the perturbation, but, after the perturbation vanishes, the trajectories of the followers stop shifting and converge towards the bipartite containment set spanned by cooperative leaders' final states and competitive leaders' mirrored final states and all agents' velocities converge to zero. We obtain the same limit values as before for the followers.

In a third run of simulations, we tested the bipartite-containment control law (3.53) on the system (3.50), using the same initial conditions and controller gains as above. Therefore, in the simulations we consider that the system is subject to a disturbance $d_i = \sigma_i(t) \begin{bmatrix} 1 & 1 \end{bmatrix}^\top$, where $\sigma_i(t)$ is given by

$$\sigma_i(t) = \begin{cases} -\tanh(t-5) - 1 + \frac{1}{(t+5)} & i = 5 \\ \tanh(t-10) - 1 + \frac{1}{(t+10)} & i \in \{4, 7, 9\} \\ -\tanh(t-10) + 1 - \frac{1}{(t+10)} & i = 6 \\ 0 & i \in \{1, 2, 3, 8\}. \end{cases}$$

The simulation results can be appreciated in Figures 3.14 and 3.15. During the first 5s and 10s, leaders 5 and 4 are influenced by the perturbation, respectively, which prevents the velocity from converging to zero. However, after the perturbation vanishes, the velocities of the leaders stop increasing and converge to zero. On the other hand, during the 10 seconds, the perturbation $d(t)$ prevents followers 6, 7, and 9 from achieving bipartite containment tracking and their trajectories shift but after the perturbation vanishes, the trajectories of the followers stop shifting and converge towards the bipartite containment set spanned by cooperative leaders' final states and competitive leaders' mirrored final states and all agents' velocities converge to zero.

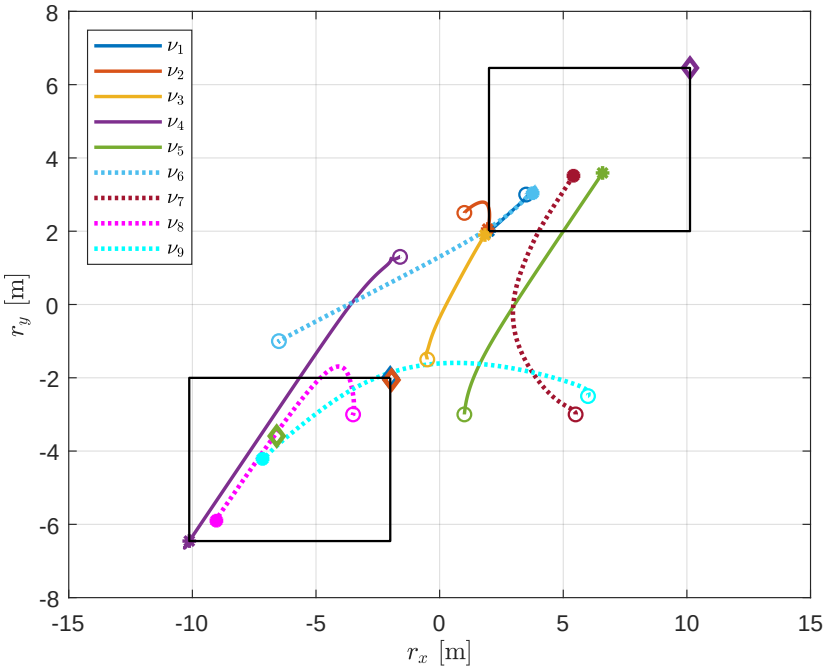

Figure 3.14: Bipartite containment tracking of (3.41) on the plane.

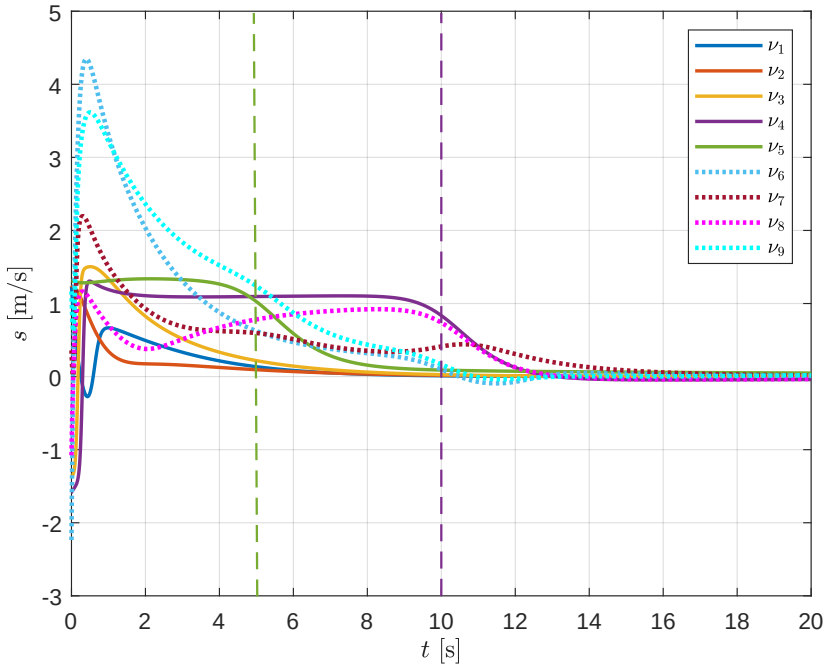

Figure 3.15: Bipartite containment tracking of (3.41) on velocity.

3.5.2.2 Structurally unbalanced networks

Now, consider a network of $N = 9$ agents containing five leaders $\nu_i, i \leq 5$, three leader groups $\{\nu_1, \nu_2, \nu_3\}$, $\{\nu_4\}$, $\{\nu_5\}$, and four followers $\nu_j, 6 \leq j \leq 9$, provided in Figure 3.16.

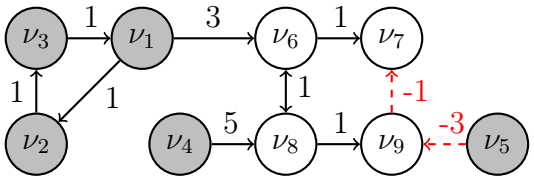

Figure 3.16: Network 2: A network of nine mobile robots

The Laplacian matrix corresponding to the graph is

$$L_s = \begin{bmatrix} 1 & 0 & -1 & 0 & 0 & 0 & 0 & 0 & 0 \\ -1 & 1 & 0 & 0 & 0 & 0 & 0 & 0 & 0 \\ 0 & -1 & 1 & 0 & 0 & 0 & 0 & 0 & 0 \\ 0 & 0 & 0 & 0 & 0 & 0 & 0 & 0 & 0 \\ 0 & 0 & 0 & 0 & 0 & 0 & 0 & 0 & 0 \\ -3 & 0 & 0 & 0 & 0 & 4 & 0 & -1 & 0 \\ 0 & 0 & 0 & 0 & 0 & -1 & 2 & 0 & 1 \\ 0 & 0 & 0 & -5 & 0 & -1 & 0 & 6 & 0 \\ 0 & 0 & 0 & 0 & 3 & 0 & -1 & 0 & 4 \end{bmatrix}$$

and its eigenvalues are $\lambda_L = 0, 0, 0, 1.5 \pm 0.86i$, 2, 3.59, 4, and 6.41. The network may not be bipartitioned into two subgroups, so is structurally unbalanced. The matrix V_l is calculated as in (3.54) and V_f is calculated as

$$V_f = \begin{bmatrix} 0.26 & 0.26 & 0.26 & 0.22 & 0 \\ 0.125 & 0.125 & 0.125 & 0 & 0.375 \\ 0.04 & 0.04 & 0.04 & 0.87 & 0 \\ 0.01 & 0.01 & 0.01 & 0.22 & -0.75 \end{bmatrix}.$$

We notice that V_f has the properties stated in Items (i)-(iv) of Lemma 7 since the network is structurally unbalanced. Since all followers are influenced by more than one leader, there are no agents corresponding to the exclusive part of a reach, and as a result, V_f does not have an element equal to ± 1, but the absolute values of each element is less than one. We also remark that the sum of the absolute value of the terms on each row is less than 1.

Now, let P be generated by (3.13) with $Q = I_N$ and $\alpha = 20$, then we obtain $\overline{\lambda}_P = 0.4839$. Consider the system (3.50) and the bipartite containment law (3.53) with the same controller gains as before. The respective agents' inertial positions and linear speeds are the same as before, while the orientations are

$$\theta(0) = [0.25 \;\; 0.61 \;\; -1.27 \;\; 0.32 \;\; 1.42 \;\; 0.46 \;\; 0.98 \;\; 1.19 \;\; 1.03]^\top.$$

The simulation results are depicted in Figures 3.17 and 3.18.

Note that all followers converge to the convex hull spanned by leaders' final states and mirrored final states and all agents' velocities converge to zero. Using relations in (3.36) and the coordinate transformation, we obtain the following limit values for followers' states,

$$\lim_{t\to\infty} r_x(t) = [1.5 \;\; 1.1 \;\; 0.01 \;\; -0.94]^\top, \quad \lim_{t\to\infty} r_y(t) = [1.79 \;\; -0.01 \;\; 0.89 \;\; 1.54]^\top,$$

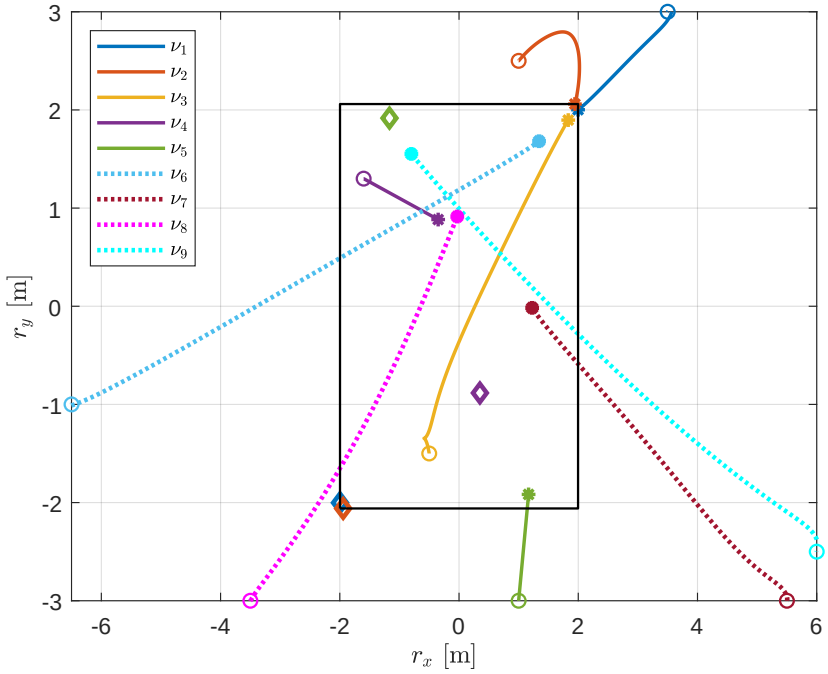

Figure 3.17: Bipartite containment tracking of (3.24) on position. The filled dots are the final states of the agents. The diamonds represent the mirrored final states of the leaders.

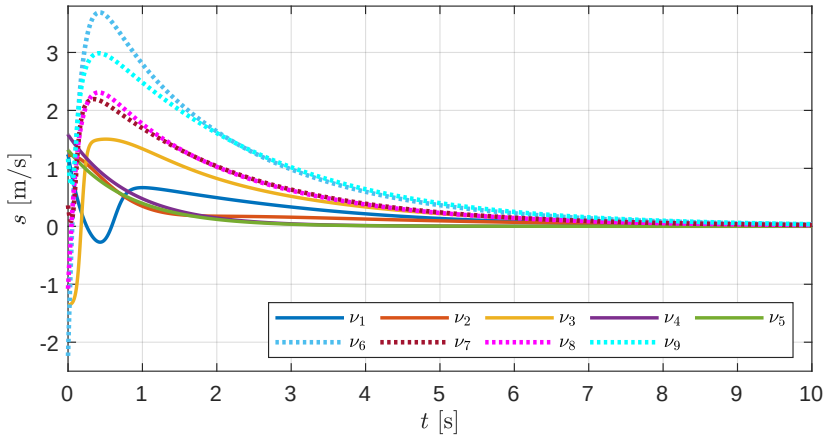

Figure 3.18: Bipartite containment tracking of (3.24) on velocity.

$$\lim_{t\to\infty} s(t) = [0\ \ 0\ \ 0\ \ 0]^\top.$$

We remark that for structurally balanced signed networks, the followers' final states converge to the bipartite containment set spanned by cooperative leaders' final states and antagonistic leaders' mirrored states. However, in the case of a structurally unbalanced network, this cannot be observed because the agents cannot be partitioned into two disjoint subsets.

In a second run of simulations, we tested the bipartite-containment control law (3.53) on the system (3.50), using the same initial conditions and controller gains as above. Therefore, in the simulations we consider that the system is subject to a

disturbance $d_i = \sigma_i(t) \begin{bmatrix} 1 & 1 \end{bmatrix}^\top$, where $\sigma_i(t)$ is given by

$$\sigma_i(t) = \begin{cases} -\tanh(t-5) - 1 + \frac{1}{(t+5)} & i = 5 \\ \tanh(t-10) - 1 + \frac{1}{(t+10)} & i \in \{4, 7, 9\} \\ -\tanh(t-10) + 1 - \frac{1}{(t+10)} & i = 6 \\ 0 & i \in \{1, 2, 3, 8\}. \end{cases}$$

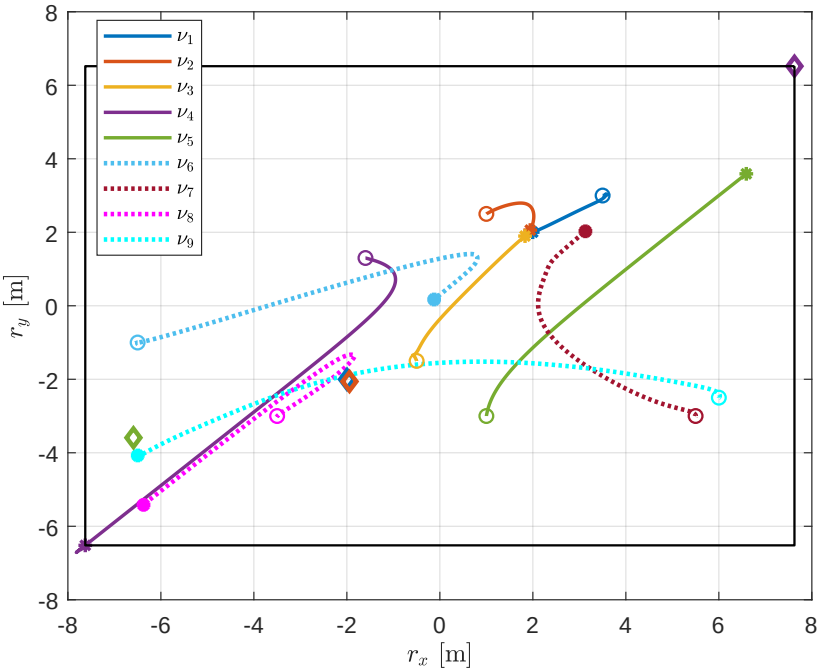

Figure 3.19: Bipartite containment tracking of (3.41) on the plane.

The simulation results can be appreciated in Figures 3.19 and 3.20. During the first 5s and 10s, leaders 5 and 4 are influenced by the perturbation, respectively, which prevents the velocity from converging to zero. However, after the perturbation vanishes, the velocities of the leaders stop increasing and converge to zero. All followers converge towards the bipartite containment set spanned by cooperative and competitive leaders' final states and symmetric final states. Moreover, all agents' velocities converge to zero.

3.6 CONCLUSIONS

In this chapter, we presented a Lyapunov approach to analyze the exponential stability of the bipartite containment tracking problem of simple and double integrators over structurally balanced and unbalanced multi-leader signed networks. Via a change of coordinates, we have shown a bound for the convergence set of the followers, as well as the limiting set points for all the agents. This is significant because the construction of a Lyapunov function may serve to extend our study to cover bipartite containment for complex non-linear systems, such as Lagrangian systems. Moreover, we have generalized the Lyapunov equation characterization of the Hurwitz property of a matrix

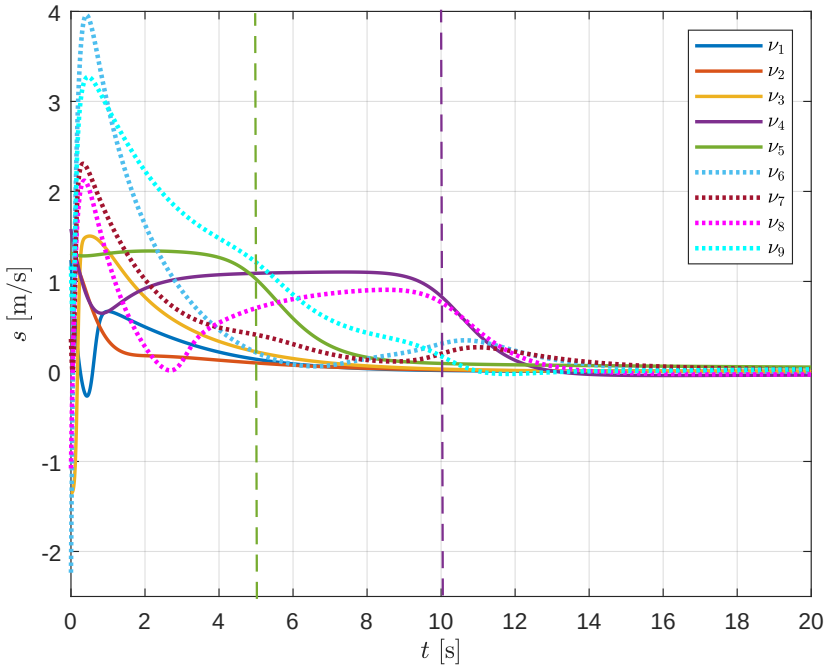

Figure 3.20: Bipartite containment tracking of (3.41) on velocity.

to matrices having more than one zero eigenvalue, which allowed us to construct strict Lyapunov functions. Disposing of strict Lyapunov functions allowed us to establish the robustness of the system with respect to a bounded disturbance.

CHAPTER 4

BIPARTITE FORMATION-CONSENSUS WITH COLLISION AVOIDANCE AND CONNECTIVITY MAINTENANCE

In this chapter, we address the bipartite formation-consensus problem for a group of vehicles over structurally balanced signed networks described by first- and second-order systems under inter-agent distance constraints. Bipartite formation in multi-agent systems is relevant, for example, when a group of autonomous vehicles operates amidst hostile conditions alongside enemy vehicles and gathers around a desired point or a safety zone. Distance constraints concern restrictions on the distance between two agents to avoid collision and, at the same time, to avoid losing communication if it does occur.

To address this problem, we propose a distributed barrier-Lyapunov-function-gradient-based bipartite formation control law that prevents inter-vehicle collisions and keeps vehicles in their sensors' range. First, we present our control laws and analysis in node coordinates expressed for each agent. Then, we use the edge-based representation for signed networks [23], where the control law is expressed for each edge interconnecting a pair of agents. The edge-based formulation corresponds well to the study of our problem as a stability problem and allows us to recast the bipartite formation-consensus problem into the space of the error coordinates.

The bipartite consensus problem has already been studied in the literature, *e.g.*, in [2, 30, 104, 95]. However, in contrast to the latter references, we address the bipartite consensus problem under collision avoidance and connectivity maintenance. The constrained non-cooperative herding problem has been studied in [15] and [26] but with optimization-based approaches, and the constrained bipartite-flocking problem is studied in [24], using artificial potential functions. In our work, compared to [15], [26], and [24], we encode the inter-agent constraints using barrier-Lyapunov functions, and our controller is based on the gradient of a barrier-Lyapunov function. Moreover, contrary to [24], a minimal safety distance is guaranteed between any two agents.

Thus, compared to the literature, we contribute with a distributed control law that solves the bipartite formation-consensus-control problem for structurally balanced signed networks. We consider, in particular, undirected signed networks and strongly connected directed signed networks described by first and second-order systems. Furthermore, we establish asymptotic stability of the bipartite formation-consensus manifold by applying Lyapunov's direct method and, in some cases, employing edge-based formulation for signed networks.

4.1 PROBLEM FORMULATION

Consider N physical systems with non-negligible dimensions, and let $x_i \in \mathbb{R}^n$ be a state of interest, typically, a position of a point in the physical space of the agent i. Let them be modeled by

$$\dot{x}_i = u_i,$$

where $u_i \in \mathbb{R}^n$ is the control input. Consider the problem of ensuring all systems achieve formation consensus, meaning they converge to configurations around a non-predefined rendezvous point. Then, for each agent let $b_i \in \mathbb{R}^n$ denote the relative displacement of agent i with respect to the rendezvous point and define

$$\bar{x}_i = x_i - b_i.$$

Then, the agent dynamics take the form

$$\dot{\bar{x}}_i = u_i. \tag{4.1}$$

Now, consider the group of agents (4.1) interconnected through inputs u_i, forming a communication network with a signed, undirected, connected, and structurally balanced graph. Here, we address two kinds of problems: leaderless bipartite consensus and leader-follower bipartite consensus. In the first case, the final states of the agents are defined by their initial conditions, and they converge to two opposite equilibria. In the second case, all the agents still converge to two symmetric equilibria, but the final states are defined by the leaders. The study of these problems is important because their solutions form a basis for addressing more realistic and complex problems. First, we are interested in the conditions under which the following is achieved.

Definition 6 (Leaderless bipartite consensus) *The systems* (4.1)-(2.33) *are said to achieve bipartite position consensus if*

$$\lim_{t\to\infty} \bar{e}_{x_k} = 0, \tag{4.2}$$

where

$$\bar{e}_{x_k} := \bar{x}_i - sgn(a_{ij})\bar{x}_j, \tag{4.3}$$

are the synchronization errors in position for each pair of communicating agents with $k \leq M$, the index of the interconnection between the ith and jth agents, and M, the total number of edges interconnecting agents in the network.

That is, for agents i and j cooperative with each other, bipartite consensus implies that $\bar{x}_i \to \bar{x}_j$ while for agents competitive with each other we have $\bar{x}_i \to -\bar{x}_j$.

Thus, bipartite consensus is achieved for cooperative agents if $\bar{x}_i - \bar{x}_j = 0$, or equivalently if

$$x_i - x_j = \bar{b}_{ij},$$

where $\bar{b}_{ij} = b_i - \operatorname{sgn}(a_{ij})b_j$. For competitive agents, bipartite consensus is attained if $\bar{e}_{x_k} = \bar{x}_i + \bar{x}_j = 0$, that is, if

$$x_i + x_j = \bar{b}_{ij}.$$

In the case of leader-follower bipartite consensus, as mentioned before, the final states of the agents depend on the leader's states. Then, to address the leader-follower bipartite consensus problem, a natural and widely used approach in the literature is to add a virtual leader in a group of agents that communicate over an undirected graph—cf. [60, 89, 6] and [7, Chapter 4]. Assume that the dynamics of the virtual leader are described by

$$\dot{x}_0 = 0, \quad x_0 \in \mathbb{R}^n. \tag{4.4}$$

Next, to account for the nature of the interaction between the virtual leader and the followers, let ϕ_i describe the interaction between the virtual leader and the agents $\nu_i, i \leq N$, such that $\phi_i = 1$ if the leader is cooperative with the agent i and $\phi_i = -1$ otherwise. Then, we define

$$\hat{e}_i := \bar{x}_i - \phi_i x_0, \quad i \leq N. \tag{4.5}$$

So, in compact form, we have

$$\hat{e} = \bar{x} - \Phi x_0, \tag{4.6}$$

where

$$\Phi = [\phi_1,\ \phi_2,\ \cdots, \phi_N]^\top, \quad \phi_i \in \{1,\ -1\}. \tag{4.7}$$

That is, the leader-follower bipartite consensus is achieved when both synchronization errors in (4.2) and the errors with respect to the leader defined in (4.5) converge to zero. Then, we can formally define the leader-follower bipartite consensus problem as follows.

Definition 7 (Leader-follower bipartite consensus) *Let $x_0 \in \mathbb{R}^n$ be the position of the virtual leader ν_0, whose dynamics is given in (4.4). The leader has a direct interconnection with at least one follower. Then, the systems (4.1)-(2.33) are said to achieve leader-follower bipartite position and velocity consensus if (4.2) and*

$$\lim_{t\to\infty} \hat{e}_i(t) = 0, \qquad i \leq N \tag{4.8}$$

hold.

That is, for agents labeled i that are cooperative with the virtual leader, bipartite consensus implies that $\bar{x}_i \to x_0$ while for agents competitive with the virtual leader we have $\bar{x}_i \to -x_0$.

Remark 12 *In this chapter, we are interested in the problem of stabilization at a point, whence the assumption on the dynamics of the leader. This can be seen, e.g., as part of a more complex maneuver requiring the robots to gather statically around a rendezvous point before starting a scouting mission—cf.* [21, 43]. •

In the context of the problem studied in this chapter, the agents are asked to achieve (leader-follower) bipartite consensus while satisfying inter-agent constraints to ensure collision avoidance and connectivity maintenance. Then, for each pair of communicating nodes ν_i and $\nu_j \in \mathcal{V}$, labeled $k \leq M$, let $\delta_k := x_i - x_j$ be the physical distance. The distance between positions remains in certain constraint sets, which are defined as follows. Let $\mathcal{E}_m$ denote the set of indices k corresponding to edges containing pairs of cooperative agents, *i.e.,* $i, j \in \mathcal{V}_l$ with $l \in \{1, 2\}$. In addition, for each $k \leq M$, let $R_k > 0$ and $\Delta_k > 0$. Then, we define the set of proximity constraints $\mathcal{I}_r$ and the set of collision-avoidance constraints $\mathcal{I}_c$ as

$$\textit{(Proximity constraints)} \qquad \mathcal{I}_r := \{\delta_k \in \mathbb{R}^n : |\delta_k| < R_k,\ k \in \mathcal{E}_m\} \tag{4.9a}$$

$$\textit{(Collision-avoidance constraints)} \qquad \mathcal{I}_c := \{\delta_k \in \mathbb{R}^n : |\delta_k| > \Delta_k\ k \leq M\}. \tag{4.9b}$$

Under these conditions, it is required to design a distributed bipartite consensus control law u_i such that the synchronization errors $\bar{e}_{x_k}$ in (4.3) satisfy (4.2) and the agents' trajectories satisfy the proximity and collision-avoidance constraints. That is, it must hold that $\delta(t) \in \mathcal{I}$ for all $t \geq 0$, with $\delta := [\delta_1\ \delta_2\ \cdots\ \delta_M]^\top$, $\mathcal{I} := \mathcal{I}_r \cap \mathcal{I}_c$ for cooperative agents and $\mathcal{I} := \mathcal{I}_c$ for competitive agents.

Remark 13 *Proximity constraints are only imposed on agents interconnected by a cooperative edge. They are not imposed on competitive interactions since it is assumed that the competitive agents have different objectives, so they do not stay close to each other.* •

In the next section, we explain how we design the control law using the gradient of a nonlinear function to solve the constrained bipartite formation-consensus problem.

4.2 ANALYSIS AND CONTROL APPROACH

In the control approach, we are inspired by the classical bipartite consensus problem without constraints to design the control law that achieves the bipartite consensus of agents while guaranteeing the inter-agent constraints encoded in (4.9). The control design and stability analysis both rely on the ability to construct appropriate Lyapunov functions. For the purpose of guaranteeing the satisfaction of the constraints, we use so-called barrier Lyapunov functions (BLFs). We study four cases depending on whether the topology is directed or undirected and whether the individual dynamics are of first or second order. For technical reasons, for second-order systems interconnected over undirected networks, we use edge coordinates, and for the other cases, we use node coordinates. Hence, we start by showing how we construct BLFs with domain in either coordinate space.

4.2.1 Barrier-Lyapunov functions in node coordinates

To put our contributions in perspective, let us consider first the systems modeled by (4.1) without constraints in the multivariable form

$$\dot{\bar{x}} = u,$$

i.e., with $\bar{x} = [\bar{x}_1 \ \bar{x}_2 \ \dots \bar{x}_N]^\top$ and $u = [u_1 \ u_2 \ \dots u_N]^\top$, and interconnected via the control law

$$u = -L_s \bar{x}, \tag{4.10}$$

where L_s is the resulting signed Laplacian matrix associated with the considered undirected signed network—see Section 2.3. Then, the closed-loop system is

$$\dot{\bar{x}} = -L_s \bar{x},$$

which has been abundantly studied in the literature—see also Chapter 2. For the purposes of this chapter, we remark the other evident fact that we can express the control law (4.10) in the form of the gradient of a function, *i.e.,*

$$-L_s \bar{x} = -\nabla_{\bar{x}} V,$$

where

$$V(\bar{x}) := \frac{1}{2} \bar{x}^\top L_s \bar{x}$$

so

$$\nabla_{\bar{x}} V := \frac{\partial V}{\partial x} = L_s \bar{x}.$$

The latter follows from the fact that

$$V(\bar{x}) = \frac{1}{4} \sum_{i,j=1}^{N} |a_{ij}| (x_i - \operatorname{sgn}(a_{ij}) x_j)^2,$$

which is the commonly used Lyapunov function candidate (LFC) in the literature, *e.g.,* [2, 109].

Similarly, to address the problem of bipartite consensus under inter-agent constraints, for the first-order systems (4.1), the control input takes the general form

$$u = -\nabla V, \tag{4.11}$$

where V is a nonlinear function encoding the control objective and the constraints, whereas its gradient makes the synchronization errors in (4.3) converge to zero and guarantees the collision-avoidance and connectivity maintenance constraints defined in (4.9) between agents.

Following the works in [66, 77, 22, 91, 92], we choose to encode the constraints using a barrier-Lyapunov function, and define our control law as a set of its gradient. Thus, we first define a *barrier-Lyapunov function* (BLF)—cf. [54], [66], [76].

Definition 8 *Consider the system $\dot{x} = f(x)$ and let $\mathcal{I}$ be an open set containing the origin. A BLF is a positive definite function $W : \mathcal{I} \to \mathbb{R}_{\geq 0}$, $x \mapsto W(x)$, that is $\mathcal{C}^1$, satisfies $\nabla W(x) f(x) \leq 0$, where $\nabla W(x) := \partial W / \partial x$, and has the property that $W(x) \to \infty$, and $\nabla W(x) \to \infty$ as $x \to \partial\mathcal{I}$, where $\partial\mathcal{I}$ denotes the border of $\mathcal{I}$.*

Now, for each agent $\dot{\bar{x}}_i = v_i$, we consider the BLF $V_{ij} : \mathbb{R} \to \mathbb{R}_{\geq 0}$,

$$V_{ij}(s) = \frac{1}{2}\left[|s|^2 + B_{ij}(s)\right], \tag{4.12}$$

where the first term is used to encode the control objective defined in (4.2) so that its gradient achieves the bipartite formation objective, and $B_{ij}(s)$ encodes the constraints in (4.9). More precisely, $B_{ij}(s)$ consists of two functions $B_{c_{ij}}(s)$ and $B_{r_{ij}}(s)$ satisfying Definition 8, and is defined as

$$B_{ij}(s) = B_{c_{ij}}(s) + \frac{1}{2}(1 + \sigma_{ij}) B_{r_{ij}}(s), \tag{4.13}$$

where $B_{c_{ij}}(s)$ encodes the inter-agent collision avoidance constraints of agents interconnected over each edge. $B_{r_{ij}}(s)$ encodes the connectivity maintenance constraints of agents interconnected over each cooperative edge, such that $\sigma_{ij} = 1$ if the agents i and j are cooperative and $\sigma_{ij} = -1$ otherwise. Furthermore, let $B_{r_{ij}}(s)$ and $B_{c_{ij}}(s)$ be such that $B_{r_{ij}}(s) \to \infty$ as $|s| \to R_k$ and $B_{c_{ij}}(s) \to \infty$ as $|s| \to \Delta_k$. Thus, $B_{ij}(s)$ is non-negative and satisfies $B_{ij}(0) = 0$ and $B_{ij}(s) \to \infty$ as $|s| \to \Delta_k$ for all edges and as $|s| \to R_k$ for cooperative edges. A particular choice for these functions is given by

$$B_{r_{ij}}(s) = \ln\left(\frac{R_k^2}{R_k^2 - |s|^2}\right), \qquad B_{c_{ij}}(s) = \ln\left(\frac{|s|^2}{|s|^2 - \Delta_k^2}\right). \tag{4.14}$$

Remark 14 *The barrier-Lyapunov functions in (4.14) are tailored to deal with symmetric constraints, but our results also apply to asymmetric constraints. For this, $B_{r_{ij}}$ and $B_{c_{ij}}$ may be redefined as*

$$B_{r_{ij}}(s) = \frac{1+\gamma}{2} \ln\left(\frac{R_{k_a}^2}{R_{k_a}^2 - |s|^2}\right) + \frac{1-\gamma}{2} \ln\left(\frac{R_{k_b}^2}{R_{k_b}^2 - |s|^2}\right),$$
$$B_{c_{ij}}(s) = \frac{1+\gamma}{2} \ln\left(\frac{|s|^2}{|s|^2 - \Delta_{k_a}^2}\right) + \frac{1-\gamma}{2} \ln\left(\frac{|s|^2}{|s|^2 - \Delta_{k_b}^2}\right),$$

where $\gamma = -1$ when $s > 0$ and $\gamma = 1$ when $s \leq 0$, as in [86, 91, 92]. •

Now, after (4.12), we see that if we define B_{ij} in function of the errors $\bar{e}_{x_k}$, $B_{ij}(\bar{e}_{x_k})$ has a minimum at $\{\bar{x}_i - \text{sgn}(a_{ij})\bar{x}_j = 0\}$ as desired, but $B_{ij}(\bar{e}_{x_k}) \to \infty$ as $|\bar{x}_i - \text{sgn}(a_{ij})\bar{x}_j| \to \Delta_k$ or $|\bar{x}_i - \text{sgn}(a_{ij})\bar{x}_j| \to R_k$, which is not the objective. Indeed, the constraints are defined with respect to the relative quantities $\delta_k = x_i - x_j$ and not with respect to the synchronization errors $\bar{e}_{x_k} = \bar{x}_i - \text{sgn}(a_{ij})\bar{x}_j$ defined in (4.3). Therefore, the barrier function must be defined to satisfy the control objective in (4.3) expressed in terms of $\bar{e}_{x_k}$ while guaranteeing the constraints in (4.9) imposed on δ_k. To this end,

for agents that are interconnected with cooperative edges, we define a *weight-recentered barrier function* [25]. We define, for a pair of cooperative agents,

$$\tilde{V}_{ij}(x_i, x_j) = \frac{1}{2}|\bar{x}_i - \bar{x}_j|^2 + \tilde{B}_{ij}(x_i - x_j) \tag{4.15}$$

with

$$\tilde{B}_{ij}(x_i - x_j) = \kappa_{1_{ij}} \left[B_{r_{ij}}(x_i - x_j) - B_{r_{ij}}(\bar{b}_{ij})\right] + \kappa_{2_{ij}} \left[B_{c_{ij}}(x_i - x_j) - B_{c_{ij}}(\bar{b}_{ij})\right], \tag{4.16}$$

where $B_{r_{ij}}(\cdot)$ and $B_{r_{ij}}(\cdot)$ are defined in (4.14) and

$$\kappa_{1_{ij}} = \frac{1}{2}\frac{\Delta_k^2}{|\bar{b}_{ij}|^2[|\bar{b}_{ij}|^2 - \Delta_k^2]}, \qquad \kappa_{2_{ij}} = \frac{1}{2}\frac{1}{R_k^2 - |\bar{b}_{ij}|^2}. \tag{4.17}$$

The weight-recentered BLF in (4.15) combines a quadratic term and barrier functions to enforce constraints on the relative positions and penalizes deviations within constrained regions defined by Δ_k and R_k. The recentering and weighting adapt the barrier's influence dynamically based on $\bar{b}_{ij}$ and constraint parameters. Moreover, the weight-recentered BF in (4.16) satisfies $\tilde{B}_{ij}(\bar{b}_{ij}) = 0$ and $\nabla_{x_i}\tilde{B}_{ij}(\bar{b}_{ij}) = 0$, and we also have $\tilde{B}_{ij}(x_i - x_j) \to \infty$ as either $|x_i - x_j| \to \Delta_k$ or $|x_i - x_j| \to R_k$, as desired.

On the other hand, for agents that are interconnected with competitive edges, we use *gradient recentered barrier functions* [101], and we define

$$\widehat{V}_{ij}(x_i, x_j) := V_{ij}(x_i - x_j) - V_{ij}(-2x_j + \bar{b}_{ij}) - \frac{\partial V_{ij}}{\partial s}(-2x_j + \bar{b}_{ij})(\bar{x}_i + \bar{x}_j), \tag{4.18}$$

where $V_{ij}(\cdot)$ is defined in (4.12). In this case, $B_{ij}(s)$ only contains the function $B_{c_{ij}}$ since connectivity constraints are not imposed on competitive edges ($\sigma_{ij} = -1$). The gradient recentered BF in (4.18) modifies the original barrier function defined in (4.12) by subtracting a reference term $V_{ij}(-2x_j + \bar{b}_{ij})$ and a linear correction term based on the gradient of V_{ij} at the recentering point $-2x_j + \bar{b}_{ij}$. Moreover, it satisfies $\widehat{V}_{ij}(x_i, x_j) = 0$ and $\nabla_{x_i}\widehat{V}_{ij}(x_i, x_j) = 0$ as $\bar{e}_{x_k} = \bar{x}_i + \bar{x}_j = 0$, and $\widehat{V}_{ij}(x_i, x_j) \to \infty$ as $|\delta_k| \to \Delta_k$ for all $k \leq M$.

We define different BLFs to address cooperative and competitive edges because there are two inter-agent constraints for cooperative edges: connectivity and collision avoidance, whereas there are only collision avoidance constraints for competitive ones. The weight-recentered BLF allows us not to impose conservative conditions on the initial conditions of the agents while dealing with two constraints. On the other hand, in the case of agents interconnected with competitive interactions, we use gradient recentered barrier functions to shift the minimum of the function at the desired equilibrium while dealing with the competitive edges. Thus, for the system in (4.1), we define the BLF for each edge as the sum of BLFs in (4.15) and (4.18), *i.e.*,

$$\bar{V}_{ij}(x_i, x_j) := \frac{1 + \sigma_{ij}}{2}\tilde{V}_{ij}(x_i, x_j) - \frac{\sigma_{ij} - 1}{2}\widehat{V}_{ij}(x_i, x_j), \tag{4.19}$$

where $\sigma_{ij} = 1$ if the agents i and j are cooperative and $\sigma_{ij} = -1$ otherwise.

Notice that $\bar{V}_{ij}$ in (4.19) has the desired properties by the definition of $\tilde{V}_{ij}$ in (4.15) and $\widehat{V}_{ij}$ in (4.18), since when $\bar{x}_i - \text{sgn}(a_{ij})\bar{x}_j = 0$ it satisfies $\bar{V}_{ij}(x_i, x_j) \equiv 0$, $\nabla_{x_i}\bar{V}_{ij}(x_i, x_j) \equiv 0$, and $\bar{V}_{ij}(x_i, x_j) \to \infty$ as $|\delta_k| \to \Delta_k$ for $k \leq M$, and as $|\delta_k| \to R_k$ for all $k \in \mathcal{E}_m$. Also, we note that $\{\bar{x}_i - \text{sgn}(a_{ij})\bar{x}_j = 0\}$ is a minimum of $\bar{V}(x_i, x_j)$ and, as a matter of fact, it is also a unique minimum even though $\bar{V}(x_i, x_j)$ has a second critical point, which we denote s^*_{ij}—see Appendix A.3.1. Then, we define $\bar{\mathcal{W}} := \cup_{i,j\leq N}\bar{\mathcal{W}}_{ij}$, where

$$\bar{\mathcal{W}}_{ij} := \{\bar{\alpha}_{ij}, s^*_{ij}\},$$

$\bar{\alpha}_{ij} = \bar{b}_{ij}$ if agents i and j are cooperative and $\bar{\alpha}_{ij} = -2x_j + \bar{b}_{ij}$, otherwise, for any $k \leq M$. Then, we define

$$\bar{V}(x) := \sum_{i=1}^{N}\sum_{j\in\mathcal{N}_i}\bar{V}_{ij}(x_i, x_j), \tag{4.20}$$

where $\bar{V}_{ij}(x_i, x_j)$ is defined in (4.19) and $\mathcal{N}_i$ corresponds to the set of the neighbors of agent i. We remark for further development that

$$\frac{\kappa_2}{2}|\delta|^2_{\bar{\mathcal{W}}} \leq \bar{V}(x), \tag{4.21}$$

where $|\delta|_{\bar{\mathcal{W}}} := \min\{|\delta - \bar{\alpha}|, |\delta - s^*|\}$, $\alpha := [\alpha_1\ \alpha_2\ \cdots\ \alpha_M]^\top$ and $s^* := [s^*_1\ s^*_2\ \cdots\ s^*_M]^\top$. In addition, we assume the following:

Assumption 3 *The gradient of the barrier-Lyapunov function $\bar{V}$ in (4.20) satisfies the bound*

$$\frac{1}{2}|\delta|^2_{\bar{\mathcal{W}}} \leq \kappa_1|\nabla_x\bar{V}|^2,$$

where κ_1 is a positive constant.

The domain of $\bar{V}(x)$ in (4.20) is the nodes' state space, which is appropriate for control design. In particular, the BLF in (4.20) encodes collision-avoidance constraints for each edge and connectivity constraints for cooperative edges and is used to design the gradient-based control law, which is used for first-order systems and directed networks. For the other case studies, we use edge coordinates. Therefore, we recall below some facts and notations related to consensus analysis in edge coordinates, and we show how to redefine the BLF given in (4.20), in edge coordinates in graph theory [54, 23].

4.2.2 Barrier-Lyapunov functions in edge coordinates

Using the incidence matrix defined in Definition 2, we may express the synchronization errors in (4.44) in the form

$$\bar{e}_x = \left[E_s^\top \otimes I_n\right]\bar{x}, \quad \bar{e}_v = \left[E_s^\top \otimes I_n\right]v. \tag{4.22}$$

Then, for the purpose of analysis, we proceed to redefine the BLF in (4.20) in these new coordinates. To that end, we note that the constraints, which are imposed on the relative distances between the nodes, may be expressed in function of the edge-coordinates $\bar{e}_{x_k}$ as

$$\delta_k = \bar{e}_{x_k} + \bar{b}_k, \quad i, j \in \mathcal{V}_l,\ l \in \{1, 2\}, \tag{4.23}$$

while for a pair of agents competitive with each other, the synchronization errors are

$$\delta_k = \bar{e}_{x_k} + \bar{d}_k - 2x_j, \quad i \in \mathcal{V}_p,\ j \in \mathcal{V}_q,\ p, q \in \{1, 2\}\ p \neq q, \tag{4.24}$$

with $\bar{b}_k = b_i - \text{sgn}(a_{ij})b_j$. Then, from (4.23) and (4.24), the constraints sets in (4.9) may be rewritten as

$$\mathcal{I}_r = \{\bar{e}_{x_k} \in \mathbb{R}^n : |\bar{e}_{x_k} + \alpha_k| < R_k,\ k \in \mathcal{E}_m\}, \tag{4.25a}$$
$$\mathcal{I}_c = \{\bar{e}_{x_k} \in \mathbb{R}^n : \Delta_k < |\bar{e}_{x_k} + \alpha_k|,\ k \leq M\}, \tag{4.25b}$$

and α_k is defined as

$$\alpha_k := \delta_k - \bar{e}_{x_k}. \tag{4.26}$$

Then, for each cooperative edge, we define the *weight recentered barrier function* [25] in edge coordinates as

$$\begin{aligned}\tilde{W}_k(\alpha_k, \bar{e}_k) = \frac{1}{2}|\bar{e}_k|^2 &+ \kappa_{1_k}\left[\ln\left(\frac{R_k^2}{R_k^2 - |\bar{e}_k + \alpha_k|^2}\right) - \ln\left(\frac{R_k^2}{R_k^2 - |\alpha_k|^2}\right)\right] \\ &+ \kappa_{2_k}\left[\ln\left(\frac{|\bar{e}_k + \alpha_k|^2}{|\bar{e}_k + \alpha_k|^2 - \Delta_k^2}\right) - \ln\left(\frac{|\alpha_k|^2}{|\alpha_k|^2 - \Delta_k^2}\right)\right],\end{aligned} \tag{4.27}$$

where

$$\kappa_{1_k} = \frac{1}{2}\frac{\Delta_k^2}{|\alpha_k|^2(|\alpha_k|^2 - \Delta_k^2)}, \qquad \kappa_{2_k} = \frac{1}{2}\frac{1}{R_k^2 - |\alpha_k|^2}. \tag{4.28}$$

and $\alpha_k = b_k$. The weight recentered BLF in (4.27) satisfies $\tilde{W}_k(\alpha_k, 0) = 0$ and $\nabla_{\bar{e}_x}\tilde{W}_k(\alpha_k, 0) = 0$, where $\nabla_{\bar{e}_{x_k}}\tilde{W}_k = \frac{\partial \tilde{W}_k}{\partial \bar{e}_{x_k}}$. Moreover, we also have that $\tilde{W}_k(\alpha_k, \bar{e}_k) \to \infty$ as either $|\delta_k| \to \Delta_k$ or $|\delta_k| \to R_k$. On the other hand, for agents that are interconnected with competitive edges, we define the *gradient recentered barrier function* [101] as

$$\widehat{W}_k(\alpha_k, \bar{e}_{x_k}) := W_k(\bar{e}_{x_k} + \alpha_k) - W_k(\alpha_k) - \frac{\partial W_k}{\partial s}(\alpha_k)\bar{e}_{x_k}. \tag{4.29}$$

The gradient recentered barrier function in (4.29) satisfies $\widehat{W}_k(\alpha_k, 0) = 0$, $\nabla_{\bar{e}_{x_k}}\widehat{W}_k(\alpha_k, 0) = 0$ and $\widehat{W}_k(\alpha_k, \bar{e}_{x_k}) \to \infty$ as $|\delta_k| \to \Delta_k$ for $k \leq M$, and as $|\delta_k| \to R_k$ for all $\sigma_k = 1$.

Now, for the system in (4.1), we define the BLF for each edge as the sum of the BLFs in (4.27) and (4.29), *i.e.*,

$$\bar{W}_k := \frac{1 + \sigma_k}{2}\tilde{W}_k(\alpha_k, \bar{e}_{x_k}) - \frac{\sigma_k - 1}{2}\widehat{W}_k(\alpha_k, \bar{e}_{x_k}), \tag{4.30}$$

with $\sigma_k = 1$ if agents i and j are cooperative and $\sigma_k = -1$ otherwise. Notice that $\bar{W}_k$ in (4.30) has the desired properties by the definition of $\tilde{W}_k$ in (4.27) and $\widehat{W}_k$ in (4.29), since it satisfies $\bar{W}_k(\alpha_k, 0) \equiv 0$, $\nabla_{\bar{e}_{x_k}}\bar{W}_k(\alpha_k, 0) \equiv 0$, where $\nabla_{\bar{e}_{x_k}}\bar{W}_k = \partial \bar{W}_k / \partial \bar{e}_{x_k}$, and $\bar{W}_k(\alpha_k, \bar{e}_{x_k}) \to \infty$ as $|\delta_k| \to \Delta_k$ for $k \leq M$, and as $|\delta_k| \to R_k$ for all $k \in \mathcal{E}_m$. Also, we note that $\{\bar{e}_{x_k} = 0\}$ is a minimum of $\bar{W}(\alpha_k, \cdot)$. As a matter of fact, it is also a unique

minimum even though $\bar{W}(\alpha_k, \cdot)$ has a second critical point, which we denote by e_k^*—see Appendix A.3.2—and we define $\mathcal{W} := \cup_{k \leq M} \mathcal{W}_k$, where

$$\mathcal{W}_k := \{0, e_k^*\}$$

for any $k \leq M$. Then, let

$$\bar{W}(\alpha, \bar{e}_x) := \sum_{k=1}^{M} \bar{W}_k(\alpha_k, \bar{e}_{x_k}), \tag{4.31}$$

where $\bar{W}_k(\alpha_k, \bar{e}_{x_k})$ is defined in (4.30). Thus, to solve the constrained bipartite formation problem, we provide below control laws of the generic form (4.11) in edge coordinates, that is,

$$u = -k_1 \left[E_s \otimes I_n\right] \nabla_{\bar{e}_x} \bar{W} + \ldots,$$

where $\bar{W}$ is the nonlinear function defined in (4.31), in edge coordinates and encoding the inter-agent distance constraints and the bipartite consensus objective in position. The dots represent additional terms depending on the control objective and due to the presence of competitive interactions and collision avoidance constraints.

For the purpose of analysis, we use another artifice, which consists in splitting the state variables and which applies to structurally balanced signed graphs containing a spanning tree (sufficient and necessary condition for bipartite consensus), is to distinguish the state-variables related to an underlying-tree graph $\mathcal{G}_t$, from the rest of states, corresponding to the graph $\mathcal{G}_c := \mathcal{G} \backslash \mathcal{G}_t$. Then, the consensus problem may be addressed as that of the stabilization of the origin for a reduced-order system—see Appendix A.1 for an example. To better see this, let the incidence matrix E_s be partitioned as [23, 54]

$$E_s = \begin{bmatrix} E_{t_s} & E_{c_s} \end{bmatrix}, \tag{4.32}$$

where $E_{t_s} \in \mathbb{R}^{N \times N-1}$ is the incidence matrix representing the edges of the spanning tree of and $E_{c_s} \in \mathbb{R}^{N \times M-(N-1)}$ is the incidence matrix representing the remaining edges. In the Proposition 9 below we define E_s in terms of E_{t_s}. Then, after (4.22) and (4.32) we have

$$\bar{e}_x = \left[(E_{t_s}^\top \bar{x})^\top \ (E_{c_s}^\top \bar{x})^\top\right]^\top,$$

so we may define $\bar{e}_x =: [\bar{e}_{x_t}^\top \quad \bar{e}_{x_c}^\top]^\top$. The indices $_t$ and $_c$ refer to states of the graphs $\mathcal{G}_t$ and $\mathcal{G}_c$ respectively. Proposition 9 establishes a relation between the consensus errors $\bar{e}_x$ and the spanning-tree errors $\bar{e}_{x_t}$, from which it follows that the objective (4.2) is attained if $\bar{e}_{x_t} \to 0$.

Proposition 9 ([84]). *For a structurally balanced signed graph, there exists a matrix R_s such that*

$$E_s = E_{t_s} R_s, \tag{4.33}$$

where

$$R_s := \begin{bmatrix} I_{N-1} & T_s \end{bmatrix}, \quad T_s := (E_{t_s}^\top E_{t_s})^{-1} E_{t_s}^\top E_{c_s}. \tag{4.34}$$

Proof: Applying the edge-gauge transformation and using the partition of E_s as in (4.32) we express the incidence matrix of an unsigned graph E as

$$E = D[E_{t_s} \quad E_{c_s}]D_e = [DE_{t_s}D_{e_t} \quad DE_{c_s}D_{e_c}], \tag{4.35}$$

where $D_e = \text{diag}([\sigma_{e_t},\ \sigma_{e_c}])$ with $\sigma_{e_{t_j}} = \{\pm 1\}$ and $\sigma_{e_{cl}} = \{\pm 1\}$ for $j < N-1$ and $l \leq M - N + 1$, $D_{e_t} = \text{diag}(\sigma_{e_t})$ and $D_{e_c} = \text{diag}(\sigma_{e_c})$ are the parts of the edge-gauge transformation matrix corresponding to the spanning tree and the remaining edges, respectively. For an unsigned network, the columns of the incidence matrix representing the remaining edges, E_c, are linearly dependent on the columns of the incidence matrix representing the spanning tree, E_t, and this can be expressed using a matrix T by $E_c = E_t T$ [54, Theorem 4.3]. So, replacing E_c and E_t by the expressions in (4.35) and left multiplying it by $(DE_{t_s}D_{e_t})^\top$, we obtain

$$\begin{aligned}(DE_{t_s}D_{e_t})^\top DE_{c_s}D_{e_c} &= (DE_{t_s}D_{e_t})^\top DE_{t_s}D_{e_t}T \\ T &= D_{e_t}(E_{t_s}^\top E_{t_s})^{-1}E_{t_s}^\top E_{c_s}D_{e_c}.\end{aligned}$$

Then, we define $T_s := D_{e_t}TD_{e_c}$ and $R_s := [I_{N-1} \quad T_s]$, and the statement in (4.33) follows. ■

The utility of Proposition 9 resides in the fact that

$$\bar{e}_x = [(E_{t_s}R_s)^\top \otimes I_n]\bar{x} = [R_s^\top \otimes I_n]\bar{e}_{x_t}. \tag{4.36}$$

Therefore, the bipartite consensus problem may be addressed as that of stabilizing the origin of a *reduced-order* system in terms of the spanning-tree errors. In particular, the objective (4.2) is attained if $\bar{e}_{x_t} \to 0$. We use this fact in what follows.

4.3 CONTROL OVER UNDIRECTED SIGNED NETWORKS

Now that we have modeled the dynamics and imposed constraints accordingly, we address the constrained bipartite consensus problem for first- and second-order systems interconnected over undirected signed networks.

Assumption 4 *The signed undirected graph is connected and structurally balanced.*

We consider agents under inter-agent constraints and interconnected over undirected signed networks that are connected and structurally balanced, as stated in Assumption 4.

We know from Chapter 2 that in the case of an undirected and structurally unbalanced graph, all of the agents' states converge to zero. Thus, if we relax the *structural balance* property assumption on the undirected signed graph, the resulting Laplacian matrix would not have a zero eigenvalue but only positive eigenvalues, making all agents converge to zero. In the considered problem, as it is required to design a control law that guarantees inter-agent collision avoidance, making them converge to the same state does not respect the imposed constraint. Thus, we only consider undirected signed networks that are structurally balanced, both for first- and second-order systems.

4.3.1 First-order systems

Consider a group of N dynamical systems modeled by (4.1) over an undirected and structurally balanced signed graph and subject to inter-agent distance constraints encoded by (4.9). Then, for the purpose of making them achieve bipartite consensus, consider the BLF-gradient-based bipartite consensus control law,

$$u_i = -k_1 \sum_{j \in \mathcal{N}_i} \nabla_{x_i} \bar{V}_{ij}, \tag{4.37}$$

where $\bar{V}_{ij}$ is defined in (4.19) and encodes the inter-agents constraints defined in (4.9). Thus, the control can be written in vector form as

$$u = -k_1 \nabla_x \bar{V}. \tag{4.38}$$

Replacing (4.38) in (4.1), the closed-loop system reads

$$\dot{x} = -k_1 \nabla_x \bar{V}. \tag{4.39}$$

For this system, we have the following.

Proposition 10 *(Leaderless bipartite formation-consensus). Consider the system (4.1) in closed loop with the control law (4.38), where $\bar{V}(x)$ is defined in (4.20), and under Assumptions 3 and 4. Then, the closed-loop system achieves bipartite formation-consensus, that is (4.2) holds, while the collision-avoidance and connectivity-maintenance constraints are maintained for almost all initial conditions such that $\delta(0) \in \mathcal{I}$, $|\alpha_{ij}(0)| > \Delta_k$ for any $i, j \leq N$. Moreover, the set $\mathcal{I}$ defined in (4.9) is rendered forward invariant.*

Proof: Consider the function $\bar{V}(x)$ defined in (4.20). $\bar{V}(x)$ is such that $\bar{V}(x) = 0$ for $\forall x \in \{\bar{e}_x = 0\}$ and its total derivate yields

$$\begin{aligned} \dot{\bar{V}} &= \nabla_x \bar{V}^\top \dot{x} \\ &= \nabla_x \bar{V}^\top (-k_1 \nabla_x \bar{V}) = -k_1 |\nabla_x \bar{V}|^2. \end{aligned} \tag{4.40}$$

Then, under the Assumption 3, we also have

$$\dot{\bar{V}} \leq -\frac{k_1}{2\kappa_1} |\delta|^2_{\bar{\mathcal{W}}} \leq 0, \tag{4.41}$$

where we recall that $\bar{\mathcal{W}} = \{\bar{\alpha}, s^*\}$ and s^* are the saddle points of $\bar{V}$.

Now, for any $\epsilon > 0$, let us define $\mathcal{I}_\epsilon$, where $\mathcal{I}_\epsilon := \mathcal{I}_{r_\epsilon} \cap \mathcal{I}_{c_\epsilon}$ for cooperative agents and $\mathcal{I}_\epsilon := \mathcal{I}_{c_\epsilon}$ for competitive agents, while $\mathcal{I}_{r_\epsilon} := \{\delta_k \in \mathbb{R}^n : |\delta_k| < R_k - \epsilon,\ k \in \mathcal{E}_m\}$ and $\mathcal{I}_{c_\epsilon} := \{\delta_k \in \mathbb{R}^n : \Delta_k + \epsilon < |\delta_k|,\ k \in \mathcal{E}_m\}$. Then, from the second inequality in (4.41) and (4.21), $\delta(0) \in \mathcal{I}_\epsilon \Rightarrow \delta(t) \in \mathcal{I}'$, where

$$\mathcal{I}' := \left\{ \delta \in \mathcal{I} : V(x) \leq \sup_{\delta \in \mathcal{I}_\epsilon} \sqrt{2 \frac{V(x)}{\kappa_2}} \right\}.$$

Moreover, from the latter and the first inequality in (4.41), $|\delta|_{\bar{\mathcal{W}}} \to 0$ as $t \to \infty$. Furthermore, this holds for $\epsilon > 0$ arbitrarily small, which implies asymptotic stability of $\bar{\mathcal{W}}$ for all initial conditions, such that $\delta(0) \in \mathcal{I}$. However, since s^* is a saddle point of $\bar{V}$, the set of initial conditions generating solutions that converge to s^* has zero Lebesgue measure. Thus, almost all initial conditions generate trajectories that converge to $\{\delta = \bar{\alpha}\}$, which corresponds to $\{\bar{e}_x = 0\}$, or equivalently, $\{x_i - x_j = \bar{b}_{ij}\}$ if the agents i and j are cooperative and to $\{x_i + x_j = \bar{b}_{ij}\}$ if the agents i and j are competitive. Thus, the statement follows. ■

Remark 15 ([84]). *The condition in Proposition 10 on $\alpha_{ij}(0)$ is not restrictive. For cooperative agents, $\alpha_{ij} = \bar{b}_{ij}$, so $|\alpha_{ij}(0)| > \Delta_{ij}$ means that the formation must respect the collision-avoidance constraints (the formation must be "safe"). For competitive agents, $|\alpha_{ij}(0)| > \Delta_{ij}$ means that $|-2x_j(0) + \bar{b}_{ij}| > \Delta_{ij}$, which restricts the initial conditions in absolute coordinates, i.e., with respect to a fixed frame. However, in the scenario considered in this section, the measurements are relative (edge coordinates). That is, absolute positions are irrelevant, so $x_j(0)$ may be conveniently redefined by replacing the origin of the fixed frame, if needed.* •

In the next subsection, we extend the results from first-order systems to second-order systems.

4.3.2 Second-order systems

Consider now a network of N dynamical systems having the following dynamics.

$$\dot{\bar{x}}_i = v_i, \tag{4.42a}$$

$$\dot{v}_i = u_i, \qquad \bar{x}_i \in \mathbb{R}^n,\ i \leq N, \tag{4.42b}$$

where $\bar{x}_i = x_i - b_i$, x_i is the agent's position, and b_i is a relative displacement defining the desired geometric shape of the formation. In the absence of constraints, bipartite consensus within a network of second-order systems over a signed graph may be achieved via the control law—cf. [104],

$$u_i = -\sum_{j=1}^{N} |a_{ij}| \Big[k_1[\bar{x}_i - \operatorname{sgn}(a_{ij})\bar{x}_j] + k_2[v_i - \operatorname{sgn}(a_{ij})v_j] \Big], \quad k_1, k_2 > 0. \tag{4.43}$$

In (4.43), the first term of the control law guarantees the bipartite consensus on position, and the second term guarantees the bipartite consensus on velocity. Moreover, as for first-order systems, we may define the synchronization errors

$$\bar{e}_{x_k} := \bar{x}_i - \operatorname{sgn}(a_{ij})\bar{x}_j, \quad \bar{e}_{v_k} := v_i - \operatorname{sgn}(a_{ij})v_j, \quad k \leq M, \tag{4.44}$$

where k denotes the index of the interconnection between the ith and jth agents. Then, we formulate the following problem of interest.

Definition 9 (Leaderless bipartite consensus for 2nd-order systems) *The systems (4.42)-(4.43) are said to achieve bipartite position and velocity consensus if*

$$\lim_{t\to\infty} \bar{e}_{x_k}(t) = 0, \quad \lim_{t\to\infty} \bar{e}_{v_k}(t) = 0, \qquad k \leq M. \tag{4.45}$$

That is, for agents i and j cooperative with each other, bipartite consensus implies that $(\bar{x}_i, v_i) \to (\bar{x}_j, v_j)$ while for agents competitive with each other we have $(\bar{x}_i, v_i) \to (-\bar{x}_j, -v_j)$.

Definition 10 (Leader-follower bipartite consensus for 2nd-order systems) *Let $x_0 \in \mathbb{R}^n$ be the position of the virtual leader ν_0, whose dynamics is given in (4.4) and is accessible to at least one follower. Then, the systems (4.42)-(4.43) are said to achieve leader-follower bipartite position and velocity consensus if (4.45) and*

$$\lim_{t\to\infty} \hat{e}_i(t) = 0, \qquad i \leq N. \tag{4.46}$$

That is, for agents i cooperative with the static virtual leader, bipartite consensus implies that $(\bar{x}_i, v_i) \to (x_0, 0)$ while for agents competitive with the static virtual leader we have $(\bar{x}_i, v_i) \to (-x_0, 0)$.

Under these conditions, it is required to design a distributed bipartite consensus control law u_i such that the synchronization errors in position and velocity, as defined in (4.44), satisfy (4.45) and the agents' trajectories satisfy the connectivity maintenance and collision-avoidance constraints, that is, $\delta(t) \in \mathcal{I}$—see (4.9).

As we explained before, for second-order systems interconnected over undirected networks, for technical reasons, we choose to work in edge coordinates. Let k_1, $k_2 > 0$ and $k_3 \geq 0$. Then, we introduce the BLF-gradient-based bipartite formation-consensus control law,

$$u_i := -k_1 \sum_{k=1}^{M} [E_s]_{ik} \nabla_{\bar{e}_{x_k}} \bar{W}_k - k_1 \sum_{k=1}^{M} [\mathbb{E}]_{ik} \nabla_{\alpha_k} \bar{W}_k - k_2 \sum_{k=1}^{M} [E_s]_{ik} \bar{e}_{v_k} - k_3 v_i, \tag{4.47}$$

where $\bar{W}$ is defined in (4.31) and $\mathbb{E} := E - E_s$, where E corresponds to the incidence matrix of the unsigned version of the signed network —See Definition 2.38.[1] From its definition, $\mathbb{E}$ is a matrix containing only the information of competitive interactions in the network. Thus, the control law in (4.47) is given in the vector form as

$$u = -k_1 \left[E_s \otimes I_n\right] \nabla_{\bar{e}_x} \bar{W} - k_1 \left[\mathbb{E} \otimes I_n\right] \nabla_{\alpha} \bar{W} - k_2 \left[E_s \otimes I_n\right] \bar{e}_v - k_3 v, \tag{4.48}$$

where the first two terms in (4.48) ensure bipartite position consensus while the third guarantees velocity bipartite consensus, *i.e.*, that (4.45) holds. The second term is needed specifically to cope with competitive agents; technically, it stems from a Lyapunov-control redesign—elucidated in the proof of Proposition 11. In the last term, if $k_3 > 0$, the velocities $v \to 0$. Therefore, this gain may be set to a positive value or zero, depending on the control goal, be that the vehicles continue to advance ($v \not\to 0$) or that they converge to two rendezvous points in formation ($v \to 0$), one for cooperative and one for competitive agents—see Section 4.3.3 for an example.

[1] A structurally balanced signed network can be transformed into an unsigned one using the gauge transformation —see Subsection 2.3 and [2, 23].

Remark 16 *In [19], the authors propose a bipartite formation control law for multi-agent systems over undirected signed networks and under inter-agent distance constraints. This control law is given by*

$$u_i := -k_1 \sum_{k=1}^{M} [E_s]_{ik} \nabla_{\bar{e}_{x_k}} \widehat{W}_k - k_1 \sum_{k=1}^{M} [\mathbb{B}]_{ik} \nabla_{\alpha_k} \widehat{W}_k - k_2 \sum_{k=1}^{M} [E_s]_{ik} \bar{e}_{v_k} - k_3 v_i, \tag{4.49}$$

where $\mathbb{B} = (1+\beta)(\beta I + E_{t_s} L_{e_{ts}}^{-1} E_{t_s}^\top)^{-1}(E - E_s), \beta > 0$. *Note that to compute* $\mathbb{B}$, *global knowledge of the network is needed. This renders the control law* (4.49) *centralized. In contrast to this, the control law proposed in* (4.47) *is distributed and solves leaderless and leader-follower bipartite formation control problems.* •

We perform the stability analysis of the system (4.42) in closed loop with the bipartite formation control law (4.48), in terms of spanning-tree coordinates. To that end, using the definitions of the edge-based formulation, we express the control law (4.48) in terms of the spanning tree errors $\bar{e}_{x_t}$—see equations (4.36)—by introducing a function $\tilde{W}_k$ defined as $\tilde{W}(\alpha, \bar{e}_{x_t}) = \bar{W}(\alpha, \left[R_s^\top \otimes I_n\right] \bar{e}_{x_t})$, with $\bar{W}$ defined in (4.31). Then, after (4.36), the gradient of $\tilde{W}$ with respect to $\bar{e}_{x_t}$ yields,

$$\nabla_{\bar{e}_{x_t}} \tilde{W} = \frac{\partial \tilde{W}(\alpha, \bar{e}_{x_t})}{\partial \bar{e}_x}^\top \frac{\partial \bar{e}_x}{\partial \bar{e}_{x_t}} = \nabla_{\bar{e}_x} \bar{W}^\top \left[R_s \otimes I_n\right]^\top. \tag{4.50}$$

After (4.33) and (4.50), the control law in (4.48) may be wirtten in spanning-tree coordinates as

$$u = -k_1 \left[E_{t_s} \otimes I_n\right] \nabla_{\bar{e}_{x_t}} \tilde{W} - k_2 \left[E_{t_s} R_s R_s^\top \otimes I_n\right] \bar{e}_{v_t} - k_3 v - k_1 \left[\mathbb{E} \otimes I_n\right] \nabla_\alpha \tilde{W}. \tag{4.51}$$

Then, differentiating (4.22) on both sides and using $\dot{v} = u$, with u defined in (4.51), we obtain the following in terms of the errors corresponding to the spanning-tree:

$$\dot{\bar{e}}_{x_t} = \bar{e}_{v_t} \tag{4.52a}$$

$$\begin{aligned} \dot{\bar{e}}_{v_t} = &- k_1 \left[L_{e_{ts}} \otimes I_n\right] \nabla_{\bar{e}_{x_t}} \tilde{W} - k_1 \left[E_{t_s}^\top \mathbb{E} \otimes I_n\right] \nabla_\alpha \tilde{W} \\ &- k_2 \left[L_{e_{ts}} R_s R_s^\top \otimes I_n\right] \bar{e}_{v_t} - k_3 \bar{e}_{v_t}, \end{aligned} \tag{4.52b}$$

where $E_{t_s}^\top E_{t_s} = L_{e_{ts}}$ corresponds to the edge Laplacian associated with a spanning tree and has $N-1$ edges. This can be easily seen by using the edge-gauge transformation and obtaining the edge Laplacian matrix corresponding to a spanning tree of an unsigned network, *i.e.*, $L_{e_t} = D_e L_{e_{ts}} D_e$. Also, we have $D_e = D_e^\top = D_e^{-1}$ so $D_e L_{e_{ts}} D_e$ is a similarity transformation, which implies that the spectra of L_{e_t} and $L_{e_{ts}}$ coincide. Consequently, as L_{e_t} has the same $N-1$ non-zero eigenvalues of the Laplacian matrix L, and so does $L_{e_{ts}}$—see [19, Remark 3].

In what follows, we present two statements on leaderless and leader-follower bipartite consensus, using control laws of the form (4.48).

4.3.2.1 Leaderless bipartite formation-consensus-control problem

For the closed-loop system (4.52), in spanning-tree coordinates, we have the following.

Proposition 11 (*Leaderless bipartite formation-consensus* [84]). *Consider the system (4.42) in closed loop with the distributed control law (4.48), with $\bar{W}(\alpha, \bar{e}_x)$ as defined in (4.31). Assume that the resulting network is structurally balanced and contains a directed spanning tree. Then, the set $\{(\bar{e}_x, v) = (0, 0)\}$ is asymptotically stable for almost all initial conditions such that $(\bar{e}_x(0), v(0)) \in \mathcal{I} \times \mathbb{R}^{nN}$ and $|\alpha_k(0)| > \Delta_k$ for any $k \leq M$.*

Proof: First, employing (4.36), we express the inter-agent distance constraints in (4.25) in terms of the errors corresponding to the spanning tree. Let $\mathcal{I}_t := \mathcal{I}_{r_t} \cap \mathcal{I}_{c_t}$ for cooperative agents and $\mathcal{I}_t := \mathcal{I}_{c_t}$ for competitive agents, where

$$\mathcal{I}_{r_t} := \{\bar{e}_{x_t} \in \mathbb{R}^{n(N-1)} : |[r_{s_k} \otimes I_n]^\top \bar{e}_{x_{t_k}} + \alpha_k| < R_k,\ k \in \mathcal{E}_{m_t}\}, \tag{4.53}$$

$$\mathcal{I}_{c_t} := \{\bar{e}_{x_t} \in \mathbb{R}^{n(N-1)} : \Delta_k < |[r_{s_k} \otimes I_n]^\top \bar{e}_{x_{t_k}} + \alpha_k|,\ k \leq N-1\}, \tag{4.54}$$

r_{s_k} is the kth column of R_s and $\mathcal{E}_{m_t}$ denotes the set of indices k corresponding to the $N-1$ edges of the spanning-tree graph interconnecting pairs of cooperative agents.

Next, we proceed to analyze the system (4.52). To that end, consider the Lyapunov function candidate

$$V(\alpha, \bar{e}_{x_t}, v) = k_1 \tilde{W}(\alpha, \bar{e}_{x_t}) + \frac{1}{2}|v|^2, \tag{4.55}$$

where $\tilde{W}(\alpha, \bar{e}_{x_t})$ is defined in (4.31), and $k_1 > 0$. Therefore, V in (4.55) is positive definite with respect to the state variables $\bar{e}_{x_t}$ and $\bar{e}_{v_t}$. In addition, by its construction, $V(\alpha, \bar{e}_{x_t}, v) \to \infty$ as $\bar{e}_{x_t}$ approaches the boundary $\partial\mathcal{I}_t$ of the set $\mathcal{I}_t$ in (4.53), for a given $\bar{e}_{v_t}$ and v. We also remark that the positivity of V holds uniformly in α. More precisely, there exists $\mu > 0$ such that $\mu[|\bar{e}_{x_t}|^2 + |v|^2] \leq V(\alpha, \bar{e}_{x_t}, v)$ and $V(\alpha, \bar{e}_{x_t}, v) \to 0$ as $|\bar{e}_{x_t}| \to 0$ and $|v| \to 0$.

Next, we compute the total derivative of V. For (4.42b) and (4.51), we have

$$\dot{v} = -k_1 [E_{t_s} \otimes I_n] \nabla_{\bar{e}_{x_t}} \tilde{W} - k_2 \left[E_{t_s} R_s R_s^\top \otimes I_n\right] \bar{e}_{v_t} - k_3 v - k_1 [\mathbb{E} \otimes I_n] \nabla_\alpha \tilde{W}. \tag{4.56}$$

Then,

$$\begin{aligned}\dot{V}(\alpha, \bar{e}_{x_t}, v) = k_1 \nabla_{\bar{e}_{x_t}} \tilde{W}^\top \dot{\bar{e}}_{x_t} + k_1 \nabla_\alpha \tilde{W}^\top [\mathbb{E} \otimes I_n]^\top v + v^\top \Big[-k_1 [E_{t_s} \otimes I_n] \nabla_{\bar{e}_{x_t}} \tilde{W} \\ -k_2 \left[E_{t_s} R_s R_s^\top \otimes I_n\right] \bar{e}_{v_t} - k_3 v - k_1 [\mathbb{E} \otimes I_n] \nabla_\alpha \tilde{W}\Big],\end{aligned}$$

so using (4.33) and (4.36), we obtain

$$\dot{V}(\alpha, \bar{e}_{x_t}, v) = -k_2 |\bar{e}_v|^2 - k_3 |v|^2, \tag{4.57}$$

which is negative semidefinite for all $(\bar{e}_{x_t}, v) \in \mathcal{I}_t \times \mathbb{R}^{nN}$.

Next, we use LaSalle's invariance theorem. On the set $\{(\bar{e}, v) : \dot{V} = 0\}$ we have $\bar{e}_v = 0$ and $v = 0$. We also remark that from the definition of α in (4.26), we have

$\alpha = [E \otimes I_n]^\top x - [E_s \otimes I_n]^\top \bar{x}$, so $\dot{\alpha} = [(E - E_s) \otimes I_n]^\top v = [\mathbb{E} \otimes I_n]^\top v$. Consequently, $\dot{\alpha} = 0$ meaning that α is constant. Furthermore, after (4.56), we have

$$- k_1 [E_{t_s} \otimes I_n] \nabla_{\bar{e}_{x_t}} \tilde{W} = k_1 [\mathbb{E} \otimes I_n] \nabla_\alpha \tilde{W}, \tag{4.58}$$

and after (4.29), we also have

$$\nabla_\alpha \tilde{W} = \nabla_{\bar{e}_{x_t}} \tilde{W} - \frac{\partial}{\partial \alpha} \left\{ \frac{\partial W}{\partial \alpha}(\alpha) \right\} \bar{e}_{x_t}. \tag{4.59}$$

Since α remains constant on $\{\dot{V} = 0\}$, the last term on the right-hand-side of (4.59) equals to zero. Thus, (4.58) holds if and only if $-k_1 [(E_{t_s} + E_t - E_{t_s}) \otimes I_n] \nabla_{\bar{e}_{x_t}} \tilde{W} = 0$. Now, since E_t is full rank (because it corresponds to the incidence matrix of a spanning tree) it follows that $\nabla_{\bar{e}_{x_t}} \tilde{W} = 0$, which holds if and only if $\bar{e}_t \in \mathcal{W}^t$, where $\mathcal{W}^t = \{0, e_t^*\}$ and e_t^* is the saddle point of $\tilde{W}$. Therefore, the solutions converge to the set $\mathcal{W}^t \times \{0\}$. However, since e_t^* is a saddle point of $\tilde{W}$, the set of initial conditions generating solutions that converge to $(e_t^*, 0)$ has zero Lebesgue measure. Thus, almost all initial conditions generate trajectories that converge to the origin. Asymptotic stability follows.

Next, we show that asymptotic stability holds for almost all initial conditions in $\mathcal{I}_t \times \mathbb{R}^{nN}$. Referring to (4.53), $\bar{e}_t \in \mathcal{I}_t$ implies $\bar{e} \in \mathcal{I}$, so we must show that $\mathcal{I}_t \times \mathbb{R}^{nN}$ is forward invariant. To that end, for any r and $\epsilon \geq 0$, let us define

$$\mathcal{D}_{r,\epsilon} := \{v \in B_r,\ \bar{e}_t \in \mathcal{I}_\epsilon\},$$

where $\mathcal{I}_\epsilon := \mathcal{I}_{c_\epsilon} \cap \mathcal{I}_{r_\epsilon}$ for cooperative agents and $\mathcal{I}_\epsilon := \mathcal{I}_{c_\epsilon}$ for competitive agents, while

$$\mathcal{I}_{\epsilon_r} := \{\bar{e}_{x t_k} \in \mathbb{R}^n : |\bar{e}_{x t_k} + \alpha_k| < R_k - \epsilon,\ k \in \mathcal{E}_{m_t}\}, \tag{4.60a}$$

$$\mathcal{I}_{\epsilon_c} := \{\bar{e}_{x t_k} \in \mathbb{R}^n : \Delta_k + \epsilon < |\bar{e}_{x t_k} + \alpha_k|,\ k \leq N - 1\}. \tag{4.60b}$$

From the definition of $\tilde{W}(\alpha, \bar{e}_t)$, $V(\alpha, \bar{e}_{x_t}, v)$ is positive definite on $\mathcal{I}_\epsilon$ for all $\bar{e}_{x_t} \in \mathcal{I}_\epsilon$, $v \in \mathbb{R}^{nN}$ and for all ϵ. From (4.57), we have

$$|\bar{e}_{x_t}(t)|^2 + |v(t)|^2 \leq \frac{1}{\mu} V(\alpha(0), \bar{e}_{x_t}(0), v(0)).$$

Then,

$$(\bar{e}_{x_t}(0), v(0)) \in \mathcal{D}_{r,\epsilon} \Rightarrow (\bar{e}_{x_t}(t), v(t)) \in \mathcal{D}', \tag{4.61}$$

where

$$\mathcal{D}' := \left\{ (\bar{e}_{x_t}, v) \in \mathcal{I}_t \times \mathbb{R}^{nN} : V(\alpha, \bar{e}_{x_t}, v) \leq \gamma_{r,\epsilon} \right\},$$

and

$$\gamma_{r,\epsilon} := \sup_{\substack{(\bar{e}_{x_t}, v) \in \mathcal{D}_{r,\epsilon} \\ \alpha \in \mathbb{R}^{nN}}} \sqrt{\frac{V(\alpha, \bar{e}_{x_t}, v)}{\mu}}.$$

Note that $\gamma_{r,\epsilon}$ is well defined because V is uniformly bounded in α and $\mathcal{D}_{r,\epsilon}$ is bounded. After LaSalle's invariance principle, we conclude that all the trajectories contained in $\mathcal{D}'$ converge to the set $\mathcal{W}^t \times \{0\}$. After (4.61), that is all the trajectories starting in $\mathcal{D}_{r,\epsilon}$. This holds for any $r > 0$ arbitrarily large and $\epsilon > 0$ arbitrarily small. Thus, again because $\mathcal{W}^t = \{0, e_t^*\}$, and e_t^* is a saddle point, we conclude that the origin is asymptotically stable for almost all trajectories $\bar{e}_{x_t}(t), v(t)$ starting in $\mathcal{I}_t \times \mathbb{R}^{nN}$, or equivalently for almost all trajectories $\bar{e}_x(t), v(t)$ starting in $\mathcal{I} \times \mathbb{R}^{nN}$. ■

We now address the problem of leader-follower bipartite formation.

4.3.2.2 Leader-follower bipartite formation-consensus-control problem

Proposition 11 addresses the leaderless bipartite consensus problem. As in previous sections, it takes simple modifications to our control law to address the leader-follower bipartite problem. To that end, we introduce now a virtual leader to the system, and we modify the BLF-gradient-based bipartite formation-consensus control input as

$$\begin{aligned} u_i := &- k_1 \sum_{k=1}^{M} [E_s]_{ik} \nabla_{\bar{e}_{x_k}} \bar{W}_k - k_1 \sum_{k=1}^{M} [\mathbb{E}]_{ik} \nabla_{\alpha_k} \bar{W}_k - k_2 \sum_{k=1}^{M} [E_s]_{ik} \bar{e}_{v_k} \\ &- k_3 v_i - k_1 a_{l_i} \hat{e}_i, \end{aligned} \tag{4.62}$$

where $a_{l_i} = 1$ if there is an information exchange between the virtual leader and the agent i and $a_{l_i} = 0$ otherwise, $\mathbb{E} := E - E_s$, and the BLF is redefined as

$$\bar{W}(\alpha, \bar{e}_x, \hat{e}) = \sum_{k=1}^{M} \left(\frac{1 + \sigma_k}{2} \tilde{W}_k(\alpha_k, \bar{e}_x) - \frac{\sigma_k - 1}{2} \widehat{W}_k(\alpha_k, \bar{e}_x) \right) + \frac{1}{2} \sum_{i=1}^{N} a_{l_i} |\hat{e}_i|^2. \tag{4.63}$$

Thus, the control law in (4.62) can be written in the vector form as

$$u = -k_1 \left[E_s \otimes I_n \right] \nabla_{\bar{e}_x} \bar{W} - k_1 \left[\mathbb{E} \otimes I_n \right] \nabla_{\alpha} \bar{W} - k_2 \left[E_s \otimes I_n \right] \bar{e}_v - k_3 v - k_1 \nabla_{\hat{e}} \bar{W}. \tag{4.64}$$

We analyze the stability of (4.42) and (4.4) in closed loop with the bipartite formation control law (4.64). Now, after (4.36), (4.33) and (4.50), the control law in (4.64) becomes

$$\begin{aligned} u = &- k_1 \left[E_{t_s} \otimes I_n \right] \nabla_{\bar{e}_{x_t}} \tilde{W} - k_2 \left[E_{t_s} R_s R_s^\top \otimes I_n \right] \bar{e}_{v_t} - k_3 v \\ &- k_1 \left[\mathbb{E} \otimes I_n \right] \nabla_{\alpha} \tilde{W} - k_1 \nabla_{\hat{e}} \tilde{W}, \end{aligned} \tag{4.65}$$

where the last term ensures that all agents cooperative with the virtual leader converge to the virtual leader's position and to its symmetric states if they are competitive, and k_3 should be greater than zero. The new closed-loop system, in spanning-tree coordinates, is

$$\dot{\bar{e}}_{x_t} = \bar{e}_{v_t} \tag{4.66a}$$

$$\begin{aligned} \dot{\bar{e}}_{v_t} = &- k_1 \left[L_{e_{ts}} \otimes I_n \right] \nabla_{\bar{e}_{x_t}} \tilde{W} - k_2 \left[L_{e_{ts}} R_s R_s^\top \otimes I_n \right] \bar{e}_{v_t} - k_3 \bar{e}_{v_t} \\ &- k_1 \left[E_{t_s}^\top \mathbb{E} \otimes I_n \right] \nabla_{\alpha} \tilde{W} - k_1 \left[E_{t_s} \otimes I_n \right]^\top \nabla_{\hat{e}} \tilde{W} \end{aligned} \tag{4.66b}$$

For the latter, we have the following.

Proposition 12 *(Leader-follower bipartite formation-consensus [84]). Consider the system (4.42) and (4.4) in closed loop with the distributed control law (4.65), with $\tilde{W}(\alpha, \bar{e}_x)$ as defined in (4.63), and assume that the resulting network is structurally balanced and contains an underlying spanning tree. Then, the set $\{(\bar{e}_x, v, \hat{e}) = (0, 0, 0)\}$ is asymptotically stable for almost all initial conditions such that $(\bar{e}_x(0), v(0), \hat{e}(0)) \in \mathcal{I} \times \mathbb{R}^{nN} \times \mathbb{R}^{nN}$ and $|\alpha_k(0)| > \Delta_k$ for any $k \leq M$.*

Proof: We consider the Lyapunov function candidate in (4.55). In this context, a virtual leader is considered in the network, so the Lyapunov function also depends on $\hat{e}$, defined in (4.6), that is

$$V(\alpha, \bar{e}_{x_t}, v, \hat{e}) = k_1 \tilde{W}(\alpha, \bar{e}_{x_t}, \hat{e}) + \frac{1}{2}|v|^2, \tag{4.67}$$

where $\tilde{W}(\alpha, \bar{e}_{x_t}, \hat{e})$ is defined in (4.63). Therefore, V is positive definite with respect to the state variables $\bar{e}_{x_t}$, $\bar{e}_{v_t}$ and $\hat{e}$. In addition, by its construction, $V(\alpha, \bar{e}_{x_t}, v, \hat{e}) \to \infty$ as $\bar{e}_{x_t}$ approaches the boundary $\partial\mathcal{I}_t$ of the set $\mathcal{I}_t$ in (4.53) and $|\hat{e}| \to \infty$, for a given $\bar{e}_{v_t}$ and v. We also remark that the positivity of V holds uniformly in α. More precisely, there exists $\mu > 0$ such that $\mu[|\bar{e}_{x_t}|^2 + |v|^2 + |\hat{e}|^2] \leq V(\alpha, \bar{e}_{x_t}, v, \hat{e})$ and $V(\alpha, \bar{e}_{x_t}, v, \hat{e}) \to 0$ as $|\bar{e}_{x_t}| \to 0$, $|v| \to 0$ and $|\hat{e}| \to 0$.

Next, we compute its total derivative along the trajectories of

$$\dot{\hat{e}} = v \tag{4.68a}$$

$$\begin{aligned}\dot{v} = &-k_1 \left[E_{t_s} \otimes I_n\right] \nabla_{\bar{e}_{x_t}} \tilde{W} - k_2 \left[E_{t_s} R_s R_s^\top \otimes I_n\right] \bar{e}_{v_t} - k_3 v \\ &- k_1 \left[\mathbb{E} \otimes I_n\right] \nabla_\alpha \tilde{W} - k_1 \nabla_{\hat{e}} \tilde{W}.\end{aligned} \tag{4.68b}$$

We obtain

$$\begin{aligned}\dot{V}(\alpha, \bar{e}_{x_t}, v, \hat{e}) = &\, k_1 \nabla_{\bar{e}_{x_t}} \tilde{W}^\top \dot{\bar{e}}_{x_t} + k_1 \nabla_\alpha \tilde{W}^\top \left[\mathbb{E}^\top \otimes I_n\right] v + k_1 \nabla_{\hat{e}} \bar{W}^\top \dot{\hat{e}} + v^\top \big[-k_3 v \\ &- k_1 [E_{t_s} \otimes I_n] \nabla_{\bar{e}_{x_t}} \tilde{W} - k_2 [E_{t_s} R_s R_s^\top \otimes I_n] \bar{e}_{v_t} - k_1 [\mathbb{E} \otimes I_n] \nabla_\alpha \tilde{W} - k_1 \nabla_{\hat{e}} \tilde{W}\Big],\end{aligned}$$

so using (4.68a), (4.33) and (4.36), we obtain

$$\dot{V}(\alpha, \bar{e}_{x_t}, v) = -\, k_2 |\bar{e}_v|^2 - k_3 |v|^2, \tag{4.69}$$

which is negative semidefinite for all $(\bar{e}_x(0), v(0), \hat{e}(0)) \in \mathcal{I} \times \mathbb{R}^{nN} \times \mathbb{R}^{nN}$ so the origin is stable.

Next, we use LaSalle's invariance theorem. On the set $\{(\bar{e},\, v,\, \hat{e}) : \dot{V} = 0\}$, we have $\bar{e}_v = 0$ and $v = 0$, which means that α is constant. In turn, after (4.68), we have

$$-\, k_1 \left[E_{t_s} \otimes I_n\right] \nabla_{\bar{e}_{x_t}} \tilde{W} - k_1 \nabla_{\hat{e}} \tilde{W} = k_1 \left[\mathbb{E} \otimes I_n\right] \nabla_\alpha \tilde{W}. \tag{4.70}$$

On the other hand, since $\alpha \equiv \text{const}$ on $\{\dot{V} = 0\}$, and with (4.59), it follows that

$$-\left[E_t \otimes I_n\right] \nabla_{\bar{e}_{x_t}} \tilde{W} - \nabla_{\hat{e}} \tilde{W} = 0 \quad \Leftrightarrow \quad -\begin{bmatrix} E_t & I_N \end{bmatrix} \begin{bmatrix} \nabla_{\bar{e}_{x_t}} \tilde{W} \\ \nabla_{\hat{e}} \tilde{W} \end{bmatrix} = 0.$$

E_t corresponds to the incidence matrix of a spanning tree, so it is full rank, and I_N is also full rank. The matrix $\begin{bmatrix} E_t & I_N \end{bmatrix}$ has linearly independent columns, so is also full rank. It follows that $\nabla_{\bar{e}_{x_t}} \tilde{W} = 0$ and $\nabla_{\hat{e}} \tilde{W} = 0$, which holds if and only if $\bar{e}_t \in \mathcal{W}^t$ and $\hat{e} = 0$. Therefore, the solutions converge to the set $\mathcal{W}^t \times \{0\} \times \{0\}$. However, since e_t^* is a saddle point of $\tilde{W}$, the set of initial conditions generating solutions that converge to $(e_t^*, 0, 0)$ has zero Lebesgue measure. Thus, almost all initial conditions generate trajectories that converge to the origin. Asymptotic stability follows.

The rest of the proof follows similar lines as in the proof of Proposition 11. We show that asymptotic stability holds for almost all initial conditions in $\mathcal{I}_t \times \mathbb{R}^{nN} \times \mathbb{R}^{nN}$. Referring to (4.53), $\bar{e}_t \in \mathcal{I}_t$ implies $\bar{e} \in \mathcal{I}$, so we must show that $\mathcal{I}_t \times \mathbb{R}^{nN}$ is forward invariant. To that end, for any r_1, r_2 and $\epsilon \geq 0$, let us define $\mathcal{D}_{r_1,r_2,\epsilon} := \{v \in B_{r_1},\ \hat{e} \in B_{r_2},\ \bar{e}_t \in \mathcal{I}_\epsilon\}$, where $\mathcal{I}_\epsilon$ is defined in (4.60). From the definition of $\tilde{W}(\alpha, \bar{e}_{x_t}, \hat{e})$, $V(\alpha, \bar{e}_{x_t}, v, \hat{e})$ is positive definite on $\mathcal{I}_\epsilon$ for all $\bar{e}_{x_t} \in \mathcal{I}_\epsilon$, $v \in \mathbb{R}^{nN}$, $\hat{e} \in \mathbb{R}^{nN}$ and for all ϵ. From (4.69), we have

$$|\bar{e}_{x_t}(t)|^2 + |v(t)|^2 + |\hat{e}(t)|^2 \leq \frac{1}{\mu} V(\alpha(0), \bar{e}_{x_t}(0), v(0), \hat{e}(0)).$$

Then,

$$(\bar{e}_{x_t}(0), v(0), \hat{e}(0)) \in \mathcal{D}_{r_1,r_2,\epsilon} \Rightarrow (\bar{e}_{x_t}(t), v(t), \hat{e}(t)) \in \mathcal{D}', \tag{4.71}$$

where

$$\mathcal{D}' := \left\{ (\bar{e}_{x_t}, v, \hat{e}) \in \mathcal{I}_t \times \mathbb{R}^{nN} \times \mathbb{R}^{nN} : V(\alpha, \bar{e}_{x_t}, v, \hat{e}) \leq \gamma_{r,\epsilon} \right\},$$

and

$$\gamma_{r,\epsilon} := \sup_{\substack{(\bar{e}_{x_t}, v, \hat{e}) \in \mathcal{D}_{r_1,r_2,\epsilon} \\ \alpha \in \mathbb{R}^{nN}}} \sqrt{\frac{V(\alpha, \bar{e}_{x_t}, v, \hat{e})}{\mu}}.$$

Note that $\gamma_{r,\epsilon}$ is well defined because V is uniformly bounded in α and $\mathcal{D}_{r,\epsilon}$ is bounded. After LaSalle's invariance principle, we conclude that all the trajectories contained in $\mathcal{D}'$ converge to the set $\mathcal{W}^t \times \{0\} \times \{0\}$. After (4.71), that is all the trajectories starting in $\mathcal{D}_{r_1,r_2,\epsilon}$. This holds for any $r > 0$ arbitrarily large and $\epsilon > 0$ arbitrarily small. Thus, again because $\mathcal{W}^t = \{0, e_t^*\}$, and e_t^* is a saddle point, we conclude that the origin is asymptotically stable for almost all trajectories starting in $\mathcal{I}_t \times \mathbb{R}^{nN} \times \mathbb{R}^{nN}$. ■

4.3.3 Numerical examples

We present some numerical examples to show the performance of our control laws (4.48) and (4.64). We consider a structurally balanced signed network of nonholonomic mobile robots. Let $r_i = [r_{x_i}\ r_{y_i}]^\top$ be the inertial position, θ_i the orientation, v_i the linear speed, ω_i the angular speed, m_i the mass, J_i the moment of inertia, F_i be the applied force and torque, and $\eta_i := [F_i\ \tau_i]^\top$. Then, the robot's model is given by the equations in (3.50). Then, defining $s_{\theta_i} := \sin\theta_i$ and $c_{\theta_i} := \cos\theta_i$ and choose the reference point $p_i = r_i + \delta_i \begin{bmatrix} c_{\theta_i} & s_{\theta_i} \end{bmatrix}^\top$ located at a distance $\delta_i = 0.1$m along the line that is perpendicular

to the wheels' axis and we express the system in terms of new coordinates defined in (3.51). Then, differentiating on both sides of the latter and using (3.50), we obtain (3.52). The feedback-linearizing control η_i is given by (3.53), which yields

$$\begin{bmatrix}\dot{\zeta}_{1_i} & \dot{\zeta}_{2_i}\end{bmatrix}^\top = \begin{bmatrix}\zeta_{3_i} & \zeta_{4_i}\end{bmatrix}^\top, \tag{4.72a}$$

$$\begin{bmatrix}\dot{\zeta}_{3_i} & \dot{\zeta}_{4_i}\end{bmatrix}^\top = u_i. \tag{4.72b}$$

4.3.3.1 Leaderless bipartite formation-consensus

We first provide a numerical example to show the performance of our control law (4.48) with $k_1 = 1$, $k_2 = 1.2$, $k_3 = 1$ and the barrier-Lyapunov function in (4.31). To that end, we implement (3.53) with u_i as in (4.48), $x_i = [\zeta_{1_i}\ \zeta_{2_i}]^\top$, $v_i = [\zeta_{3_i}\ \zeta_{4_i}]^\top$, $m_i = 8\text{kg}$ and $J_i = 0.12\text{kg/m}^2$, $\forall i \leq N$.

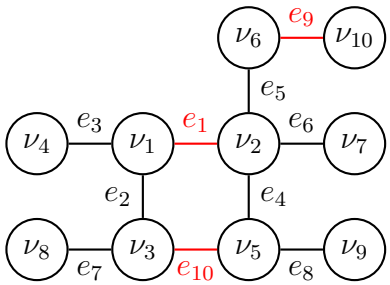

Figure 4.1: Network 1: A structurally balanced, leaderless, and undirected signed network of 10 mobile robots. The black lines represent cooperative edges, and the red lines represent the competitive ones.

We consider an undirected signed network of 10 agents and 10 edges as the one depicted in Figure 4.1, subject to inter-agent collision avoidance and connectivity maintenance restrictions. We define the orientation of the edges as follows:

$$e_1 = \nu_1 + \nu_2,\ e_2 = \nu_1 - \nu_3,\ e_3 = \nu_1 - \nu_4,\ e_4 = \nu_2 - \nu_5,\ e_5 = \nu_2 - \nu_6,$$
$$e_6 = \nu_2 - \nu_7,\ e_7 = \nu_3 - \nu_8,\ e_8 = \nu_5 - \nu_9,\ e_9 = \nu_6 + \nu_{10},\ e_{10} = \nu_3 + \nu_5.$$

The incidence matrix corresponding to the graph is

$$E_s = \begin{bmatrix}
1 & 1 & 1 & 0 & 0 & 0 & 0 & 0 & 0 & 0\\
1 & 0 & 0 & 1 & 1 & 1 & 0 & 0 & 0 & 0\\
0 & -1 & 0 & 0 & 0 & 0 & 1 & 0 & 0 & 1\\
0 & 0 & -1 & 0 & 0 & 0 & 0 & 0 & 0 & 0\\
0 & 0 & 0 & -1 & 0 & 0 & 0 & 1 & 0 & 1\\
0 & 0 & 0 & 0 & -1 & 0 & 0 & 0 & 1 & 0\\
0 & 0 & 0 & 0 & 0 & -1 & 0 & 0 & 0 & 0\\
0 & 0 & 0 & 0 & 0 & 0 & -1 & 0 & 0 & 0\\
0 & 0 & 0 & 0 & 0 & 0 & 0 & -1 & 0 & 0\\
0 & 0 & 0 & 0 & 0 & 0 & 0 & 0 & 1 & 0
\end{bmatrix}.$$

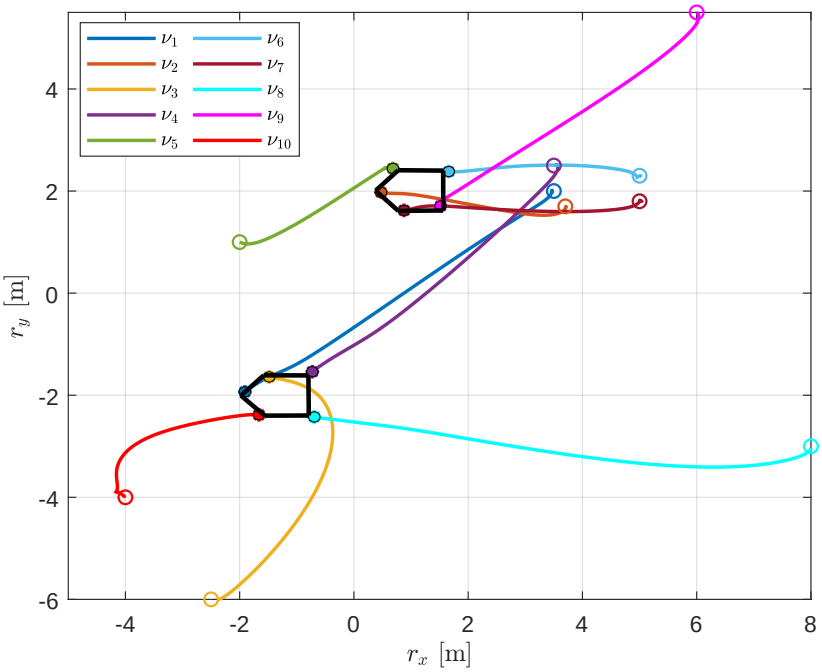

Figure 4.2: Bipartite formation of system (4.42) with control input (4.48). The asterisks are the inertial positions of the robots. The reference points p_i of the mobile robots, on the black circles around the asterisks, of the two disjoint subgroups form a formation around two symmetric consensus points.

The set of nodes may be split into two disjoint subsets, such as

$$\mathcal{V}_1 = \{\nu_1,\ \nu_3,\ \nu_4,\ \nu_8,\ \nu_{10}\}, \quad \mathcal{V}_2 = \{\nu_2,\ \nu_5,\ \nu_6,\ \nu_7,\ \nu_9\}$$

so the network is structurally balanced.

From the decomposition in (4.32), edges $e_i,\ i \leq 9$ correspond to $\mathcal{G}_t$ and the remaining edge e_{10} corresponds to $\mathcal{G}_c$. Since the considered network has the same number of edges as the number of nodes, the eigenvalues of L_s and L_{e_s} are

$$\lambda_{L_s} = \lambda_{L_{e_s}} = 0,\ 0.33,\ 0.58,\ 0.67,\ 0.79,\ 2,\ 2.5,\ 3.41,\ 4,\ 5.7.$$

The respective agents' initial states are

$$r_x(0) = \begin{bmatrix}3.5 & 3.7 & -2.5 & 3.5 & -2 & 5 & 5 & 8 & 6 & -4\end{bmatrix}^\top,$$

$$r_y(0) = \begin{bmatrix}2 & 1.7 & -6 & 2.5 & 1 & 2.3 & 1.8 & -3 & 5.5 & -4\end{bmatrix}^\top,$$

$$v(0) = \begin{bmatrix}0.2 & 0.45 & 0.32 & 0.32 & 1.12 & 0.3 & 0.4 & 0.22 & 0.42 & -0.14\end{bmatrix}^\top,$$

$$\theta(0) = \begin{bmatrix}0 & -0.46 & -1.25 & 0.32 & -0.46 & 0 & 0 & -1.11 & -0.79 & -0.79\end{bmatrix}^\top,$$

and the relative displacements are

$$d_x = \begin{bmatrix}-0.8 & -0.8 & -0.4 & 0.4 & -0.4 & 0.4 & -0.4 & 0.4 & 0.4 & -0.4\end{bmatrix}^\top,$$

$$d_y = \begin{bmatrix}0 & 0 & 0.4 & 0.4 & 0.4 & 0.4 & -0.4 & -0.4 & -0.4 & -0.4\end{bmatrix}^\top.$$

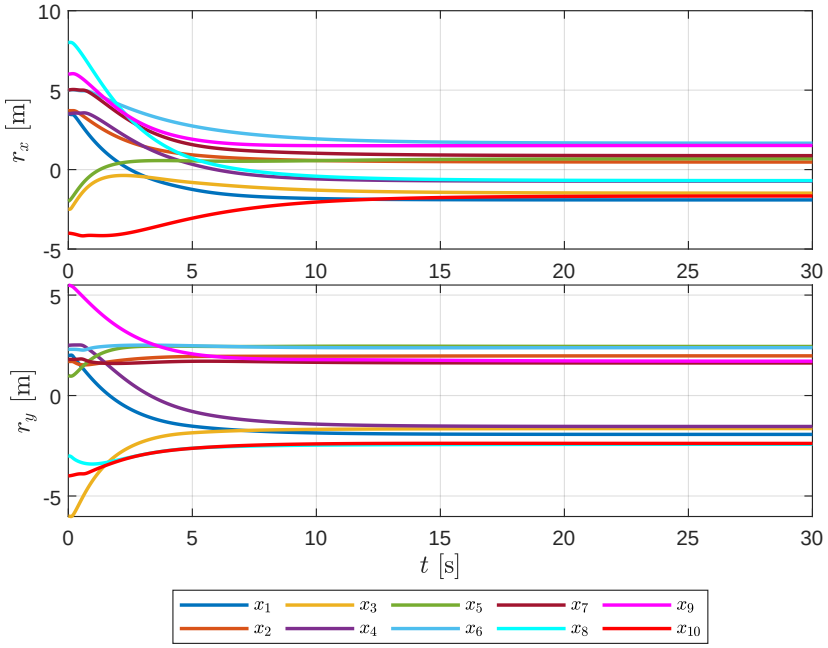

Figure 4.3: Bipartite formation of system (4.42) with control input (4.48) on position.

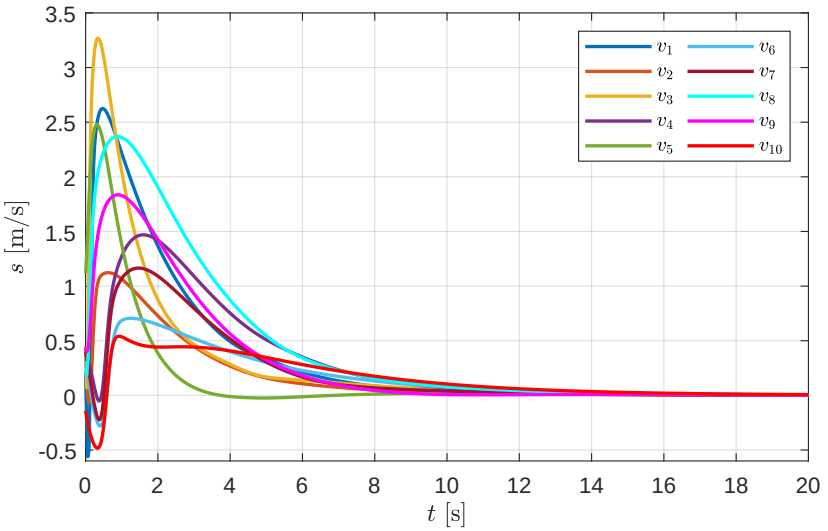

Figure 4.4: Bipartite formation of system (4.42) with control input (4.48) on velocity, where $k_3 > 0$. The velocities of all agents converge to zero.

The constraint sets are $\Delta_k = 0.2$ for all $k \leq M$ and $R_k = 11$ for all $k \in \mathcal{E}_m$. The paths of each agent up to bipartite formation are depicted in Figure 4.2. The reference points of the mobile robots reach the desired formation around two symmetric consensus points. The velocities of mobile robots are depicted in Figure 4.4, and velocities converge to zero. Moreover, it is clear from Figures 4.3, and 4.5 that the inter-agent collision avoidance and connectivity maintenance constraints in (4.9a)–(4.9b) are always respected.

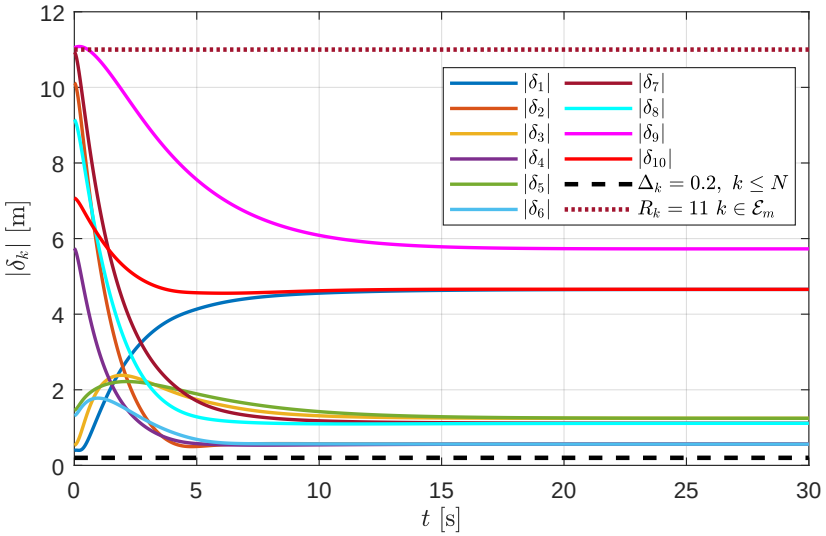

Figure 4.5: Trajectories of the norm of the inter-agent distances with control input (4.48). The dashed lines are the minimum, and the dotted lines are the maximum distance constraints for agents. All inter-agent safety proximity constraints are respected.

4.3.3.2 Leader-follower bipartite formation-consensus

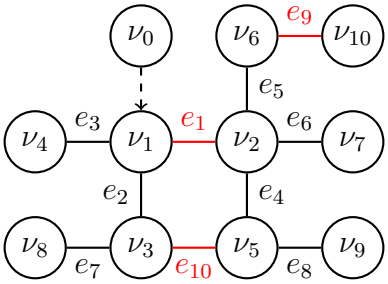

Figure 4.6: Network 2: A structurally balanced undirected signed network of 10 mobile robots with a virtual leader ν_0.

We then provide a numerical example to show the performance of our control law (4.64), in the presence of a virtual leader ν_0, with $k_1 = 1$, $k_2 = 1.2$, $k_3 = 1$ and the barrier-Lyapunov function in (4.63). We consider the same undirected signed network in Figure 4.1 with a virtual leader ν_0 giving information to agent ν_1, depicted in Figure 4.6. The virtual leader's position is

$$x_0 = [-2 \ \ -3]^\top,$$

and

$$A_l = \text{diag}(1, 0, \ldots, 0), \quad \Phi = \begin{bmatrix} 1 & -1 & 1 & 1 & -1 & -1 & -1 & 1 & -1 & 1 \end{bmatrix}^\top.$$

The respective agents' inertial positions, velocities, and orientations are the same as before, while the relative displacements are

$$d_x = \begin{bmatrix} -0.8 & 0.8 & -0.4 & 0.4 & -0.4 & 0.4 & 0.4 & 0.4 & -0.4 & -0.4 \end{bmatrix}^\top,$$

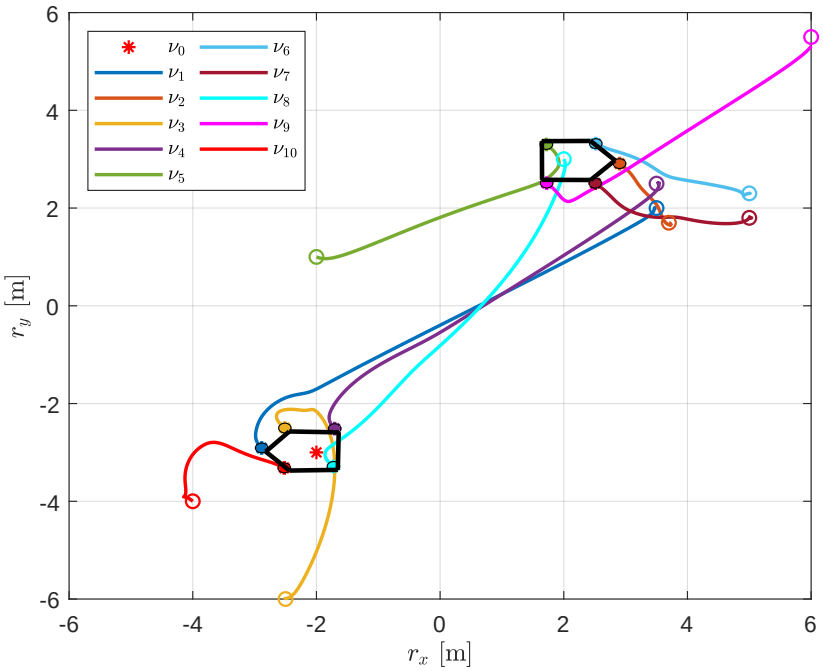

Figure 4.7: Bipartite formation of system (4.42) with control input (4.64). The asterisks are the inertial positions of the robots. The reference points p_i of the mobile robots, on the black circles around the asterisks, of the two disjoint subgroups form a formation around two symmetric consensus points.

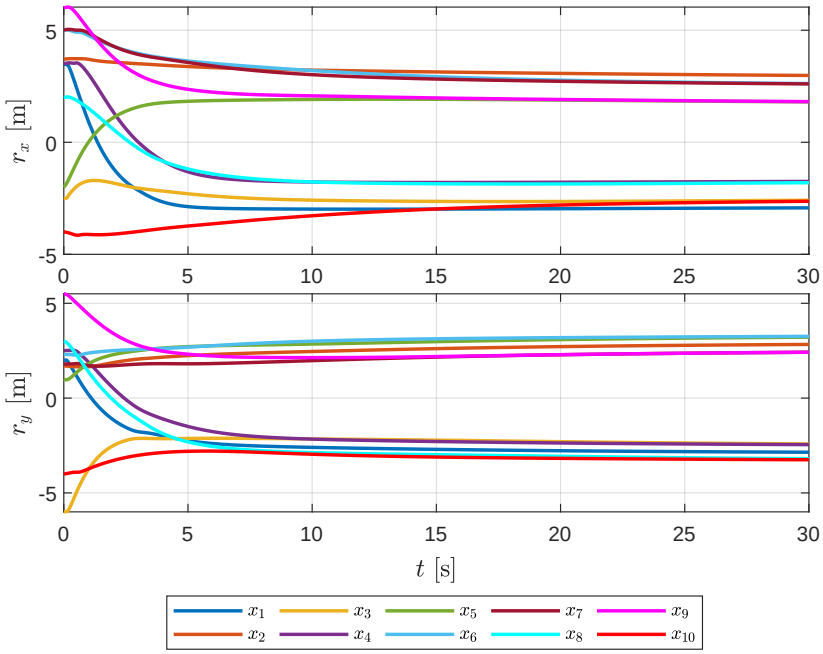

Figure 4.8: Bipartite formation of system (4.42) with control input (4.64) on position.

$$d_y = \begin{bmatrix} 0 & 0 & 0.4 & 0.4 & 0.4 & 0.4 & -0.4 & -0.4 & -0.4 & -0.4 \end{bmatrix}^\top.$$

The constraints are also set as before. The paths of each agent up to leader-follower bipartite formation are depicted in Figure 4.7. Agents in $\mathcal{V}_1$ converge around the virtual leader's position, while agents in $\mathcal{V}_2$ reach formation around the virtual leader's

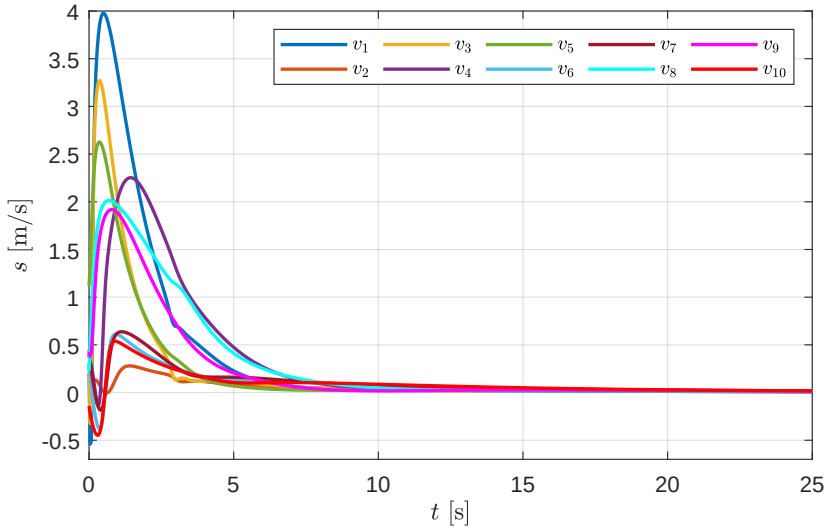

Figure 4.9: Bipartite formation of system (4.42) with control input (4.64) on velocity, where $k_3 > 0$. The velocities of all agents converge to zero.

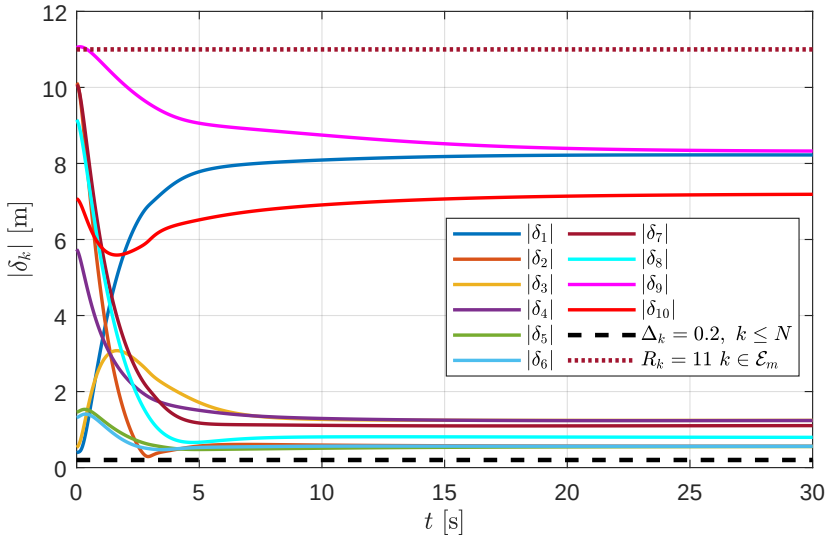

Figure 4.10: Trajectories of the norm of the inter-agent distances with control input (4.64). The dashed lines are the minimum, and the dotted lines are the maximum distance constraints for agents. All inter-agent safety proximity constraints are respected.

symmetric position. The velocities of mobile robots are depicted in Figure 4.9, and velocities converge to zero. Moreover, it is clear from Figures 4.8 and 4.10 that the inter-agent collision avoidance and connectivity maintenance constraints in (4.9a)–(4.9b) are always respected.

4.4 CONTROL OVER DIRECTED SIGNED NETWORKS

In this section, we extend our previous results to the case of directed topology networks. The results of this section on a class of directed signed graphs are new to the literature. In particular, we address the constrained bipartite consensus problem for first- and second-order systems interconnected over directed signed networks and we do so in

node coordinates.

As we explained in Chapter 2, in the case of a directed and structurally unbalanced graph, there are many possibilities for the behavior of the agents, depending on the presence of a root node. For instance, if the structurally unbalanced digraph is strongly connected, which rules out the presence of a root node, then all the agents' states converge to zero. Technically, this can be inferred from the fact that, in this case, the resulting Laplacian matrix does not have a zero eigenvalue but only positive ones. Note that having all the agents converging to the origin (or any other common equilibrium) is an undesirable behavior because that implies that they collide. In contrast, if the digraph contains a root node and is structurally unbalanced, multiple equilibria may appear. This, in turn, prevents achieving bipartite consensus, which necessarily implies the existence of only two equilibria. Thus, we only consider directed signed networks satisfying the following.

Assumption 5 *The signed directed graph is structurally balanced and contains a directed spanning tree.*

4.4.1 First-order systems

Consider a group of N dynamical systems modeled by (4.1) over an undirected and structurally balanced signed graph and subject to inter-agent distance constraints encoded by (4.9). Then, for the purpose of making them achieve bipartite consensus, consider the BLF-gradient-based bipartite consensus control law (4.38), where $\bar{V}_{ij}$ is defined in (4.19) and encodes the inter-agents constraints defined in (4.9). Thus, the closed-loop system reads

$$\dot{\bar{x}} = -k_1 \nabla_x \bar{V}. \tag{4.73}$$

For this system, we have the following.

Proposition 13 *Consider the system (4.1) in closed loop with the control law (4.38), with $\bar{V}(x)$ as defined in (4.20), under Assumptions 3 and 5. Then, the closed-loop system achieves bipartite formation-consensus, that is (4.2) holds, while the collision-avoidance and connectivity-maintenance constraints are satisfied, for almost all initial conditions such that $\delta(0) \in \mathcal{I}$ and $|\alpha_k(0)| > \Delta_k$ for any $k \leq M$.*

Proof: Consider the Lyapunov function candidate $\bar{V}(x)$ defined in (4.20). Its total derivate reads

$$\dot{\bar{V}} = -k_1 |\nabla_x \bar{V}|^2 \leq -\frac{k_1}{2\kappa} |\delta|^2_{\bar{\mathcal{W}}}. \tag{4.74}$$

As in the proof of Proposition 10, from (4.74) we conclude that $\bar{\mathcal{W}}$ is asymptotically stable so this statement of Proposition 13 follows using similar arguments as for Proposition 10. ■

We wrap up the technical contents of this chapter by addressing the bipartite consensus problem with collision avoidance and connectivity maintenance for networks of second-order systems.

4.4.2 Second-order systems

We consider a group of N dynamical systems modeled by (4.42) over a structurally balanced digraph, as in the previous section, but for technical reasons, we strengthen Assumption 5 to the following.

Assumption 6 *The signed directed graph is strongly connected, weight-balanced, and structurally balanced.*

Then, for the purpose of making the agents achieve bipartite consensus, as we did in Section 4.3.2, we consider a BLF-gradient-based bipartite consensus control law defined as

$$u = -k_1 \nabla_x \bar{V} - k_2 \left[L_s \otimes I_n\right] v - k_3 v, \tag{4.75}$$

where, in this case, $\bar{V}_{ij}$ is defined in node coordinates in (4.19). This function encodes the inter-agents constraints defined in (4.9), and L_s is the resulting Laplacian matrix associated with the directed graph under Assumption 6. Thus, the closed-loop system reads

$$\dot{\tilde{x}} = -k_1 \nabla_x \bar{V} - k_2 \left[L_s \otimes I_n\right] v - k_3 v, \tag{4.76}$$

For this system, we have the following.

Proposition 14 *Consider the system (4.42). Under Assumption 6, the controller (4.75), with $\bar{V}(x)$ as defined in (4.20), guarantees bipartite formation-consensus, that is (4.45) holds, and the inter-agent collision avoidance and connectivity maintenance constraints are respected for almost all initial conditions such that $(\delta(0), v(0)) \in \mathcal{I} \times \mathbb{R}^{nN}$, where $\mathcal{I}$ is defined in (4.9), and $|\alpha_k(0)| > \Delta_k$ for any $k \leq M$.*

Proof: Consider the following Lyapunov function.

$$V(x, v) = k_1 \bar{V}(x) + \frac{1}{2}|v|^2,$$

where $\bar{V}(x)$ is defined in (4.20). More precisely, there exists $\bar{\mu} > 0$ such that $\bar{\mu}[|\delta - \alpha|^2 + |v|^2] \leq V(x, v)$ and $V(x, v) \to 0$ as $|\delta| \to \alpha$ and $|v| \to 0$. Its derivative gives

$$\begin{aligned}
\dot{V} &= k_1 \nabla_x \bar{V}^\top \dot{x} + v^\top \dot{v} \\
&= k_1 \nabla_x \bar{V}^\top v + \frac{1}{2} v^\top (-k_1 \nabla_x \bar{V} - k_2 \left[L_s \otimes I_n\right] v - k_3 v) \\
&\quad + \frac{1}{2}(-k_1 \nabla_x \bar{V} - k_2 \left[L_s \otimes I_n\right] v - k_3 v)^\top v \\
&= -\frac{1}{2} k_2 v^\top \left[(L_s + L_s^\top) \otimes I_n\right] v - k_3 v^\top v.
\end{aligned}$$

In view of Assumption 6, $L_s + L_s^\top$ is a symmetric positive semidefinite matrix with a single zero eigenvalue so $L_s + L_s^\top \geq 0$—see [54, 2]. Then $\dot{V} \leq 0$, which is negative semi-definite for all $(\delta, v) \in \mathcal{I} \times \mathbb{R}^{nN}$.

Next, we use LaSalle's invariance theorem. On the set $\{\dot{V} = 0\}$ we have $v = 0$ and $L_s v = 0$, which gives $v_i - \text{sgn}(a_{ij}) v_j = 0$. Then from (4.75), we have $\nabla_x \bar{V} = 0$,

which holds if and only if $\delta \in \bar{\mathcal{W}}$, where $\bar{\mathcal{W}} = \{\bar{\alpha}, s^*\}$ and s^* are the saddle points of $\bar{V}$. Therefore, the solutions converge to the set $\bar{\mathcal{W}}$. However, since s^* is a saddle point of $\bar{V}$, the set of initial conditions generating solutions that converge to $(s^*, 0)$ has zero Lebesgue measure. Thus, almost all initial conditions generate trajectories that converge to $(\bar{\alpha}, 0)$, (*i.e.*, $x_i - x_j = \bar{b}_{ij}$ if the agents i and j are cooperative and $x_i + x_j = \bar{b}_{ij}$ if the agents i and j are competitive and $v = 0$). Asymptotic stability follows. The rest of the proof follows similar arguments as in the proof of Proposition 11. ■

4.4.3 Numerical examples

We present some numerical examples to show the performance of our control laws (4.73) and (4.75). We consider a structurally balanced signed network of mobile robots. We first consider the constrained bipartite consensus problem of first-order systems, then that of second-order systems.

4.4.3.1 First-order systems

We present a numerical example to show the performance of our control law (4.73), where $k_1 = 1$, and the barrier-Lyapunov function $\bar{V}(x)$ as defined in (4.20). We consider a structurally-balanced directed signed network of 6 nonholonomic mobile robots, with a competitive leader, as the one illustrated in Figure 4.11. The competitive leader represents a static obstacle that other mobile robots should avoid. The robot's model is given by the equations in (3.50).

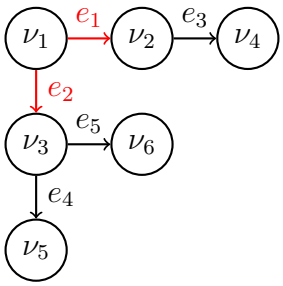

Figure 4.11: A structurally-balanced and directed signed network of 6 mobile robots. The black lines represent cooperative edges, and the red line represents the competitive one. The competitive leader represents a static obstacle.

The incidence and the in-incidence matrices corresponding to the graph are

$$E_s = \begin{bmatrix} 1 & 1 & 0 & 0 & 0 \\ 1 & 0 & 1 & 0 & 0 \\ 0 & 1 & 0 & 1 & 1 \\ 0 & 0 & -1 & 0 & 0 \\ 0 & 0 & 0 & -1 & 0 \\ 0 & 0 & 0 & 0 & -1 \end{bmatrix}, \quad E_{s\odot} = \begin{bmatrix} 0 & 0 & 0 & 0 & 0 \\ 1 & 0 & 0 & 0 & 0 \\ 0 & 1 & 0 & 0 & 0 \\ 0 & 0 & -1 & 0 & 0 \\ 0 & 0 & 0 & -1 & 0 \\ 0 & 0 & 0 & 0 & -1 \end{bmatrix}.$$

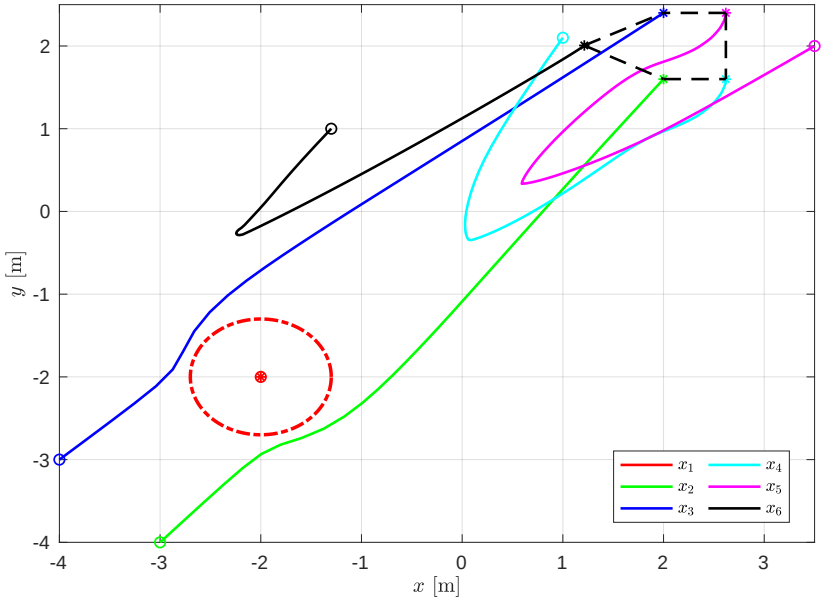

Figure 4.12: Bipartite formation of system (4.73). The asterisks are the inertial positions of the robots. The mobile robots avoid the obstacle, represented by agent 1 in red, and form a formation around the obstacle's symmetric state.

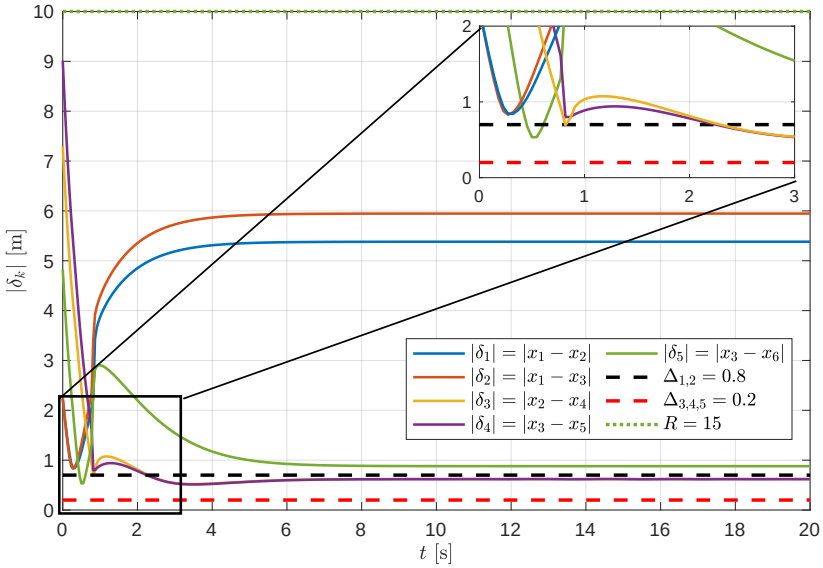

Figure 4.13: Trajectories of the norm of the inter-agent distances of system (4.73). The dashed lines are the minimum, and the dotted lines are the maximum distance constraints for agents. All inter-agent safety proximity constraints are respected.

The set of nodes may be split into two disjoint subsets, such as

$$\mathcal{V}_1 = \{\nu_1\}, \quad \mathcal{V}_2 = \{\nu_2,\ \nu_3,\ \nu_4,\ \nu_5,\ \nu_6\}$$

so the network is structurally balanced. The respective agents' initial states are

$$r_x(0) = \begin{bmatrix} -2 & -3 & -4 & 1 & 3.5 & -1.3 \end{bmatrix}^\top, \quad r_y(0) = \begin{bmatrix} -2 & -4 & -3 & 2.1 & 2 & 1 \end{bmatrix}^\top,$$

and the relative displacements are

$$d_x = \begin{bmatrix} 0 & 0 & 0 & -0.4 & -0.4 & -0.8 \end{bmatrix}^\top, \quad d_y = \begin{bmatrix} 0 & -0.4 & 0.4 & -0.4 & 0.4 & 0 \end{bmatrix}^\top.$$

The constraint sets are $\Delta_{1,1} = 0.8$ and $\Delta_{3,4,5} = 0.2$ and $R_k = 10$ for all $k \in \mathcal{E}_m$. The paths of each agent up to bipartite formation are depicted in Figure 4.12. The mobile robots avoid the obstacle and reach the desired formation around the obstacle's symmetric position. It is clear from Figure 4.13 that the inter-agent collision avoidance and connectivity maintenance constraints in (4.9a)–(4.9b) are always respected.

4.4.3.2 Second-order systems

We present a numerical example to show the performance of our control law (4.75), where $k_1 = 1$, $k_2 = 1.2$, $k_3 = 1$ and the barrier-Lyapunov function in (4.20). We consider a strongly connected, weight-balanced, and structurally-balanced directed signed network of 6 nonholonomic mobile robots, as the one illustrated in Figure 4.14. The robot's model is given by the equations in (3.50).

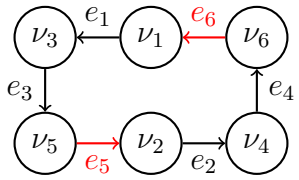

Figure 4.14: A strongly connected, weight-balanced, and structurally-balanced directed signed network of 6 mobile robots. The black lines represent cooperative edges, and the red lines represent the competitive ones.

The incidence and the in-incidence matrices corresponding to the graph are

$$E_s = \begin{bmatrix} 1 & 0 & 0 & 0 & 0 & 1 \\ 0 & 1 & 0 & 0 & 1 & 0 \\ -1 & 0 & 1 & 0 & 0 & 0 \\ 0 & -1 & 0 & 1 & 0 & 0 \\ 0 & 0 & -1 & 0 & 1 & 0 \\ 0 & 0 & 0 & -1 & 0 & 1 \end{bmatrix}, \quad E_{s\odot} = \begin{bmatrix} 0 & 0 & 0 & 0 & 0 & 1 \\ 0 & 0 & 0 & 0 & 1 & 0 \\ -1 & 0 & 0 & 0 & 0 & 0 \\ 0 & -1 & 0 & 0 & 0 & 0 \\ 0 & 0 & -1 & 0 & 0 & 0 \\ 0 & 0 & 0 & -1 & 0 & 0 \end{bmatrix}.$$

The set of nodes may be split into two disjoint subsets, such as

$$\mathcal{V}_1 = \{\nu_1,\ \nu_3,\ \nu_5\}, \quad \mathcal{V}_2 = \{\nu_2,\ \nu_4,\ \nu_6\}$$

so the network is structurally balanced. The respective agents' initial states are

$$r_x(0) = \begin{bmatrix} 3.5 & -3.6 & -2.5 & -5.3 & -2 & 0.5 \end{bmatrix}^\top, \quad r_y(0) = \begin{bmatrix} -2 & 1.7 & -0.6 & 2 & 1 & 2 \end{bmatrix}^\top,$$

$$v(0) = \begin{bmatrix} 0 & 0 & 0 & 0 & 0 & 0 \end{bmatrix}^\top,$$

and the relative displacements are

$$d_x = \begin{bmatrix} -0.6 & -0.6 & 0.6 & 0 & 0 & 0.6 \end{bmatrix}^\top, \quad d_y = \begin{bmatrix} 0.6 & -0.6 & 0.6 & 0.6 & -0.6 & -0.6 \end{bmatrix}^\top.$$

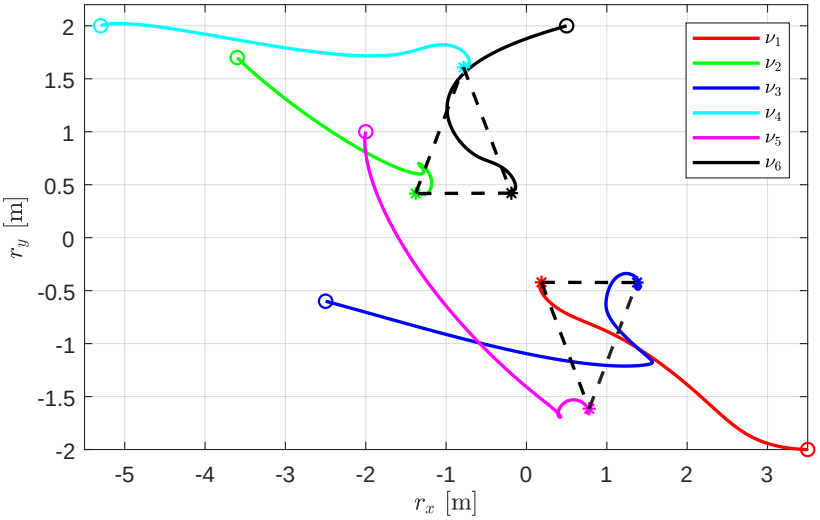

Figure 4.15: Bipartite formation of system (4.42) with control input (4.75). The asterisks are the inertial positions of the robots. The mobile robots form a formation around two symmetric consensus points.

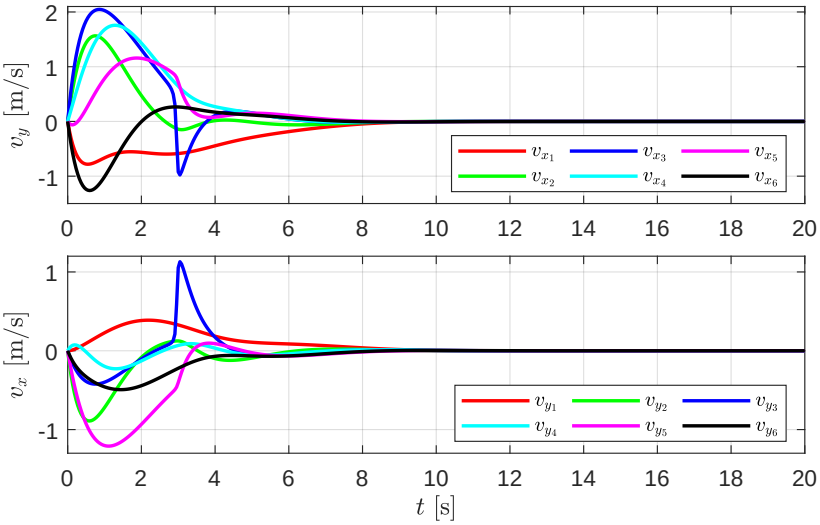

Figure 4.16: Bipartite formation of system (4.42) with control input (4.75) on velocity, where $k_3 > 0$. The velocities of all agents converge to zero.

The constraint sets are $\Delta_k = 0.1$ for all $k \leq M$ and $R_k = 8$ for all $k \in \mathcal{E}_m$. The paths of each agent up to bipartite formation are depicted in Figure 4.15. The mobile robots reach the desired formation around two symmetric consensus points. The velocities of mobile robots are depicted in Figure 4.16, and velocities converge to zero. Moreover, it is clear from Figure 4.17 that the inter-agent collision avoidance and connectivity maintenance constraints in (4.9a)–(4.9b) are always respected.

4.5 CONCLUSIONS

We presented a BLF-based distributed control law to solve the constrained bipartite formation-consensus control problem for first- and second-order systems over struc-

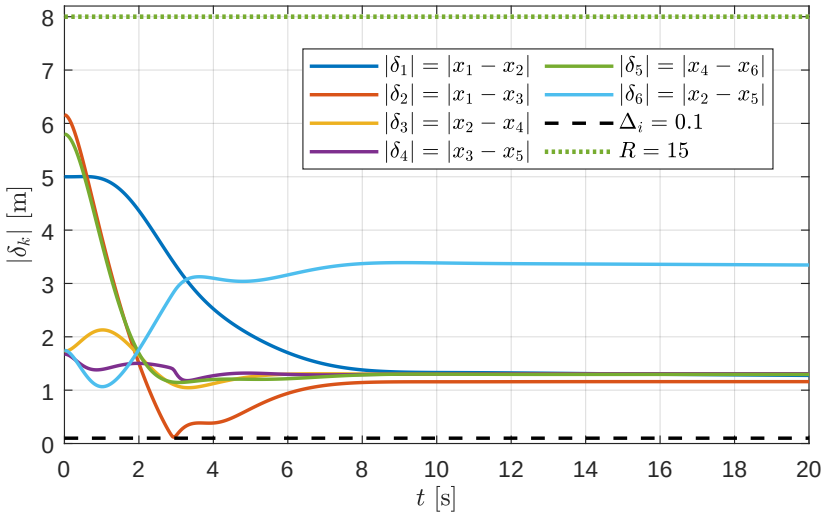

Figure 4.17: Trajectories of the norm of the inter-agent distances with control input (4.75). The dashed lines are the minimum, and the dotted lines are the maximum distance constraints for agents. All inter-agent safety proximity constraints are respected.

turally balanced signed networks that are undirected and directed. Compared to the literature, the proposed control laws are based on the gradient of a BLF and guarantee inter-agent collision avoidance for every agent in the networks and connectivity maintenance for two cooperative agents. We performed the stability analysis of the systems, first in terms of the node coordinates and then in terms of the synchronization errors, using Lyapunov's direct method. We also illustrated the practical application of our results through numerical simulations involving the formation-consensus control of nonholonomic vehicles. In the next Chapter, we will use the results presented here to address nonlinear systems, *i.e.,* robot manipulators, satellites, etc.

CHAPTER 5

FORMATION CONTROL OF EULER-LAGRANGE SYSTEMS WITH INTER-AGENT CONSTRAINTS

In this chapter, we first address the bipartite formation-control problem of robot manipulators' end-effectors under relative-distance constraints and in the presence of disturbances. Next, we tackle the bipartite formation problem of a flying spacecraft containing competitive satellites under collision avoidance and connectivity maintenance constraints. In both cases, we model the networked system of cooperative-competitive agents, interconnected over a structurally balanced undirected signed graph, using the Euler-Lagrange equations.

We consider first a networked system of cooperative-competitive robot manipulators. The formation goal is imposed on the manipulators' end-effectors. Such scenarios are motivated, for example, by applications in industrial robotics in which the robots share the same workspace but are assigned symmetric tasks by the team. Ideally, the robot manipulators should occupy the minimum space while evolving with guaranteed safety and increased reactivity.

The study of this problem has a solid precedent. Compared to the related literature—see *e.g.,* [79, 103, 102], our results apply to networks of robot manipulators having both cooperative and competitive interactions. Then, in contrast to the literature on the bipartite consensus problem of robot manipulators over signed networks—see *e.g.,* [45, 29, 111, 20, 115, 31, 46, 42, 40, 65], we address the problem under inter-agent constraints. We consider inter-agent constraints on the end-effectors to keep a minimum safety distance between any pair of interconnected end-effectors to avoid collisions and a maximum distance maintenance to make certain the task requirements for cooperative end-effectors are guaranteed. Compared to [15, 26], in which the control strategies rely on optimization techniques, and to [24], in which artificial potential functions are used, we base our controller on the gradient of a barrier-Lyapunov function. In contrast to [15, 26], our controller applies to signed networks, and contrary to [24], a minimal safety distance between agents is ensured. Our results follow up on our findings described in Chapter 4, but here we consider robot manipulators modeled by Euler-Lagrange

equations, not simple integrators, and we establish robustness with respect to external perturbations. To that end, we follow the frameworks of [99, 61, 102], to use an internal model to reject the disturbances, but contrary to these references, our work considers signed networks. Compared to [20, 115, 31] and [65], in which the presence of disturbances is considered, we also address minimum and maximum distance constraints on the end-effectors.

Then, we consider the bipartite formation-control problem of a network of flying spacecraft under collision avoidance and connectivity maintenance constraints. Such a scenario is motivated by aerospace applications, in which the spacecraft has the objective to recognize objects in space while avoiding enemy satellites or other obstacles during the mission. We address the problem by using the relative translational dynamics developed in [1]. Compared to the related literature—see *e.g.,* [64, 16, 70, 1, 47], our results apply to networks of satellites having both cooperative and competitive interactions. Moreover, in contrast to [64, 16, 70, 1, 47] and the literature on the bipartite consensus problem of flying spacecraft over signed networks—see *e.g.,* [114, 113], we address the problem under inter-agent constraints.

Our control design and analysis, to address both problems described above, rely on the edge-based formulation for signed networks [23] described in Section 2.4.2, which allows to recast the problem into one of stabilization of the origin in error coordinates. We establish asymptotic stability of the bipartite formation manifold using Lyapunov's direct method. To the best of our knowledge, similar results are not available in the literature for robot manipulators or satellites interconnected over networks containing competitive interactions.

5.1 LAGRANGIAN FORMULATION

We consider a network of N systems with n-degrees-of-freedom, modeled by the Euler-Lagrange equations

$$M_i(q_i)\ddot{q}_i + C_i(q_i, \dot{q}_i)\dot{q}_i + \frac{\partial}{\partial q_i}U_i(q_i) = \tau_i^*, \quad i \leq N, \tag{5.1}$$

where $q_i, \dot{q}_i, \ddot{q}_i \in \mathbb{R}^n$ are the generalized joint position, velocity, and acceleration respectively, $M_i(q_i) \in \mathbb{R}^{n\times n}$ is the inertia matrix, $U : \mathbb{R}^n \to \mathbb{R}$ is the potential energy function and $\tau_i^* \in \mathbb{R}^p$ is the control input. As it is customary, we assume the following.

Assumption 7 *The following properties hold.*

1. *There exist* $\underline{c}_i$ *and* $\bar{c}_i > 0$ *such that,* $\underline{c}_i I \leq M_i(q_i) \leq \bar{c}_i I$ *for all* $q_i \in \mathbb{R}^n$.
2. *The matrix* $\dot{M}_i(q_i) - 2C_i(q_i, \dot{q}_i)$ *is skew-symmetric.*
3. *The Coriolis matrix* $C_i(q_i, \dot{q}_i)$ *is uniformly bounded in* q_i. *Moreover*

$$|C_i(q_i, \dot{q}_i)\dot{q}_i| \leq k_{c_i}|\dot{q}_i|^2$$

for $k_{c_i} > 0$.

We first address the bipartite formation of cooperative-competitive robot manipulators with inter-agent end-effector constraints. This work was carried out during my research stay at the University of Groningen. Then, we study the constrained bipartite formation of a network of cooperative and competitive satellites. For both of the addressed problems, we consider a structurally balanced and undirected signed network, and the agents are modeled by the Euler-Lagrange equations in (5.1).

5.2 ROBUST FORMATION OF ROBOT MANIPULATORS WITH INTER-AGENT END-EFFECTOR CONSTRAINTS

The study of the bipartite formation-control problem of robot manipulators' end-effector under constraints is motivated, as mentioned before, by applications in industrial robotics for robots working on opposite surfaces or on opposite corners of a product without collisions. It can also be used for robot manipulators that are placed at opposite sides of a conveyor with the mission of placing the products on the conveyor with antisymmetric movements. By placing signs on certain edges, we force one group of manipulators to perform the task on one side and the other group to perform its task on the other (symmetric) side. In such applications, the realistic objective is for cooperative manipulators either to follow a leader who may be interacting with a human operator, or to execute a predefined task and follow a trajectory. One way to tackle this type of problem is to solve the basic problem of signed networks, *i.e.*, the bipartite consensus or bipartite formation problem, as are the consensus and leader-tracking control problems for traditional cooperative agents.

5.2.1 Problem statement

Let

$$x_i = x_{i_0} + h_i(q_i), \tag{5.2}$$

denote the position of the end-effector of the ith manipulator, where x_{i_0} is the position of the manipulator's base and $h_i : \mathbb{R}^n \to \mathbb{R}^p$ is the mapping from joint-space to the task space [57]. Differentiating (5.2) with respect to time, we obtain the relation between the task-space velocity and joint velocity [57]

$$\dot{x}_i = J_i(q_i)\dot{q}_i, \quad J_i(q_i) := \frac{\partial h_i(q_i)}{\partial q_i}\dot{q}_i, \tag{5.3}$$

where $J_i(q_i) \in \mathbb{R}^{n\times p}$ is the Jacobian matrix of the forward kinematics.

The bipartite-formation-control problem consists in the end-effectors' positions of the cooperative agents reaching a desired geometric shape around a consensus value, while the end-effectors' positions of non-cooperative agents converge to another spatial configuration. The characteristics of the formation shape are defined through the relative biases b_i and b_j with respect to the consensus points. Formally, we can thus define the bipartite formation control objective as

$$\lim_{t\to\infty} \bar{x}_i(t) - \mathrm{sgn}(a_{ij})\bar{x}_j(t) \to 0, \quad i, j \leq N, \tag{5.4}$$

where

$$\bar{x}_i := x_i - b_i, \tag{5.5}$$

and $a_{ij} \in \mathbb{R}$ is the adjacency weight between the two agents.

In an all-cooperative-agents setting, consensus means that all $\bar{x}_i$ converge to the same value, but in this case, since some robot manipulators are cooperative and others are competitive, all the end-effectors reach two symmetrical consensus values. For the purpose of control design and analysis, this boils down to making certain synchronization errors to converge to zero. Akin to Chapter 2 these errors correspond to the edges on the graph and are defined as

$$\bar{e}_{x_k} := \bar{x}_i - \operatorname{sgn}(a_{ij})\bar{x}_j, \quad k \leq M, \tag{5.6}$$

where $\bar{x}_i$ is defined in (5.5) and k denotes the index of the interconnection between the ith and jth end-effectors. As described in Section 2.3, since a_{ij} is either positive or negative, the resulting network is modeled by a signed graph.

Now, as mentioned in Chapter 4, in view of the constraints imposed on the end-effectors, considering the structurally unbalanced case for undirected signed networks is not interesting since making all end-effectors converge to the origin does not respect the collision-avoidance objective. Therefore, we impose the following.

Assumption 8 *The systems described in (5.1), which are interconnected via inputs τ_i, form a structurally balanced (see Definition 1), undirected, and connected signed graph.*

In addition, it is imposed that the controller τ_i^* ensures that the end-effectors do not collide and remain within their sensing ranges. Akin to the previous chapter, this comes to ensuring that for any pair of communicating nodes ν_i and $\nu_j \in \mathcal{V}$, the corresponding positions remain in certain constraint sets, which are defined as follows. Let $\mathcal{E}_m$ denote the set of indices k corresponding to edges containing pairs of cooperative agents, *i.e.*, $i, j \in \mathcal{V}_l$ with $l \in \{1, 2\}$ and $\delta_k := x_i - x_j$. In addition, for each $k \leq M$, let $R_k > 0$ and $\Delta_k > 0$. Then, we define

$$\text{(Task requirement constraints)} \qquad \mathcal{I}_r := \{\delta_k \in \mathbb{R}^n : |\delta_k| < R_k,\ k \in \mathcal{E}_m\} \tag{5.7a}$$

$$\text{(Collision-avoidance constraints)} \qquad \mathcal{I}_c := \{\delta_k \in \mathbb{R}^n : |\delta_k| > \Delta_k\ k \leq M\}, \tag{5.7b}$$

where $\mathcal{I}_r$ is the set of task requirement constraints and $\mathcal{I}_c$ is the set of collision-avoidance constraints. Under these conditions, it is required to design a distributed bipartite formation dynamic controller of the form

$$\tau_i^* = f_i(\bar{e}_{x_k}, q_i, \dot{q}_i),$$

that ensures that,

$$\lim_{t\to\infty} \bar{e}_{x_k}(t) = 0, \quad \lim_{t\to\infty} \dot{q}_i(t) = 0, \quad k \leq M, i \leq N, \tag{5.8}$$

and the manipulators' end-effector's trajectories satisfy the proximity and collision-avoidance constraints. That is, it must hold that $\delta(t) \in \mathcal{I}$ for all $t \geq 0$, with $\delta := [\delta_1\ \delta_2\ \cdots\ \delta_M]^\top$, $\mathcal{I} := \mathcal{I}_r \cap \mathcal{I}_c$ for cooperative manipulators and $\mathcal{I} := \mathcal{I}_c$ for competitive manipulators.

5.2.2 Control in the absence of disturbance

The control approach follows the developments in Chapter 4. That is, we address the considered problem as one of stabilization of the origin in edge coordinates, which in this case correspond exactly to the synchronization errors in (5.6). Then, in order to respect the inter-agent constraints, the control input is designed as the gradient of a so-called barrier-Lyapunov function. Next, we discuss in more detail each aspect of the control design.

5.2.2.1 Control design

For the purpose of analysis, we define the BLF in edge coordinates corresponding to the synchronization errors, defined in (5.6). On the other hand, as was the case in Chapter 4, the constraints are imposed on relative distances δ_k whereas the control objective for the end-effectors is defined in terms of $\bar{e}_{x_k}$. Then, we can express the relative distance between two end-effectors in terms of $\bar{e}_{x_k}$ as in (4.23) if they are cooperative, and as in (4.24) otherwise. Then, considering the constraints as defined in (4.25) in function of the synchronization errors and the definition of α_k in (4.26), we define

$$\bar{W}_k(\alpha_k, \bar{e}_{x_k}) := \sum_{k=1}^{M} \left(\frac{1+\sigma_k}{2} \tilde{W}_k(\alpha_k, \bar{e}_{x_k}) - \frac{\sigma_k - 1}{2} \widehat{W}_k(\alpha_k, \bar{e}_{x_k}) \right), \tag{5.9}$$

where $\sigma_k = 1$ if end-effectors i and j are cooperative and $\sigma_k = -1$ otherwise, $\tilde{W}_k$ is defined in (4.27) for cooperative edges and $\widehat{W}_k$ is defined in (4.29) for competitive edges. The BLF in (5.9) encodes collision-avoidance constraints for each edge between end-effectors and connectivity constraints for cooperative edges and is used to design the gradient-based control law. Moreover, it satisfies $\bar{W}_k(\alpha_k, 0) = 0$, $\nabla_{\bar{e}_{x_k}} \bar{W}_k(\alpha_k, 0) = 0$ and $\bar{W}_k(\alpha_k, \bar{e}_{x_k}) \to \infty$ as $|\delta_k| \to \Delta_k$ for all $k \leq M$, and as $|\delta_k| \to R_k$ for all $\sigma_k = 1$. Also, we note that $\{\bar{e}_{x_k} = 0\}$ is a minimum of $\bar{W}(\alpha_k, \cdot)$ and, as a matter of fact, it is also a unique minimum even though $\bar{W}(\alpha_k, \cdot)$ has a second critical point, which we denote e_k^*. Then, as in Chapter 4, defining $\mathcal{W} := \cup_{k \leq M} \mathcal{W}_k$, where

$$\mathcal{W}_k := \{0, e_k^*\}$$

for any $k \leq M$, we have

$$\frac{\kappa_1}{2} |\bar{e}_{x_k}|_{\mathcal{W}_k}^2 \leq \bar{W}_k(\alpha_k, \bar{e}_k) \tag{5.10}$$

for all $\alpha_k \in \mathbb{R}^n$ and $\bar{e}_k$ such that $\bar{e} \in \mathcal{I}$, where $|\bar{e}_k|_{\mathcal{W}_k} := \min\{|\bar{e}_k|, |\bar{e}_k - e_k^*|\}$.

Thus, using the BLF above, we define the BLF-gradient-based bipartite formation control law as

$$\tau_i^* = -k_{1_i} J_i(q_i)^\top \left[\sum_{k=1}^{M} [E_s]_{ik} \nabla_{\bar{e}_{x_k}} \bar{W}_k + \sum_{k=1}^{M} [\mathbb{E}]_{ik} \nabla_{\alpha_k} \bar{W} \right] - k_{2_i} \dot{q}_i + \frac{\partial}{\partial q_i} U_i(q_i), \tag{5.11}$$

where $k_{1_i} > 0$, $k_{2_i} > 0$ for all $i \leq N$,

$$\mathbb{E} = E - E_s, \tag{5.12}$$

E is the incidence matrix of the cooperative version of the considered network, and E_s is the incidence matrix of the considered signed network.

The control law in (5.11) is reminiscent of the one in (4.47), but includes extra terms proper to the nonlinear model of robot manipulators. The first two terms in the control law in (5.11) are needed to ensure the bipartite formation of end-effectors while respecting the inter-agent constraints imposed on the task space. The second term is needed specifically because of the use of the gradient recentered barrier function and the presence of competitive interactions between agents. These two terms are multiplied by the elements of the Jacobian matrix since the torque enters from the joint levels, but the bipartite formation objective and the constraints are imposed on the end-effectors. The rest of the control law is the usual passivity-based control. The third term is needed to control the joint velocity. It corresponds to a damping injection to steer the joint velocity at zero. The last term compensates for the gravitational force.

5.2.2.2 Stability analysis in the absence of disturbances

We analyze the stability of the bipartite formation manifold in (5.6) for the closed-loop system (5.1) interconnected by the control law (5.11). To that end, using the definition of the incidence matrix, we represent the synchronization errors in (5.6) and α_k defined in (4.26), in vector form

$$\bar{e}_x = \left[E_s^\top \otimes I_n\right] \bar{x}, \tag{5.13a}$$

$$\alpha = \left[E^\top \otimes I_n\right] x - \left[E_s^\top \otimes I_n\right] \bar{x}. \tag{5.13b}$$

Let

$$\bar{W}(\alpha, \bar{e}_x) = \sum_{k=1}^{M} \bar{W}_k(\alpha_k, \bar{e}_{x_k}) \tag{5.14}$$

where $\bar{W}_k$ is defined in (5.9). Then, we write the closed-loop system (5.1)–(5.11) in the compact form

$$\begin{aligned} \ddot{q} = &- M(q)^{-1}\Big[C(q,\dot{q})\dot{q} + K_1 J(q)^\top [E_s \otimes I_n] \nabla_{\bar{e}_x} \bar{W}(\alpha, \bar{e}_x) \\ &+ K_1 J(q)^\top [\mathbb{E} \otimes I_n] \nabla_\alpha \bar{W}(\alpha, \bar{e}_x) + [K_2 \otimes I_n]\dot{q}\Big], \end{aligned} \tag{5.15}$$

where $q = [q_i]$, $M(q) = \text{blkdiag}[M_i(q_i)]$, $C(q,\dot{q}) = \text{blkdiag}[C_i(q_i,\dot{q}_i)]$, $K_1 = \text{diag}(k_{1_i})$, $K_2 = \text{diag}(k_{2_i})$ and $J(q)^\top = \text{blkdiag}[J_i(q_i)^\top]$, $\forall i \leq N$. For this system, we have the following.

Proposition 15 ([81]) *Consider N robot manipulators modeled by (5.1), with $d_i = 0$ and satisfying the Assumptions 7 and 8, in closed loop with the distributed control law (5.11), with k_{1i}, $k_{2i} > 0$, for all $i \leq N$ and $\bar{W}_k$ as defined in (5.9). Then, for any given formation shape reachable by the end-effectors, the set $\{(\bar{e}_x, \dot{q}) = (0,0)\}$ is asymptotically stable for almost all initial conditions such that $(\bar{e}_x(0), \dot{q}(0)) \in \mathcal{I} \times \mathbb{R}^{nN}$ and $|\alpha_k(0)| > \Delta_k$ for any $k \leq M$.*

Proof: After Assumption 8, the considered graph is undirected and connected, so it contains a spanning tree. Then, as for the more ordinary scenario of consensus, the result may be assessed by analyzing the dynamics of the agents that belong to the spanning-tree—see [23], [54], [76]. To obtain the closed-loop equations in spanning-tree coordinates, following the latter, we first recall that

$$E_s = [E_{t_s} \quad E_{c_s}], \tag{5.16}$$

where $E_{t_s} \in \mathbb{R}^{N\times N-1}$ is the incidence matrix representing the edges of the spanning tree, corresponding to the spanning-tree graph $\mathcal{G}_t$, and $E_{c_s} \in \mathbb{R}^{N\times M-(N-1)}$ is the incidence matrix representing the remaining edges, corresponding to $\mathcal{G}_c := \mathcal{G}\backslash\mathcal{G}_t$. Consequently, after (5.13a) and (5.16), the errors can be expressed as $\bar{e}_x = [(E_{t_s}^\top \bar{x})^\top \ (E_{c_s}^\top \bar{x})^\top]^\top$, which gives $\bar{e}_x := [\bar{e}_{x_t}^\top \quad \bar{e}_{x_c}^\top]^\top$. Furthermore, for a structurally balanced signed graph, there exists a matrix R_s such that

$$E_s = E_{t_s} R_s, \tag{5.17}$$

where $R_s := [I_{N-1} \quad T_s]$ and $T_s := (E_{t_s}^\top E_{t_s})^{-1} E_{t_s}^\top E_{c_s}$—see Proposition 1 in [19]. Notably, the following relationship between the synchronization errors $\bar{e}$ and the spanning-tree errors $\bar{e}_{x_t}$ holds:

$$\bar{e}_x = [(E_{t_s} R_s)^\top \otimes I_n]\bar{x} = [R_s^\top \otimes I_n]\bar{e}_{x_t}, \tag{5.18}$$

so the bipartite formation objective (5.8) is achieved if $\bar{e}_{x_t} \to 0$ and $\dot{q} \to 0$. On the other hand, a similar relation holds for α defined in (5.13b):

$$\alpha = [\mathbb{E}^\top \otimes I_n]x + [E_s^\top \otimes I_n]b, \tag{5.19}$$

where $\mathbb{E}$ is defined in (5.12), $b := [b_1 \ b_2 \ \cdots \ b_M]^\top$ with $b_k := b_i - \text{sgn}(a_{ij})b_j$ and $k \leq M$. The matrix $\mathbb{E}$ corresponds only to competitive edges. Thus, akin to (5.16), we can write $\mathbb{E} = [\mathbb{E}_t \quad \mathbb{E}_c]$ and $\alpha = [\alpha_t^\top \ \alpha_c^\top]^\top$. Thus,

$$\mathbb{E} = \mathbb{E}_t R_s \tag{5.20}$$

and

$$\alpha = R_s^\top \left[[\mathbb{E}_t^\top \otimes I_n]x + [E_{t_s}^\top \otimes I_n]b\right] = [R_s^\top \otimes I_n]\alpha_t. \tag{5.21}$$

Next, to express the control law in spanning-tree coordinates, we introduce

$$\tilde{W}(\alpha_t, \bar{e}_{x_t}) := \bar{W}(R_s^\top \alpha_t, R_s^\top \bar{e}_{x_t}). \tag{5.22}$$

That is, in view of (5.18) and (5.21), $\tilde{W}(\alpha_t, \bar{e}_{x_t})$ denotes the same quantity as the right-hand-side of (5.14), but in spanning-tree coordinates, so $\tilde{W}$ maps $\mathcal{I}_t \times \mathbb{R}^{nN} \to \mathbb{R}^{nN}_{\geq 0}$, where $\mathcal{I}_t := \mathcal{I}_{r_t} \cap \mathcal{I}_{c_t}$ for cooperative agents and $\mathcal{I}_t := \mathcal{I}_{c_t}$ for competitive agents, and

$$\mathcal{I}_{r_t} := \{\bar{e}_{t_{x_k}} \in \mathbb{R}^n : |[r_{s_k}^\top \otimes I_n][\bar{e}_{t_{x_k}} + \alpha_{t_k}]| < R_k \ , k \in \mathcal{E}_{m_t}\}, \tag{5.23}$$

$$\mathcal{I}_{c_t} := \{\bar{e}_{t_{x_k}} \in \mathbb{R}^n : \Delta_k < |[r_{s_k}^\top \otimes I_n][\bar{e}_{t_{x_k}} + \alpha_{t_k}]|, \ k \leq N-1\}, \tag{5.24}$$

$\mathcal{E}_{m_t}$ denotes the set of indices k corresponding to the $N-1$ edges of the spanning-tree graph containing pairs of cooperative agents, and r_{s_k} is the kth column of R_s. The

set $\mathcal{I}_t$ defines the constraints in spanning-tree coordinates. Using $\tilde{W}$, we define the gradient-based control terms

$$\begin{aligned}\nabla_{\bar{e}_{x_t}}\tilde{W} &\equiv \frac{\partial \bar{W}(\alpha,\bar{e}_x)}{\partial \bar{e}_x}^\top \frac{\partial \bar{e}_x}{\partial \bar{e}_{x_t}} = \nabla_{\bar{e}_x}\bar{W}^\top[R_s^\top \otimes I_n],\\ \nabla_{\alpha_t}\tilde{W} &\equiv \frac{\partial \bar{W}(\alpha,\bar{e}_x)}{\partial \alpha}^\top \frac{\partial \alpha}{\partial \alpha_t} = \nabla_{\alpha}\bar{W}^\top[R_s^\top \otimes I_n].\end{aligned} \tag{5.25}$$

Thus, in spanning-tree edge coordinates, Eq. (5.15) becomes

$$\begin{aligned}\ddot{q} = &- M(q)^{-1}\Big[C(q,\dot{q})\dot{q} + K_1 J(q)^\top[E_{t_s}\otimes I_n]\nabla_{\bar{e}_{x_t}}\tilde{W}(\alpha_t,\bar{e}_{x_t})\\ &+ K_1 J(q)^\top[\mathbb{E}_t\otimes I_n]\nabla_{\alpha_t}\tilde{W}(\alpha_t,\bar{e}_{x_t}) + [K_2\otimes I_n]\dot{q}\Big].\end{aligned} \tag{5.26}$$

The rest of the proof consists in establishing asymptotic stability of the origin $\{(\bar{e}_{x_t},\dot{q}) = (0,0)\}$ and forward invariance of the set $\mathcal{I}_t\times\mathbb{R}^{nN}$, for the trajectories of (5.26). First, consider the Lyapunov function candidate

$$V(\alpha_t,\bar{e}_{x_t},\dot{q}) = \tilde{W}(\alpha_t,\bar{e}_{x_t}) + \frac{1}{2}\dot{q}^\top M(q)\dot{q}, \tag{5.27}$$

where $M(q) = M(q)^\top$. Also, we remark that V is positive definite in $\bar{e}_{x_t}$ and $\dot{q}$, and bounded from above uniformly in α_t. More precisely, there exist $\mu_1 > 0$ such that $\mu_1\left[|\bar{e}_{x_t}|^2 + |\dot{q}|^2\right] \leq V(\alpha_t,\bar{e}_{x_t},\dot{q})$, and $V(\alpha_t,\bar{e}_{x_t},\dot{q}) \to 0$ as $|\bar{e}_{x_t}| \to 0$ and $|\dot{q}| \to 0$.

Now, its derivative satisfies

$$\begin{aligned}\dot{V} =&\nabla_{\bar{e}_{x_t}}\tilde{W}^\top[E_{t_s}\otimes I_n]^\top J\dot{q} + \nabla_{\alpha_t}\tilde{W}^\top[\mathbb{E}_t\otimes I_n]^\top J\dot{q}\\ &+\frac{1}{2}\dot{q}^\top\dot{M}\dot{q} - \dot{q}^\top C(q,\dot{q})\dot{q} - \dot{q}^\top[K\otimes I_n]\dot{q}\\ &-\dot{q}^\top J(q)^\top[E_{t_s}\otimes I_n]\nabla_{\bar{e}_{x_t}}\tilde{W} - \dot{q}^\top J(q)^\top[\mathbb{E}_t\otimes I_n]\nabla_{\alpha_t}\tilde{W}\\ =&-\frac{1}{2}\dot{q}^\top\left[\dot{M} - 2C(q,\dot{q})\right]\dot{q} - \dot{q}^\top[K\otimes I_n]\dot{q}.\end{aligned}$$

But since $\dot{M} - 2C(q,\dot{q})$ is skew-symmetric, we obtain

$$\dot{V}(\alpha_t,\bar{e}_{x_t},\dot{q}) = -\dot{q}^\top[K\otimes I_n]\dot{q} \leq 0, \tag{5.28}$$

for all $(\bar{e}_{x_t},\dot{q}) \in \mathcal{I}_t\times\mathbb{R}^{nN}$ so the origin is stable and the solutions are uniformly bounded. Next, we use LaSalle's invariance theorem. To that end, we first note that on the set $\{\dot{q}\in\mathbb{R}^{nN} : \dot{V} = 0\}$, we have $\dot{q} = 0$, and consequently, $\ddot{q} = 0$. In view of (5.3), it follows that $\dot{x} = 0$ because $\dot{x} = J(q)\dot{q}$. In turn, since all the functions on the right-hand-side of (5.26) are continuous, we have

$$J(q)^\top[E_{t_s}\otimes I_n]\nabla_{\bar{e}_{x_t}}\tilde{W} + J(q)^\top[\mathbb{E}_t\otimes I_n]\nabla_{\alpha_t}\tilde{W} = 0. \tag{5.29}$$

On the one hand, we have

$$\nabla_{\alpha_t}\tilde{W} = \nabla_{\bar{e}_{x_t}}\tilde{W} - \frac{\partial}{\partial\alpha_t}\left\{\frac{\partial W}{\partial\alpha_t}(\alpha_t)\right\}\bar{e}_{x_t}, \tag{5.30}$$

and, because $\alpha = [E^\top \otimes I_n]x - [E_s^\top \otimes I_n]\bar{x}$, then $\dot{\alpha} = [\mathbb{E} \otimes I_n]^\top \dot{x}$ and $\dot{\alpha}_t = [\mathbb{E}_t \otimes I_n]^\top \dot{x}$. Thus, $\dot{\alpha}_t = 0$, which is equivalent to $\alpha_t \equiv \text{const}$ on $\{\dot{V} = 0\}$. In turn, the last term of the right-hand-side of (5.30) equals to zero. Then, from (5.29) and using (5.12), $J(q)^\top[(E_{t_s} + E_t - E_{t_s}) \otimes I_n]\nabla_{\bar{e}_{x_t}}\tilde{W} = J(q)^\top[E_t \otimes I_n]\nabla_{\bar{e}_{x_t}}\tilde{W} = 0$. Now, since E_t is full rank (because it corresponds to the incidence matrix of a spanning tree) it follows that $\nabla_{\bar{e}_{x_t}}\tilde{W} = 0$, which holds if and only if $\bar{e}_{x_t} \in \mathcal{W}^t$, where $\mathcal{W}^t = \{0, e_t^*\}$ and e_t^* is the saddle point of $\tilde{W}$. Therefore, the solutions converge to the set $\mathcal{W}^t \times \{0\}$. However, since e_t^* is a saddle point of $\tilde{W}$, the set of initial conditions generating solutions that converge to $(e_t^*, 0)$ has zero Lebesgue measure. Thus, almost all initial conditions generate trajectories that converge to the origin. Asymptotic stability follows. The rest of the proof follows similar arguments as in the proof of Proposition 11. ■

Remark 17 *The workspace of a manipulator is the total volume or area within which the end-effector can move, determined by joint configurations and link lengths. The reachable set is a subset of this workspace, representing the specific points the end-effector can access while satisfying certain constraints. The reachable set is always smaller than or equal to the workspace, as it includes only those points achievable under specific conditions.* •

Remark 18 *The statement of Proposition 15 goes beyond the control of manipulators' end-effectors. This analysis may also serve as a basis for solutions to other problems, such as the control formation of cooperative-competitive satellites under inter-agent constraints. The latter is addressed at the end of the chapter.* •

5.2.3 Control in the presence of disturbances

Consider now a network of N robot manipulators with n-degrees-of-freedom, in the presence of disturbances, *i.e.,* modeled by

$$M_i(q_i)\ddot{q}_i + C_i(q_i, \dot{q}_i)\dot{q}_i + \frac{\partial}{\partial q_i}U_i(q_i) = \tau_i + d_i, \quad i \leq N, \tag{5.31}$$

where $d_i \in \mathbb{R}^n$ represents an external disturbance generated by an exosystem. As in [61] and [102], we consider that the external disturbances are modeled by

$$d_i = d_{M,i} + J_i(q_i)^\top d_{E,i}, \tag{5.32}$$

where $d_{M,i} \in \mathbb{R}^n$, $d_{E,i} \in \mathbb{R}^p$ and $J_i(q_i) \in \mathbb{R}^{n \times p}$ is the Jacobian matrix. The disturbance d_i is generated by an exosystem of the form

$$\dot{w}_{M,i} = S_{M,i}w_{M,i}, \qquad d_{M,i} = C_{M,i}w_{M,i}, \tag{5.33a}$$

$$\dot{w}_{E,i} = S_{E,i}w_{E,i}, \qquad d_{E,i} = C_{E,i}w_{E,i}, \quad i \leq N \tag{5.33b}$$

where $w_{M,i}, w_{E,i} \in \mathbb{R}^{l_i}$, $S_{M,i}, S_{E,i} \in \mathbb{R}^{l_i \times l_i}$ and $C_{M,i}, C_{E,i} \in \mathbb{R}^{n \times l_i}$. As in [99], we assume the following.

Assumption 9 *The exosystems $S_{M,i}$ and $S_{E,i}$ are assumed to be neutrally stable, that is, all the eigenvalues of $S_{M,i}$ and $S_{E,i}$ are different and lie on the imaginary axis, and they are nonsingular. Moreover, they are assumed to be known.*

Such an assumption is satisfied in various scenarios involving human-robot-environment interactions because the disturbance is expressed as a sum of sinusoidals—cf. [99], which is a truncated finite Fourier approximation of general external bounded disturbances.

The control design for perturbed systems as in (5.31) builds on the control law τ^* in (5.11), which is effective to achieve bipartite formation among the end-effectors while respecting the imposed constraints. To cope with the disturbances, however, the controller is endowed with its own dynamics. That is, let

$$\begin{aligned}\dot{\chi}_i &= f_{1_i}(\bar{e}_{x_k}, q_i, \dot{q}_i, \chi_i)\\ \tau_i &= f_{2_i}(\bar{e}_{x_k}, q_i, \dot{q}_i, \chi_i).\end{aligned}$$

The dynamical system $\dot{\chi}_i$ is designed to estimate the disturbances, and the control law τ_i is defined by redesigning τ_i^* to contain a disturbance-rejection term that depends on χ_i.

5.2.3.1 Robust control redesign

The disturbance estimator is designed based on an internal model-based approach [61, 102, 99]. Let

$$\dot{\chi}_{1_i} = A_{M,i}\chi_{1_i} - B_{M,i}u_i, \tag{5.34a}$$
$$\dot{\chi}_{2_i} = A_{E,i}\chi_{2_i} - B_{E,i}J_i(q_i)u_i, \tag{5.34b}$$

where $\chi_{1_i} \in \mathbb{R}^{l_i}$, $\chi_{2_i} \in \mathbb{R}^{l_i}$, $A_{M,i} \in \mathbb{R}^{l_i \times l_i}$, $A_{E,i} \in \mathbb{R}^{l_i \times l_i}$, $B_{M,i} \in \mathbb{R}^{l_i \times n}$, $B_{E,i} \in \mathbb{R}^{l_i \times n}$, $u_i \in \mathbb{R}^n$ is the input to the internal model dynamics, which is defined later, $A_{M,i} + A_{M,i}^\top = 0$, $A_{E,i} + A_{E,i}^\top = 0$ and the pairs $(B_{M,i}^\top, A_{M,i})$ and $(B_{E,i}^\top, A_{E,i})$ are observable. We also assume, as in [61] and [102], that the eigenvalues of the matrix $S_{M,i}$ in (5.33) and $A_{M,i}$ and the eigenvalues of $S_{E,i}$ in (5.33) and $A_{E,i}$ are identical. Under these conditions, there exist transformation matrices $T_{M,i} \in \mathbb{R}^{l_i \times p_i}$ and $T_{E,i} \in \mathbb{R}^{l_i \times p_i}$, such that—cf. [33, Section 4.2]

$$T_{M,i}S_{M,i} = A_{M,i}T_{M,i}, \qquad B_{M,i}^\top T_{M,i} + C_{M,i} = 0 \tag{5.35a}$$
$$T_{E,i}S_{E,i} = A_{E,i}T_{E,i}, \qquad B_{E,i}^\top T_{E,i} + C_{E,i} = 0. \tag{5.35b}$$

Then, we can rewrite (5.34) in the compact form as

$$\dot{\chi}_i = A_i\chi_i - B_i(q_i)u_i, \tag{5.36}$$

where

$$\chi_i = \begin{bmatrix}\chi_{1_i} & \chi_{2_i}\end{bmatrix}^\top, \quad A_i = \begin{bmatrix}A_{M,i} & 0\\ 0 & A_{E,i}\end{bmatrix}, \quad B_i(q_i) = \begin{bmatrix}B_{M,i} & J_i(q_i)^\top B_{E,i}\end{bmatrix}.$$

Next, the control law is redesigned using χ_i, and the input u_i will be defined later, using the internal model. Then, we define the following estimation error coordinates: $\tilde{\chi}_i$, for the estimate of the disturbance, and $\tilde{d}_i$, for the disturbance, that is

$$\tilde{\chi}_i = \chi_i - T_i w_i \tag{5.37a}$$
$$\tilde{d}_i = B_i^\top(q_i)\chi_i + d_i, \tag{5.37b}$$

where $T_i = \begin{bmatrix} T_{M,i} & T_{E,i} \end{bmatrix}$ and $w_i = \begin{bmatrix} w_{M,i} & w_{E,i} \end{bmatrix}^\top$. Next, taking the derivative of (5.37a) and using (5.33) for (5.37b), we obtain

$$\begin{aligned} \dot{\tilde{\chi}}_i &= \dot{\chi}_i - T_i \dot{w}_i \\ \tilde{d}_i &= B_i(q_i)^\top \chi_i + C_i w_i. \end{aligned}$$

Now, replacing (5.36) and (5.33) then using (5.37a) in the first equation and using (5.35) and (5.37a) in the second equation, we obtain the estimation-error dynamics.

$$\begin{aligned} \dot{\tilde{\chi}}_i &= A_i \chi_i - B_i(q_i) u_i - T_i S_i w_i \\ &= A_i \tilde{\chi}_i - B_i(q_i) u_i \qquad (5.38a) \\ \tilde{d}_i &= B_i(q_i)^\top \chi_i - B_i(q_i)^\top T_i w_i \\ &= B_i(q_i)^\top (\chi_i - T_i w_i) = B_i(q_i)^\top \tilde{\chi}_i. \qquad (5.38b) \end{aligned}$$

The equations in (5.38) are important because they define a passive map from u_i to $\tilde{d}_i$. To see that, consider the storage function $H_i(\tilde{\chi}_i) = \frac{1}{2}|\tilde{\chi}_i|^2$. Its derivative gives

$$\begin{aligned} \dot{H}_i(\tilde{\chi}_i) &= \tilde{\chi}_i^\top \dot{\tilde{\chi}}_i \\ &= \frac{1}{2} \tilde{\chi}_i^\top (A_i + A_i^\top) \tilde{\chi}_i - \tilde{\chi}_i^\top B_i(q_i) u_i \\ &= \tilde{\chi}_i^\top (A_i \tilde{\chi}_i - B_i u_i) \\ &= -\tilde{\chi}_i^\top B_i(q_i) u_i = u_i^\top \tilde{d}_i. \end{aligned}$$

In the previous computations, we used $A_i + A_i^\top = 0$. Thus, the system in (5.38) is lossless from the input u_i to the output $\tilde{d}_i = B_i^\top \tilde{\chi}_i$. This observation guides our choice to redesign the control law in (5.11) as

$$\tau_i = \tau_i^* + B_i^\top(q_i) \chi_i. \qquad (5.39)$$

5.2.3.2 Stability analysis in the presence of disturbance

We analyze the system (5.31) in the presence of disturbances and driven by the control law (5.39), where χ_i is defined by (5.36), with $u_i = \dot{q}_i$. We have the following.

Proposition 16 ([82]) *Consider N robot manipulators modeled by (5.31) and satisfying the Assumptions 7 and 8 in closed-loop with the distributed controller defined by (5.39), (5.11), and (5.36), with $u_i = \dot{q}_i$ and k_{1i}, $k_{2i} > 0$, for all $i \leq N$. Then, for any given formation shape reachable by the end-effectors, the set $\{(\bar{e}_x, \dot{q}) = (0,0)\}$ is asymptotically stable for almost all initial conditions such that $(\bar{e}_x(0), \dot{q}(0)) \in \mathcal{I} \times \mathbb{R}^{nN}$ and $|\alpha_k(0)| > \Delta_k$ for any $k \leq M$.*

Proof: As for Proposition 15 the statement follows if we establish asymptotic stability of the origin in spanning-tree coordinates and forward invariance of $\mathcal{I}_t \times \mathbb{R}^{nN}$.

First, proceeding as in Section 5.2.2.2, we obtain that the closed-loop equations now read

$$\begin{aligned} \ddot{q} = &- M(q)^{-1} \Big[C(q,\dot{q})\dot{q} + K_1 J(q)^\top [E_{t_s} \otimes I_n] \nabla_{\bar{e}_{x_t}} \tilde{W}(\alpha_t, \bar{e}_{x_t}) \\ &+ K_1 J(q)^\top [\mathbb{E}_t \otimes I_n] \nabla_{\alpha_t} \tilde{W}(\alpha_t, \bar{e}_{x_t}) + [K_2 \otimes I_n]\dot{q} - [B(q) \otimes I_n]^\top \chi - d \Big], \qquad (5.40) \end{aligned}$$

where $d := \text{col}[d_i]$, $i \leq N$.

Next, we consider the Lyapunov function candidate

$$V(\alpha_t, \bar{e}_{x_t}, \dot{q}, \tilde{\chi}) = \tilde{W}(\alpha_t, \bar{e}_{x_t}) + \frac{1}{2}\left[\dot{q}^\top M(q)\dot{q} + |\tilde{\chi}|^2\right], \tag{5.41}$$

whose derivative yields

$$\begin{aligned}
\dot{V} =& \nabla_{\bar{e}_{x_t}} \tilde{W}^\top [E_{t_s} \otimes I_n]^\top J(q)\dot{q} + \nabla_{\alpha_t} \tilde{W}^\top [\mathbb{E}_t \otimes I_n]^\top J(q)\dot{q} \\
&+ \frac{1}{2}\dot{q}^\top \dot{M}\dot{q} - \dot{q}^\top C(q,\dot{q})\dot{q} - \dot{q}^\top [K \otimes I_n]\dot{q} \\
&- \dot{q}^\top J(q)^\top \left[[E_{t_s} \otimes I_n]\nabla_{\bar{e}_{x_t}} \tilde{W} + [\mathbb{E}_t \otimes I_n]\nabla_{\alpha_t} \tilde{W}\right] \\
&- \tilde{\chi}^\top [B(q) \otimes I_n]u + \dot{q}^\top [B(q) \otimes I_n]^\top \chi + \dot{q}^\top d.
\end{aligned} \tag{5.42}$$

Then, we use (5.37), the skew symmetry of $\dot{M} - 2C(q,\dot{q})$ and $u = \dot{q}$ to obtain

$$\begin{aligned}
\dot{V} =& -\tilde{\chi}^\top [B(q) \otimes I_n]u + \frac{1}{2}\dot{q}^\top \left[\dot{M} - 2C(q,\dot{q})\right]\dot{q} \\
&+ \dot{q}^\top [B(q) \otimes I_n]^\top \chi - \dot{q}^\top [K \otimes I_n]\dot{q} + \dot{q}^\top \left[\tilde{d} - [B(q) \otimes I_n]^\top \chi\right] \\
=& -\tilde{\chi}^\top [B(q) \otimes I_n]u + \dot{q}^\top [B(q) \otimes I_n]^\top \chi - \dot{q}^\top [K \otimes I_n]\dot{q} \\
&+ \dot{q}^\top [B(q) \otimes I_n]^\top \tilde{\chi} - \dot{q}^\top [B(q) \otimes I_n]^\top \chi \\
=& -\dot{q}^\top [K \otimes I_n]\dot{q} \leq 0.
\end{aligned}$$

Note that on the set $\{\dot{q} \in \mathbb{R}^{nN} : \dot{V} = 0\}$, we have $\dot{q} = 0$ and $\ddot{q} = 0$. In turn, after (5.40), we have

$$K_1 J(q)^\top [E_{t_s} \otimes I_n]\nabla_{\bar{e}_{x_t}} \tilde{W} + K_1 J(q)^\top [\mathbb{E}_t \otimes I_n]\nabla_{\alpha_t} \tilde{W} - [B(q) \otimes I_n]^\top \chi - d = 0. \tag{5.43}$$

As in the Proof of Proposition 15, on $\{\dot{V} = 0\}$, we have $\dot{x} = 0$ and $\dot{\alpha}_t = 0$. Consequently, α_t is constant. Then, from (5.43) and using (5.12), we obtain

$$K_1 J(q)^\top [E_t \otimes I_n]\nabla_{\bar{e}_{x_t}} \tilde{W} - [B(q) \otimes I_n]^\top \chi - d = 0,$$

after (5.37b), we get

$$K_1 J(q)^\top [E_t \otimes I_n]\nabla_{\bar{e}_{x_t}} \tilde{W} - [B(q) \otimes I_n]^\top \chi - \left[\tilde{d} - [B(q) \otimes I_n]^\top \chi\right] = 0,$$

that is, $K_1 J(q)^\top [E_t \otimes I_n]\nabla_{\bar{e}_{x_t}} \tilde{W} - \tilde{d} = 0$. Then, replacing (5.38b) in the previous equation, we obtain

$$K_1 J(q)^\top [E_t \otimes I_n]\nabla_{\bar{e}_{x_t}} \tilde{W} = [B(q) \otimes I_n]^\top \tilde{\chi}. \tag{5.44}$$

Next, we differentiate on both sides of the latter to obtain

$$K_1 J(q)^\top [E_t \otimes I_n]\frac{\partial^2 \tilde{W}}{\partial \bar{e}_t^2}\dot{\bar{e}}_{x_t} + K_1 \dot{J}(q)^\top [E_t \otimes I_n]\nabla_{\bar{e}_{x_t}} \tilde{W} = [B(q) \otimes I_n]^\top \dot{\tilde{\chi}} + [\dot{B}(q) \otimes I_n]^\top \tilde{\chi},$$

but since $\dot{\bar{e}}_{x_t} = E_{t_s}^\top J\dot{q} = 0$, $\dot{J}(q) = \frac{\partial J(q)}{\partial q}\dot{q} = 0$, and $\dot{B}(q) = \frac{\partial B(q)}{\partial q}\dot{q} = 0$, it follows that

$$[B(q) \otimes I_n]^\top \dot{\tilde{\chi}} = 0.$$

Then, we replace (5.36) in the latter to obtain

$$[B(q) \otimes I_n]^\top \left[[A \otimes I_n]\tilde{\chi} - [B(q) \otimes I_n]u\right] = \left[[B(q)^\top A] \otimes I_n\right] \tilde{\chi} = 0.$$

The last identity comes from using $u = \dot{q} = 0$. Differentiating on both sides of this identity, we have

$$\begin{cases} \left[[B(q)^\top A] \otimes I_n\right] \dot{\tilde{\chi}} = \left[[B(q)^\top A^2] \otimes I_n\right] \tilde{\chi} = 0 \\ \left[[B(q)^\top A^2] \otimes I_n\right] \dot{\tilde{\chi}} = \left[[B(q)^\top A^3] \otimes I_n\right] \tilde{\chi} = 0 \\ \vdots \\ \left[[B(q)^\top A^{l_i-1}] \otimes I_n\right] \dot{\tilde{\chi}} = \left[[B(q)^\top A^{l_i}] \otimes I_n\right] \tilde{\chi} = 0. \end{cases} \tag{5.45}$$

On the other hand, consider the characteristic polynomial of A:

$$p(\lambda) = \lambda^{l_i} + c_{l_{i-1}}\lambda^{l_i-1} + \cdots + c_1\lambda + c_0. \tag{5.46}$$

After Cayley-Hamilton's Theorem, $p(A) = 0$. Therefore,

$$\frac{1}{c_0} B(q)^\top [p(A) \otimes I_n]\tilde{\chi} = 0,$$

that is,

$$\frac{1}{c_0}\left[B(q)^\top \left(A^{l_i} + c_{l_i-1}A^{l_i-1} + \cdots + c_1 A\right) \otimes I_n\right] \tilde{\chi} + \frac{1}{c_0} B(q)^\top [c_0 \otimes I_n]\tilde{\chi} = 0,$$

or, equivalently,

$$-\frac{1}{c_0}\left[B(q)^\top \left[A^{l_i} + c_{l_i-1}A^{l_i-1} + \cdots + c_1 A\right] \otimes I_n\right] \tilde{\chi} = [B(q) \otimes I_n]^\top \tilde{\chi}. \tag{5.47}$$

The last identity is useful in view of the fact that the equations in (5.45) continue to hold if the left-hand sides are multiplied by the coefficients c_k of $p(\lambda)$ in (5.46) with $k \leq l_i$. Therefore, since $c_{l_i} = 1$,

$$\left[B(q)^\top \left[A^{l_i} + c_{l_{i-1}}A^{l_i-1} + \cdots + c_2 A^2 + c_1 A\right] \otimes I_n\right] \tilde{\chi} = 0.$$

From the latter and (5.47), we conclude that $[B(q) \otimes I_n]^\top \tilde{\chi} = 0$. In turn, from (5.44) we have $J(q)^\top [E_t \otimes I_n]\nabla_{\bar{e}_{x_t}} \tilde{W} = 0$, which holds if and only if $\nabla_{\bar{e}_{x_t}} \tilde{W} = 0$. The rest of the proof follows as for Proposition 11. ■

5.2.4 Numerical example

We provide a numerical example to show the performance of our control laws, first the one in (5.11) in the absence of disturbance and then the one in (5.39) in the presence of disturbance. For that, we consider a system of $N = 6$ two-link robot manipulators interconnected over a structurally balanced undirected signed network, modeled by a graph as the one depicted in Figure 5.1. For the corresponding graph, we define the orientation of the seven edges as

$$e_1 = \nu_1 + \nu_2,\ e_2 = \nu_1 - \nu_3,\ e_3 = \nu_1 + \nu_4,\ e_4 = \nu_2 + \nu_5,$$
$$e_5 = \nu_2 - \nu_6,\ e_6 = \nu_3 + \nu_4,\ e_7 = \nu_5 + \nu_6.$$

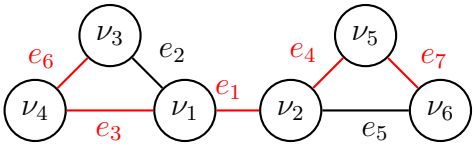

Figure 5.1: An undirected signed network of 6 robot manipulators. The black lines (e_2 and e_5) represent cooperative edges, and the red lines the competitive edges.

The set of nodes may be split into two disjoint subgroups as

$$\mathcal{V}_1 = \{\nu_1, \nu_3, \nu_5\}, \qquad \mathcal{V}_2 = \{\nu_2, \nu_4, \nu_6\},$$

so the network is structurally balanced. From (4.32), the edges $e_i, i \leq 5$ correspond to the edges of the spanning tree, and the remaining edges, e_6 and e_7, correspond to the cycles. The corresponding incidence matrix is given by

$$E_s = \begin{bmatrix} 1 & 1 & 1 & 0 & 0 & 0 & 0 \\ 1 & 0 & 0 & 1 & 1 & 0 & 0 \\ 0 & -1 & 0 & 0 & 0 & 1 & 0 \\ 0 & 0 & 1 & 0 & 0 & 1 & 0 \\ 0 & 0 & 0 & 1 & 0 & 0 & 1 \\ 0 & 0 & 0 & 0 & -1 & 0 & 1 \end{bmatrix}.$$

Each manipulator is modeled by the Euler-Lagrange equations in (5.1), with inertia and Coriolis matrices given by

$$M_i(q_i) = \begin{bmatrix} \alpha_i + 2\beta_i \cos(q_{2_i}) & \delta_i + \beta_i \cos(q_{2_i}) \\ \delta_i + \beta_i \cos(q_{2_i}) & \delta_i \end{bmatrix},$$
$$C_i(q_i, \dot{q}_i) = \delta_i \begin{bmatrix} -\sin(q_{2_i})\dot{q}_{2_i} & -\sin(q_{2_i})(\dot{q}_{1_i} + \dot{q}_{2_i}) \\ -\sin(q_{2_i})\dot{q}_{1_i} & 0 \end{bmatrix},$$

where $\alpha_i = l_{2_i}^2 m_{2_i} + l_{1_i}^2 (m_{1_i} + m_{2_i})$, $\beta_i = l_{1_i} l_{2_i} m_{2_i}$ and $\delta_i = l_{2_i}^2 m_{2_i}$ with l_{1_i}, l_{2_i} and m_{1_i}, m_{2_i} are the length and the mass of links 1 and 2. The physical parameters are

$m_1 = 1.2\text{kg}$, $m_2 = 1\text{kg}$, and $l_1 = l_2 = 1\text{m}$ for all $i \leq N$. The kinematic model for each manipulator is given by

$$x_i = \begin{bmatrix} l_1 \cos(q_{i_1}) + l_2 \cos(q_{1_i} + q_{2_i}) \\ l_1 \sin(q_{i_1}) + l_2 \sin(q_{1_i} + q_{2_i}) \end{bmatrix} + x_{i_0},$$

and the Jacobian matrix

$$J_i(q_i) = \begin{bmatrix} -l_1 \sin(q_{i_1}) - l_2 \sin(q_{1_i} + q_{2_i}) & -l_2 \sin(q_{1_i} + q_{2_i}) \\ l_1 \cos(q_{i_1}) + l_2 \cos(q_{1_i} + q_{2_i}) & l_2 \cos(q_{1_i} + q_{2_i}) \end{bmatrix}.$$

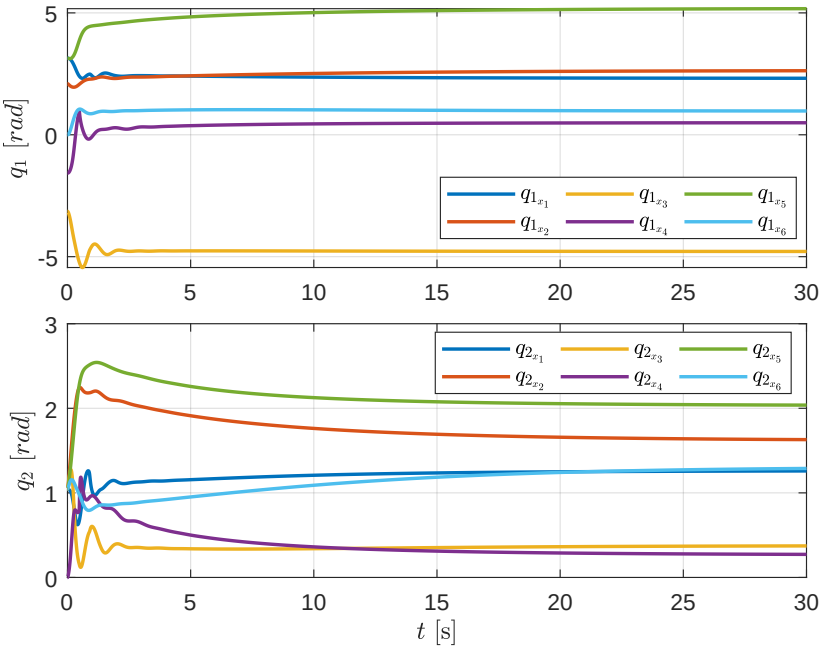

Figure 5.2: Bipartite formation of system (5.1) with control input (5.11) on joint trajectories.

First, consider the system (5.1) interconnected with the bipartite formation control law (5.11), where $k_{1_i} = 20$, $k_{2_i} = 15$ for all $i \leq N$. The bases of six robot manipulators are located at

$$x_{1_0} = \begin{bmatrix} 0 & 0.5 \end{bmatrix}^\top, \; x_{2_0} = \begin{bmatrix} 2.5 & 0 \end{bmatrix}^\top, \; x_{3_0} = \begin{bmatrix} -1 & 0 \end{bmatrix}^\top,$$
$$x_{4_0} = \begin{bmatrix} 0 & -2 \end{bmatrix}^\top, \; x_{5_0} = \begin{bmatrix} -3 & 0.5 \end{bmatrix}^\top, \; x_{6_0} = \begin{bmatrix} 2 & -2 \end{bmatrix}^\top.$$

The initial conditions for each agent are

$$q_1(0) = \begin{bmatrix} \pi & \pi/3 \end{bmatrix}^\top, \; q_2(0) = \begin{bmatrix} 2\pi/3 & \pi/3 \end{bmatrix}^\top, \; q_3(0) = \begin{bmatrix} -\pi & \pi/3 \end{bmatrix}^\top,$$
$$q_4(0) = \begin{bmatrix} -\pi/2 & 0 \end{bmatrix}^\top, \; q_5(0) = \begin{bmatrix} \pi & \pi/3 \end{bmatrix}^\top, \; q_6(0) = \begin{bmatrix} 0 & \pi/3 \end{bmatrix}^\top,$$
$$\dot{q}_1(0) = \dot{q}_2(0) = \dot{q}_3(0) = \dot{q}_4(0) = \dot{q}_5(0) = \dot{q}_6(0) = \begin{bmatrix} 0 & 0 \end{bmatrix}^\top,$$

with $q = \begin{bmatrix} q_1 & q_2 \end{bmatrix}^\top$ and $\dot{q} = \begin{bmatrix} \dot{q}_1 & \dot{q}_2 \end{bmatrix}^\top$. The relative displacements of the end-effectors are

$$b_1 = \begin{bmatrix} 0 & 0.4 \end{bmatrix}^\top, \; b_2 = \begin{bmatrix} -0.4 & 0 \end{bmatrix}^\top, \; b_3 = \begin{bmatrix} 0.4 & 0 \end{bmatrix}^\top,$$
$$b_4 = \begin{bmatrix} 0 & -0.4 \end{bmatrix}^\top, \; b_5 = \begin{bmatrix} -0.4 & 0 \end{bmatrix}^\top, \; b_6 = \begin{bmatrix} 0.4 & 0 \end{bmatrix}^\top,$$

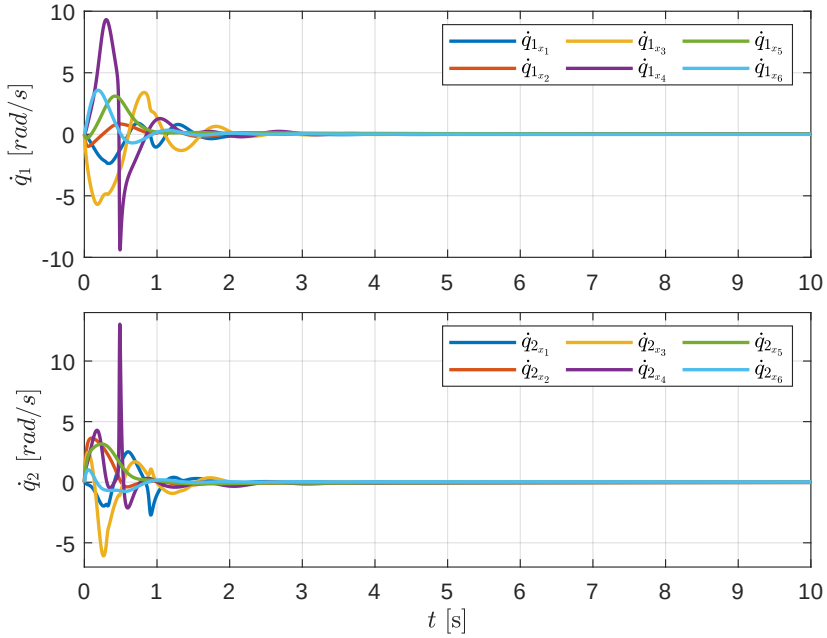

Figure 5.3: Bipartite formation of system (5.1) with control input (5.11) on joint velocities.

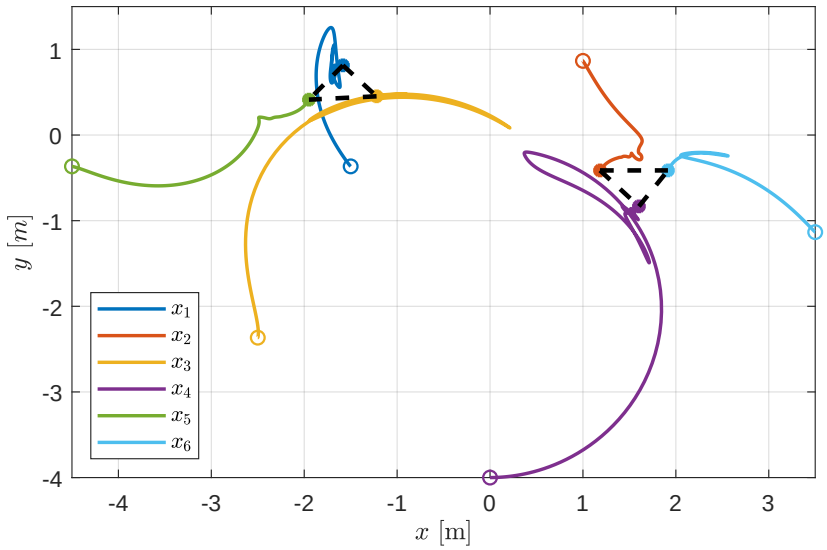

Figure 5.4: Evolution of the manipulators' end-effector from the initial positions (o) to the final positions (*). Each group of end-effectors forms a triangle around the symmetric equilibrium points.

with $b = \begin{bmatrix} b_x & b_y \end{bmatrix}^\top$. The constraint sets are set to $\Delta_k = 0.2$m for all edges, and the connectivity constraints for the two cooperative edges e_2 and e_5 are given as $R_2 = 2.5$m and $R_5 = 3.5$m.

The joint positions and velocities are depicted in Figures 5.2 and 5.3, respectively, and all velocities converge to zero. The paths of each end-effector up to bipartite formation are depicted in Figure 5.4, and their final configuration is depicted in Figure 5.6[1]. Moreover, it is clear from Figure 5.5 that the minimum safety distance between

[1]A video of the simulation is available at: http://tinyurl.com/simulationRM.

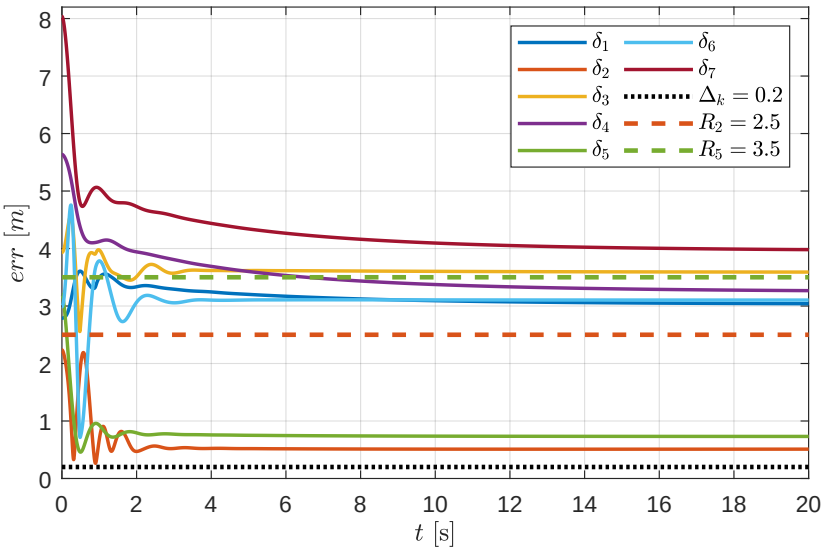

Figure 5.5: Trajectories of the norm of inter-agent distances with control input (5.11). The black dashed line is the minimum distance constraint for a pair of end-effectors corresponding to each edge, and the red and green dashed lines are the maximum distance constraints for the edges e_2 and e_5, respectively.

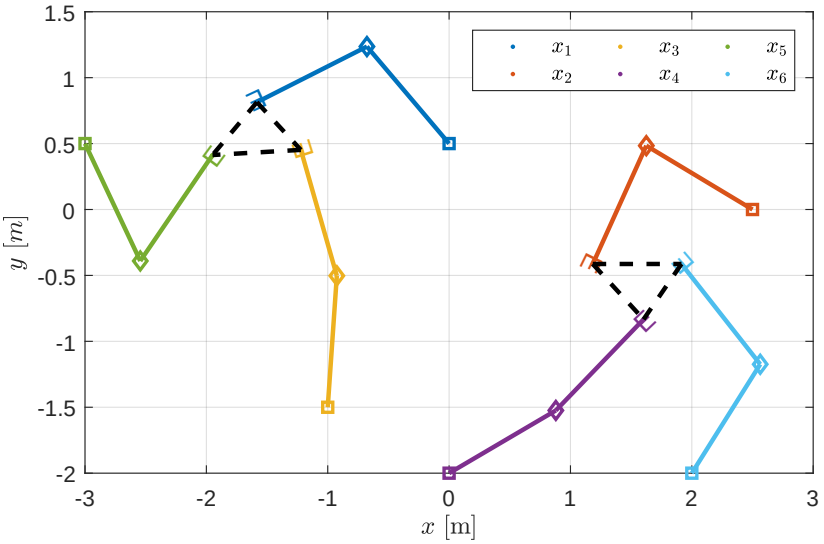

Figure 5.6: Final positions of the manipulators and their end-effector.

each pair of end-effectors is respected. In addition, for the two cooperative edges, e_2 and e_5, the maximum distance between the end-effectors is also respected. Thus, collision avoidance and connectivity maintenance among the manipulators' end-effectors are both guaranteed.

In a second run of simulations, we consider the system (5.1), where $d_i \neq 0$ and with the robust bipartite formation control law in (5.39). We take the same initial conditions as before. Let $k_{1_i} = 200$ and $k_{2_i} = 300$ for all $i \leq N$. The matrices in (5.33)

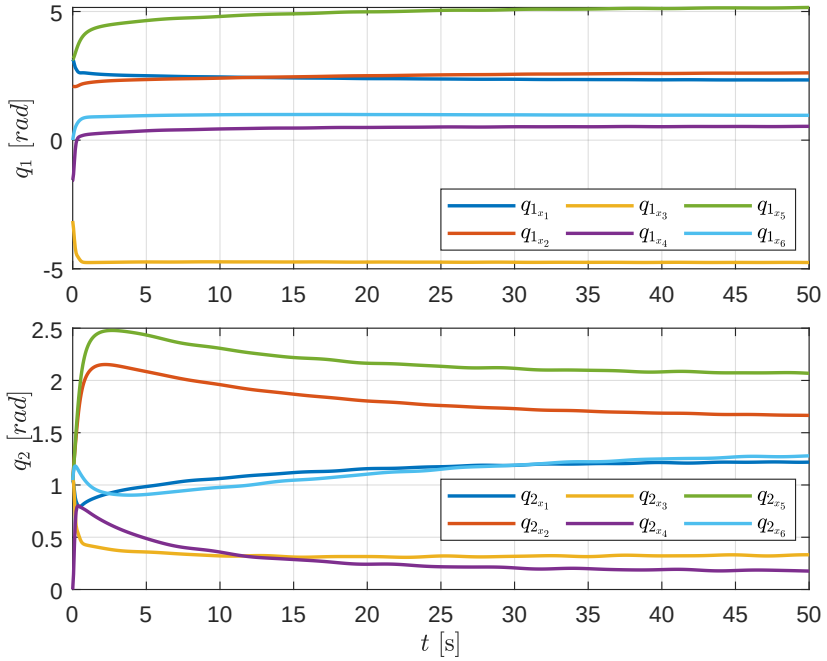

Figure 5.7: Bipartite formation of system (5.1) with control input (5.39) on joint trajectories.

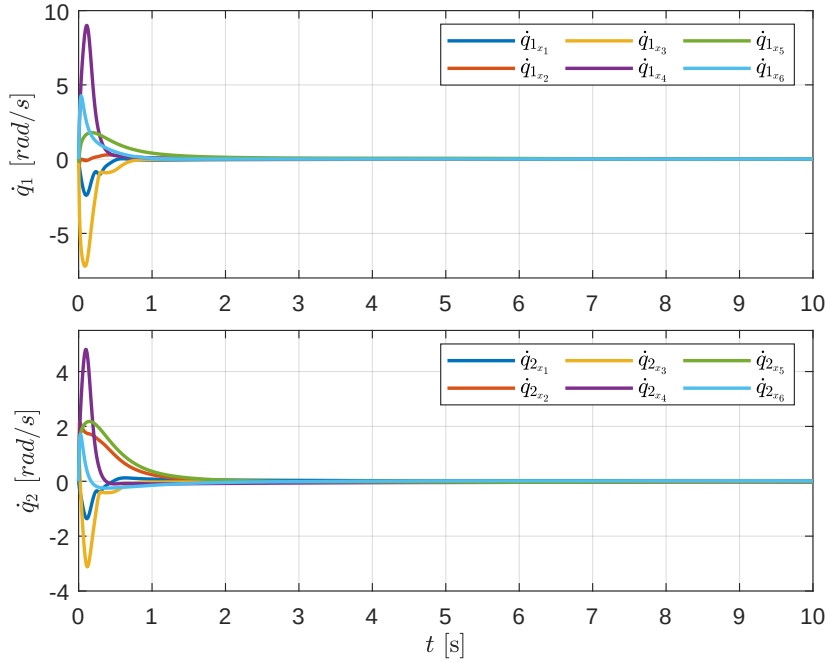

Figure 5.8: Bipartite formation of system (5.1) with control input (5.39) on joint velocities.

of the exosystem generating the disturbance are given as

$$S_{M_i} = S_{E_i} = \begin{bmatrix} 0 & 1 \\ -1 & 0 \end{bmatrix}, \; C_{M_i} = C_{E_i} = \begin{bmatrix} 1 & 0 \\ 0 & 1 \end{bmatrix}.$$

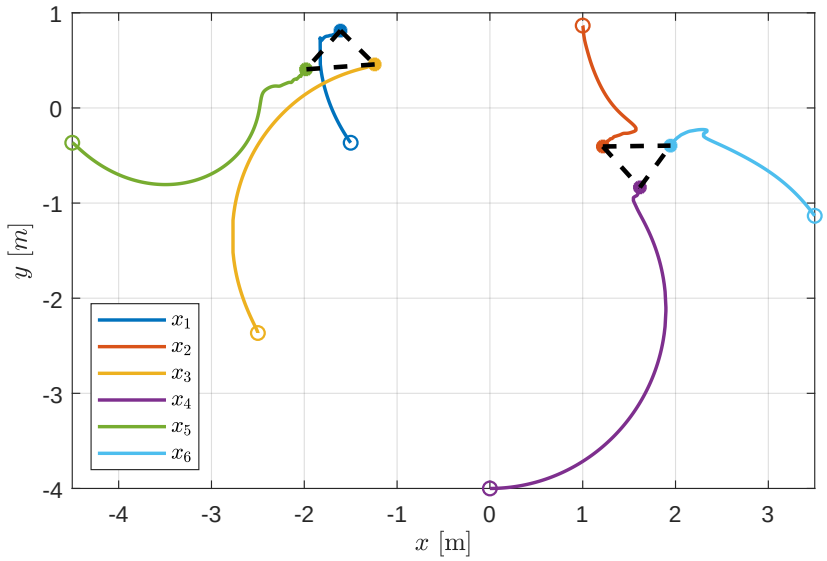

Figure 5.9: Evolution of the manipulators' end-effector from the initial positions (o) to the final positions (*). Each group of end-effectors forms a triangle around the symmetric consensus points.

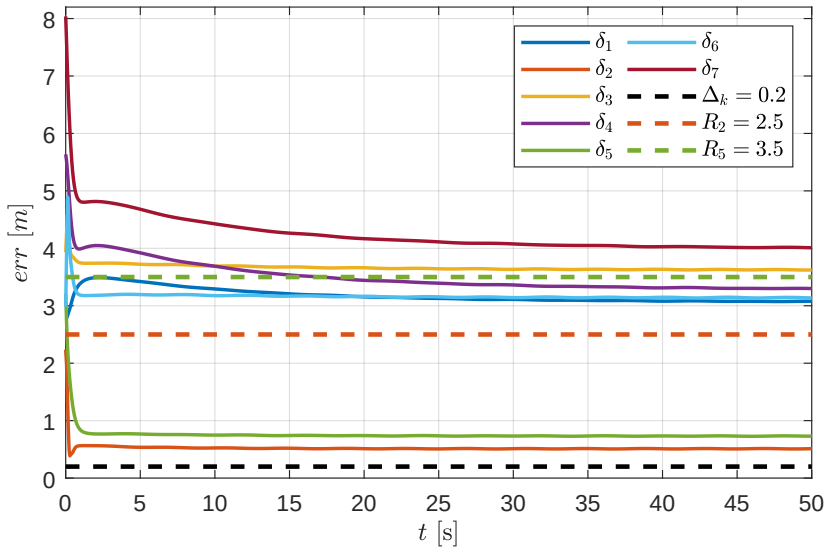

Figure 5.10: Trajectories of the norm of inter-agent distances with control input (5.39). The black dashed line is the minimum distance constraint, and the red dashed line is the maximum distance constraint for end-effectors.

The matrices of the internal model in (5.36) are given as

$$A_{M_i} = \begin{bmatrix} 0 & 1 \\ -1 & 0 \end{bmatrix}, \; A_{E_i} = \begin{bmatrix} 0 & \pi/2 \\ -\pi/2 & 0 \end{bmatrix},$$
$$B_{M_i} = \begin{bmatrix} 1 & 0 \\ 0 & 1 \end{bmatrix}, \; B_{E_i} = \begin{bmatrix} 1 & 0 \\ 0 & 1 \end{bmatrix}.$$

The joint positions and velocities are depicted in Figures 5.7 and 5.8, respectively, and all velocities converge to zero. The paths of each end-effector up to bipartite formation are depicted in Figure 5.9. Their final configuration is the same as in Figure

5.6. Moreover, it is clear from Figure 5.10 that collision avoidance and connectivity maintenance are guaranteed among the manipulators' end-effectors.

5.3 FLYING SPACECRAFT FORMATION WITH INTER-AGENT CONSTRAINTS

We wrap up this chapter with a brief presentation of the constrained bipartite formation-control problem of a network of flying spacecraft, using our previous results. Loosely speaking, the problem that we address consists in having all the satellites achieve formation under the assumption that some of them may be competitive. This study is motivated, as mentioned before, by aerospace applications. A network of spacecraft works in cooperation with the objective of providing unprecedented image resolution for astronomy purposes or to recognize planets or objects in space [16]. On the other hand, during their mission, they should avoid collisions with other satellites, or debris in space. Moreover, the network of spacecraft must also avoid collisions with each other and stay within a certain distance to stay within their sensors' range and be able to communicate.

5.3.1 Problem statement and translational equations of motion

We model a network of satellites by the relative translational dynamics developed in [1]. To that end, we first consider N satellites with n-degrees-of-freedom in low earth orbit in the Earth-Centered Inertial (ECI) frame F^l. We assume that the attitude dynamics of the satellites have a weak influence on the translational dynamics, so it is ignored. First, following [1], we write the dynamics of the translational motion in the (ECI) frame to address a satellite formation orbiting the Earth. The ECI frame is defined to have its origin at the center of the Earth, its x-axis pointing towards the vernal equinox, z-axis pointing towards the celestial north pole [1]—see Figure 5.11. This frame does not rotate with the Earth but moves as the Earth orbits around the Sun.

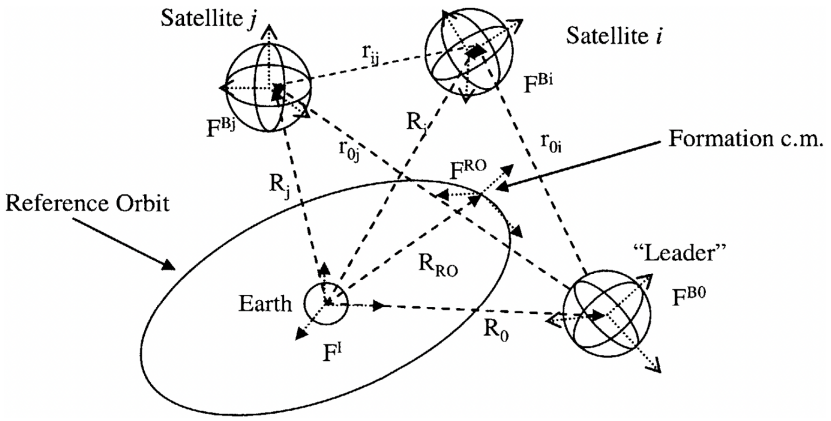

Figure 5.11: Geometry of different reference frames [1].

For each satellite, let $q_i \in \mathbb{R}^3$ be the position of the ith satellite in the ECI frame, where $q_i = [q_{x_i}\ q_{y_i}\ q_{z_i}]^\top$ and $b_i \in \mathbb{R}^3$ denote the relative displacement with respect to

the rendezvous point and define

$$\bar{q}_i = q_i - b_i. \tag{5.48}$$

Then, the kinetic energy of the satellite $T_i(\dot{q}_i)$, and the sum of the potential energy of the satellite $V_i(q_i)$ are calculated as

$$T_i(\dot{q}_i) = \frac{1}{2} m_i \dot{q}_i^\top \dot{q}_i, \quad V_i(q_i) = V_i^g(q_i) + V_i^m(q_i), \tag{5.49}$$

where $\dot{q}_i$ is the velocity of satellite i. V_i^g is the potential energy of the satellite i in Earth's gravitational field and is given by

$$V_i^g(q_i, \phi) = -\frac{\mu_e m_i}{R_i} \left[1 - \sum_{k=2}^{\infty} J_k \left(\frac{R_e}{R_i} \right)^2 P_k \cos(\phi) \right],$$

where ϕ is the angle between Earth's North Pole direction and the direction of q_i, J_k is the kth zonal harmonic of Earth (J_2, J_3, J_3), and P_k Legendre polynomials. Note that the J_2 term is dominant with respect to other J_k terms, so

$$V_i^g(q_i) = -\frac{\mu_e m_i}{R_i} \left[1 - J_2 \left(\frac{R_e}{R_i} \right)^2 \left(3 \left(\frac{q_{z_i}}{R_i} \right)^2 - 1 \right) \right], \tag{5.50}$$

where we used $\cos(\phi) = \frac{q_{z_i}}{R_i}$ in the ECI reference frame. V_i^m is the total magnetic potential energy of satellite i due to the magnetic field of other satellites and Earth's magnetic field and is given by

$$V_i^m(q_i, q_j) = -\mu_i \left[\sum_{j=1 \ j \neq i}^{N} B_{ij}(q_i - q_j) + B_e(q_i) \right], \tag{5.51}$$

where μ_i is the dipole strength of the ith satellite, B_{ij} is the magnetic field strength at the position of the ith satellite due to satellite j, and B_e is the Earth's magnetic field vector at the position of the ith satellite.

Then, using the Lagrangian equations [63]

$$\frac{d}{dt} \frac{\partial L_i}{\partial \dot{q}_i}(q_i, \dot{q}_i) - \frac{\partial L_i}{\partial q_i}(q_i, \dot{q}_i) = \bar{\tau}_i, \tag{5.52}$$

where

$$L_i(q_i, \dot{q}_i) = \sum_{i=1}^{N} T_i(\dot{q}_i) - \sum_{i=1}^{N} \left(V_i^g(q_i) + V_i^m(q_i) \right),$$

the dynamics of the satellite i in the ECI reference frame is given by

$$m_i \ddot{q}_{x_i} - \frac{\partial V_i}{\partial q_{x_i}} = \bar{\tau}_{x_i} \tag{5.53a}$$

$$m_i \ddot{q}_{y_i} - \frac{\partial V_i}{\partial q_{y_i}} = \bar{\tau}_{y_i} \tag{5.53b}$$

$$m_i \ddot{q}_{z_i} - \frac{\partial V_i}{\partial q_{z_i}} = \bar{\tau}_{z_i}, \tag{5.53c}$$

where m_i is the mass of the satellite i and is constant, and $\bar{\tau}_i = [\bar{\tau}_{x_i}\ \bar{\tau}_{y_i}\ \bar{\tau}_{z_i}]^\top$ is the vector containing the sum of the external disturbance forces acting on satellite i. Using (5.50), the gradient of the gravitational potential energy gives

$$\frac{\partial V_i^g}{\partial q_i} = -\frac{\mu_e m_i}{R_i^3}\begin{bmatrix} q_{x_i} \\ q_{y_i} \\ q_{z_i} \end{bmatrix} + \frac{3\mu_e R_e^2 J_2 m_i}{2R_i^7}\begin{bmatrix} q_{x_i}(5q_{z_i}^2 - R_i^2) \\ q_{y_i}(5q_{z_i}^2 - R_i^2) \\ q_{z_i}(5q_{z_i}^2 - 3R_i^2) \end{bmatrix}, \tag{5.54}$$

where R_e is the equatorial radius of Earth, R_i is the distance between the Earth's center and the ith satellite, defined as

$$R_i = \sqrt{x_i^2 + (y_i + R_0)^2 + z_i^2},$$

and R_0 is the radius of the formation's center of mass orbit. Using (5.51), the gradient of the magnetic potential energy gives

$$\frac{\partial V_i^m}{\partial q_i} = \tilde{\tau}_i(q_i, \mu_i). \tag{5.55}$$

Then, replacing (5.54) and (5.55) in (5.53) and ignoring the external disturbances $\bar{\tau}_i$, we obtain

$$m_i\ddot{q}_{x_i} + \frac{\mu_e m_i}{R_i^3}q_{x_i} - \frac{3\mu_e R_e^2 J_2 m_i}{2R_i^7}(5q_{z_i}^2 - R_i^2)q_{x_i} = \tilde{\tau}_{x_i} \tag{5.56a}$$

$$m_i\ddot{q}_{y_i} + \frac{\mu_e m_i}{R_i^3}q_{y_i} - \frac{3\mu_e R_e^2 J_2 m_i}{2R_i^7}(5q_{z_i}^2 - R_i^2)q_{y_i} = \tilde{\tau}_{y_i} \tag{5.56b}$$

$$m_i\ddot{q}_{z_i} + \frac{\mu_e m_i}{R_i^3}q_{z_i} - \frac{3\mu_e R_e^2 J_2 m_i}{2R_i^7}(5q_{z_i}^2 - 3R_i^2)q_{z_i} = \tilde{\tau}_{z_i}, \tag{5.56c}$$

where $\tilde{\tau}_i = [\tilde{\tau}_{x_i}\ \tilde{\tau}_{y_i}\ \tilde{\tau}_{z_i}]^\top$ are the control forces.

Now, using (5.53), we develop the relative translational dynamics in the orbital frame F^{RO}. F^{RO} is defined with its origin attached to the center of mass of the formation, where its y-axis is defined by the vector $\vec{R}_{RO}$, which represents the position of the formation center of mass in the ECI frame [1]—see Figure 5.11. Then, the translational dynamics of the ith satellite in the ECI frame is given by

$$m_i\ddot{q}_i + \frac{\mu_e m_i q_i}{R_i^3} - \frac{3\mu_e R_e^2 J_2 m_i}{2R_i^7}(5q_{z_i}^2 - pR_i^2)q_i = \tilde{\tau}_i, \tag{5.57}$$

where $q_i = [q_{x_i}\ q_{y_i}\ q_{z_i}]^\top$ is the position of the satellite i, $\tilde{\tau}_i = [\tilde{\tau}_{x_i}\ \tilde{\tau}_{y_i}\ \tilde{\tau}_{z_i}]^\top$ is the control force and $p = [1\ 1\ 3]^\top$. Similar to (5.57), the translational dynamics of the kth satellite, is given by

$$m_k\ddot{q}_k + \frac{\mu_e m_k q_k}{R_k^3} - \frac{3\mu_e R_e^2 J_2 m_k}{2R_k^7}(5q_{z_k}^2 - pR_k^2)q_k = \tilde{\tau}_k, \tag{5.58}$$

where $q_k = [q_{x_k}\ q_{y_k}\ q_{z_k}]^\top$ is the position of the satellite k, R_k is the distance between the Earth's center and the kth satellite and $\tilde{\tau}_k = [\tilde{\tau}_{x_k}\ \tilde{\tau}_{y_k}\ \tilde{\tau}_{z_k}]^\top$ is the control force.

Then, subtracting (5.57) from (5.58), we obtain

$$\ddot{q}_i - \ddot{q}_k + \frac{\mu_e q_i}{R_i^3} - \frac{\mu_e q_k}{R_k^3} + \frac{3\mu_e R_e^2 J_2 m_i}{2R_i^7}(pR_i^2 - 5q_{z_i}^2)q_i \\ - \frac{3\mu_e R_e^2 J_2 m_k}{2R_k^7}(pR_k^2 - 5q_{z_k}^2)q_k = \frac{\tau_i}{m_i} - \frac{\tau_k}{m_k},$$

or equivalently, defining $q_{ik} = q_i - q_k$ as the position of satellite i with respect to satellite k and r_{ik} is the distance of satellite i with respect to satellite k, we have

$$\ddot{q}_{ik} + \frac{\mu_e(q_k + q_{ik})}{(R_k + r_{ik})^3} - \frac{\mu_e q_k}{R_k^3} - \frac{3\mu_e R_e^2 J_2 m_k}{2R_k^7}\left(pR_k^2 - 5q_{z_k}^2\right) q_k \\ + \frac{3\mu_e R_e^2 J_2 m_i}{2(R_k + r_{ik})^7}\left(p(R_k + r_{ik})^2 - 5(q_{z_k} + q_{z_{ik}})^2\right)(q_k + q_{ik}) = \frac{\tau_i}{m_i} - \frac{\tau_k}{m_k}.$$

Following the works of [1, 16], we assume a circular reference orbit for the formation center of mass, and its angular velocity with respect to the ECI frame is

$$\omega_0 = \sqrt{\frac{\mu_e}{R_0^3}}, \tag{5.59}$$

where μ_e is the gravitational constant of the Earth. Let the relative position q_{ik} in the ECI frame be expressed by $q_{ik,ECI}$. Then, using the transport theorem [37], the velocity and the acceleration in the orbital frame F^{RO} can be expressed as

$$\dot{q}_{ik,ECI} = \dot{q}_{ik,F^{RO}} + \omega_0 \times q_{ik,F^{RO}}, \\ \ddot{q}_{ik,ECI} = \ddot{q}_{ik,F^{RO}} + 2\omega_0 \times \dot{q}_{ik,F^{RO}} + \omega_0 \times \omega_0 \times q_{ik,F^{RO}}.$$

Then, defining

$$q_{ik,F^{RO}} = [x_i \ y_i \ z_i]^\top,$$

the relative dynamics of the ith satellite with respect to kth satellite, attached to a body frame with its origin at the center of mass of formation, in the orbital frame F^{RO}, is given as

$$\ddot{x}_i - 2\omega_0\dot{y}_i - \omega_0^2 x_i + \frac{\mu_e x_i}{R_i^3} + \frac{3\mu_e R_e^2 J_2}{2R_i^7}\left(R_i^2 - 5z_i^2\right)x_i = \frac{\tau_{x_i}}{m_i} \tag{5.60a}$$

$$\ddot{y}_i + 2\omega_0\dot{x}_i - \omega_0^2 y_i + \frac{\mu_e(R_0 + y_i)}{R_i^3} + \frac{3\mu_e R_e^2 J_2}{2R_i^7}\left(R_i^2 - 5z_i^2\right)(R_0 + y_i) = \frac{\tau_{y_i}}{m_i} \tag{5.60b}$$

$$\ddot{z}_i + \frac{\mu_e z_i}{R_i^3} + \frac{3\mu_e R_e^2 J_2}{2R_i^7}\left(3R_i^2 - 5z_i^2\right)z_i = \frac{\tau_{z_i}}{m_i}. \tag{5.60c}$$

Then, the relative translational dynamics of satellites in (5.60) can be written in a Lagrangian form as

$$M_i\ddot{q}_{ik,F^{RO}} + C_i\dot{q}_{ik,F^{RO}} + \frac{\partial}{\partial q_{ik,F^{RO}}}U_i(q_{ik,F^{RO}}) = \tau_i + d_{J_2,i}, \tag{5.61}$$

where

$$M_i = \begin{bmatrix} m_i & 0 & 0 \\ 0 & m_i & 0 \\ 0 & 0 & m_i \end{bmatrix}, \quad C_i = \begin{bmatrix} 0 & -2m_i\omega_0 & 0 \\ 2m_i\omega_0 & 0 & 0 \\ 0 & 0 & 0 \end{bmatrix}, \quad q_i = \begin{bmatrix} x_i \\ y_i \\ z_i \end{bmatrix}, \quad \tau_i = \begin{bmatrix} \tau_x \\ \tau_y \\ \tau_z \end{bmatrix},$$

$$\frac{\partial}{\partial q_{ik,F^{RO}}} U_i(q_{ik,F^{RO}}) = \begin{bmatrix} -m\left(\omega_0^2 - \frac{\mu_e}{R_i^3}\right) x_i \\ m\left(\frac{\mu_e R_0}{R_i^3} - \frac{\mu_e}{R_0^2}\right) - m\left(\omega_0^2 - \frac{\mu_e}{R_i^3}\right) y_i \\ \frac{\mu_e}{R_i^3} z_i \end{bmatrix},$$

$$d_{J_2,i} = -\frac{3\mu_e R_e^2 J_2}{2R_i^7} \begin{bmatrix} (R_i^2 - 5z_i^2)\, x_i \\ (R_i^2 - 5z_i^2)\,(R_0 + y_i) \\ (3R_i^2 - 5z_i^2)\, z_i \end{bmatrix}. \tag{5.62}$$

Here, as opposed to the case of robot manipulators, the matrices M_i and C_i are constant, but $\dot{M}_i - 2C_i$ is still skew-symmetric for all $i \leq N$. Moreover, if the difference between R_i and R_0 is reasonably small, then replacing (5.59) in $\frac{\partial}{\partial q_{ik,F^{RO}}} U_i(q_{ik,F^{RO}})$, we obtain

$$\frac{\partial}{\partial q_{ik,F^{RO}}} U_i(q_{ik,F^{RO}}) = \begin{bmatrix} -m\left(\omega_0^2 - \frac{\mu_e}{R_i^3}\right) x_i \\ m\left(\frac{\mu_e R_0}{R_i^3} - \frac{\mu_e}{R_0^2}\right) - m\left(\omega_0^2 - \frac{\mu_e}{R_i^3}\right) y_i \\ \frac{\mu_e}{R_i^3} z_i \end{bmatrix} \approx \begin{bmatrix} 0 \\ m\left(\frac{\mu_e R_0}{R_i^3} - \frac{\mu_e}{R_0^2}\right) \\ \omega_0^2 \end{bmatrix}, \tag{5.63}$$

which is constant.

Now that the network of satellites is expressed in Lagrangian form, we can use our result from Section 5.2 to address the bipartite formation-control problem of satellites. For simplicity, we express the relative distance $q_{ik,F^{RO}}$ as q_i. We consider the problem of making N satellites, modeled by (5.61) and interconnected over an undirected and structurally balanced graph, achieve bipartite formation consensus, that is, converge around two symmetric rendezvous points, *i.e.,*

$$\lim_{t\to\infty} \bar{e}_{q_k}(t) = 0, \quad \lim_{t\to\infty} \dot{q}_i(t) = 0, \quad \forall k \leq M,\ i \leq N \tag{5.64}$$

where

$$\bar{e}_{q_k} := \bar{q}_i - \operatorname{sgn}(a_{ij})\bar{q}_j, \tag{5.65}$$

and $\bar{q}_i$ is defined in (5.48), under the connectivity-maintenance and collision-avoidance constraints, as defined in (5.7).

Remark 19 *At this point, we were unable to establish that the disturbance $d_{J_2,i}$ due to the J_2 term could be generated by an internal model. However, since the effect of this perturbation is crucial for applications, it was necessary to address its influence. Instead of making some unjustified ad-hoc assumptions on this disturbance, we chose to include it in our simulations and evaluate the robustness of our closed-loop system in its presence.* •

5.3.2 Formation control of flying spacecraft under constraints

The control design follows the lines of Section 5.2.2 as the network of satellites is also modeled by the Euler-Lagrange equations. The only distinction for the case of satellites is the absence of the Jacobian matrix, as we control the position $\bar{q}$ of the satellites, rather than with robot manipulators where a Jacobian matrix maps the joint-space to the end-effector's task space. Then, we introduce the BLF-gradient-based bipartite formation-consensus control law, which is very similar to the control law in (5.11), as

$$\tau_i := -k_{1_i} \sum_{k=1}^{M} [E_s]_{ik} \nabla_{\bar{e}_{q_k}} \widetilde{W}_k - k_{1_i} \sum_{k=1}^{M} [\mathbb{E}]_{ik} \nabla_{\alpha_k} \widetilde{W}_k - k_{2_i} \dot{q}_i + \frac{\partial}{\partial q_i} U_i(q_i), \tag{5.66}$$

where $\widetilde{W}$ is defined in (5.9), $\mathbb{E} := E - E_s$, and

$$\alpha_k := \delta_k - \bar{e}_{q_k}. \tag{5.67}$$

Next, we analyze the stability of the bipartite formation manifold in (5.65) for the closed-loop system (5.61) interconnected by the control law (5.66). To that end, using the definition of the incidence matrix, we represent the synchronization errors in (5.65) and α_k defined in (5.67), in vector form

$$\bar{e}_q = [E_s^\top \otimes I_n]\bar{q}, \tag{5.68a}$$

$$\alpha = [E^\top \otimes I_n]q - [E_s^\top \otimes I_n]\bar{q}. \tag{5.68b}$$

Then, the closed-loop system (5.61)–(5.66) in the compact form

$$\ddot{q} = -M^{-1}\Big[C\dot{q} + K_1[E_s \otimes I_n]\nabla_{\bar{e}_q}\widetilde{W}(\alpha, \bar{e}_q) + K_1[\mathbb{E} \otimes I_n]\nabla_\alpha \widetilde{W}(\alpha, \bar{e}_q) + [K_2 \otimes I_n]\dot{q}\Big]. \tag{5.69}$$

For this system, we have the following statement, whose proof is omitted because it follows the proof of Proposition 15.

Proposition 17 *Consider N satellites modeled by (5.61), where $d_i = 0$ for all $i \leq N$, and satisfying the Assumptions 7 and 8, in closed-loop with the distributed control law (5.66), with k_{1_i}, $k_{2_i} > 0$, for all $i \leq N$ and $\widetilde{W}$ as defined in (5.9). Then, the set $\{(\bar{e}_q, \dot{q}) = (0, 0)\}$ is asymptotically stable for almost all initial conditions such that $(\bar{e}_q(0), \dot{q}(0)) \in \mathcal{I} \times \mathbb{R}^{3N}$ and $|\alpha_k(0)| > \Delta_k$ for any $k \leq M$.*

5.3.3 Numerical example

We consider an undirected signed network of 4 satellites interconnected by 4 edges over a structurally balanced undirected signed network, modeled by a graph as the one depicted in Figure 5.12. We define the orientation of the edges as follows:

$$e_1 = \nu_1 - \nu_2, \quad e_2 = \nu_1 + \nu_3, \quad e_3 = \nu_2 + \nu_4, \quad e_4 = \nu_3 - \nu_4.$$

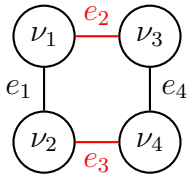

Figure 5.12: A structurally balanced undirected signed network of 4 satellites. The black lines represent cooperative edges, and the red lines represent the competitive ones.

The incidence matrix corresponding to the graph is

$$E_s = \begin{bmatrix} 1 & 1 & 0 & 0 \\ -1 & 0 & 1 & 0 \\ 0 & 1 & 0 & 1 \\ 0 & 0 & 1 & -1 \end{bmatrix}.$$

The set of nodes may be split into two disjoint subsets, such as $\mathcal{V}_1 = \{\nu_1,\ \nu_2\}$, $\mathcal{V}_2 = \{\nu_3,\ \nu_4\}$ so the network is structurally balanced. From (4.32), edges $e_i,\ i \leq 3$ correspond to $\mathcal{G}_t$ and the remaining edge e_4 corresponds to $\mathcal{G}_c$.

5.3.3.1 In the absence of J_2 effects

Each satellite is modeled by the Euler-Lagrange equations in (5.61), where $d_{J_2,i} = 0$ for all $i \leq N$. The internia and Coriolis matrices are given in (5.62), where $m_i = 2000$kg for all $i \leq N$ and $\mu_e = 398600 \times 10^9 m^3/s^2$. Moreover, the radius of the Earth is $R_e = 6000 \times 10^3$m, and the radius of the orbit is $R_0 = R_e + 2000 \times 10^3$m [1].

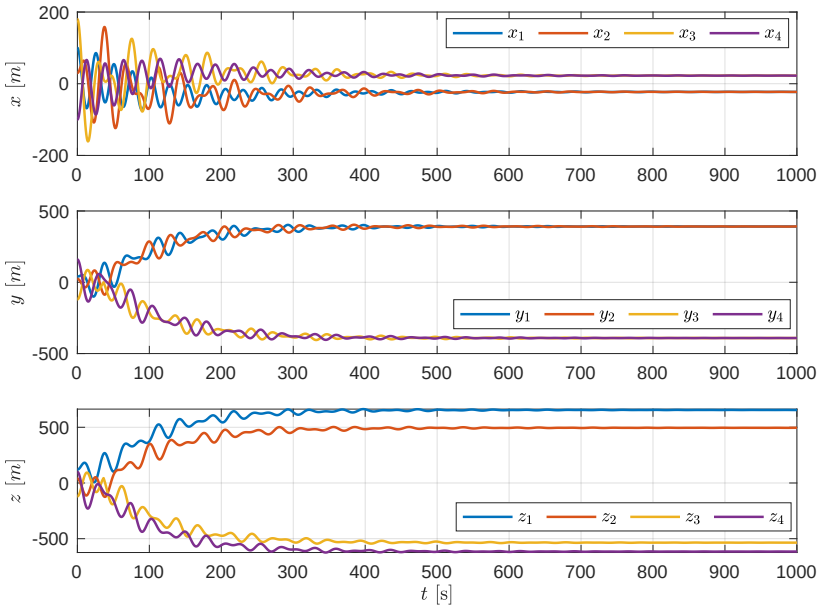

Figure 5.13: Bipartite formation of system (5.61), where $d_{J_2,i} = 0$, interconnected with the control input (5.66) on position, in the orbital frame F^{RO}.

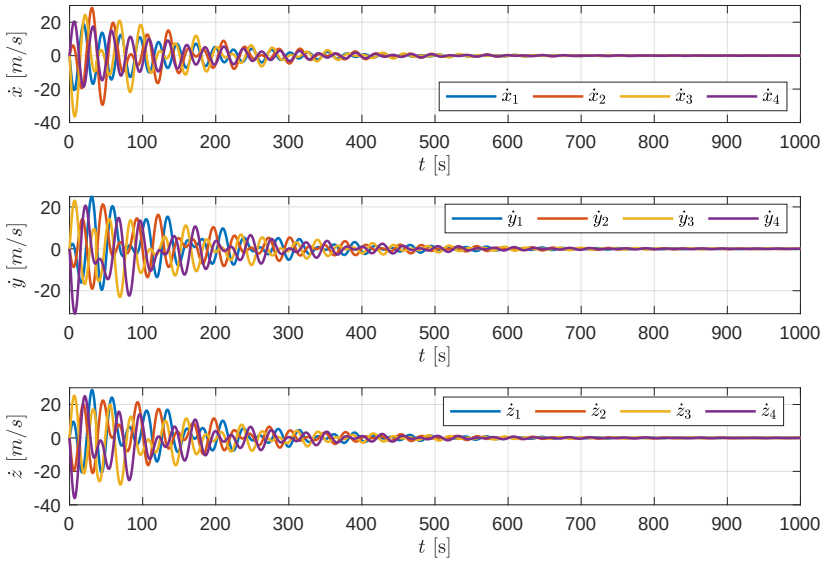

Figure 5.14: Bipartite formation of system(5.61), where $d_{J_2,i} = 0$, interconnected with the control input (5.66) on velocity, in the orbital frame F^{RO}. The velocities of all satellites converge to zero.

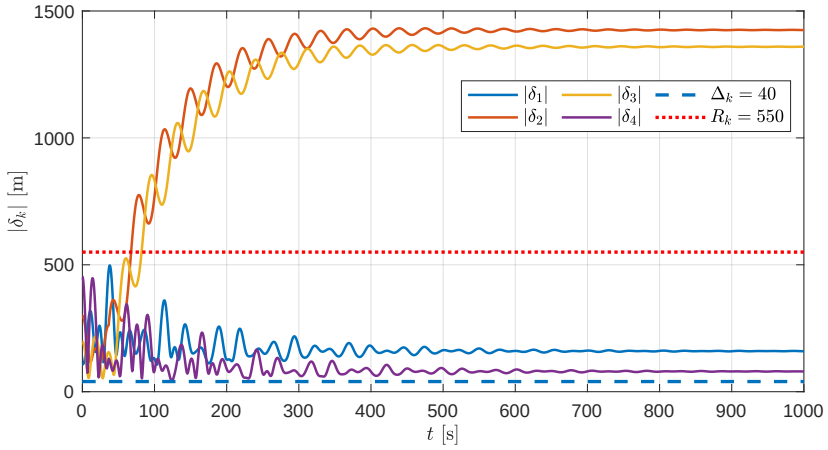

Figure 5.15: Trajectories of the norm of the inter-agent distances with control input (5.66). The dashed lines are the minimum, and the dotted line is the maximum distance constraints for satellites. All inter-agent safety and connectivity constraints are respected.

The network of satellites is interconnected via the control law (5.66), where $k_1 = 30$ and $k_2 = 25$, and subject to inter-agent collision avoidance and connectivity maintenance restrictions. The respective agents' initial states are

$$x(0) = \begin{bmatrix} 100 & 30 & 180 & -100 \end{bmatrix}^\top, \; y(0) = \begin{bmatrix} 40 & 24 & -120 & 160 \end{bmatrix}^\top,$$
$$z(0) = \begin{bmatrix} 120 & 40 & -120 & 100 \end{bmatrix}^\top, \; v_x(0) = v_y(0) = v_y(0) = \begin{bmatrix} 0 & 0 & 0 & 0 \end{bmatrix}^\top,$$

and the relative displacements are

$$d_x = d_y = \begin{bmatrix} 0 & 0 & 0 & 0 \end{bmatrix}^\top, d_z = \begin{bmatrix} 80 & -80 & 40 & -40 \end{bmatrix}^\top.$$

The constraint sets are defined as $\Delta_k = 40$m for all $k \leq M$ and $R_k = 550$m for $k \in \mathcal{E}_m$. The paths of each agent up to bipartite formation are depicted in Figure 5.13. The

center of satellites reach the desired formation around two symmetric consensus points. The velocities of the satellites are depicted in Figure 5.14, and velocities converge to zero. Moreover, it is clear from Figure 5.15 that the inter-agent collision avoidance and connectivity maintenance constraints in (5.7) are always respected. The oscillations in the Figures are due to significant distances between satellites, their considerable masses, and the relatively weak values chosen for k_1 and k_2.

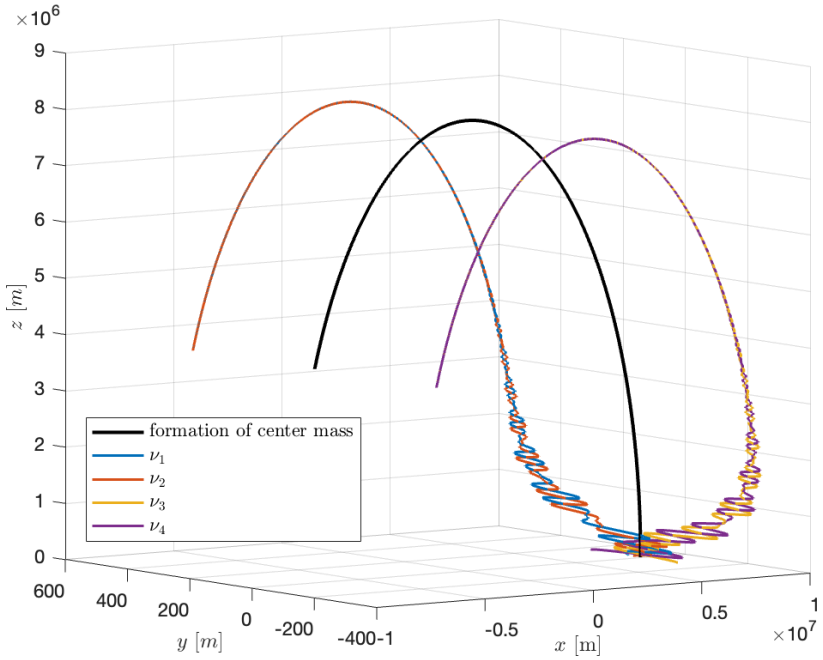

Figure 5.16: Evolution of the satellites from the initial positions to the final positions, in the ECI frame at $t = 50$ minutes. Each group of satellites gathers around two symmetric equilibrium points and advances with the orbit.

5.3.3.2 In the presence of J_2 effects

In a second run of simulations, we consider the system (5.61), where $d_{J_2,i} \neq 0$, interconnected over the control law (5.66). We take the same initial conditions as before. The constraint sets are defined as $\Delta_k = 35$m for all $k \leq M$ and $R_k = 550$m for $k \in \mathcal{E}_m$. The paths of each agent up to bipartite formation are depicted in Figure 5.17. The center of satellites reach the desired formation around two symmetric consensus points. The velocities of the satellites are depicted in Figure 5.18, and velocities converge to zero. Moreover, it is clear from Figure 5.19 that even in the presence of J_2 perturbations, the inter-agent collision avoidance and connectivity maintenance constraints in (5.7) are always respected.

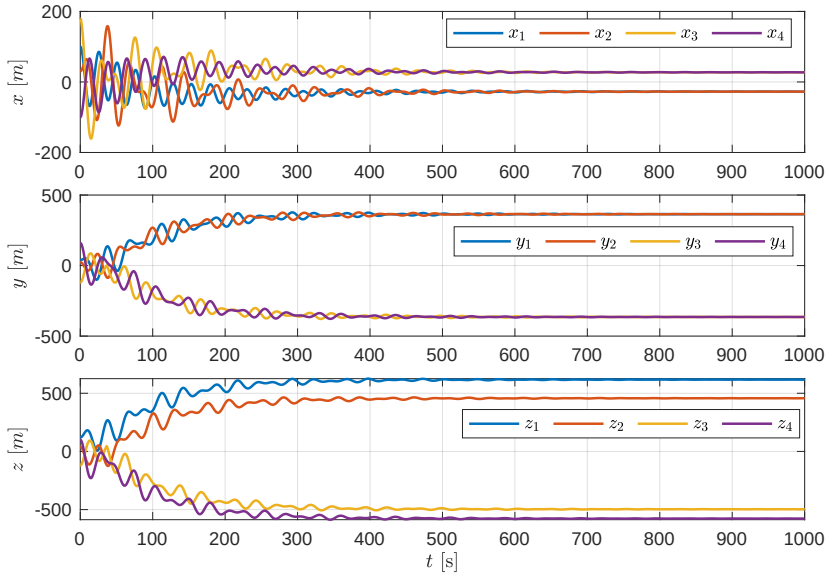

Figure 5.17: Bipartite formation of system (5.61), where $d_{J_2,i} \neq 0$, interconnected with the control input (5.66) on position, in the orbital frame F^{RO}.

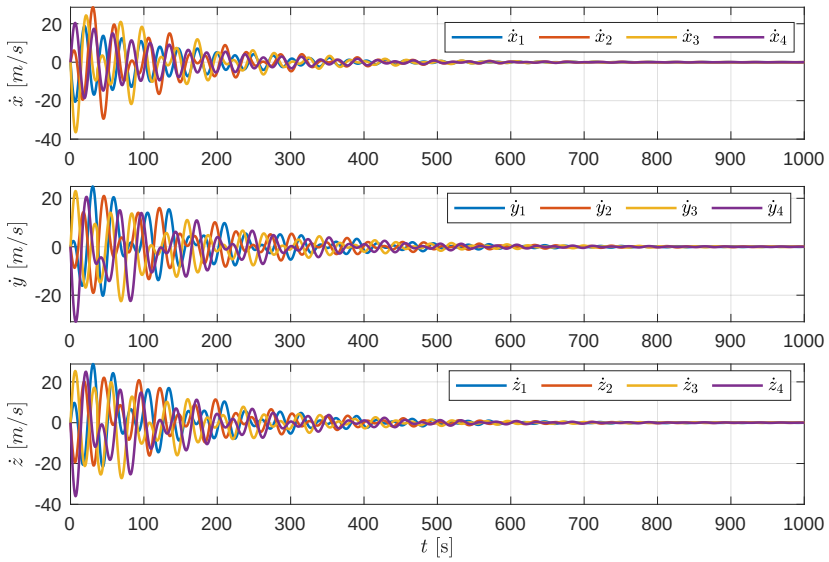

Figure 5.18: Bipartite formation of system (5.61), where $d_{J_2,i} \neq 0$, interconnected with the control input (5.66) on velocity, in the orbital frame F^{RO}. The velocities of all satellites converge to zero.

5.4 CONCLUSIONS

We addressed the problem of constrained bipartite formation of cooperative and competitive robot manipulators modeled by Euler-Lagrange equations over structurally balanced and undirected signed graphs under inter-agent end-effector constraints. First, we presented a bipartite formation control law based on the gradient of a barrier-Lyapunov function that guarantees that manipulators' end-effectors do not collide and stay within their maximum distance imposed by the task requirements. Then, in order to deal with perturbed robot manipulators, we robustified our controller with an

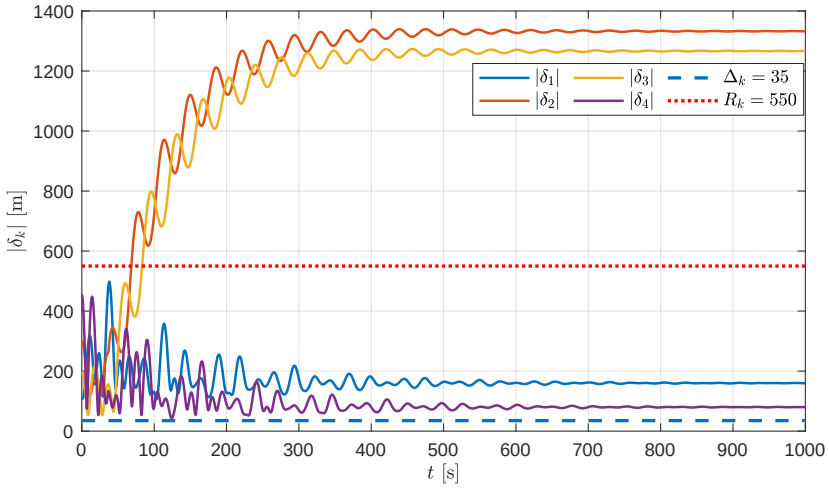

Figure 5.19: Trajectories of the norm of the inter-agent distances with control input (5.66). The dashed lines are the minimum, and the dotted line is the maximum distance constraints for satellites. All inter-agent safety and connectivity constraints are respected.

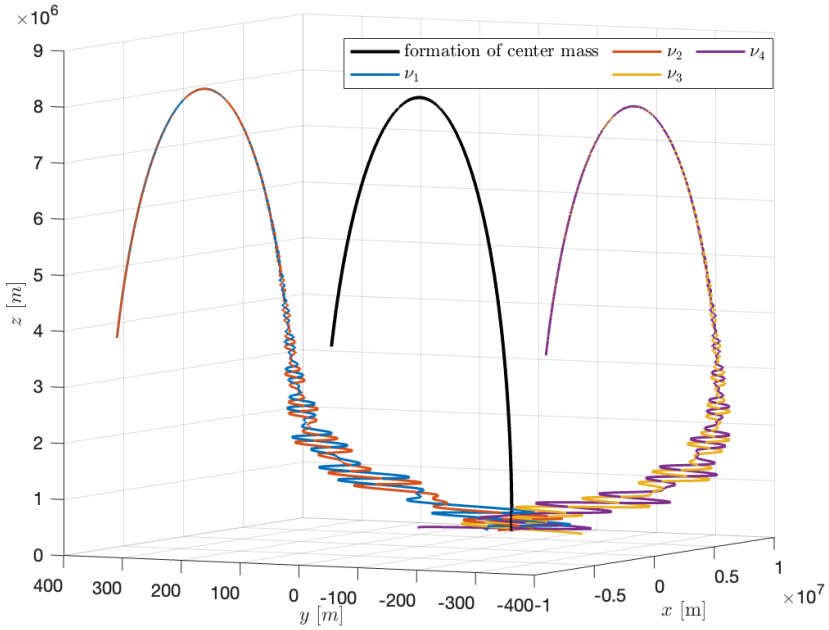

Figure 5.20: Evolution of the satellites, under J_2 effects, from the initial positions to the final positions, in the ECI frame at $t = 50$ minutes. Each group of satellites gathers around two symmetric equilibrium points and advances with the orbit.

internal model-based approach to reject disturbances. Compared to the literature, we contributed with a robust bipartite formation control law that ensures that the manipulator's end-effectors achieve the desired formation while avoiding inter-agent collisions. We established asymptotic stability of the bipartite formation manifold and robustness with respect to external perturbations.

We believe that the utility of our results goes beyond the case of collision avoidance and maximum distance maintenance for cooperative-competitive robot manipulators' end-effectors. It may also apply to other Lagrangian systems. In that regard, we considered a network of cooperative-competitive satellites. We presented BLF-gradient-

based control laws that solve the constrained bipartite formation problem for satellites subject to collision avoidance and connectivity maintenance constraints. Not only the extension is direct, but it is another contribution since, to the best of our knowledge, there are no results on the constrained bipartite formation of satellites interconnected over a signed graph. This being said the significant problem of bipartite formation in the presence of disturbance remains open.

CONCLUSIONS AND FURTHER RESEARCH

SUMMARY

In this work, we addressed multiple control problems for multi-agent systems over networks containing cooperative and competitive interactions, with the purpose of addressing relevant robotic application scenarios. We considered signed networks with multiple leaders under inter-agent constraints and subject to disturbances. To this end, we proposed multiple contributions in terms of stability analysis and control design for a variety of linear and nonlinear systems. These contributions are summarized as follows.

Networks with cooperative and antagonistic interactions. In this work, we considered the presence of both cooperative and antagonistic interactions among the agents in each problem that we addressed. Thus, our results are more general than those of the literature focusing only on all-cooperative networks. Moreover, competitive interactions are representative of multi-objectives in the multi-agent system, where agents converge to two symmetric equilibria or realize symmetric tasks. On the other hand, competitive edges are used to represent the presence of groups of enemy agents and static obstacle(s) to be avoided in the system or to define dangerous zones from which agents should stay away.

Bipartite containment tracking control over signed networks containing multiple leaders. We addressed the problem of bipartite containment tracking for first- and second-order systems over structurally balanced and unbalanced signed networks containing multiple cooperative and/or competitive leaders. With respect to the literature, we contributed with a novel stability analysis approach of the bipartite containment set. First, we contributed by giving a possible form of the right and left eigenvectors associated with the zero eigenvalues of the Laplacian matrix of a structurally balanced or unbalanced signed network. Then, we calculated the explicit limit values of the followers by extending the definition of the average system and synchronization errors to the case of multileader signed networks. We also constructed strict Lyapunov functions by extending the results on the Lyapunov characterization of the

necessary and sufficient condition of having a directed spanning tree in the network to the case of signed networks with multiple leaders. We also established exponential stability and robustness of the systems in the sense of input-to-state stability via strict Lyapunov functions. The latter cannot be ascertained if the Lyapunov functions are not strict.

Bipartite consensus with collision avoidance and connectivity maintenance. We addressed the problem of constrained bipartite formation-consensus for first- and second-order systems. We first considered first- and second-order systems over structurally balanced undirected signed graphs. Then, we studied first-order systems over directed signed networks containing a spanning tree and second-order systems over strongly connected and weight-balanced directed signed graphs. For both cases, we contributed by proposing a control law based on the gradient of a BLF, guaranteeing inter-agent collision avoidance and connectivity maintenance. We conducted the stability analysis of the systems using Lyapunov's direct method, both in terms of the node coordinates and the synchronization errors.

Control of cooperative and competitive Euler-Lagrange systems. We addressed the problem of constrained bipartite formation of cooperative-competitive Euler-Lagrange systems. We first addressed the bipartite formation robot manipulators' end-effectors with inter-agent end-effector constraints and subject to external disturbances. To deal with perturbed robot manipulators under constraints, we presented a bipartite formation control law based on the gradient of a barrier-Lyapunov function and then robustified the controller with an internal model-based approach to reject disturbances. Then, we addressed the bipartite formation of a network of satellites with inter-satellite collision avoidance and connectivity maintenance. For both problems, we established the asymptotic stability of the bipartite formation manifold. Compared to the literature, our contributions include, first, a BLF-based robust bipartite formation control law that ensures the manipulator's end-effectors achieve the desired formation while avoiding inter-agent collisions and remaining close to each other as imposed by the task requirements, and second, a BLF-based bipartite formation control law that guarantees satellite formation with collision avoidance and connectivity maintenance constraints.

FURTHER RESEARCH

The contributions of this thesis successfully addressed some of the important challenges related to the aspects presented at the beginning of the memoir. These aspects included the presence of both cooperative and antagonistic interactions, multiple leaders, control under inter-agent constraints, and dealing with disturbances. Still, there are a number of open problems to be addressed to be able to consider the general problem of guiding a swarm of robots required to advance in formation or to be contained in a safe zone in realistic and constrained environments. Some of these problems arise directly from the contributions presented in this thesis and are as follows.

General directed signed graphs. One of the original contributions of this memoir is to address the bipartite containment problem for signed networks containing multiple cooperative and/or competitive leaders, as shown in Chapter 2. On the other hand, another contribution is to address the constrained bipartite consensus problem for some classes of directed signed networks. However, we stress that the results obtained for the latter problem apply only to two classes of directed topologies. For first-order systems, we solve the problem over a structurally balanced directed graph containing a spanning tree, and for second-order systems, we address the problem over a strongly connected, weight-balanced, and structurally balanced directed graph. Nonetheless, for the general problem that is addressed in this memoir, an interesting direction of research is to study the constrained bipartite consensus problem for multi-leader signed networks, as we do in Chapter 3. A possible starting point for considering general directed signed graphs with inter-agent constraints may be to follow the approach introduced in [67] and used in Chapter 3 to express the system with constraints in terms of two interconnected dynamical systems and then construct strict Lyapunov functions to deal with general directed signed graphs.

Open multi-agent systems and collision-avoidance for all agents. In Chapter 4, we address the bipartite formation with collision avoidance, but only agents that are *interconnected* with each other avoid collisions. But in realistic scenarios, the collision should be avoided by *all* agents. For instance, for the network represented in Figure 4.11, only agents 2 and 3 are interconnected with the competitive leader, representing the obstacle. These two agents are also the only ones able to avoid the obstacle, as shown in Figure 4.12. If the other agents were close to the obstacle, obstacle avoidance would not be possible for those. A natural way to address this problem is for the agents to take into account all other agents within their sensing ranges. If an agent comes close to an obstacle, it will detect it and be able to avoid it. On the other hand, when the agent moves away from the obstacle and is no longer in a dangerous zone where a collision is likely, it will cease to detect the obstacle and will not be influenced by its state. This means that interconnections will be added to and removed from the network. Furthermore, this also implies that for the bipartite consensus problem, groups of cooperative agents will stop being influenced by competitive agents, and their final positions will not be affected.

Collision-avoidance of robot manipulators. In Chapter 5, we address the bipartite formation of robot manipulators' end-effecter under collision avoidance constraints. More precisely, in this memoir, collision avoidance is only guaranteed for end-effectors and not for the links. To the best of our knowledge, guaranteeing inter-link collision avoidance in multi-agent systems is an open problem. As a matter of fact, so is the problem that we solved: the constrained bipartite formation for the manipulators' end-effectors. Collision avoidance for the link has been addressed, e.g., in [96], but not for cooperative and competitive agents. In future research, collision avoidance between the links of the manipulators may be addressed, *e.g.,* by considering each link as an agent, so as a node of the graph, and the links can be modeled using the 2D or 3D ellipsoidal agent approach. For instance, in [96], each agent is modeled by an

ellipsoid approximation, and the inter-agent collisions are represented as two planar ellipsoids that intersect with each other.

Control redesign via strict Lyapunov functions. In Chapters 4 and 5, we address the bipartite formation-consensus problems for linear and non-linear systems. In both of the chapters, we construct non-strict Lyapunov functions, and we design our controllers based on the gradient of these non-strict Lyapunov functions. An interesting direction of research may be to figure out how to render these BLFs strict and modify the controller using the gradient-based term to take care of the disturbances. The analysis given in Chapters 4 and 5 is promising because it may be a first step to construct strict Lyapunov functions to deal with disturbances, especially to tackle the formation-control problem of satellites under J_2 effects.

APPENDIX A

APPENDICES

A.1 GRAPH THEORY

Example Consider the undirected signed network depicted in Figure A.1.

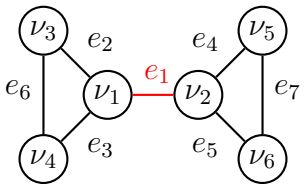

Figure A.1: An undirected signed network of 6 agents. The black lines represent cooperative edges and the red line represents the competitive edge.

The graph has $N = 6$ nodes and $M = 7$ edges. We can split the nodes into two disjoint subgroups, such as

$$\mathcal{V}_1 = \{\nu_1,\ \nu_3,\ \nu_4\}, \quad \mathcal{V}_2 = \{\nu_2,\ \nu_5,\ \nu_6\},$$

so the graph is structurally balanced. We define the orientation of the edges as

$$e_1 = \nu_1 + \nu_2, \quad e_2 = \nu_1 - \nu_3, \quad e_3 = \nu_1 - \nu_4, \quad e_4 = \nu_2 - \nu_5,$$
$$e_5 = \nu_2 - \nu_6, \quad e_6 = \nu_3 - \nu_4, \quad e_7 = \nu_5 - \nu_6.$$

We define the gauge transformation matrix $D \in \mathbb{R}^{N\times N}$ as

$$D = \text{diag}([1,\ -1,\ 1,\ 1,\ -1,\ -1]).$$

For the edges $e_1,\ e_2$ and e_3, the initial node is $\nu_1 \in \mathcal{V}_1$ and for the edge e_6, the initial node is $\nu_3 \in \mathcal{V}_1$ so $\sigma_{e_i} = 1,\ i \in \{1,\ 2,\ 3,\ 6\}$. For the edges e_4 and e_5 the initial node is $\nu_2 \in \mathcal{V}_2$ and for the edge e_7, the initial node is $\nu_5 \in \mathcal{V}_2$ so $\sigma_{e_j} = -1,\ j \in \{5,\ 6,\ 7\}$. As a result, the matrix $D_e \in \mathbb{R}^{M\times M}$ for the edge-gauge transformation is defined as

$$D_e = \text{diag}([1,\ 1,\ 1,\ -1,\ -1,\ 1,\ -1]).$$

The incidence matrix $E \in \mathbb{R}^{N\times M}$ of the unsigned graph is given below.

$$E = \begin{bmatrix} 1 & 1 & 1 & 0 & 0 & 0 & 0 \\ -1 & 0 & 0 & 1 & 1 & 0 & 0 \\ 0 & -1 & 0 & 0 & 0 & 1 & 0 \\ 0 & 0 & -1 & 0 & 0 & -1 & 0 \\ 0 & 0 & 0 & -1 & 0 & 0 & 1 \\ 0 & 0 & 0 & 0 & -1 & 0 & -1 \end{bmatrix}.$$

Applying the gauge transformations on the incidence matrix E, we obtain

$$E_s = DED_e = \begin{bmatrix} 1 & 1 & 1 & 0 & 0 & 0 & 0 \\ 1 & 0 & 0 & 1 & 1 & 0 & 0 \\ 0 & -1 & 0 & 0 & 0 & 1 & 0 \\ 0 & 0 & -1 & 0 & 0 & -1 & 0 \\ 0 & 0 & 0 & -1 & 0 & 0 & 1 \\ 0 & 0 & 0 & 0 & -1 & 0 & -1 \end{bmatrix},$$

which corresponds to the incidence matrix of a signed graph, given in (2.38). Then, the Laplacian matrix $L_s = E_s E_s^\top \in \mathbb{R}^{N\times N}$ and the edge Laplacian matrix $L_{e_s} = E_s^\top E_s \in \mathbb{R}^{M\times M}$ associated to the undirected signed graph are calculated as

$$L_s = \begin{bmatrix} 3 & 1 & -1 & -1 & 0 & 0 \\ 1 & 3 & 0 & 0 & -1 & -1 \\ -1 & 0 & 2 & -1 & 0 & 0 \\ -1 & 0 & -1 & 2 & 0 & 0 \\ 0 & -1 & 0 & 0 & 2 & -1 \\ 0 & -1 & 0 & 0 & -1 & 2 \end{bmatrix}, \quad L_{e_s} = \begin{bmatrix} 2 & 1 & 1 & 1 & 1 & 0 & 0 \\ 1 & 2 & 1 & 0 & 0 & -1 & 0 \\ 1 & 1 & 2 & 0 & 0 & 1 & 0 \\ 1 & 0 & 0 & 2 & 1 & 0 & -1 \\ 1 & 0 & 0 & 1 & 2 & 0 & 1 \\ 0 & -1 & 1 & 0 & 0 & 2 & 0 \\ 0 & 0 & 0 & -1 & 1 & 0 & 2 \end{bmatrix}.$$

The eigenvalues of the Laplacian matrix and the edge Laplacian matrix are

$$\lambda_{L_s} = \{0,\ 0.4384,\ 3,\ 3,\ 3,\ 4.5616\}, \quad \lambda_{L_{e_s}} = \{0,\ 0,\ 0.4384,\ 3,\ 3,\ 3,\ 4.5616\}.$$

The Laplacian matrix L_s has exactly one zero eigenvalue and is positive semi-definite. As the graph has 7 edges, which is more than the number of nodes, the edge Laplacian L_{e_s} has exactly $M - N + 1 = 2$ zero eigenvalues.

On the other hand, since the undirected graph is structurally balanced and contains a spanning tree, it can be decomposed into the union of two subgraphs: the first subgraph consists of the edges corresponding to the spanning tree, while the second subgraph contains the remaining edges, as depicted in Figure A.2.

Then, the incidence matrix E_s is partitioned into $[E_{t_s} \quad E_{c_s}]$ as in (4.32), where $E_{t_s} \in \mathbb{R}^{N\times N-1}$ is the incidence matrix representing the spanning tree of the graph, and $E_{c_s} \in \mathbb{R}^{N\times M-(N-1)}$ is the incidence matrix representing the remaining edges

$$E_{t_s} = \begin{bmatrix} 1 & 1 & 1 & 0 & 0 \\ 1 & 0 & 0 & 1 & 1 \\ 0 & -1 & 0 & 0 & 0 \\ 0 & 0 & -1 & 0 & 0 \\ 0 & 0 & 0 & -1 & 0 \\ 0 & 0 & 0 & 0 & -1 \end{bmatrix}, \quad E_{c_s} = \begin{bmatrix} 0 & 0 \\ 0 & 0 \\ 1 & 0 \\ -1 & 0 \\ 0 & 1 \\ 0 & -1 \end{bmatrix}.$$

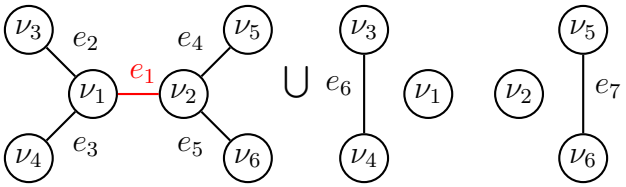

Figure A.2: Partition of the undirected structurally balanced signed graph on Figure A.1 into a spanning tree and the remaining edges.

From (4.34), we obtain

$$T_s = (E_{t_s}^\top E_{t_s})^{-1} E_{t_s}^\top E_{c_s} = \begin{bmatrix} 0 & 0 \\ -1 & 0 \\ 1 & 0 \\ 0 & -1 \\ 0 & 1 \end{bmatrix}, \quad R_s = [I_{N-1} \quad T_s] = \begin{bmatrix} 1 & 0 & 0 & 0 & 0 & 0 & 0 \\ 0 & 1 & 0 & 0 & 0 & -1 & 0 \\ 0 & 0 & 1 & 0 & 0 & 1 & 0 \\ 0 & 0 & 0 & 1 & 0 & 0 & -1 \\ 0 & 0 & 0 & 0 & 1 & 0 & 1 \end{bmatrix},$$

which satisfy (4.33).

A.2 LYAPUNOV FUNCTIONS AND STABILITY THEOREMS

Theorem A.2.1 (Lyapunov's stability theorem [38]) *Let $x = 0$ be an equilibrium point for*

$$\dot{x} = f(x), \tag{A.1}$$

where $f : \mathcal{D} \to \mathbb{R}^n$, and $\mathcal{D} \subset \mathbb{R}^n$ is a domain containing $x = 0$. Let $V : \mathcal{D} \to \mathbb{R}_{\geq 0}$ be a continuously differentiable function such that

$$V(0) = 0 \text{ and } V(x) > 0 \quad \text{in} \quad \mathcal{D}\backslash\{0\} \tag{A.2}$$

$$\dot{V}(x) \leq 0 \quad \text{in} \quad \mathcal{D} \tag{A.3}$$

Then, $x = 0$ is stable. Moreover, if

$$\dot{V} < 0 \quad \text{in} \quad \mathcal{D}\backslash\{0\} \tag{A.4}$$

then $x = 0$ is asymptotically stable.

Consider the general nonlinear systems of the form

$$\dot{x} = f(x, u) \tag{A.5}$$

where $x(t) \in \mathbb{R}^n$ is the state, $u \in \mathcal{U}^m$ denotes an external input, and $f : \mathbb{R}^n \times \mathbb{R}^m$ is continuously differentiable satisfying $f(0, 0) = 0$.

Definition A.2.1 ($\mathcal{K}$ and $\mathcal{K}_\infty$ functions [38]) *A continuous function $\alpha : [0, a) \to [0, \infty)$ is said to belong to class $\mathcal{K}$ if it is strictly increasing and $\alpha(0) = 0$. It is said to belong to class $\mathcal{K}_\infty$ if $a = \infty$ and $\alpha(r) \to \infty$ as $r \to \infty$.*

Definition A.2.2 ($\mathcal{KL}$ function [38]) *A continuous function $\beta : [0, a) \times [0, \infty) \to [0, \infty)$ is said to belong to class $\mathcal{KL}$ if, for each fixed s, the mapping $\beta(r, s)$ belongs to class $\mathcal{K}$ with respect to r and, for each fixed r, the mapping $\beta(r, s)$ is decreasing with respect to s and $\beta(r, s) \to 0$ as $s \to \infty$.*

Definition A.2.3 (Input-to-state stability [88]) *The system (A.5) is (globally) input-to-state stable if there exist a $\mathcal{KL}$-function $\beta : \mathbb{R}_{\geq 0} \times \mathbb{R}_{\geq 0}$ and a $\mathcal{K}$-function γ such that, for each input $u \in \mathcal{L}_\infty$ and each $\xi \in \mathbb{R}^n$, it holds that*

$$|x(t, \xi, u)| \leq \beta(|\xi|, t) + \gamma(||u||) \tag{A.6}$$

for each $t \geq 0$.

Definition A.2.4 (ISS-Lyapunov function [88]) *A smooth function $V : \mathbb{R}^n \to \mathbb{R}_{\geq 0}$ is called an ISS-Lyapunov function for system (A.5) if there exist $\mathcal{K}_\infty$-functions α_1, α_2, and $\mathcal{K}$-functions α_3 and χ, such that*

$$\alpha_1(|\xi|) \leq V(\xi) \leq \alpha_2(|\xi|) \tag{A.7}$$

for any $\xi \in \mathbb{R}^n$ and

$$\nabla V(\xi) \cdot f(\xi, u) \leq \alpha_3(|\xi|) \tag{A.8}$$

for any $\xi \in \mathbb{R}^n$ and any $\mu \in \mathbb{R}^m$ so that $|\xi| \geq \chi(|u|)$.

A.3 CRITICAL POINTS OF THE BARRIER-LYAPUNOV FUNCTIONS

A.3.1 Barrier-Lyapunov functions in node coordinates

For cooperative agents, the BLF in node coordinates is defined as

$$\begin{aligned}\tilde{W}_{ij}(x_i, x_j) = &\frac{1}{2}|\bar{x}_i - \bar{x}_j|^2 \\ &+ \frac{1}{2}\frac{\Delta_k^2}{|\bar{b}_{ij}|^2(|\bar{b}_{ij}|^2 - \Delta_k^2)}\left[\ln\left(\frac{R_k^2}{R_k^2 - |x_i - x_j|^2}\right) - \ln\left(\frac{R_k^2}{R_k^2 - |\bar{b}_{ij}|^2}\right)\right] \\ &+ \frac{1}{2}\frac{1}{R_k^2 - |\bar{b}_{ij}|^2}\left[\ln\left(\frac{|x_i - x_j|^2}{|x_i - x_j|^2 - \Delta_k^2}\right) - \ln\left(\frac{|\bar{b}_{ij}|^2}{|\bar{b}_{ij}|^2 - \Delta_k^2}\right)\right].\end{aligned} \tag{A.9}$$

Its gradient may be written as

$$\nabla\tilde{W}_{ij} = \begin{bmatrix}\nabla_{x_i}\tilde{W}_{ij} \\ \nabla_{x_j}\tilde{W}_{ij}\end{bmatrix},$$

where

$$\begin{aligned}\nabla_{x_i}\tilde{W}_{ij} = &\left[1 + \frac{\Delta_k^2}{|\bar{b}_{ij}|^2(|\bar{b}_{ij}|^2 - \Delta_k^2)} \cdot \frac{1}{R_k^2 - |x_i - x_j|^2}\right. \\ &- \left.\frac{1}{R_k^2 - |\bar{b}_{ij}|^2} \cdot \frac{\Delta_k^2}{|x_i - x_j|^2(|x_i - x_j|^2 - \Delta_k^2)}\right](x_i - x_j) - \bar{b}_{ij}.\end{aligned} \tag{A.10}$$

and $\nabla_{x_j}\tilde{W}_{ij} = -\nabla_{x_i}\tilde{W}_{ij}$. Then, the Hessian of the function reads

$$H(\tilde{W}_{ij}) = \begin{bmatrix} \frac{\partial^2 \tilde{W}_{ij}}{\partial x_i^2} & \frac{\partial^2 \tilde{W}_{ij}}{\partial x_i x_j} \\ \frac{\partial^2 \tilde{W}_{ij}}{\partial x_i x_j} & \frac{\partial^2 \tilde{W}_{ij}}{\partial x_j^2} \end{bmatrix},$$

where

$$\begin{aligned} \frac{\partial^2 \tilde{W}_{ij}}{\partial x_i^2} = & \Bigg[1 + \frac{\Delta_k^2}{|\bar{b}_{ij}|^2(|\bar{b}_{ij}|^2 - \Delta_k^2)} \cdot \frac{1}{R_k^2 - |x_i - x_j|^2} \\ & - \frac{1}{R_k^2 - |\bar{b}_{ij}|^2} \cdot \frac{\Delta_k^2}{|x_i - x_j|^2(|x_i - x_j|^2 - \Delta_k^2)}\Bigg] I_n \\ & + 2\Bigg[\frac{1}{R_k^2 - |\bar{b}_{ij}|^2} \cdot \frac{\Delta_k^2\,(2|x_i - x_j|^2 - \Delta_k^2)}{|x_i - x_j|^4(|x_i - x_j|^2 - \Delta_k^2)^2} \\ & + \frac{\Delta_k^2}{|\bar{b}_{ij}|^2(|\bar{b}_{ij}|^2 - \Delta_k^2)} \cdot \frac{1}{(R_k^2 - |x_i - x_j|^2)^2}\Bigg](x_i - x_j)(x_i - x_j)^\top, \end{aligned} \tag{A.11}$$

$\frac{\partial^2 \tilde{W}_{ij}}{\partial x_i^2} = \frac{\partial^2 \tilde{W}_{ij}}{\partial x_j^2}$ and $\frac{\partial^2 \tilde{W}_{ij}}{\partial x_i x_j} = -\frac{\partial^2 \tilde{W}_{ij}}{\partial x_i^2}$. The eigenvalues of the Hessian are

$$\begin{aligned} \lambda_l(s_k) = & 1 + \frac{\Delta_k^2}{|\bar{b}_{ij}|^2(|\bar{b}_{ij}|^2 - \Delta_k^2)} \cdot \frac{1}{R_k^2 - |x_i - x_j|^2} \\ & - \frac{1}{R_k^2 - |\bar{b}_{ij}|^2} \cdot \frac{\Delta_k^2}{|x_i - x_j|^2 - \Delta_k^2}, \quad l \in \{1,\ 2, \cdots, n-1\} \end{aligned} \tag{A.12a}$$

$$\begin{aligned} \lambda_n(s_k) = & 2\Bigg[1 + \frac{\Delta_k^2}{|\bar{b}_{ij}|^2(|\bar{b}_{ij}|^2 - \Delta_k^2)} \cdot \frac{1}{R_k^2 - |x_i - x_j|^2} \\ & - \frac{1}{R_k^2 - |\bar{b}_{ij}|^2} \cdot \frac{\Delta_k^2}{|x_i - x_j|^2 - \Delta_k^2}\Bigg]. \end{aligned} \tag{A.12b}$$

Now, we look at the critical points, where $\nabla_{x_i}\tilde{W}_{ij} = 0$ and $\nabla_{x_j}\tilde{W}_{ij} = 0$. Looking at the form of the BLF, it has two critical points with opposite signs. The first one is $x_i - x_j = \bar{b}_{ij}$, that is,

$$\frac{\Delta_k^2}{|\bar{b}_{ij}|^2(|\bar{b}_{ij}|^2 - \Delta_k^2)} \cdot \frac{\bar{b}_{ij}}{R_k^2 - |\bar{b}_{ij}|^2} - \frac{1}{R_k^2 - |\bar{b}_{ij}|^2} \cdot \frac{\Delta_k^2 \alpha_k}{|\bar{b}_{ij}|^2(|\bar{b}_{ij}|^2 - \Delta_k^2)} = 0.$$

To prove that it is a minimum, we show that $\lambda_l(0) > 0$, that is,

$$\lambda_l(0) = 1 + \frac{\Delta_k^2}{|\bar{b}_{ij}|^2(|\bar{b}_{ij}|^2 - \Delta_k^2)} \cdot \frac{1}{R_k^2 - |\bar{b}_{ij}|^2} - \frac{1}{R_k^2 - |\bar{b}_{ij}|^2} \cdot \frac{\Delta_k^2}{|\bar{b}_{ij}|^2 - \Delta_k^2} = 1.$$

The other critical point s_k^* is aligned with $\bar{b}_{ij}$. Then, there exists $a > 0$ such that $s^* = -a\bar{b}_{ij}$. So,

$$\left[1 + \frac{\Delta_k^2}{|\bar{b}_{ij}|^2(|\bar{b}_{ij}|^2 - \Delta_k^2)} \cdot \frac{1}{R_k^2 - |-a\bar{b}_{ij}|^2} - \frac{1}{R_k^2 - |\bar{b}_{ij}|^2} \cdot \frac{\Delta_k^2}{|-a\bar{b}_{ij}|^2(|-a\bar{b}_{ij}|^2 - \Delta_k^2)}\right] \times(-a\bar{b}_{ij}) = \bar{b}_{ij}$$

$$\left[1 + \frac{\Delta_k^2}{|\bar{b}_{ij}|^2(|\bar{b}_{ij}|^2 - \Delta_k^2)} \cdot \frac{1}{R_k^2 - |-a\bar{b}_{ij}|^2} - \frac{1}{R_k^2 - |\bar{b}_{ij}|^2} \cdot \frac{\Delta_k^2}{|-a\bar{b}_{ij}|^2(|-a\bar{b}_{ij}|^2 - \Delta_k^2)}\right] = -\frac{1}{a} < 0.$$

Then, $\lambda_l(-a\bar{b}_{ij}) < 0$ and $s^* = -a\bar{b}_{ij}$ is a saddle point.

On the other hand, for competitive agents, the BLF in node coordinates is defined as

$$\begin{aligned}\hat{W}_{ij}(x_i, x_j) = &\frac{1}{2}\left[(x_i - x_j)^2 + \ln\left(\frac{|x_i - x_j|^2}{|x_i - x_j|^2 - \Delta^2}\right)\right] \\ &- \frac{1}{2}\left[(-2x_j + \bar{b}_{ij})^2 + \ln\left(\frac{|-2x_j + \bar{b}_{ij}|^2}{|-2x_j + \bar{b}_{ij}|^2 - \Delta^2}\right)\right] \\ &- \left[(-2x_j + \bar{b}_{ij}) - \Delta^2 \frac{-2x_j + \bar{b}_{ij}}{|-2x_j + \bar{b}_{ij}|^2(|-2x_j + \bar{b}_{ij}|^2 - \Delta^2)}\right](\bar{x}_i + \bar{x}_j).\end{aligned}$$

Its gradient may be written as

$$\nabla\tilde{W}_{ij} = \begin{bmatrix}\nabla_{x_i}\tilde{W}_{ij} \\ \nabla_{x_j}\tilde{W}_{ij}\end{bmatrix},$$

where

$$\begin{aligned}\nabla_{x_i}\hat{W}_{ij} = &\left[1 + \Delta^2 \frac{1}{|x_i - x_j|^2(|x_i - x_j|^2 - \Delta^2)}\right](x_i - x_j) \\ &+ \left[1 - \Delta^2 \frac{1}{|-2x_j + \bar{b}_{ij}|^2(|-2x_j + \bar{b}_{ij}|^2 - \Delta^2)}\right][-2x_j + \bar{b}_{ij}]. \qquad \text{(A.13)}\end{aligned}$$

and

$$\begin{aligned}\nabla_{x_j}\hat{W}_{ij} = &-\left[1 + \Delta^2 \frac{1}{|x_i - x_j|^2(|x_i - x_j|^2 - \Delta^2)}\right](x_i - x_j) \\ &+ \left[4 - 4\Delta^2 \frac{1}{|-2x_j + \bar{b}_{ij}|^2(|-2x_j + \bar{b}_{ij}|^2 - \Delta^2)}\right][-2x_j + \bar{b}_{ij}]. \qquad \text{(A.14)}\end{aligned}$$

Then, its Hessian reads

$$H(\tilde{W}_{ij}) = \begin{bmatrix}\frac{\partial^2\tilde{W}_{ij}}{\partial x_i^2} & \frac{\partial^2\tilde{W}_{ij}}{\partial x_i x_j} \\ \frac{\partial^2\tilde{W}_{ij}}{\partial x_i x_j} & \frac{\partial^2\tilde{W}_{ij}}{\partial x_j^2}\end{bmatrix},$$

where

$$\frac{\partial^2 \hat{W}}{\partial x_i^2} = \left[1 + \Delta^2 \frac{1}{|x_i - x_j|^2(|x_i - x_j|^2 - \Delta^2)}\right] I_n + \left[\frac{2\Delta^2[2|x_i - x_j|^2 - \Delta^2]}{|x_i - x_j|^4(|x_i - x_j|^2 - \Delta^2)^2}\right](x_i - x_j)(x_i - x_j)^\top, \tag{A.15}$$

$$\frac{\partial^2 \hat{W}_{ij}}{\partial x_j^2} = \left(1 + 2\left[\frac{1}{|x_i - x_j|^2} + \frac{2\Delta^2}{(|x_i - x_j|^2 - \Delta^2)^2}\right]\right) I_n + \left(4 + 4\left[\frac{1}{|-2x_j + \bar{b}_{ij}|^2} + \frac{2\Delta^2}{\left(|-2x_j + \bar{b}_{ij}|^2 - \Delta^2\right)^2}\right]\right) I_n + \left(4\Delta^2\left[\frac{1}{|-2x_j + \bar{b}_{ij}|^2\left(|-2x_j + \bar{b}_{ij}|^2 - \Delta^2\right)} + \frac{4\Delta^2}{\left(|-2x_j + \bar{b}_{ij}|^2 - \Delta^2\right)^2}\right]\right) I_n.$$

and

$$\frac{\partial^2 \hat{W}_{ij}}{\partial x_i x_j} = -2\Delta^2\left[\frac{(x_i - x_j)}{|x_i - x_j|^4(|x_i - x_j|^2 - \Delta^2)} + \frac{(x_i - x_j)}{|x_i - x_j|^2(|x_i - x_j|^2 - \Delta^2)^2}\right](x_i - x_j) - \left[1 + \Delta^2 \frac{1}{|x_i - x_j|^2(|x_i - x_j|^2 - \Delta^2)} 2 - 2\Delta^2 \frac{1}{|-2x_j + \bar{b}_{ij}|^2(|-2x_j + \bar{b}_{ij}|^2 - \Delta^2)}\right] I_n$$

$$+4\Delta^2\left[\frac{(-2x_j + \bar{b}_{ij})}{|-2x_j + \bar{b}_{ij}|^4(|-2x_j + \bar{b}_{ij}|^2 - \Delta^2)} + \frac{(-2x_j + \bar{b}_{ij})}{|-2x_j + \bar{b}_{ij}|^2(|-2x_j + \bar{b}_{ij}|^2 - \Delta^2)^2}\right](-2x_j + \bar{b}_{ij}).$$

Let $s = x_i - x_j$. The eigenvalues of its Hessian are

$$\lambda_l(s_k) = 1 + \Delta^2 \frac{1}{|s_k|^2(|s_k|^2 - \Delta^2)}, \quad l \in \{1,\ 2, \cdots, n-1\} \tag{A.16a}$$

$$\lambda_n(s_k) = 2\left[1 + \Delta^2 \frac{1}{|s_k|^2(|s_k|^2 - \Delta^2)}\right]. \tag{A.16b}$$

First, we look at the critical points, where $\nabla_{x_i} \hat{W}_{ij} = 0$ and $\nabla_{x_j} \hat{W}_{ij} = 0$. Looking at the form of the BLF, we see that there are two critical points with opposite signs. The first one is $s_k = -2x_j + \bar{b}_{ij}$, that is,

$$\left[1 + \Delta^2 \frac{1}{|-2x_j + \bar{b}_{ij}|^2(|-2x_j + \bar{b}_{ij}|^2 - \Delta^2)}\right](-2x_j + \bar{b}_{ij}) = \left[1 + \Delta^2 \frac{1}{|-2x_j + \bar{b}_{ij}|^2(|-2x_j + \bar{b}_{ij}|^2 - \Delta^2)}\right][-2x_j + \bar{b}_{ij}] = 0.$$

To prove that it is a minimum, we show that $\lambda_l(-2x_j + \bar{b}_{ij}) > 0$, where

$$\lambda_l(-2x_j + \bar{b}_{ij}) = 1 + \Delta^2 \frac{1}{|-2x_j + \bar{b}_{ij}|^2(|-2x_j + \bar{b}_{ij}|^2 - \Delta^2)} > 0/$$

The other critical point s_k^* is aligned with $s_k = -2x_j + \bar{b}_{ij}$. Then, there exists $a > 0$ such that $s^* = -a(-2x_j + \bar{b}_{ij})$. So,

$$\left[1 + \Delta^2 \frac{1}{|s_k^*|^2(|s_k^*|^2 - \Delta^2)}\right] - a(-2x_j + \bar{b}_{ij}) \\ = \left[1 + \Delta^2 \frac{1}{|-2x_j + \bar{b}_{ij}|^2(|-2x_j + \bar{b}_{ij}|^2 - \Delta^2)}\right][-2x_j + \bar{b}_{ij}],$$

and

$$\lambda_l(s_k^*) = -\frac{1}{a}\lambda_l(s_k).$$

As $\lambda_l(s_k) > 0$, we have that $\lambda_l(s_k^*) < 0$, so $s^* = -a(-2x_j + \bar{b}_{ij})$ is a saddle point.

A.3.2 Barrier-Lyapunov functions in edge coordinates

For cooperative agents, the BLF in edge coordinates is defined as

$$\begin{aligned}\tilde{W}_k(\bar{e}_{x_k}, \alpha_k) = &\frac{1}{2}|\bar{e}_{x_k}|^2 \\ &+ \frac{1}{2}\frac{\Delta_k^2}{|\alpha_k|^2(|\alpha_k|^2 - \Delta_k^2)}\left[\ln\left(\frac{R_k^2}{R_k^2 - |\bar{e}_{x_k} + \alpha_k|^2}\right) - \ln\left(\frac{R_k^2}{R_k^2 - |\alpha_k|^2}\right)\right] \\ &+ \frac{1}{2}\frac{1}{R_k^2 - |\alpha_k|^2}\left[\ln\left(\frac{|\bar{e}_{x_k} + \alpha_k|^2}{|\bar{e}_{x_k} + \alpha_k|^2 - \Delta_k^2}\right) - \ln\left(\frac{|\alpha_k|^2}{|\alpha_k|^2 - \Delta_k^2}\right)\right], \end{aligned} \tag{A.17}$$

where $\alpha_k = b_k$. Its gradient may be written as

$$\begin{aligned}\nabla_{\bar{e}_{x_k}}\tilde{W}_k = &\left[1 + \frac{\Delta_k^2}{|\alpha_k|^2(|\alpha_k|^2 - \Delta_k^2)} \cdot \frac{1}{R_k^2 - |\bar{e}_{x_k} + \alpha_k|^2}\right. \\ &- \left.\frac{1}{R_k^2 - |\alpha_k|^2} \cdot \frac{\Delta_k^2}{|\bar{e}_{x_k} + \alpha_k|^2(|\bar{e}_{x_k} + \alpha_k|^2 - \Delta_k^2)}\right](\bar{e}_{x_k} + \alpha_k) - \alpha_k. \end{aligned} \tag{A.18}$$

Then, the Hessian of the function reads

$$\begin{aligned}\frac{\partial^2 \tilde{W}_k}{\partial \bar{e}_{x_k}^2} = &\left[1 + \frac{\Delta_k^2}{|\alpha_k|^2(|\alpha_k|^2 - \Delta_k^2)} \cdot \frac{1}{R_k^2 - |\bar{e}_{x_k} + \alpha_k|^2}\right. \\ &- \left.\frac{1}{R_k^2 - |\alpha_k|^2} \cdot \frac{\Delta_k^2}{|\bar{e}_{x_k} + \alpha_k|^2(|\bar{e}_{x_k} + \alpha_k|^2 - \Delta_k^2)}\right] I_n \\ &+ 2\left[\frac{1}{R_k^2 - |\alpha_k|^2} \cdot \frac{\Delta_k^2\,(2|\bar{e}_{x_k} + \alpha_k|^2 - \Delta_k^2)}{|\bar{e}_{x_k} + \alpha_k|^4(|\bar{e}_{x_k} + \alpha_k|^2 - \Delta_k^2)^2}\right. \\ &+ \left.\frac{\Delta_k^2}{|\alpha_k|^2(|\alpha_k|^2 - \Delta_k^2)} \cdot \frac{1}{(R_k^2 - |\bar{e}_{x_k} + \alpha_k|^2)^2}\right](\bar{e}_{x_k} + \alpha_k)(\bar{e}_{x_k} + \alpha_k)^\top. \end{aligned} \tag{A.19}$$

The eigenvalues of the Hessian are

$$\lambda_l(s_k) = 1 + \frac{\Delta_k^2}{|\alpha_k|^2(|\alpha_k|^2 - \Delta_k^2)} \cdot \frac{1}{R_k^2 - |\bar{e}_{x_k} + \alpha_k|^2} - \frac{1}{R_k^2 - |\alpha_k|^2} \cdot \frac{\Delta_k^2}{|\bar{e}_{x_k} + \alpha_k|^2 - \Delta_k^2}, \quad l \in \{1,\ 2, \cdots, n-1\} \tag{A.20a}$$

$$\begin{aligned}\lambda_n(s_k) = 1 &+ \frac{\Delta_k^2}{|\alpha_k|^2(|\alpha_k|^2 - \Delta_k^2)} \cdot \frac{1}{R_k^2 - |\bar{e}_{x_k} + \alpha_k|^2} - \frac{1}{R_k^2 - |\alpha_k|^2} \cdot \frac{\Delta_k^2}{|\bar{e}_{x_k} + \alpha_k|^2 - \Delta_k^2} \\ &+ 2\left[\frac{1}{R_k^2 - |\alpha_k|^2} \cdot \frac{\Delta_k^2\,(2|\bar{e}_{x_k} + \alpha_k|^2 - \Delta_k^2)}{|\bar{e}_{x_k} + \alpha_k|^4(|\bar{e}_{x_k} + \alpha_k|^2 - \Delta_k^2)^2}\right. \\ &+ \left.\frac{\Delta_k^2}{|\alpha_k|^2(|\alpha_k|^2 - \Delta_k^2)} \cdot \frac{1}{\left(R_k^2 - |\bar{e}_{x_k} + \alpha_k|^2\right)^2}\right] |\bar{e}_{x_k} + \alpha_k|^2.\end{aligned} \tag{A.20b}$$

For all $|\bar{e}_{x_k} + \alpha_k| > \Delta_k$, $|\alpha_k| > \Delta_k$, $|\bar{e}_{x_k} + \alpha_k| < R_k$ and $|\alpha_k| < R_k$, we have that

$$\begin{aligned}\lambda_n(s_k) = 1 &+ \frac{1}{R_k^2 - |\bar{e}_{x_k} + \alpha_k|^2} \cdot \frac{\Delta_k^2(3|\bar{e}_{x_k} + \alpha_k|^2 - \Delta_k^2)}{|\bar{e}_{x_k} + \alpha_k|^2(|\bar{e}_{x_k} + \alpha_k|^2 - \Delta_k^2)^2} \\ &+ \frac{\Delta_k^2}{|\alpha_k|^2(|\alpha_k|^2 - \Delta_k^2)} \cdot \frac{R_k^2 + |\bar{e}_{x_k} + \alpha_k|^2}{\left(R_k^2 - |\bar{e}_{x_k} + \alpha_k|^2\right)^2} > 1.\end{aligned}$$

Now, we look at the critical points, where $\nabla_{\bar{e}_{x_k}} \tilde{W}_k = 0$. Looking at the form of the BLF, it has two critical points with opposite signs. The first one is $\bar{e}_{x_k} = 0$, that is,

$$\frac{\Delta_k^2}{|\alpha_k|^2(|\alpha_k|^2 - \Delta_k^2)} \cdot \frac{\alpha_k}{R_k^2 - |\alpha_k|^2} - \frac{1}{R_k^2 - |\alpha_k|^2} \cdot \frac{\Delta_k^2 \alpha_k}{|\alpha_k|^2(|\alpha_k|^2 - \Delta_k^2)} = 0.$$

To prove that it is a minimum, we show that $\lambda_l(0) > 0$, that is,

$$\lambda_l(0) = 1 + \frac{\Delta_k^2}{|\alpha_k|^2(|\alpha_k|^2 - \Delta_k^2)} \cdot \frac{1}{R_k^2 - |\alpha_k|^2} - \frac{1}{R_k^2 - |\alpha_k|^2} \cdot \frac{\Delta_k^2}{|\alpha_k|^2 - \Delta_k^2} = 1.$$

For the other critical point e_k^*, we have

$$\left[1 + \frac{\Delta_k^2}{|\alpha_k|^2(|\alpha_k|^2 - \Delta_k^2)} \cdot \frac{1}{R_k^2 - |e_k^* + \alpha_k|^2} - \frac{1}{R_k^2 - |\alpha_k|^2} \cdot \frac{\Delta_k^2}{|e_k^* + \alpha_k|^2(|e_k^* + \alpha_k|^2 - \Delta_k^2)}\right](e_k^* + \alpha_k) = \alpha_k.$$

In original relative distance coordinates, we have $e_k^* + \alpha_k = s_k^*$, which is aligned with the other critical point $\alpha_k = b_k$, so there exists $a > 0$ such that $s_k^* = -a\alpha_k$.

$$\left[1 + \frac{\Delta_k^2}{|\alpha_k|^2(|\alpha_k|^2 - \Delta_k^2)} \cdot \frac{1}{R_k^2 - |-a\alpha_k|^2} - \frac{1}{R_k^2 - |\alpha_k|^2} \cdot \frac{\Delta_k^2}{|-a\alpha_k|^2(|-a\alpha_k|^2 - \Delta_k^2)}\right] -a\alpha_k = \alpha_k$$

$$\left[1 + \frac{\Delta_k^2}{|\alpha_k|^2(|\alpha_k|^2 - \Delta_k^2)} \cdot \frac{1}{R_k^2 - |-a\alpha_k|^2} - \frac{1}{R_k^2 - |\alpha_k|^2} \cdot \frac{\Delta_k^2}{|-a\alpha_k|^2(|-a\alpha_k|^2 - \Delta_k^2)}\right] = -\frac{1}{a} < 0.$$

Then, $\lambda_l(s^*) < 0$ and $s^* = -a\alpha_k$ is a saddle point.

On the other hand, for competitive agents, the BLF in edge coordinates is defined as

$$\begin{aligned}\hat{W}_k(\bar{e}_{x_k}, \alpha_k) =& \frac{1}{2}\left[|\bar{e}_{x_k} + \alpha_k|^2 + \ln\left(\frac{|\bar{e}_{x_k} + \alpha_k|^2}{|\bar{e}_{x_k} + \alpha_k|^2 - \Delta_k^2}\right)\right] - \frac{1}{2}\left[|\alpha_k|^2 + \ln\left(\frac{|\alpha_k|^2}{|\alpha_k|^2 - \Delta_k^2}\right)\right] \\ & - \left[\alpha_k - \frac{\Delta^2(\alpha_k)}{|\alpha_k|^2\left(|\alpha_k|^2 - \Delta^2\right)}\right]\bar{e}_{x_k}, \end{aligned} \tag{A.21}$$

Its gradient with respect to the synchronization errors $\bar{e}_{x_k}$, may be written as

$$\begin{aligned}\nabla_{\bar{e}_{x_k}}\hat{W}_k(\bar{e}_{x_k}, \alpha_k) = & \left[1 - \frac{\Delta^2}{|\bar{e}_{x_k} + \alpha_k|^2(|\bar{e}_{x_k} + \alpha_k|^2 - \Delta^2)}\right](\bar{e}_{x_k} + \alpha_k) \\ & - \left[1 - \frac{\Delta^2}{|\alpha_k|^2\left(|\alpha_k|^2 - \Delta^2\right)}\right]\alpha_k. \end{aligned} \tag{A.22}$$

Its Hessian, with respect to the synchronization errors, reads

$$\begin{aligned}\frac{\partial^2\hat{W}}{\partial\bar{e}_{x_k}^2} = & \left[1 - \frac{\Delta_k^2}{|\bar{e}_{x_k} + \alpha_k|^2(|\bar{e}_{x_k} + \alpha_k|^2 - \Delta_k^2)}\right] I_n \\ & + 2\left[\frac{\Delta_k^2\left(2|\bar{e}_{x_k} + \alpha_k|^2 - \Delta_k^2\right)}{|\bar{e}_{x_k} + \alpha_k|^4(|\bar{e}_{x_k} + \alpha_k|^2 - \Delta_k^2)^2}\right](\bar{e}_{x_k} + \alpha_k)(\bar{e}_{x_k} + \alpha_k)^\top. \end{aligned} \tag{A.23}$$

Let $s_k = \bar{e}_{x_k} + \alpha_k$. The eigenvalues of the Hessian are

$$\lambda_l(s_k) = 1 - \frac{\Delta_k^2}{|s_k|^2(|s_k|^2 - \Delta_k^2)}, \quad l \in \{1,\ 2, \cdots, n-1\} \tag{A.24a}$$

$$\lambda_n(s_k) = 1 - \frac{\Delta_k^2}{|s_k|^2(|s_k|^2 - \Delta_k^2)} + 2\frac{\Delta_k^2\left(2|s_k|^2 - \Delta_k^2\right)}{|s_k|^4(|s_k|^2 - \Delta_k^2)^2}|s_k|^2 \tag{A.24b}$$

For all $|s_k| > \Delta_k$, we have that

$$\lambda_n(s_k) = 1 + \frac{\Delta^2(|s_k|^2 - \Delta^2) + 2\Delta^2|s_k|^2}{|s_k|^2(|s_k|^2 - \Delta^2)^2} > 1.$$

Now, we look at the critical points, where $\nabla_{\bar{e}_{x_k}}\hat{W}_k = 0$. Looking at the form of the BLF, it has two critical points with opposite signs. The first one is $\bar{e}_{x_k} = 0$ and $\alpha_k = -2x_j + b_k$ since

$$\begin{aligned}&\left[1 - \frac{\Delta^2}{|-2x_j + b_k|^2(|-2x_j + b_k|^2 - \Delta^2)}\right](-2x_j + b_k) \\ &- \left[1 - \frac{\Delta^2}{|-2x_j + b_k|^2\left(|-2x_j + b_k|^2 - \Delta^2\right)}\right](-2x_j + b_k) = 0.\end{aligned}$$

Then, to prove that it is a minimum, we show that $\lambda_l(-2x_j + b_k) > 0$, that is,

$$\lambda_l(-2x_j + b_k) = 1 - \frac{\Delta_k^2}{|-2x_j + b_k|^2(|-2x_j + b_k|^2 - \Delta_k^2)} > 0,$$

if

$$\Delta^2 < \frac{|-2x_j + b_k|^4}{1 + |-2x_j + b_k|^2}. \tag{A.25}$$

The condition (A.25), which restricts the initial conditions in *absolute* coordinates, *i.e.*, with respect to a fixed frame. However, in the scenario considered in this paper, the measurements are relative (edge coordinates). That is, absolute positions are irrelevant. So, $x_j(0)$ may be conveniently defined by replacing the origin of the fixed frame if needed. Then, we have that $\lambda_l(-2x_j + b_k) > 0$ and $s_k = -2x_j + b_k$ is a minimum. There exists another critical point $\bar{e}_{x_k} = e_k^*$, so the gradient of the BLF gives

$$\begin{aligned}
&\left[1 - \Delta^2 \frac{1}{|e_k^* + b_k|^2(|e_k^* - 2x_j + b_k|^2 - \Delta^2)}\right](e_k^* - 2x_j + b_k) \\
&= \left[1 - \Delta^2 \frac{1}{|-2x_j + b_k|^2(|-2x_j + b_k|^2 - \Delta^2)}\right](-2x_j + b_k).
\end{aligned}$$

In original relative distance coordinates, we have $e_k^* - 2x_j + b_k = s_k^*$, which is aligned with the other critical point $-2x_j + b_k$, so there exists $a > 0$ such that $s^* = -a(-2x_j + b_k)$. As the BLF has only two critical points with opposite signs

$$\begin{aligned}
&\left[1 - \Delta^2 \frac{1}{|s_k^*|^2(|s_k^*|^2 - \Delta^2)}\right] - a(-2x_j + b_k) \\
&= \left[1 - \Delta^2 \frac{1}{|-2x_j + b_k|^2(|-2x_j + b_k|^2 - \Delta^2)}\right](-2x_j + b_k) \\
&\lambda_l(s_k^*) = -\frac{1}{a}\lambda_l(-2x_j + b_k)
\end{aligned}$$

As $\lambda_l(-2x_j + b_k) > 0$, we have that $\lambda_l(s_k^*) < 0$, so $s^* = -a(-2x_j + b_k)$ is a saddle point.

Bibliography

[1] U. Ahsun. *Dynamics and control of electromagnetic satellite formations*. PhD thesis, Imperial College London, Dept. of Aeronautics and Astronautics, Massachusetts Institute of Technology, Cambridge, 2007. https://dspace.mit.edu/handle/1721.1/40894.

[2] C. Altafini. Consensus problems on networks with antagonistic interactions. *IEEE Trans. on Autom. Control*, 58(4):935–946, 2013.

[3] A. D. Ames, X. Xu, J. W. Grizzle, and P. Tabuada. Control barrier function based quadratic programs for safety critical systems. *IEEE Trans. on Autom. Control*, 62(8):3861–3876, 2016.

[4] E. Aranda-Bricaire and J. González-Sierra. Formation with non-collision control strategies for second-order multi-agent systems. *Entropy*, 25(6):904, 2023.

[5] E. A. Barbashin and N. N. Krasovskiĭ. Ob ustoĭchivosti dvizheniya v tselom. *Dokl. Akad. Nauk. USSR*, 86(3):453–456, 1952. Commonly (and wrongly) cited in English under: "On the stability of motion in the large"; Correct translation: "On the stability of motion in the *whole*".

[6] Y. Cao and W. Ren. Distributed coordinated tracking with reduced interaction via a variable structure approach. *IEEE Trans. on Autom. Control*, 57(1):33–48, 2011.

[7] Y. Cao and W. Ren. *Distributed Coordination of Multi-agent Networks: Emergent Problems, Models, and Issues*. Springer-Verlag, 2011.

[8] Y. Cao, W. Ren, and M. Egerstedt. Distributed containment control with multiple stationary or dynamic leaders in fixed and switching directed networks. *Automatica*, 48(8):1586–1597, 2012.

[9] Y. Cao, D. Stuart, W. Ren, and Z. Meng. Distributed containment control for multiple autonomous vehicles with double-integrator dynamics: algorithms and experiments. *IEEE Trans. on Control Systems Technology*, 19(4):929–938, 2010.

[10] D. Cartwright and F. Harary. Structural balance: a generalization of heider's theory. *Psychological Review*, 63(5):277, 1956.

[11] J. S. Caughman and J. J. P. Veerman. Kernels of directed graph Laplacians. *The Electronic Journal of Combinatorics*, 13(1):1–8, 2006.

[12] T. H. Cheng, Z. Kan, J. A. Rosenfeldand, and W. E. Dixon. Decentralized formation control with connectivity maintenance and collision avoidance under limited and intermittent sensing. In *Proc. American Control Conf.*, pages 3201–3206, 2014.

[13] T. Chevet, C. Stoica Maniu, C. Vlad, and Y. Zhang. Guaranteed voronoi-based deployment for multi-agent systems under uncertain measurements. In *Proc. European Control Conf. (ECC)*, pages 4016–4021, 2019.

[14] T. Chevet, C. Vlad, C. Stoica Maniu, and Y. Zhang. Decentralized mpc for uavs formation deployment and reconfiguration with multiple outgoing agents. *Journal of Intelligent & Robotic Systems*, 97(1):155–170, 2020.

[15] V. S. Chipade and D. Panagou. Multi-swarm herding: Protecting against adversarial swarms. In *Proc. IEEE Conf. on Dec. and Control*, pages 5374–5379, 2020.

[16] S. J. Chung, U. Ahsun, and J. J. E. Slotine. Application of synchronization to formation flying spacecraft: Lagrangian approach. *Journal of Guidance, Control, and Dynamics*, 32(2):512–526, 2009.

[17] S. J. Chung and J. J. E. Slotine. Cooperative robot control and concurrent synchronization of Lagrangian systems. *IEEE Trans. on Robotics*, 25(3):686–700, June 2009.

[18] P. Şekercioğlu, E. Panteley, I. Sarras, A. Loría, and J. Marzat. Exponential bipartite containment tracking over multi-leader coopetition networks. In *Proc. American Control Conference*, pages 509–514, San Diego, CA, USA, 2023.

[19] P. Şekercioğlu, I. Sarras, A. Loría, E. Panteley, and J. Marzat. Bipartite formation over undirected signed networks with collision avoidance. In *Proc. IEEE Conf. on Dec. and Control*, pages 1438–1443, Singapore, 2023.

[20] Q. Deng, Y. Peng, T. Han, and D. Qu. Event-triggered bipartite consensus in networked Euler-Lagrange systems with external disturbance. *IEEE Trans. on Circuits and Systems II: Express Briefs*, 68(8):2870–2874, 2021.

[21] D. V. Dimarogonas and K. J. Kyriakopoulos. On the rendezvous problem for multiple nonholonomic agents. *IEEE Trans. on Autom. Control*, 52(5):916–922, May 2007.

[22] D. V. Dimarogonas and K. J. Kyriakopoulos. Connectedness preserving distributed swarm aggregation for multiple kinematic robots. *IEEE Trans. on Robotics*, 24(5):1213–1223, October 2008.

[23] M. Du, B. Ma, and D. Meng. Edge convergence problems on signed networks. *IEEE Trans. on Cybernetics*, 49(11):4029–4041, 2018.

[24] M. C. Fan, H. T. Zhang, and M. Wang. Bipartite flocking for multi-agent systems. *Communications in Nonlinear Science and Numerical Simulation*, 19(9):3313–3322, 2014.

[25] C. Feller and C. Ebenbauer. Weight recentered barrier functions and smooth polytopic terminal set formulations for linear model predictive control. In *Proc. American Control Conf.*, pages 1647–1652, 2015.

[26] J. Grover, N. Mohanty, C. Liu, W. Luo, and K. Sycara. Noncooperative herding with control barrier functions: Theory and experiments. In *Proc. IEEE Conf. on Dec. and Control*, pages 80–86, 2022.

[27] H. V. Henderson, F. Pukelsheim, and S. R. Searle. On the history of the kronecker product. *Linear and Multilinear Algebra*, 14(2):113–120, 1983.

[28] R. A. Horn and C. R. Johnson. *Matrix Analysis*. Cambridge University Press, 1985.

[29] H. X. Hu, G. Wen, W. Yu, J. Cao, and T. Huang. Finite-time coordination behavior of multiple Euler–Lagrange systems in cooperation-competition networks. *IEEE Trans. on Cybernetics*, 49(8):2967–2979, 2019.

[30] J. Hu and W. X. Zheng. Emergent collective behaviors on coopetition networks. *Physics Letters A*, 378(26-27):1787–1796, 2014.

[31] J. Huang and Z. Xiang. Leader-following bipartite consensus with disturbance rejection for uncertain multiple Euler-Lagrange systems over signed networks. *Journal of the Franklin Institute*, 358(15):7786–7803, 2021.

[32] D. Ioan, S. Olaru, I. Prodan, F. Stoican, and S. I. Niculescu. From obstacle-based space partitioning to corridors and path planning. a convex lifting approach. *IEEE Control Systems Letters*, 4(1):79–84, 2019.

[33] B. Jayawardhana. *Tracking and Disturbance Rejection for Passive Nonlinear Systems*. PhD thesis, Imperial College London, London, United Kingdom, 2006. https://www.rug.nl/staff/b.jayawardhana/thesis.pdf.

[34] B. Jayawardhana and G. Weiss. Tracking and disturbance rejection for fully actuated mechanical systems. *Automatica*, 44(11):2863–2868, 2008.

[35] M. Ji, G. Ferrari-Trecate, M. Egerstedt, and A. Buffa. Containment control in mobile networks. *IEEE Trans. on Autom. Control*, 53(8):1972–1975, 2008.

[36] Z. Kan, J. R. Klotz, E. L. Pasiliao Jr, and W. E. Dixon. Containment control for a social network with state-dependent connectivity. *Automatica*, 56:86–92, 2015.

[37] T. R. Kane and D. A. Levinson. *Dynamics, theory and applications.* McGraw Hill, 1985.

[38] H. Khalil. *Nonlinear systems.* Macmillan Publishing Co., 1st ed., New York, 1992.

[39] J. P. LaSalle. Stability theory and invariance principles. In *Dynamical systems*, pages 211–222. Elsevier, 1976.

[40] B. Li, T. Han, B. Xiao, X. S. Zhan, and H. Yan. Leader-following bipartite consensus of multiple uncertain Euler-Lagrange systems under deception attacks. *Applied Mathematics and Computation*, 428:127227, 2022.

[41] Z. Li, W. Ren, X. Liu, and M. Fu. Distributed containment control of multi-agent systems with general linear dynamics in the presence of multiple leaders. *International Journal of Robust and Nonlinear Control*, 23(5):534–547, 2013.

[42] D. Liang and J. Huang. Leader-following bipartite consensus of multiple uncertain Euler-Lagrange systems over signed switching digraphs. *Neurocomputing*, 405:96–102, 2020.

[43] J. Lin, A. S. Morse, and B. D. O. Anderson. The multi-agent rendezvous problem. In *Proc. IEEE Conf. on Dec. and Control*, volume 2, pages 1508–1513, 2003.

[44] H. Liu, G. Xie, and L. Wang. Necessary and sufficient conditions for containment control of networked multi-agent systems. *Automatica*, 48(7):1415–1422, 2012.

[45] J. Liu, H. Li, and J. Luo. Bipartite consensus in networked Euler-Lagrange systems with uncertain parameters under a cooperation-competition network topology. *IEEE Control Systems Letters*, 3(3):494–498, 2019.

[46] J. Liu, S. Xie, and H. Li. Oscillatory group-bipartite consensus in a swarm of robots with multiple oscillatory leaders. *IEEE Trans. on Control of Network Systems*, 10(1):124–133, 2022.

[47] F. L. Markley, J. L. Crassidis, F. L. Markley, and J. L. Crassidis. *Fundamentals of Spacecraft Attitude Determination and Control.* Springer, 2014.

[48] S. Mathavaraj and E. A. Butcher. Rigid-body attitude control, synchronization, and bipartite consensus using feedback reshaping. *Journal of Guidance, Control, and Dynamics*, 46(6):1095–1111, 2023.

[49] D. Meng. Bipartite containment tracking of signed networks. *Automatica*, 79:282–289, 2017.

[50] D. Meng, M. Du, and Y. Jia. Interval bipartite consensus of networked agents associated with signed digraphs. *IEEE Trans. on Autom. Control*, 61(12):3755–3770, 2016.

[51] D. Meng, M. Du, and Y. Wu. Extended structural balance theory and method for cooperative–antagonistic networks. *IEEE Trans. on Autom. Control*, 65(5):2147–2154, 2019.

[52] D. Meng, M. Du, and Y. Wu. *Disagreement Behavior Analysis of Signed Networks*, volume 5. Springer Nature, 2022.

[53] X. Meng and H. Gao. High-order bipartite containment control in multi-agent systems over time-varying cooperation-competition networks. *Neurocomputing*, 359:509–516, 2019.

[54] M. Mesbahi and M. Egerstedt. *Graph theoretic methods in multiagent networks*. Princeton University Press, 2010.

[55] S. Monaco and L. R. Celsi. On multi-consensus and almost equitable graph partitions. *Automatica*, 103:53–61, 2019.

[56] D. Mukherjee and D. Zelazo. Robustness of consensus over weighted digraphs. *IEEE Trans. on Network Science and Engineering*, 2018.

[57] R. Murray, Z. Li, and S. Sastry. *A mathematical introduction to robotic manipulation*. CRC Press, 1994.

[58] W. Ni and D. Cheng. Leader-following consensus of multi-agent systems under fixed and switching topologies. *Systems & control letters*, 59(3-4):209–217, 2010.

[59] H. Nijmeijer and A. Rodríguez-Angeles. *Synchronization of mechanical systems*, volume 46 of *Nonlinear Science, Series A*. World Scientific, London, 2003.

[60] E. Nuño, D. Valle, I. Sarras, and L. Basañez. Leader–follower and leaderless consensus in networks of flexible-joint manipulators. *European Journal of Control*, 20(5):249–258, 2014.

[61] E. Nuño, I. Sarras, H. Yin, and B. Jayawardhana. Robust leaderless consensus of Euler-Lagrange systems with interconnection delays. In *Proc. American Control Conf.*, pages 1547–1552, 2023.

[62] R. Olfati-Saber and R. M. Murray. Consensus problems in networks of agents with switching topology and time-delays. *IEEE Trans. on Autom. Control*, 49(9):1520–1533, 2004.

[63] R. Ortega, A. Loria, P. J. Nicklasson, and H. Sira-Ramirez. *Passivity-based Control of Euler-Lagrange Systems: Mechanical, Electrical and Electromechanical Applications*. Series Comunications and Control Engineering. Springer Verlag, London, 1998. ISBN 1-85233-016-3.

[64] H. Pan and V. Kapila. Adaptive nonlinear control for spacecraft formation flying with coupled translational and attitude dynamics. In *Proc. IEEE Conf. on Dec. and Control*, volume 3, pages 2057–2062, 2001.

[65] J. Pan, T. Han, B. Xiao, and H. Yan. Task-space multiple-bipartite consensus for networked heterogeneous Euler-Lagrange systems via hierarchical predefined-time control algorithm. *Nonlinear Dynamics*, 111(18):17095–17108, 2023.

[66] D. Panagou, D. M. Stipanovič, and P. G. Voulgaris. Multi-objective control for multi-agent systems using lyapunov-like barrier functions. In *Proc. IEEE Conf. on Dec. and Control*, pages 1478–1483, 2013.

[67] E. Panteley and A. Loría. Synchronization and dynamic consensus of heterogeneous networked systems. *IEEE Trans. on Autom. Control*, 62(8):3758–3773, 2017.

[68] E. Panteley, A. Loría, and S. Sukumar. Strict Lyapunov functions for consensus under directed connected graphs. In *Proc. European Control Conf. (ECC)*, pages 935–940, St. Petersburg, Russia, 2020.

[69] R. J. Plemmons. M-matrix characterizations.I—nonsingular M-matrices. *Linear Algebra and its Applications*, 18(2):175–188, January 1977.

[70] S. R. Ploen, F. Y. Hadaegh, and D. P. Scharf. Rigid body equations of motion for modeling and control of spacecraft formations. part 1: Absolute equations of motion. In *Proc. American Control Conference*, volume 4, pages 3646–3653, 2004.

[71] H. A. Poonawala and M. W. Spong. Preserving strong connectivity in directed proximity graphs. *IEEE Trans. on Autom. Control*, 62(9):4392–4404, September 2017.

[72] A. V. Proskurnikov, A. S. Matveev, and M. Cao. Opinion dynamics in social networks with hostile camps: Consensus vs. polarization. *IEEE Trans. on Autom. Control*, 61(6):1524–1536, 2015.

[73] W. Ren. Distributed leaderless consensus algorithms for networked Euler-Lagrange systems. *Int. Jour. of Control*, 82(11):2137–2149, 2009.

[74] W. Ren and E. Atkins. Distributed multi-vehicle coordinated control via local information exchange. *International Journal of Robust and Nonlinear Control*, 17(10-11):1002–1033, 2007.

[75] W. Ren and R. W. Beard. *Distributed consensus in multi-vehicle cooperative control*. Springer verlag, London, U.K., 2008.

[76] E. Restrepo-Ochoa. *Coordination control of autonomous robotic multi-agent systems under constraints*. PhD thesis, Univ Paris-Saclay, Gif sur Yvette, France, 2021. https://tel.archives-ouvertes.fr/tel-03537341.

[77] E. Restrepo-Ochoa, A. Loría, I. Sarras, and J. Marzat. Robust consensus of high-order systems under output constraints: Application to rendezvous of underactuated UAVs. *IEEE Trans. on Autom. Control*, 68(1):329–342, 2023.

[78] A. Rodriguez-Angeles and H. Nijmeijer. Mutual synchronization of robots via estimated state feedback: a cooperative approach. *IEEE Trans. on Control Systems Technology*, 12(4):542–554, 2004.

[79] K. Sakurama. Formation control of mechanical multi-agent systems under relative measurements and its application to robotic manipulators. In *Proc. IEEE Conf. on Dec. and Control*, pages 6445–6450, 2021.

[80] E. Sebastián, E. Montijano, and C. Sagüés. Adaptive multirobot implicit control of heterogeneous herds. *IEEE Trans. on Robotics*, 38(6):3622–3635, 2022.

[81] P. Şekercioğlu, B. Jayawardhana, I. Sarras, A. Loría, and J. Marzat. Formation control of cooperative-competitive robot manipulators with inter-agent constraints. *IFAC-PapersOnLine*, 58(21):49–54, 2024. 4th IFAC Conference on Modelling, Identification and Control of Nonlinear Systems MICNON 2024.

[82] P. Şekercioğlu, B. Jayawardhana, I. Sarras, A. Loría, and J. Marzat. Robust formation control of robot manipulators with inter-agent constraints over undirected signed networks. *IEEE Trans. on Control of Network Systems (Early Access)*, 2024. https://ieeexplore.ieee.org/document/10681470.

[83] P. Şekercioğlu, E. Panteley, I. Sarras, A. Loría, and J. Marzat. Distributed bipartite containment tracking over signed networks with multiple leaders. *IEEE Trans. on Control of Network Systems (Early Access)*, 2024. https://ieeexplore.ieee.org/document/10453997.

[84] P. Şekercioğlu, I. Sarras, A. Loría, E. Panteley, and J. Marzat. Leader-follower and leaderless bipartite formation-consensus over undirected coopetition networks and under proximity and collision-avoidance constraints. *International Journal of Control*, pages 1–15, 2024.

[85] Y. Shang. Resilient consensus in multi-agent systems with state constraints. *Automatica*, 122:109288, 2020.

[86] S. Singh and A. Jain. Collision avoidance and connectivity preservation using asymmetric barrier lyapunov function with time-varying distance-constraints. *Systems & Control Letters*, 183:105672, 2024.

[87] A. Singletary, K. Klingebiel, J. Bourne, A. Browning, P. Tokumaru, and A. Ames. Comparative analysis of control barrier functions and artificial potential fields for obstacle avoidance. In *2021 IEEE/RSJ International Conference on Intelligent Robots and Systems (IROS)*, pages 8129–8136, 2021.

[88] E. D. Sontag and Y. Wang. On characterizations of the input-to-state stability property. *Systems & Control Letters*, 24(5):351–359, 1995.

[89] H. Su, X. Wang, and Z. Lin. Flocking of multi-agents with a virtual leader. *IEEE Trans. on Autom. Control*, 54(2):293–307, 2009.

[90] T. Tao, S. Roy, and S. Baldi. Adaptive single-stage control for uncertain nonholonomic Euler-Lagrange systems. In *Proc. IEEE Conf. on Dec. and Control*, pages 2708–2713, 2022.

[91] K. P. Tee and S. S. Ge. Control of nonlinear systems with partial state constraints using a barrier lyapunov function. *International Journal of Control*, 84(12):2008–2023, 2011.

[92] K. P. Tee, S. S. Ge, and E. H. Tay. Barrier Lyapunov functions for the control of output-constrained nonlinear systems. *Automatica*, 45(4):918–927, April 2009.

[93] K. Topolewicz, S. Olaru, E. Girejko, and C. E. T. Dórea. On impact of disturbance in the deployment problem of multi-agent system. *Archives of Control Sciences*, pages 299–320, 2023.

[94] S. G. Tzafestas. *Introduction to mobile robot control.* Elsevier Inc, First ed., London, 2013.

[95] M. E. Valcher and P. Misra. On the consensus and bipartite consensus in high-order multi-agent dynamical systems with antagonistic interactions. *Syst. & Control Lett.*, 66:94 – 103, 2014.

[96] C. K. Verginis and D. V. Dimarogonas. Closed-form barrier functions for multi-agent ellipsoidal systems with uncertain lagrangian dynamics. *IEEE Control Systems Letters*, 3(3):727–732, 2019.

[97] C. K. Verginis, A. Nikou, and D. V. Dimarogonas. Position and orientation based formation control of multiple rigid bodies with collision avoidance and connectivity maintenance. In *Proc. IEEE Conf. on Dec. and Control*, pages 411–416, 2017.

[98] L. Wang, J. Wu, X. S. Zhan, T. Han, and H. Yan. Fixed-time bipartite containment of multi-agent systems subject to disturbance. *IEEE Access*, 8:77679–77688, 2020.

[99] S. Wang, H. Zhang, S. Baldi, and R. Zhong. Leaderless consensus of heterogeneous multiple Euler-Lagrange systems with unknown disturbance. *IEEE Trans. on Autom. Control*, 68(4):2399–2406, 2022.

[100] P. Wieland, J. S. Kim, H. Scheu, and F. Allgöwer. On consensus in multi-agent systems with linear high-order agents. *IFAC Proceedings Volumes*, 41(2):1541–1546, 2008.

[101] A. G. Wills and W. P. Heath. A recentred barrier for constrained receding horizon control. In *Proc. American Control Conf.*, volume 5, pages 4177–4182, 2002.

[102] H. Wu, B. Jayawardhana, H. G. De Marina, and D. Xu. Distributed formation control of manipulators' end-effector with internal model-based disturbance rejection. In *Proc. IEEE Conf. on Dec. and Control*, pages 5568–5575, 2021.

[103] H. Wu, B. Jayawardhana, H. G. de Marina, and D. Xu. Distributed formation control for manipulator end-effectors. *IEEE Trans. on Autom. Control*, pages 5413–5428, 2022.

[104] Y. Yang, R. Ding, and W. Hu. Bipartite consensus for a class of double-integrator multi-agent systems with antagonistic interactions. In *IEEE/ASME Int. Conf. Advanced Intel. Mechatr.*, pages 901–906, 2019.

[105] S. J. Yoo and T. H. Kim. Distributed formation tracking of networked mobile robots under unknown slippage effects. *Automatica*, 54:100–106, 2015.

[106] S. J. Yoo and B. S. Park. Connectivity preservation and collision avoidance in networked nonholonomic multi-robot formation systems: Unified error transformation strategy. *Automatica*, 103:274–281, 2019.

[107] D. Zelazo, A. Rahmani, and M. Mesbahi. Agreement via the edge Laplacian. In *Proc. IEEE Conf. on Dec. and Control*, pages 2309–2314, 2007.

[108] H. Zhang and J. Chen. Bipartite consensus of multi-agent systems over signed graphs: state feedback and output feedback control approaches. *Int. J. of Robust and Nonlinear Control*, 27(1):3–14, 2017.

[109] H. Zhang, F. L. Lewis, and Z. Qu. Lyapunov, adaptive, and optimal design techniques for cooperative systems on directed communication graphs. *IEEE Trans. on Industrial Electronics*, 59(7):3026–3041, 2011.

[110] H. Zhang, Y. Zhou, Y. Liu, and J. Sun. Cooperative bipartite containment control for multiagent systems based on adaptive distributed observer. *IEEE Trans. on Cybernetics*, pages 5432–5440, 2020.

[111] J. Zhang, F. Wang, and G. Wen. Bipartite consensus for networked Euler–Lagrange systems with cooperative–competitive interactions and time delays. *IET Control Theory & Applications*, 17(9):1214–1226, 2023.

[112] T. Zhang, J. Liu, H. Li, S. Xie, and L. Jun. Group consensus coordination control in networked nonholonomic multirobot systems. *Int. Jour. of Advanced Robotic Systems*, 18(4):1–14, 2021.

[113] G. Zhao, H. Cui, and C. Hua. Hybrid event-triggered bipartite consensus control of multiagent systems and application to satellite formation. *IEEE Trans. on Automation Science and Engineering*, 20(3):1760–1771, 2022.

[114] G. Zhao, C. Hua, and X. Guan. A hybrid event-triggered approach to consensus of multiagent systems with disturbances. *IEEE Trans. on Control of Network Systems*, 7(3):1259–1271, 2020.

[115] X. F. Zhao, T. Han, X. S. Zhan, and H. Yan. Distributed estimator-based fixed-time bipartite consensus of multiple Euler-Lagrange systems over a signed digraph. *IEEE Trans. on Circuits and Systems II: Express Briefs*, 69(6):2847–2851, 2022.